Title
Investigation of the Feasibility of a Small Scale Transmutation Device

Author
Sit, Roger Carson

Publication Date
2009

Peer reviewed|Thesis/dissertation

Investigation of the Feasibility of a Small Scale Transmutation Device

by

Roger Carson Sit

B.S. (Mississippi State University) 1984

M.S. (University of California, Berkeley) 1985

A dissertation submitted in partial satisfaction of the

requirements for the degree of

Doctor of Philosophy

in

Engineering-Nuclear Engineering

in the

Graduate Division

of the

University of California, Berkeley

Committee in charge:

Professor Jasmina Vujic, Chair

Professor David McNelis (University of North Carolina at Chapel Hill)

Professor Ka-Ngo Leung

Professor Dorian Liepmann

Fall 2009

Abstract

Investigation of the Feasibility of a Small Scale Transmutation Device

by

Roger Carson Sit

Doctor of Philosophy in Engineering-Nuclear Engineering

University of California, Berkeley

Professor Jasmina Vujic, Chair

This dissertation presents the design and feasibility of a small-scale, fusion-based transmutation device incorporating a commercially available neutron generator. It also presents the design features necessary to optimize the device and render it practical for the transmutation of selected long-lived fission products and actinides.

Four conceptual designs of a transmutation device were used to study the transformation of seven radionuclides: long-lived fission products (Tc-99 and I-129), short-lived fission products (Cs-137 and Sr-90), and selective actinides (Am-241, Pu-238, and Pu-239). These radionuclides were chosen because they are major components of spent nuclear fuel and also because they exist as legacy sources that are being stored pending a decision regarding their ultimate disposition.

The four designs include the use of two different devices; a Deuterium-Deuterium (D-D) neutron generator (for one design) and a Deuterium-Tritium (D-T) neutron generator (for three designs) in configurations which provide different neutron energy

spectra for targeting the radionuclide for transmutation. Key parameters analyzed include total fluence and flux requirements; transmutation effectiveness measured as irradiation effective half-life; and activation products generated along with their characteristics: activity, dose rate, decay, and ingestion and inhalation radiotoxicity.

From this investigation, conclusions were drawn about the feasibility of the device, the design and technology enhancements that would be required to make transmutation practical, the most beneficial design for each radionuclide, the consequence of the transmutation, and radiation protection issues that are important for the conceptual design of the transmutation device.

Key conclusions from this investigation include: (1) the transmutation of long-lived fission products and select actinides can be practical using a small-scale, fusion driven transmutation device; (2) the transmutation of long-lived fission products could result in an irradiation effective half-life of a few years with a three order magnitude increase in the on-target neutron flux accomplishable through a combination of technological enhancements to the source and system design optimization; (3) the transmutation of long-lived fission products requires a thermal-slow energy spectrum to prevent the generation of activation products with half-lives even longer than the original radionuclide; (4) there is no benefit in trying to transmute short-lived fission products due to the ineffectiveness of the transmutation process and the generation of a multiplicity of counterproductive activation products; (5) for actinides, irradiation effective half-lives of < 1 year can be achieved with a four orders magnitude increase in the on-target flux; (6) the ideal neutron energy spectra for transmuting actinides is highly dependent on the particular radionuclide and its fission-to-capture ratio as they determine the generation

rate of other actinides; and (7) the methodology developed in this dissertation provides a mechanism that can be used for studying the feasibility of transmuting other radionuclides, and its application can be extended to studying the production of radionuclides of interest in a transmutation process.

Although large-scale transmutation technology is presently being researched world-wide for spent fuel management applications, such technology will not be viable for a couple of decades. This dissertation investigated the concept of a small-scale transmutation device using present technology. The results of this research show that with reasonable enhancements, transmutation of specific radionuclides can be practical in the near term.

_____

Professor JasminaVujic,

Dissertation Committee Chair

Acknowledgements

I would like to express my sincere appreciation to the members of my dissertation committee Professor Jasmina Vujic, Professor David McNelis, Professor Ka-Ngo Leung, and Professor Dorian Liepmann for their scientific advice, guidance, and efforts in reviewing my dissertation.

I am incredibly indebted to and grateful for Professor Vujic who began this 11 year journey with me, expressing encouragement and inspiration all along the way. She made the completion of my degree possible by allowing me many non-traditional variances, which I consider "miracles", in my progression through the graduate program.

I especially want to thank Professor McNelis, without whom I would not have been able to complete this research. He has been a great mentor not only for this research but for my professional life. He believed in me even from the very beginning when he allowed me to join the research group without any knowledge of me, my background, or my abilities and without proof of my academic status at the time. He graciously funded my trips to meet with Professor Vujic on several occasions and has supported my research topic from its inception. Professionally, Professor McNelis has allowed me the opportunity to be involved in technical issues that I would never have had the opportunity to be involved in; ie, meetings with EPRI and members of the Russian Academy of Sciences; and a visit to the AREVA fuel fabrication facility.

I would also like to express my sincere gratitude to professor Man-Sung Yim and Dr. Jun Li. They allowed me to join their research group at NC State University and

patiently allowed me to catch up in my knowledge of the nuclear power industry. They provided me with the structure I needed to work within to conduct my research and the necessary encouragement to progress at a steady pace.

I would like to thank Lisa Zemelman who provided me with advice, guidance, and logistics over the past several years in meeting the administrative requirements of completing and filing the final manuscript. I would like to thank R.A. Forrest, Ph.D., the author of the EASY software package, for helpful discussions on the limitations of the software and rendering his scientific opinion on my proposed methodology. I would like to thank Mr. Peter Reinhardt, Director of EHS at Yale University (my previous boss), for introducing me to Professor McNelis which started the relationship leading to this research. I would like to thank my present boss, Ms. Mary Beth Koza, Director of EHS at University of North Carolina for allowing me flexibility in managing my job and my time in order to complete this research. I would like to thank my wife and two sons who had to endure many working weekends and evenings during the course of this research and whose encouragement has been vital.

Finally, and most importantly, I would like to acknowledge my lord, Jesus Christ, who I lean on daily for guidance, strength, and perseverance; and who allowed me to meet all the wonderful people aforementioned. To Him I dedicate my future experiences with the completion of this degree.

Table of Contents

List of Figures

List of Tables

Chapter 1

Introduction

1.1 Transmutation Overview

Transmutation is the transformation of one nuclide into another or other nuclides. Transmutation occurs in nuclear and radiological processes whether they are desired or undesired and unwanted. Fission and fusion energy production include both desired and undesired transmutation processes. The desired process is changing nuclides for the purpose of creating or releasing energy, e.g., fissioning of U-235, or fusing of hydrogen nuclides, and the resulting undesired process is changing non-radioactive nuclides to radioactive nuclides (activation of water, metals, and concrete.)

The application of transmutation technology can be viewed as either a production process or a depletion process. An example of a production process is the generation of radionuclides used for diagnostic and/or therapeutic medicine, e.g., for SPECT (single photon emission computed tomography) imaging and PET (positron emission tomography) imaging, such as Tc-99m, Tl-201, F-18, and C-11. An example of a depletion process is the destruction of spent nuclear fuel or other unwanted radionuclides. The scope of this dissertation will cover the application of transmutation as a depletion process and will include evaluations of both desired and undesired processes.

The focus of studying transmutation in this research is for the specific task of changing radionuclides with undesired characteristics (high radiotoxicity, high heat evolution and/or very long half-lives) to less undesirable characteristics (lower radiotoxicity, lower heat evolution and/or shorter half-lives). Presently, there is much

research being done globally on this principle as applied to nuclear waste management in an effort to reduce the long-term impacts of spent nuclear fuel storage and reprocessing or disposal; to reduce the potential of proliferation; and to increase public confidence and acceptance. With the present renaissance in nuclear energy, as a source of alternative energy to combat the effects of global warming and advance energy security, there is a need to resolve the nuclear fuel cycle issues. Present transmutation research focuses on large scale devices such as nuclear reactors and/or high energy accelerators. Although research is being conducted internationally, with the bulk of the collaborative research being done in Western European nations, a practical technology for nuclear waste transmutation is most likely a couple of decades away.

1.2 Review of Transmutation Technologies

In general, transmutation technologies can employ the use of neutrons, charged particles, or photons. Research has shown that most industrial scale transmutation technologies studied for the purpose of nuclear waste transmutation involve the use of the fundamentals of neutron generation and neutron reactions. This dissertation will focus on transmutation technology based on neutron interactions. The three most important transmutation reactions resulting from neutrons are:

- Fission; (e.g., U-235 to Kr-92 + Ba-142)
- Neutron capture/absorption; e.g.,(n, γ), (n,2n), (n,3n), (n,alpha)
- and subsequent radioactive decay and daughter product evolution (e.g., Np-239 to Pu-239)

Any type of transmutation involving either of the first two reactions will be a function of the fission and neutron capture cross sections and the spectral dependence of the material being transmuted. For certain radionuclides such as fission products, neutron capture/absorption reactions are the major processes for transmutation; whereas, for actinides, the preferred reactions would be fissions as neutron capture and absorption could serve to create additional actinides. Research into nuclear watse transmutation strategies have included the use of thermal reactors, fast reactors, fusion sources, accelerator driven subcritical reactors [9, 13]. Additionally, recent research involves the use of lasers for radionuclide transmutation [49] and charged particles such as protons or electrons for direct transmutation [70, 72].

1.2.1 Thermal Reactors

Thermal reactors are reactors in which the fission chain reaction is sustained primarily by thermal neutrons. Most current power reactors are thermal reactors. The energy of fission neutrons created is higher than thermal energy levels and moderators are used to slow down the neutrons to thermal energy levels. Thermal reactors such as boiling water reactors (BWRs) and pressurized water reactors (PWRs) have neutron fluxes in the core on the order of 10^{14} n/cm^2-s. The thermal reactor neutron energy spectrum is shown in Figure 1.1. Thermal reactor transmutation focuses mainly on the use of the thermal neutrons of the spectrum.

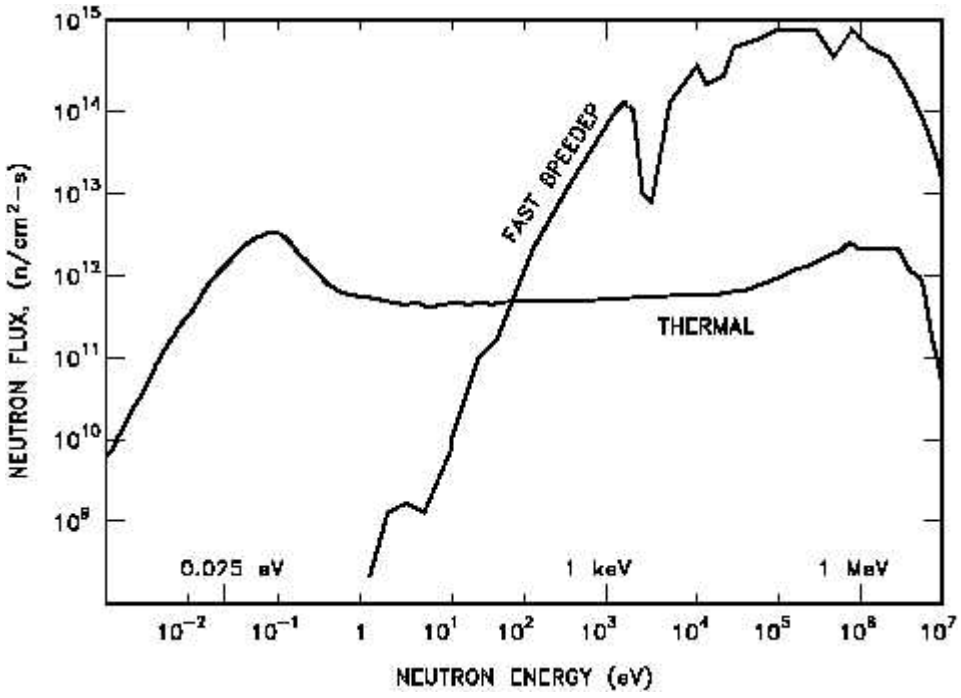

Figure 1.1 Neutron Energy Spectra of Thermal and Fast Breeder Reactors [34]

Thermal reactors are known to be good for transmutation of long-lived fission products but not very effective for transmutation of minor actinides. The neutron energy spectrum in a thermal reactor has higher fluxes in the lower energy range for which the cross sections for absorption by the long-lived fission products to stable radionuclides is higher; thereby increasing the potential transmutation efficiency. This energy spectrum is, however, disadvantageous to the transmutation of the minor actinides. The absorption reactions include not only fission but also capture reactions; therefore, the competition between the fission and capture processes is highly relevant. The capture reactions lead to the production of additional transuranic elements. For examples; neutron capture on U-238 leads to the production of Pu-239, neutron capture in Pu-242 leads to the production of Am-241, and then Curium is produced by neutron capture of Americium [50].

The thermal energy neutrons have high fission cross sections for some actinides such as Pu-238 and Pu-239 but low fission cross sections for most other actinides such as Am-241 and Np-237 (which can ultimately be transformed to other nuclides that have high fission cross sections); however, the dominant reactions for these actinides will then be capture reactions. Because the dominant reaction is capture, then actinide creation will surpass actinide destruction.

In summary, thermal reactors are good for transmutation of long-lived fission products and Plutonium; however, not very good for the minor actinides due to low fission cross sections and minor actinide formation. The CEA (French Atomic Energy Commission), JAERI (Japan Atomic Energy Research Institute), and Brookhaven National Laboratory (BNL) have researched and proposed transmutation strategies based on the thermal reactor concept. [9]

1.2.2 Fast Reactors

Fast reactors are reactors in which the fission chain reaction is sustained primarily by higher energy neutrons. These reactors do not have moderators. Fast reactors such as liquid metal fast breeder reactors (LMFBRs) and high temperature gas cooled reactors (HTGRs) have neutron fluxes in the core on the order of 10^{15} n/cm^2-s. The fast breeder reactor neutron energy spectrum is also shown in Figure 1.1. Fast reactors can fission most of the actinides; however, the cross sections are smaller than the reaction cross sections of thermal energy neutrons. The higher neutron flux of the fast reactors compensates for the lower fission probabilities. The fast neutron flux in fast reactors can be 2 – 3 orders of magnitude greater than the thermal neutron flux in thermal reactors.

The flux is higher due to the larger number of fission neutrons created in the core. Also the production of higher actinides through neutron capture is smaller with the fast neutrons than thermal neutrons. The fission to capture ratio of minor actinides increases with the mean neutron energy. Therefore, if a fast reactor with a very hard neutron spectrum is established, the minor actinides become additional fissionable resources instead of waste material as in a thermal reactor [9].

The long-lived fission products could also be transmuted in fast reactors, but at a much lower efficiency than in a thermal reactor because the cross section for reactions will be lower at the higher energies. The long-lived fission products would need to be loaded into moderated targets outside the reactor core. Another disadvantage for long-lived fission product transmutation in a fast reactor energy spectrum is that the transmuted products may be quite different (longer half-life or more radiotoxic) than the transmuted products from a thermal reactor spectrum due to the higher order nuclear reactions that occur with higher energy neutrons [50].

In summary, fast reactors are good for transmutation of minor actinides through fission thereby minimizing the production of actinides; however, not very good for the fission products. The list of research institutes that have researched transmutation strategies using the fast reactor includes CEA, JAERI, Power Reactor and Nuclear Fuel Development Corporation (PNC), General Electric Corporation (GE), Argonne National Laboratory (ANL), and Central Research Institute of Electric Power Industry (CRIEPI) [9].

1.2.3 Fusion Sources

Although fusion power reactors have not yet been developed, research has shown that due to superior neutron economy, D-T fusion reactors can produce fluence on the order of 10^{21} n/s [22]. Fusion power reactor concepts that have been studied include the ITER (a tokamak concept which is the world's largest experimental fusion facility designed to demonstrate the scientific and technological feasibility of fusion power) [45], the Z-Pinch concept [13], and a Spheromak concept [46]. Subsequently, researchers began looking at the use of fusion reactions to perform transmutation. Fusion power sources used as transmutation reactors have been studied. Concepts include the use of the In-Zinerator (using the Z-Pinch fusion source) [13], the Fusion Transmutation of Waste Reactor (FTWR) [27], and the Gas-Cooled Fast Transmutation Reactor (GCFTR) [27].

Recently, the Lawrence Livermore National Laboratory has been developing an advanced energy concept known as the Laser Inertial Fusion Engine (LIFE) based upon the technology of their new National Ignition Facility (NIF) [69]. LIFE would employ an inertial confinement fusion laser system to operate a fusion-fission hybrid reactor for the dual purpose of generating energy and burning nuclear waste. This concept would use lasers to create fusion reactions in a target releasing large numbers of neutrons (up to 10^{20} neutrons every second) which will create a chain reaction in a surrounding fission blanket [69]. This fission blanket can be made up of the spent nuclear fuel that is destined for a repository.

Sources of neutrons from fusion reactions are available today, although typically at much lower source strengths than would be found in a fusion power reactor concept. Most of these sources utilize the deuterium-deuterium (D-D) reaction or the deuterium-tritium (D-T) reaction. These neutron sources are found in gas, oil, or uranium ore well logging, non-destructive testing devices (neutron or prompt gamma activation analysis) for explosives detection or elemental fingerprinting, and medical treatment facilities (such as Boron Neutron Capture Therapy, BNCT). These technologies have not been studied with respect to transmutation to any extent because of their relatively low neutron flux produced.

1.2.4 Subcritical Reactors Driven by Proton or Electron Accelerator Systems

Accelerator-driven systems (ADS) use high energy particle accelerator reactions to create large amounts of neutrons used to drive a subcritical reactor to perform radionuclide transmutation. These systems can be referred to as accelerator-fission hybrid systems. These systems use spallation reactions from high energy proton accelerators impinging upon a high z number target to create the neutrons. Electron accelerators have also been studied to drive subcritical reactors for transmutation. The high energy reactions (electron-gamma showers) of the accelerated electrons lead to photo-neutron reactions inside the high z number target as the source of neutrons. In the electron accelerator case, intranuclear cascades also contribute to neutron generation but at a much lower production rate than the proton accelerator. The incident proton and electrons are typically accelerated to energies of about 1 GeV to impinge upon a target located in the sub-critical reactor core to produce neutrons to drive the fission reactions [5, 9].

The neutron energy spectrum in a subcritical reactor in the ADS will be more similar to that of the fast reactor than the thermal reactor. Transmutation efficacy will be similar to the fast reactor whereby fission products are not efficiently transmuted while minor actinides can be transmuted more efficiently. Like the fast reactor, transmutation of fission products can be possible if the fission product is placed in a moderated target outside of the subcritical reactor core. The neutron energy spectrum within the subcritical core will be highly dependent upon the ADS target design. The larger the diameter of the target, the lower the median energy of the neutrons exiting the spallation target. This would have a direct impact on the transmutation efficiencies of the radionculides; especially the actinides [50].

The ADS is the subject of several cooperative research programs internationally but such technology is not expected to be available for practical deployment for several more decades [11]. JAERI, CEA, BNL, Los Alamos National Laboratory (LANL), National Agency for New Technologies, Energy and the Environment (ENEA), Royal Institute of Technology, and the Institute for Theoretical and Experimental Physics (ITEP) among others have all researched the use of proton accelerator driven transmutation [9]. The CEA [21], KFKI Atomic Energy Research Institute [23] and North Carolina State University [5] have studied the electron accelerator driven transmutation concept.

Another type of accelerator driven subcritical system is being studied by the Institute des Sciences Nucleaires and the CEA in France and is considered a type of hybrid system because it uses both an accelerated driven system and fusion reactions. This technology utilizes a deuteron accelerator for impinging deuterons onto a tritium

target, thereby producing the D-T reaction fusion neutrons with average energy of about 14 MeV. This accelerator, as are the ADSs described previously, is coupled to a small subcritical reactor or assembly [26].

1.2.5 Lasers

Another transmutation strategy that is being studied involves the use of high powered lasers and is referred to as photo-transmutation. Unlike the previously described processes, neutron generation and reactions are not the focus of this process. This process proposes the use of photonuclear (γ, n) reactions for transmutation using presently available table top laser systems. The laser produces plasma on the surface of a target, the high energy electrons are then stopped in the target producing Bremsstrahlung radiation (photons). In the specific experiments conducted, the photons generated interact with I-129 (with a half-life of 15.7 million years) [43] producing a photo-neutron thereby converting it to I-128 (with a half-life of 25 minutes) [43]. This transmutation process is being studied at the University of Glasgow, University of Strathclyde, Rutherford Appleton Laboratory, and the Institute for Transuranium Elements (ITU) [19].

A major disadvantage of this technology at the present time is the power requirements that would be needed to accomplish significant transmutation. For example, a Vulcan laser was used to perform "proof of principle" experiments at the Rutherford Appleton Laboratory where I-129 atoms were transformed into I-128 successfully; however, to transform a 46 gram block of I-129 (about 7.4 mCi or 272 MBq) it would take about 10^{17} pulses of the laser at about a terawatt of power per pulse. Another disadvantage of this technology is that it would only apply to long-lived and

short-lived fission products but not to actinides. Photo-transmutation would not be effective for transmutation of the transuranics due to the low photo-fission crosssections as compared to transmutation processes using neutrons [51].

1.2.6 Charged Particle Accelerators

Charged particle accelerators can directly utilize the charged particles for transmutation. This is different from the indirect use of the charged particle to create neutrons to perform the transmutation as discussed in Section 1.2.4. Charged particle transmutation is prevalent in the medical industry where protons, alphas, and other ions are used to generate specific radionuclides such as At-211 and Sr-82. The most common charged particle studied for nuclear waste transmutation applications is the proton. Researchers in Belgium [70], Japan [71], and France [72] have studied the use of proton accelerators for transmutation of actinides, long and short-lived fission products. The studies conclude that proton induced reactions are not as effective as neutron induced fission reactions for actinides [72]; and, in general, not as effective for fission products as the indirect use of protons to create neutrons for driving a subcritical blanket for transmutation [71]. However, for select fission products such as Cs-135, Cs-137, Se-79, and Sn-126, proton reactions may require more energy but may produce transmutation products that are more favorable [70]. Therefore, when considering safety (no fission), ease of operation, and public acceptance, direct proton reaction transmutation may be competitive and worthy of more research [70].

Electrons have also been studied to create bremsstrahlung and utilize the (γ,xn) reaction to transmute neutron-rich short-lived fission products such as Cs-137 and Sr-90.

However, due to the poor efficiency and high intensity electron beam required, this transmutation strategy has not been adopted as a feasible strategy.

1.3 Motivation for Investigating a Small Scale Transmutation Device

The concept of nuclear waste transmutation is very complex. Much of the research which has been done focuses on specific radionuclide transmutation in the midst of the large number of radionuclides present in nuclear waste. There is a lack of quantitative information about what other radionuclides may be produced in addition to the transmutation product of the targeted nuclide, what quantities and activities of other radionuclides are produced, the dose rates and radiotoxicities resulting from these products, and their decay characteristics. This research will focus on single target radionuclides to be transmuted, determine the effective half-life as a function of neutron flux and energy spectrum, determine the number and activities of the radionuclide activation products, determine the external dose rates and radiotoxicities (ingestion and inhalation hazards) of the activation products, and evaluate the decay of the activation products. In addition, the research will determine if transmutation of certain radionuclides is feasible with neutron fluxes available in present day technology and, if not, what improvement in neutron fluxes would be required. The radionuclides that are the subject of this investigation are common in research and medical settings and are in the form of sealed sources as may be used for academic research. Therefore, a transmutation device, if feasible, may be immediately useful to reduce the number of these radiation sources and reduce the risk of malevolent use of such materials. In

addition, this research of a transmutation device would be beneficial to the fundamental understanding of single nuclide transmutation by revealing competing transmutation processes, how activation products may differ as a result of the different processes, and evaluating the consequences of those activation products.

As discussed in the previous sections, the transmutation technologies being studied globally are mostly non-mature at the present time. Thermal reactor technology is much more mature than fast reactor technology as well as fusion and accelerator driven systems; however, as pointed out earlier, it is not sufficiently effective in transmutation of all radionuclides of interest. Industrial scale transmutation will not be available for several more decades; therefore, if a small scale transmutation device is feasible, certain applications may be appropriate.

Chapter 2

Scope of Dissertation Research

The research presented in this dissertation will focus on investigating, using mathematical simulations, the use of a small scale transmutation device for the purpose of beneficially transforming long-lived fission products, short-lived fission products and actinides. The transmutation efficiency will be a function of the neutron flux impinging on the target radionuclide, the neutron energy spectrum available, and the amount of time available for transmutation. Several base cases will be established to designate the neutron source; determine the on-target neutron flux and neutron energy spectrum from that source; evaluate the resulting transmutation efficacy with respect to the target radionuclide; and evaluate the activation products from the transmutation process in terms of total activity, photon dose rate and radiotoxicities from the products, and the decay characteristics of the products. Conclusions will be drawn on which of the base cases is most beneficial with respect to the radionuclide being transmuted.

2.1 Description of "Small Scale" Transmutation Device Concept

For the purpose of this dissertation, the term "small scale" refers to transmutation of small quantities of single radionuclides using available technology; and also the neutron source is physically small or "bench-scale" in size. For practical transmutation, two conditions must apply [11]:

- the reaction probability for the radionuclide of interest must be sufficient for the transmutation to occur rapidly enough to be practical.

- the target radionuclide should be partitioned or separated from other nuclides otherwise; more radionuclides will be produced under the neutron bombardment.

Single radionuclides will be chosen for the transmutation studies and small quantities (typically < 1 Ci) will be used. The radionuclides would be consistent with the categories of radionuclides typically found in nuclear waste: long-lived fission products, short-lived fission products, and actinides or transuranics. In addition, the quantities used would be consistent with amounts of these materials found in typically available sealed sources.

2.2 Purpose

The purpose of this research is to determine whether a compact device for transmuting radionuclides of interest is feasible. Studying transmutation on a small scale leads to a better understanding of how individual radionuclides transmute without the complexity of the myriad of other radionuclides present in nuclear waste. This knowledge can lead to development of transmutation strategies for different radionuclides to optimize transmutation efficiency. The transmutation strategy includes using the correct energy spectrum to maximize transmutation, minimize production of activation products, and ensure that the activation products produced are not longer-lived or more hazardous than the radionuclide to be destroyed.

2.3 Potential Application

The US Department of Energy has funded the OSRP (Offsite Source Recovery Program) to reclaim unwanted radiological sources distributed around the United States that represent a potential radiological vulnerability to the security of the country. As of September 2005, the OSRP had 9,600 sealed sources in secure storage. The Project anticipates a total of 10,000 sealed sources to be packaged for disposal (above ground

storage) through 2010. These sources include actinides/transuranics such as Pu-238, Pu-239, and Am-241, as well as fission products such as I-129, Tc-99, Cs-137, and Sr-90 [16]. Although these sources are secure, they must still be under constant surveillance to alleviate the potential for their theft and use for malevolent purposes. The Department of Homeland Security, after the events of September 11, 2001, issued many new regulations to ensure the security of radionuclides in use as well as in storage (for disposal). The transmutation of these sources could reduce the radiological vulnerabilities that they present by reducing the amount of time that materials need to be stored or by changing the nuclides so that they no longer are a proliferation risk.

Table 2.1 presents an example of select radionuclides that are being handled by DOE's OSRP. This Table is not an exhaustive list but includes some of the radionuclides addressed in this research.

Table 2.1 Examples of Radionuclide Sources in DOE's OSRP [47]

Radionuclide	Number of Sources in Storage (Jan, 2007)	Activity of Stored Sources, TBq (Ci)	Number of Sources Registered for Retrieval	Activity of Registered Sources for Retrieval TBq (Ci)
Cs-137	393	310 (8,393)	600	905 (24,446)
Sr-90	10	2,740 (74,000)	100	13,500 (364,000)
Am-241	10,154	507 (13,698)	1,012	62.6 (1,689)
Pu-238	2,169	407 (10,993)	112	298 (8,043)

The table shows that there are many radionuclide sources that have no beneficial use but could present a hazard if used for malevolent purposes. Adding to the problem of these numerous sources is that presently, there are no disposal options other than the

OSRP) for these sources which would typically be considered Class C waste. The most recent disposal site for such Class C sealed sources was in Barnwell South Carolina, who closed their doors to everyone outside their waste compact in the summer of 2008 [52]. Having a feasible small scale transmutation device could contribute to helping resolve the low-level waste predicament as it pertains to Class B or C waste by providing an alternative disposal pathway.

2.4 Radionuclides to be Studied

The radionuclides studied within the scope of this dissertation include long-lived fission products: I-129 and Tc-99, short-lived fission products: Cs-137 and Sr-90, and actinides: Am-241, Pu-238, and Pu-239. Details of these radionuclides are given in Chapter 7.

Chapter 3

Review of Small Scale Neutron Sources

This research begins with a review of the neutron sources presently available. Ultimately, one of the neutron sources will be chosen to be the source for the transmutation device. The most important factor to evaluate is the neutron source strength (n/s) that the source can provide; i.e., typically the higher the source strength, the higher the transmutation efficiency.

3.1 Radionuclide Sources

There have been many different types of isotopic neutron sources that have been developed for many different purposes. These purposes include academic research in neutron science, instrument calibration, moisture density gauges, and radiography devices. Neutron sources include Cf-252 which emits neutrons through spontaneous fission; and a number of sources which produces neutrons by the (α, n) reaction; e.g. AmBe, RaBe, PuBe, PuB, PuLi, and PuF. The interaction of the alpha emitting Am, Ra, and Pu with loosely bound neutrons in the Be, B, Li, and F provides the source of the free neutrons. Different materials with which the α particle reacts creates neutrons of different average energies.

Radionuclide sources typically have neutron yields in the range from 10^4 to 10^6 neutrons/sec per curie [32]. The activity of each of these sources is typically 2-5 Ci [47]. As discussed in Section 2.3, there are many unused and excess sources (Am and Pu) that were used as neutron generators being stored for disposal. If this type of sources were considered for use as a source of neutrons for a small scale transmutation device, one

would have to consider the total neutron source strength. Even thousands of these sources collected together will only increase the total source strength by about 3 orders of magnitude from the typical neutron source strength of a single source of no more than about 10^6 neutrons per second. In addition, having thousands of sources in a single location, because of the physical size, would probably prohibit the ability to develop a small scale transmutation device.

3.2 Accelerator Based Neutron Sources

Although research is being conducted with large scale accelerators, such as the Spallation Neutron Source (SNS) at Oak Ridge, small, compact, table-top accelerator based neutron generators have evolved into affordable products recently. These accelerator based neutron generators typically create deuterium ions accelerating them into deuterium or tritium targets, thereby producing the neutrons. Deuterium-deuterium (D-D) reactions will yield neutrons with average energies of about 2.5 MeV [2]. Deuterium-tritium (D-T) reactions will yield neutrons with average energies of about 14.1 MeV [2]. These accelerators are typically sealed tube neutron generators. The ion source, accelerator column, and target are enclosed in a vacuum tight enclosure.

The source strength from these accelerator based neutron generators are typically in the range from 10^8 to 10^{10} neutrons/sec. The D-D generators have roughly two orders of magnitude lower neutron yield than the D-T generators [16].

3.3 Radiofrequency (Rf) Driven Plasma Ion Sources

The Plasma and Ion Source Technology Group at the Lawrence Berkeley National Laboratory (LBNL) along with the University of California Berkeley has developed high- yield compact neutron generators. These generators utilize a 13.5 MHz

Rf induction discharge to produce a deuterium or deuterium-tritium plasma with high concentration of atomic ions. Subsequently, ion beams with high current density can be extracted from the plasma source. These generators with different configurations (such as cylindrical, spherical, or straight-tube designs) and sizes (several mm to 10's of cm in diameter and lengths), have been designed and tested at LBNL [3, 28].

The source strength from these devices can be as high as 10^{12} for D-D generators and 10^{14} for D-T generators [14]. Novel designs such as a coaxial cylinder, where target material surrounding the ion source rather than projecting ions at a target, results in higher neutron output. The ion source is a rod-shape so the neutron production can be increased by increasing the length of the source and target cylinders. In addition, the ion sources and target can be nested (having multiple layers of plasma and target) thereby generating an even higher neutron output [14].

3.4 Pyroelectric Crystal Fusion Sources

The University of California at Los Angeles (UCLA) has developed a tabletop method for producing nuclear fusion [53]. Unlike conventional fusion reactor theory, UCLA's method doesn't use magnetic or inertial confinement. Rather, it uses a pyroelectric crystal; which is a material that will produce a strong electric field when heated. The UCLA device contains a 3-cm-diamter lithium tantalate ($LiTaO_3$) crystal and an erbium deuteride (ErD_2) target in a low-pressure deuterium atmosphere. When the crystal is gently heated, an electric field that is concentrated at the tip of a tungsten needle (attached to the crystal) will ionize deuterium molecules and accelerate them towards the ErD_2 target where the D-D reactions occur. The source strength of this device is approximately 800 - 10^3 neutrons/sec. The researchers believe that by

enhancing the system and using tritiated targets, they may be able to achieve about 10^6 neutrons/sec [20, 53].

Researchers at the Rensselaer Polytechnic Institute (RPI) have developed a similar technology but use two opposing crystals in their device. This would, in effect, double the acceleration potential and does not require cryogenic cooling, unlike the UCLA device [33]. The RPI device uses $LiTaO_3$ crystals and a deuterium gas like the UCLA device, but a different material for the target, a deuterated polystyrene target. The neutron output from this device can be about 19 x 10^3 neutrons per heating cycle per nA current [54]. When comparing by using the UCLA parameters, then the neutron output would be about 4 x 10^3 neutrons /second. Such a device will have similar applications to the accelerator based sources discussed in Section 3.2. In addition to neutron generation, another advantage of this RPI design is that higher energy x-rays (up to 200 keV) can be generated because of the increased acceleration potential which exceeds the energies of the present commercially available pyroelectric x-ray products which could lead to medical imaging applications [54].

3.5 Sonofusion

Another relatively new development in neutron generation uses acoustic energy to create a cavitation bubble collapse (or vapor bubble implosion). If the test liquid and conditions are suitable, then the environment of the imploding bubble can experience thermonuclear conditions. Researchers at Purdue University use deuterated acetone (i.e., the hydrogen in the acetone is in the form of deuterium) as the source of deuterium in the system. A D-D reaction occurs as a result of the kinetic energy released when the bubble bursts. The original experiments were done at Oak Ridge National Laboratories (ORNL)

by the researcher who is now at Purdue University, Rusi Taleyarkhan. Using his experimental set-up, Taleyarkhan measured a production of about 10^5 neutrons/sec. The implications of sonofusion technology are not well understood at this time. However, it is agreed that thermonuclear fusion through sonofusion does occur and is quite repeatable. The research into this particular technology is still not yet mature. Nevertheless, this new technology, if feasible as an energy source, appears to be inherently safe and should be much more environmentally friendly than other existing fusion/fossil energy sources (e.g., there would be no significant decay heat after reactor shutdown and the tritium produced would be burned in the D-T reactions as fuel) [29].

Recent reports have questioned Taleyarkhan's credibility. There continues to be controversy on his "misconduct" more so than his "research findings, although, independent research groups are still trying to reproduce his results [48]. The output of Taleyarken's experimental setup would indicate applications similar to those of accelerator generated neutron sources discussed in section 3.2.

3.6 Chosen Neutron Source

Of the neutron sources discussed in Sections 3.1 through 3.5, the technology that appears most promising in terms of neutron source strength is the Rf-driven plasma ion sources developed at LBNL and UC Berkeley. These sources can be developed in a number of different configurations (dependent upon the application) and have much higher source strength than the other described sources. Therefore, for the purpose of this research, the neutron source for the small-scale transmutation device will be an Rf-driven plasma ion source. Because transmutation requires a large supply of neutrons, the source configuration used is the one which could provide the largest neutron source strength.

This could ultimately lead to the highest flux on the target. A conceptual design of the generic cylindrical neutron generator is shown in Figure 3.1.

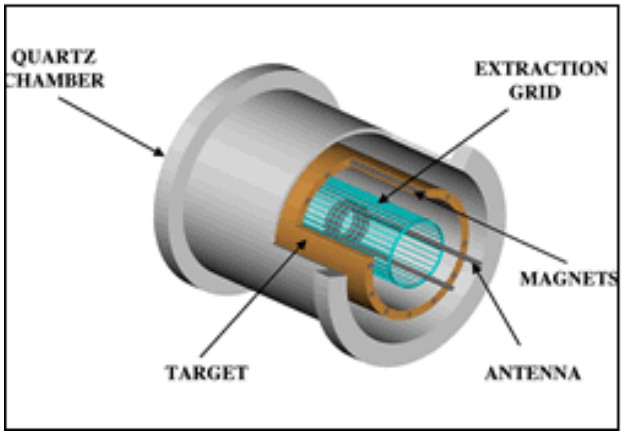

Figure 3.1 Compact Neutron Generator: Single Target Coaxial Design [14]

This neutron generator (which has been manufactured and tested at LBNL) has dimensions of 26 cm in diameter and 28 cm in length. These dimensions will be used in the analyses throughout this research. There are two types of these generators: one that operates as a D-D (deuterium-deuterium) neutron generator expected to generate about 1.2×10^{12} n/s with average energy of 2.5 MeV, and one that operates as a D-T (deuterium-tritium) neutron generator expected to generate about 3.5×10^{14} n/s with average energy of 14 MeV. For the purposes of this research, these source strengths will be modeled in the transmutation device.

However, the researchers at LBNL believe that a nested configuration of this coaxial design could generate neutrons with source strengths about an order of magnitude higher for both D-D and D-T generators [14]. This provides a promising indication for future technological advancements of these generators, whatever their application. These generators also have an advantage over the commercially available accelerator-based fusion sources; they have a much longer lifetime due to their self-loading target

design. The D or T atoms are ion implanted into the target material; thus, the target atoms are replenished by the operations of the generator [2]. These generators have been studied for many different applications from medical to industrial uses; i.e., Boron Neutron Capture Therapy (BNCT), neutron activation analysis (elemental analysis, explosives detection), neutron radiography (cargo and luggage screening), and even brachytherapy (cancer treatment where sources are applied in contact with tumors to administer a lethal dose of radiation to tumor cells) [2, 3, 7]. This research focuses on the feasibility of this compact neutron generator's for use in transmutation.

Chapter 4

Methodology of Computer Simulations

The general description of the overall methodology is to first use radiation transport calculations to determine the energy dependent neutron spectrum incident on the target radionuclide (or averaged over the target cell when dealing with the actinides). The spectrum is then applied in the activation code to calculate the transmutation products of the target radionuclide(s). The subsequent treatment and evaluation includes:

- Calculating transmutation efficiency (by evaluating effective half-lives)
- Evaluating amount and types of radionuclides produced from the irradiation of the target radionuclide(s)
- Calculating dose rates and radiotoxicities (both ingestion and inhalation) the product radionuclides over time
- Evaluating the decay characteristics (activity as a function of time) of the product radionuclides

4.1 Analytical Tools

To develop a conceptual design of a transmutation device, radiation transport calculations are required for simulation of source neutron behavior in the system. The general-purpose Monte Carlo N-Particle (MCNP) code, developed and maintained by LANL [55], is an internationally recognized code for analyzing the transport of neutrons, photons, and electrons using Monte Carlo simulation techniques. The code must be able to simulate the transport of source neutrons inside materials, evaluate their interaction

with the materials, and generate and transport secondary particles. The particular version of MCNP used in this research was MCNPX version 2.5f [30]. MCNPX (Monte Carlo N-Particle eXtended) is a version of the MCNP code having higher particle energy capabilities (ie, greater than 20 MeV for neutrons) using tabular data that exceeded energies of those in MCNP and additional mathematical physics models where tabular data is not available [30]. For example, one of the first versions of MCNPX was comprised of MCNP and the "intermediate interaction physics models" of the LAHET (Los Alamos High Energy Transport) code [56] and the "high energy physics models" of the FLUKA (a high energy radiation transport code widely used by the high energy accelerator community) code [57] for radiation transport calculations.

Transmutation of nuclides calculations were performed using the European Activation System (EASY). The version used in this research was EASY-2003 [31]. EASY is a complete code and data package for the calculation of the activation of materials in neutron fields. This code has been in development since the late 80's specifically for fusion technology applications; but can be applied to other applications involving neutrons with energies < 20 MeV. The EASY package includes a widely used and validated (in Europe) inventory code FISPACT [35]. It has been adapted by the International Thermonuclear Experimental Reactor (ITER) as the reference activation code for that project. The package includes the EAF (European Activation Files) with interaction cross sections and radionuclide decay data. ITER is a joint international (including the USA) research and development project that aims to demonstrate the scientific and technical feasibility of fusion power. The core task of the inventory code, FISPACT, is to solve the set of differential equations which determines the inventory and

quantities of different radionuclides present in a given material after irradiation in a neutron field. The governing set of differential equations is:

$$\frac{dN_i}{dt} = -N_i(\lambda_i + \sigma_i\phi) + \sum_{j \neq i} N_j(\lambda_{ij} + \sigma_{ij}\phi) + S_i$$

$$S_i = \sum_k N_k \sigma_k^f \phi Y_{ik} \qquad (4.1)$$

Where;

N_i is the amount of nuclide i at time t

λ_i is the decay constant of nuclide i (s^{-1})

λ_{ij} is the decay constant of nuclide j producing i (s^{-1})

σ_i is the total cross section for reactions on i (cm^2)

σ_{ij} is the reaction cross section for reactions on j producing i (cm^2)

σ_{fk} is the fission cross section for reactions on actinide k (cm^2)

ϕ is the neutron flux (n cm^{-2} s^{-1})

S_i is the source of nuclide i from fission

Y_{ik} is the yield of nuclide i from the fission of nuclide k

FISPACT uses a numerical method to solve the governing equations in a manner similar to the Euler method [35].

4.2 Conceptual Design of a Transmutation Device

The transmutation device that will house the neutron generator will have a spherical geometry and be made of a reflective material to maximize the neutron flux within the device and incident on a target. The target radionuclides to be transmuted will be modeled as being electroplated onto aluminum planchets and placed inside the transmuter.

The following factors will affect the neutron on-target flux:

- The reflective material of which the sphere is made
- The thickness of the sphere
- The size of the sphere (inner diameter)
- and the neutron source (D-D vs D-T)

The radiation transport code MCNPX was used to model the transmutation device in order to investigate the impact of the above parameters on maximizing the neutron flux inside the device. Appropriate tallies used were a point detector tally (F5) to determine the total neutron flux within the transmutation device, a mesh tally to investigate the neutron flux profile within the transmutation device, a surface tally (F2) to determine the energy dependent neutron spectrum incident on a target surface, a cell flux tally (F4) to determine the energy dependent neutron flux within a target cell, and an energy deposition tally (F6) to calculate heat load.

4.3 Transmutation/Activation Calculations of Target Radionuclide

Once the on-target energy dependent neutron flux was determined from MCNPX, it was used in FISPACT to determine the fluence and time that was required to diminish the target radionuclide from a preselected starting value to a ending amount. The starting and ending amounts for each radionuclide studied will be presented in the discussions of results in Chapter 7. Typically the starting amount was one curie (37 GBq) and the ending amount was based on the amount of that radionuclide that is required to be labeled by the Nuclear Regulatory Commission (NRC) in its regulations [36]. The original energy dependent flux was based on the present capability of the compact neutron generators chosen for this transmutation device. These will be referred to hereafter as the "Base Cases".

The flux from the base cases was then increased by an order of magnitude for each evaluation and the transmutation calculations repeated until the time required for eliminating the radionuclide was within a reasonable period of time. For the purposes of this research, a reasonable period of time was considered to be less than 100 years. The flux that was required for transmutation within this reasonable period of time was considered the "High Flux Cases" correlated to each of the "Base Cases"; i.e., each base case will have a high flux case associated with that base case. From this evaluation, a projection of technology need could be concluded. In other words, what increase in flux production would be required for the transmutation device to be considered practical; i.e. deplete a radionuclide to its target level with the 100 year time frame.

Transmutation calculations are performed in the EASY 2003 code package by FISPACT using the European Activation data files (EAF) which is a composite of cross section data for neutron induced reactions for energies ranging from 10^{-5} eV to 20 MeV [37]. All reactions are included for nuclides up to and including Fermium (Z=100). This leads to a total of 12, 617 reaction channels that contain data. This nuclear data base was produced by experimental data and validated world-wide by investigators from many different organizations. Origins of the data are delineated in the reference [37].

4.4 Activation Products Radiation Protection Issues

For each of the base cases, and the iterative increases in fluxes up to and including the high flux cases, FISPACT was used to determine the twenty most prevalent radionuclides generated (or more if any additional radionuclides had activities greater than 1% of the total activity); the total activity of activation products generated; the gamma dose rate from the activation products (using a semi-infinite plane source model of the resulting radionuclides); the ingestion and inhalation radiotoxicities of the activation products; and the time dependent decay of the activation products. From these evaluations, the better transmutation strategy for a specific radionuclide was determined based on what was produced (i.e., a higher energy neutron spectrum may produce activation products that are even longer in half-life, more radiotoxic, or have higher heat evolution than the target radionuclide.)

The dose rate calculations in this study used validated decay data from reference [38]. This reference contains data for 1917 nuclides including decay modes, decay energies, half-life, and gamma spectrum, if available. The source of the decay data is the

Joint Evaluated File Version 2.2 (JEF-2.2) nuclear data library, which are the standard nuclear data files for Europe [58]. Any gaps in the nuclear data in JEF-2.2 were filled with data from other nuclear data bases such as the National Nuclear Data Center (NNDC) [59].

Radiotoxicity calculations are based on dose conversion factors found in reference [39]. These dose conversion factors are called committed effective doses per unit intake. They are used to convert the activity (Bq) of an ingested or inhaled radionuclide into the dose (Sv) received by the average person over a 50 year period and has the units $SvBq^{-1}$. Much of these data come from reliable sources such as the International Commission on Radiological Protection recommendations; specifically, ICRP Report Publication 68 [60] and ICRP Publication 72 [61]. Gaps in the data in the ICRP Reports were either filled using data from the National Radiological Protection Board (NRPB) or was calculated from the NRPB methodology [62].

Finally, the time-dependent decay of the activation products also used the decay data from reference [38] which, as mentioned before, includes half-life information for the radionuclides.

4.5 Shielding Requirements for the Operation of the Transmutation Device

Following the conceptual design of the transmutation device and evaluation of the established base cases, shielding evaluations were done to determine the amount of shielding required if the device were to be operated as a self-shielded device. This

evaluation will provide a basis for radiation protection determinations during the operation of the device for workers and members of the public. The calculations of photon and neutron flux and doses are evaluated at 2 locations outside the transmutation device; at 30 cm (or one foot), and at one meter from the outer shell of the transmutation device. The calculation at 30 cm will determine the dose rate and posting requirements such as "Radiation, High Radiation, or Very High Radiation Areas" as required by regulations [36]. The one meter evaluation would be useful for facility shielding design. As shielding material was added around the transmutation device, the dose points are at one foot and one meter from the outside of the shield. The reason shielding analysis is done utilizing local shielding as opposed to facility shielding is to determine whether the device can be considered a "self-shielded" device.

MCNPX was used to determine the photon and neutron flux at these two distances from the device. Then flux to dose conversion factors for photons and neutrons were used to calculate a dose rate in mrem/hour which includes both the photon and neutron doses. The photon dose conversion factors are taken from reference [40]. The neutron dose conversion factors are taken from reference [41]. The conversion factors from reference [41] have also been codified in the Nuclear Regulatory Commission's radiation protection regulations [36].

It was necessary to use variance reduction techniques in the modeling for shielding due to the fact that so few particles or photons were actually getting through the shields (which is the purpose for the shield). Two variance reduction techniques were employed; source direction biasing [63], and geometry splitting [63]. The particular technique for source direction biasing used was restricting source emissions to a nested

cone about the bias direction which was towards the tally region. This technique eliminates the computation of particles or photons in other directions that would not contribute to the tally; thereby, shortening the computation time. The particular technique used for geometry splitting was using composite cells to model the shield and changing the importances assigned to each cell. The cells closer to the tally region have higher importances than those farther from the tally region. As particles move from cell to cell, the particle weights are adjusted according to the ratio of importances. This is done to keep the tally unbiased while providing a reliable value for the tally [30, 63].

4.6 Heat Load Calculations

The heat load to the transmutation device results from two sources. One source is the energy deposition by the neutrons, photons, and all other secondary or even tertiary particles impinging upon the transmutation device. This source was modeled by MCNPX using an F6 tally, an energy deposition tally. This tally provided results in units of MeV/sec, which was then converted to units kW. A second source of heat is the energy deposition by the decay of the activation products produced. This source was modeled by FISPACT which calculates the power (kW) produced by the total activity of the activation products.

Chapter 5

Conceptual Design of Transmutation Device

5.1 Evaluate Reflective Materials for Transmutation Device

As stated in Section 4.2, the transmutation device that will house the neutron generator will have a spherical geometry and be made of a reflective material to maximize the neutron flux incident on a target. The first step in the conceptual design was to evaluate the effect of the materials selected on the total neutron flux within the transmutation device. Common reflective materials used in the nuclear industry (reactors and accelerators) were evaluated individually and in various combinations; lead, beryllium, and carbon [34, 64]. A case was also run using depleted Uranium to ascertain its reflective properties. A thickness of one meter of material was used to provide a consistent basis in comparing effects of different material. Therefore, when combinations were used, the total thickness was kept at one meter. A large enough thickness was chosen just to ensure that, for the single materials, maximum reflection would be achieved. The results are plotted in Figure 5.1 as flux ratios normalized to a tally location when no reflector is present.

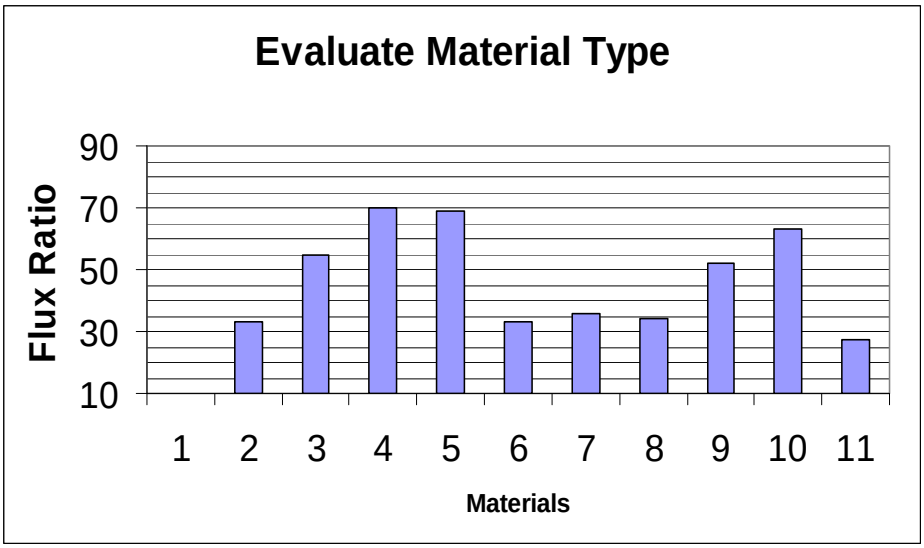

Figure 5.1 Total Neutron Flux Ratio as a Function of Reflector Material

The results show that beryllium yields the highest flux ratio and lead is the next best single material. For this evaluation, the D-T source was used, and the diameter and thickness of the sphere were held constant. The beryllium as a good reflective material is consistent with the literature such as reference [7] which also chooses a compound of beryllium as the preferred reflector material.

5.2 Evaluate D-T vs D-D Neutron Energy Spectra as Function of Reflector Material

The three principle reflector materials (Be, Pb, and C) were then evaluated using a D-T source and compared to a D-D source. The scattering cross section of the different materials varies with energy so this evaluation was done to compare the fluxes produced when using the D-D (2.5 MeV) neutrons as the source versus the D-T neutrons (14 MeV). Figure 5.2 shows the comparison of D-T and D-D fluxes as a function of the three potential reflector materials.

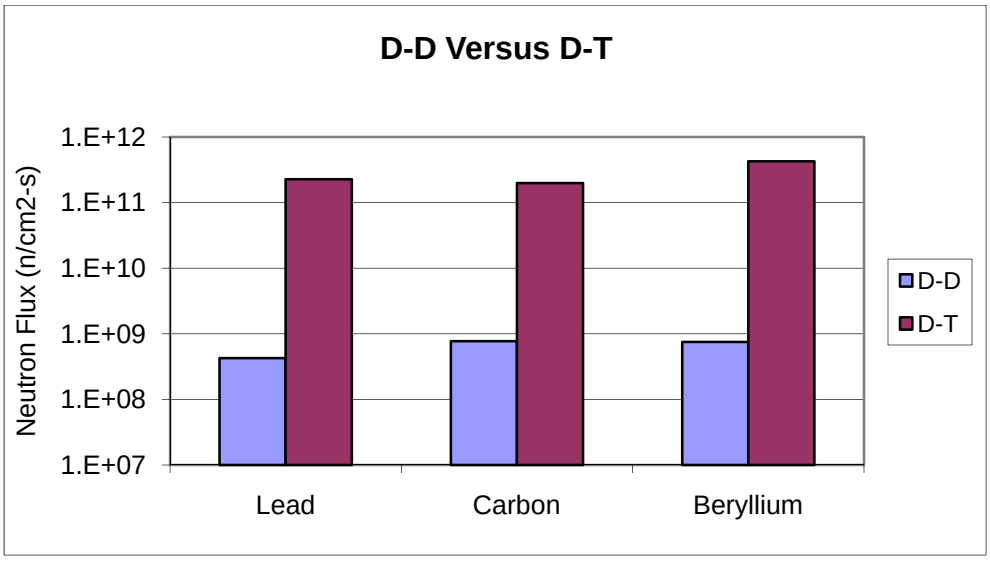

Figure 5.2 Neutron Fluxes inside Sphere as Function of Source and Reflector Material

Results show that for the D-T neutrons, the flux is highest using Be, then Pb, then C. This is consistent with the flux ratios shown in Figure 5.1. For the D-D neutrons which are of lower energies, carbon yields the highest flux, followed by beryllium and then lead. The reason for the difference between D-T and D-D is that both Pb and Be have significant (n, 2n) reaction cross-sections in the higher energy ranges so that when the D-T reaction is the source of the neutrons, neutrons are multiplied in the reflector material. This effect does not occur with the D-D neutrons. Carbon does not have (n, 2n) cross-sections in these energy ranges so does not generate neutron multiplication. This effect is confirmed in the following graphical representation of cross section data. Figure 5.3 shows the neutron cross section data for Be. The blue curve is the (n, total) cross section and the green curve is the (n, 2n) reaction curve. The (n, 2n) cross section is negligibly small below about 3 MeV and then rises to a peak between 4 and 20 MeV.

Therefore the D-D neutrons (which are 2.5 MeV) will produce insignificant (n, 2n) reactions.

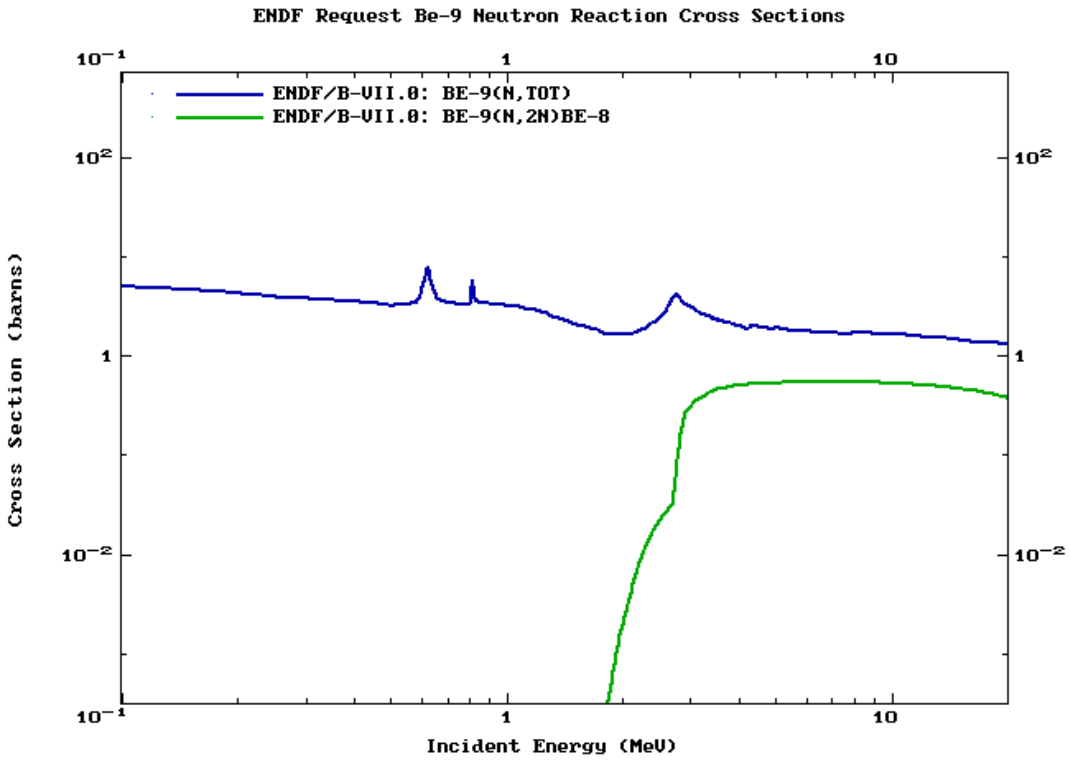

Figure 5.3 Total and (n, 2n) Neutron Cross Sections in Be [42]

The same phenomena exist for Pb as shown in Figure 5.4. The (n, 2n) reaction doesn't exist until the incident neutron energies exceed about 7 MeV. Therefore the D-D neutrons will not produce significant numbers of (n, 2n) reactions. Again, there are no (n,2n) cross-sections for carbon at these energy ranges.

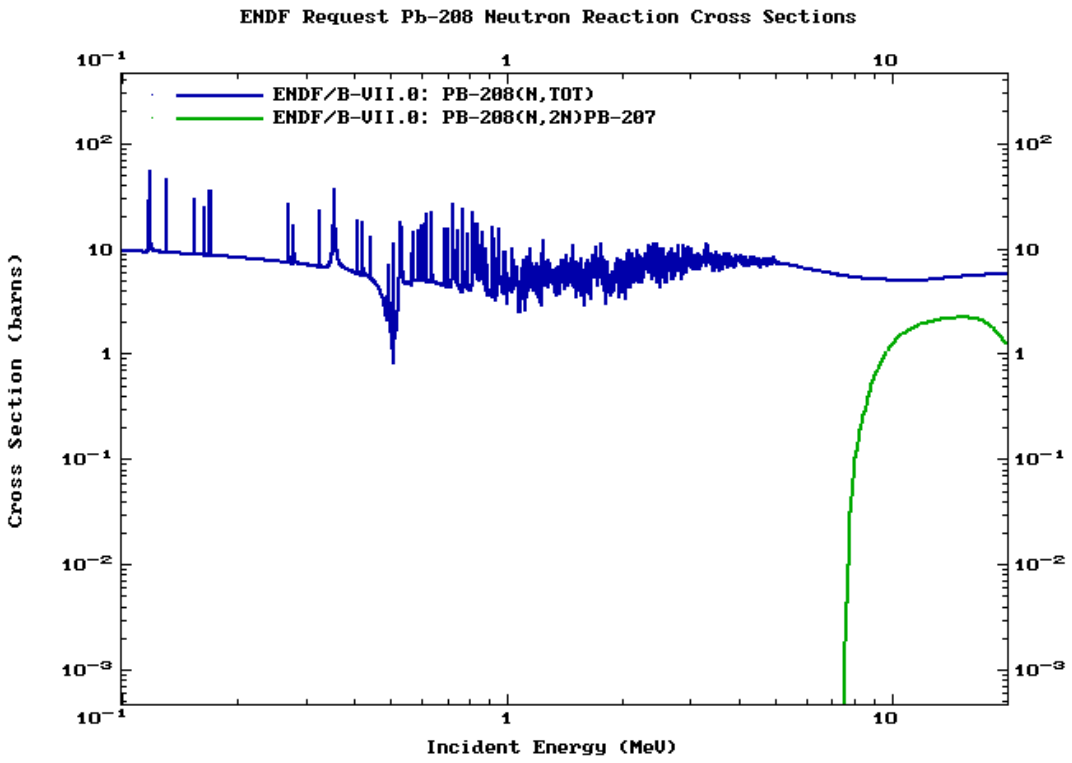

Figure 5.4: Total and (n, 2n) Neutron Cross Sections in Pb [42]

To evaluate the neutron energy spectra of the resulting fluxes using the different reflecting materials, an energy structure had to be modeled into the transport calculations. A 100-group energy spectrum was chosen to be consistent with an energy group option available in the FISPACT software; i.e., the GAM-II energy structure. Any other energy structure could have been used to model the transport; however, the results would have to be compiled to match the FISPACT cross section energy structure. The neutron flux distribution as a function of energy for the three highest reflective cases is shown in Figure 5.5.

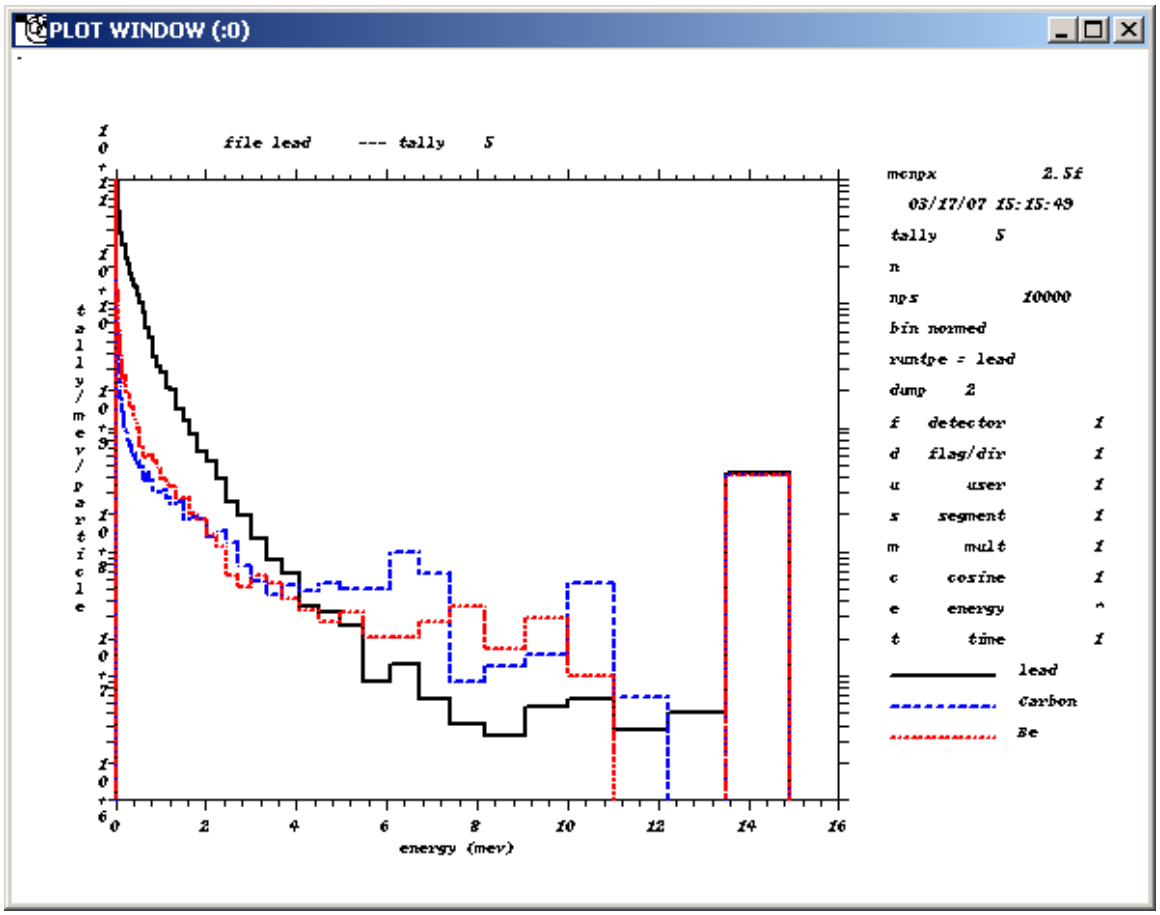

Figure 5.5 Neutron Energy Flux Spectra Within Select Reflectors

Figure 5.5 is a tally plot from MCNPX analyses and shows the differences in the resulting energy spectra inside the transmutation device due to the reflector material. There are more lower energy neutrons in a Pb reflected sphere while there are more higher energy neutrons in C and Be reflected spheres. Note the existence of the large peak of neutrons at the 14 MeV range resulting from neutrons incident from the source and inelastic scattered neutrons with minimal degradation of energy. These tally plots were evaluated at a location within the device where the target would be placed for transmutation.

The understanding of the neutron energy distribution impinging on the target is important because the reaction cross-sections of each nuclide differ with energy. Figure 5.6 shows the neutron capture cross-section spectra for both Tc-99 and I-129. Ideally, to get maximum transmutation efficiency, the target nuclide would be impacted with neutrons whose energies are associated with the highest cross sections for the desired reaction; i.e. neutron capture or absorption. In the case of these long lived fission products, the capture resonances occur below about 2 keV. The concept of using energies to match the capture resonances to get the highest efficiency possible is called "adiabatic resonance crossing" [18]

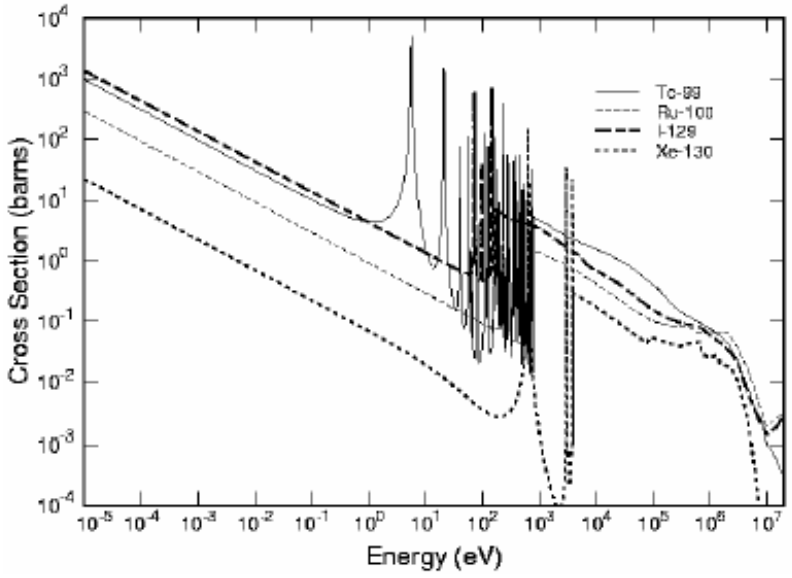

Figure 5.6 Neutron Capture Cross Sections of Tc-99 and I-129 (ENDF-B/VI) [8]

Figure 5.6 includes cross-sections for Ru-100 and Xe-130 which are the decay products (short half-lives) of Tc-100 and I-130 which result from the Tc-99 and I-129

neutron capture reaction. Tc-100 and I-130 undergo neutron capture reactions to become other stable nuclides.

5.3 Effect of Material Thickness

In an effort to maximize the neutron flux within the transmutation device, the effect of material thickness was evaluated. The D-T neutron source was used along with the two best reflecting/multiplying materials, i.e., Be and Pb. Starting with a two meter radius sphere with a wall thickness of 5 cm, MCNPX simulations were performed while increasing the thickness in increments of 5 cm. The effect on the neutron multiplication factor is shown in Figure 5.7.

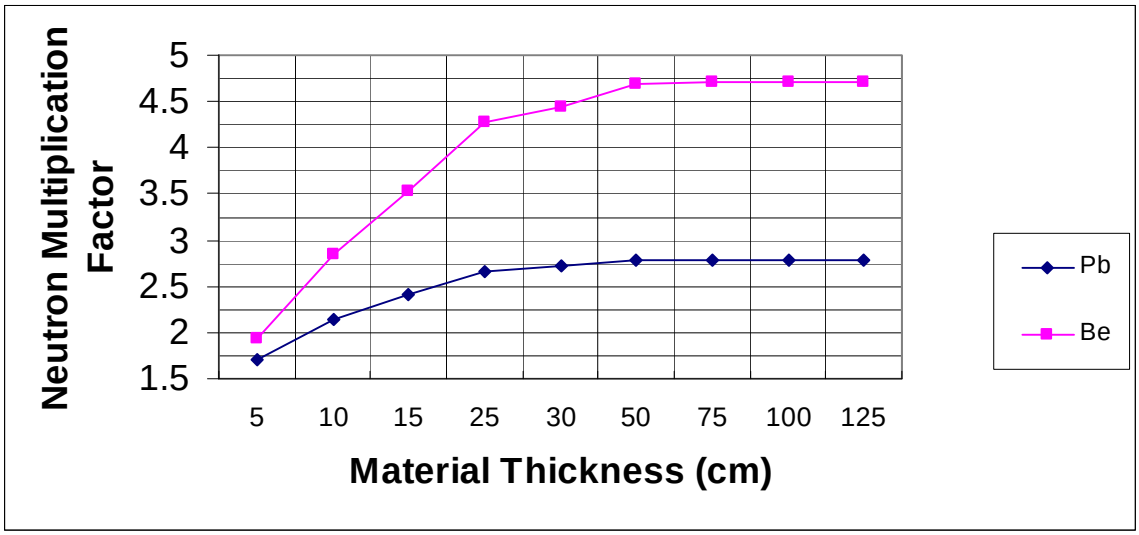

Figure 5.7 Neutron Multiplication Factor as a function of Material Thickness

These results demonstrate that a Be shell produces a higher neutron multiplication factor. However, at best, the Be neutron multiplication factor is a factor of about 1.7 higher than the Pb. For both materials, there is a thickness for which the neutron multiplication effect diminishes. Selecting this thickness would minimize the amount of

material necessary in the transmutation device while providing maximum neutron multiplication. The optimum thickness is a compromise between the thickness of material needed and the neutron multiplication achieved; i.e. about 25 centimeters.

5.4 Effect of Sphere Size

The effect of sphere size on the neutron flux inside the transmutation device was evaluated. The neutron flux is calculated using a sphere with inner diameters of one, two and four meters. The thickness of the sphere and the material was held constant. The results of these calculations are shown in Figure 5.8.

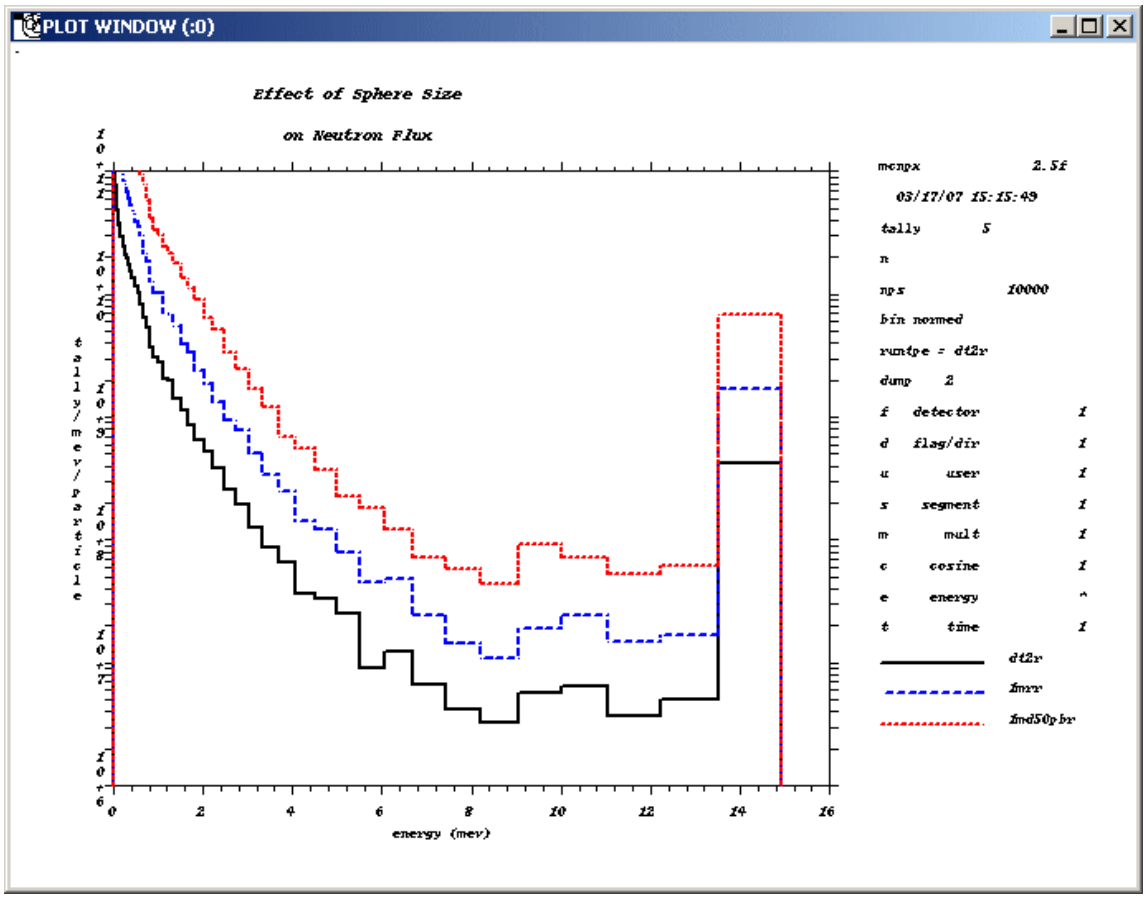

Legend: Black curve: 4m ID, Blue curve: 2m ID, Red curve: 1m ID

Figure 5.8 Neutron Flux as a Function of Sphere Inner Diameter

The results show that the neutron flux inside the transmutation device is approximately inversely proportional to the inner diameter. The one meter diameter sphere has as much as an order of magnitude higher flux over a significant portion of the energy spectrum as compared with the four meter diameter sphere. As expected, the energy distribution of the neutron flux inside the transmutation device is very consistent among the sizes because the material and thickness were constant. The only difference was the magnitude of the neutron flux.

5.5 Neutron Flux Distribution Inside the Transmutation Device

The variability of the flux was evaluated inside the spherical transmutation device. Using MCNPX, a mesh tally was used to simulate the flux using the model geometry shown in Figure 5.9.1. The model represents a lead spherical reflector shell with a neutron source located off center of the x-axis. The cylindrical neutron source is represented in this figure by a cylindrical shell seen as a rectangle where the top and bottom lines are the cylindrical walls of the source. The mesh tally of a cross section of the inside sphere (transmutation chamber) is shown in Figure 5.9.2. The mesh tally results show that the neutron flux is fairly uniform, within a factor of three, throughout the chamber. The flux is the highest directly adjacent to the source and is very uniform on hemisphere opposite the source which will be where the area that the target is mounted.

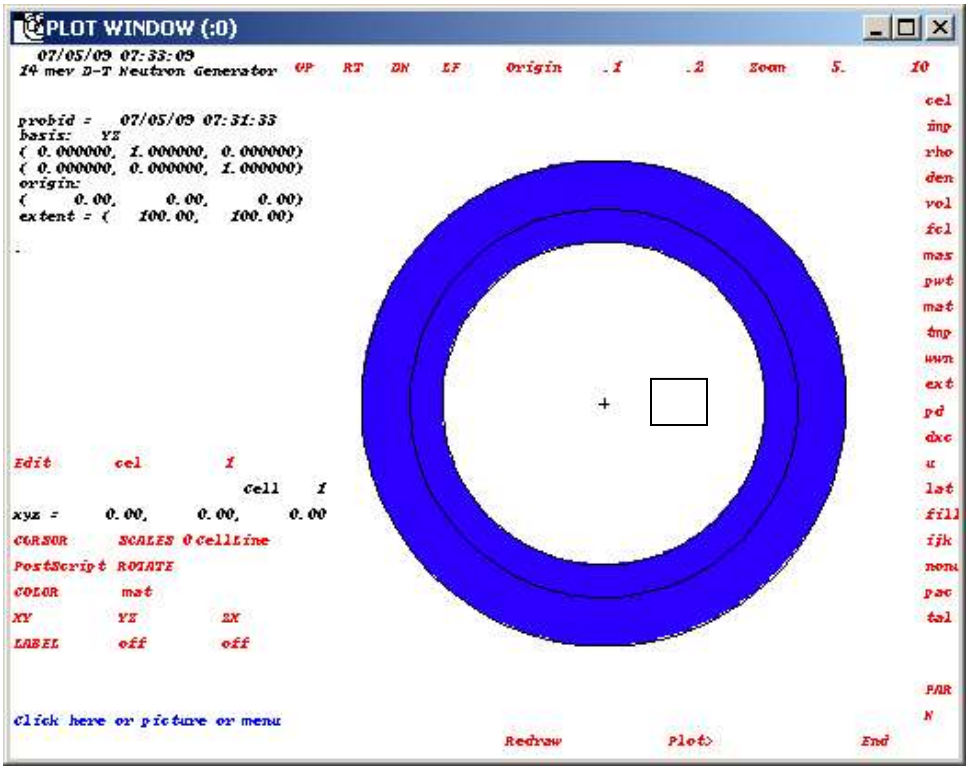

Figure 5.9.1 MCNPX Model Geometry for Mesh Tally Evaluation Inside Transmutation Device

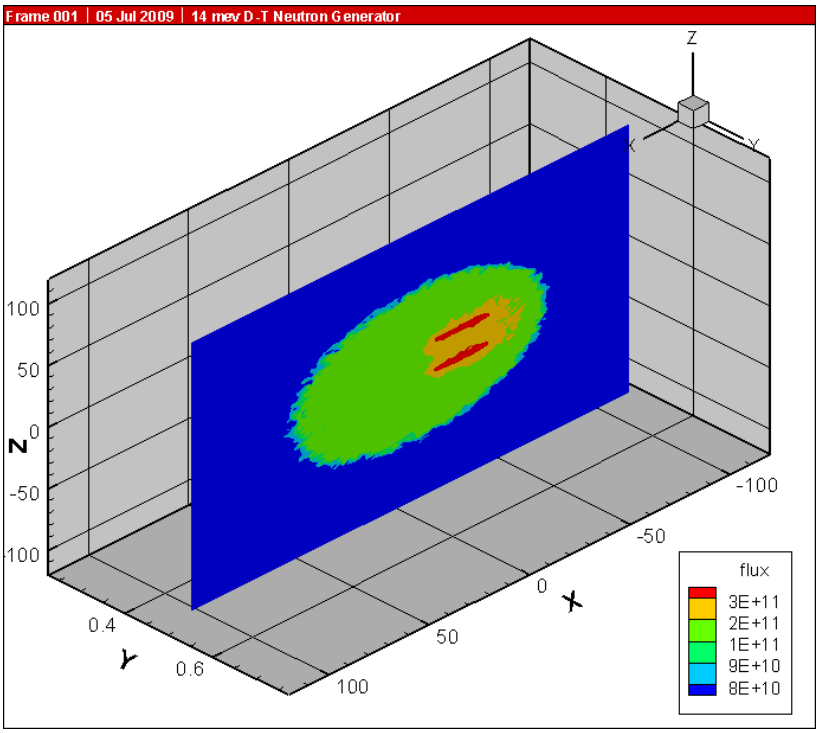

Figure 5.9 Mesh Tally Results for the Neutron Flux inside the Transmutation Device

The implication of this result is that target location is not critical within the chamber with respect to total neutron flux; however, the energy spectrum is slightly different in that locations closer to the source will have more primary neutrons as opposed to locations farther from the source which will have more scattered neutrons. This is evidenced in the output of the radiation transport calculations. Therefore, modeling the neutron flux energy spectrum at the target site is important.

5.6 Effect of Target Size on Neutron Energy Spectra

With a fixed target location, the effect of the target diameter on the neutron energy spectrum was evaluated. Aluminum target planchet diameters of 5, 6, 7.5, 10 and 15 cm were evaluated with a fixed thickness of 0.2 cm. The results show that a larger target mount introduces more structural material inside the sphere and, therefore, moderates some of the neutrons. Even though the total flux on the target changes insignificantly, the resulting neutron energy spectrum using the larger diameter planchets has a greater percentage of lower energy neutrons – a condition which is more favorable for neutron capture reactions (specifically (n, γ) reactions). Figure 5.10 shows only the lower portion of the energy spectra (< 0.01 MeV) and demonstrates the moderating effect when using the larger target and the resulting lower energy spectrum. The upper part of the spectra shows target size independence for the higher energies. The increase in the number of lower energy neutrons is important for the reasons mentioned in Section 5.2. The larger planchet is also important in that a larger surface area is available for the radionuclide to be mounted. This is important to maximize reactions for radionuclides

where the capture reaction cross sections are in the low energy range because it minimizes self shielding effects.

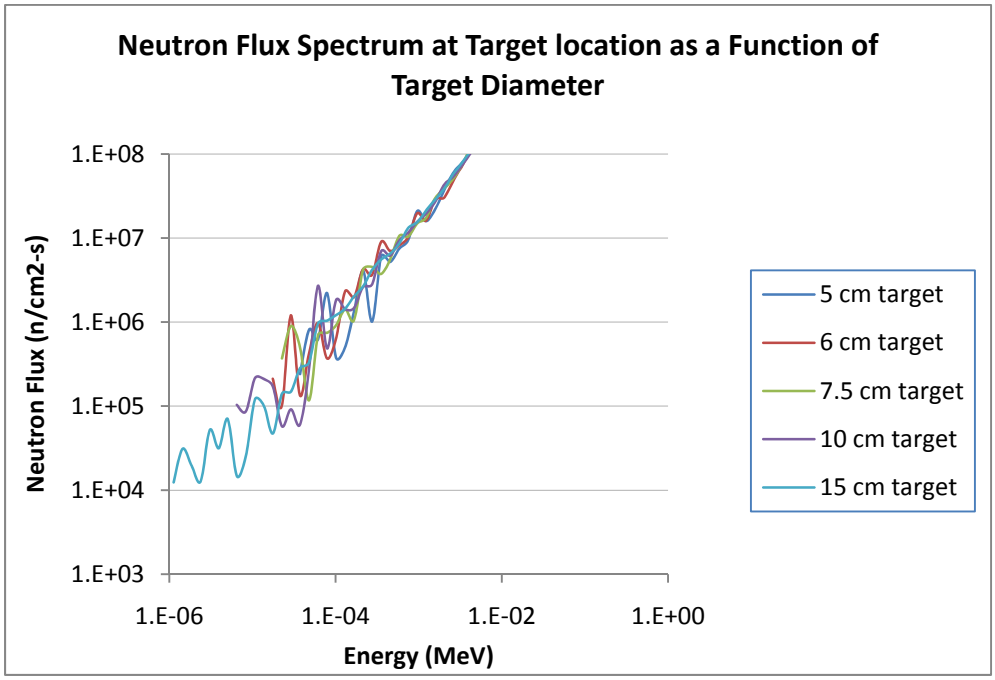

Figure 5.10 Neutron Flux Energy Spectra at Target Location for Different Target Diameters

5.7 Moderating the Transmutation Energy Spectrum

In order to maximize the transmutation of radionuclides which have high reaction cross sections in the lower energy ranges, a moderating material was added to the conceptual design of the sphere and its effect evaluated. An initial evaluation was performed using a layer of the moderating material inside the spherical transmutation device. Reference [17] indicated that Teflon® is a good moderating material; therefore, a 5 cm layer of Teflon® was added to the inside of the sphere. The moderating effect on the neutron flux energy spectrum is shown in Figure 5.11 and demonstrate that there is a

significant increase in low energy neutrons when the Teflon® moderator is added to the inside of the transmutation device.

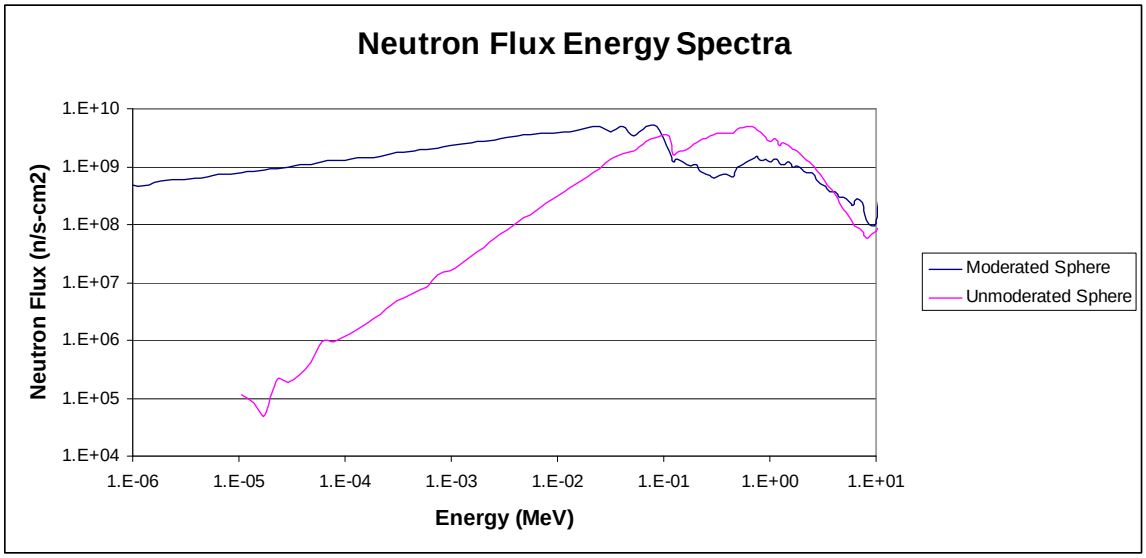

Figure 5.11 Neutron Flux Energy Spectrum Inside a Teflon Moderated versus an Un-treated Sphere

In Figure 5.11, the blue line is the neutron energy spectrum for the moderated sphere, as compared to the pink curve which is the energy spectrum for the unmoderated sphere, using the D-T generator in each case. The moderated sphere produces a neutron spectrum that is more beneficial for the (n, γ) reactions for the transmutation of the long-lived fission products as shown in Figure 5.6.

Based on this preliminary result, more moderating materials were evaluated in an effort to maximize the flux. A review of the literature [17, 18] indicated that teflon, calcium fluoride, aluminum oxide, and nickel are all good moderating materials. Water is a "classic" moderating material and lead was the reflector material used in the previous

sections. The transmutation device was then modeled with composite spherical shells so that material iterations could be performed so as to find the highest on-target neutron flux. The MCNPX model was run utilizing a three shell composite sphere and the shell materials were varied in combinations of moderator and reflector material. Figure 5.12 shows the neutron energy spectra of the different cases evaluated.

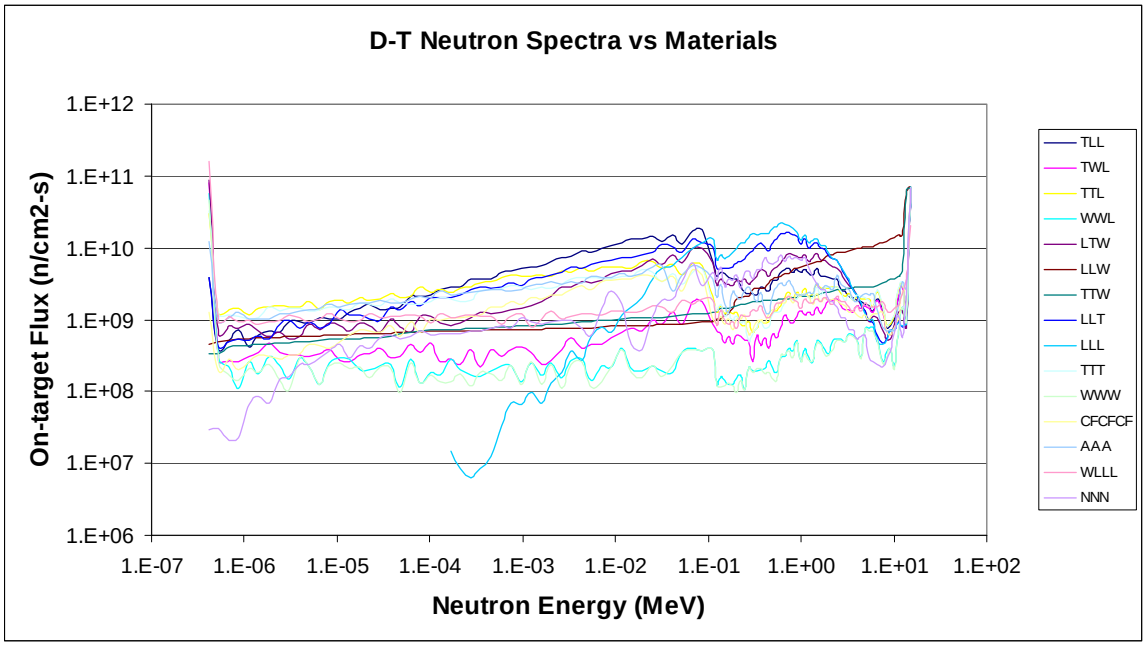

Legend: T-teflon, W-water, L-lead, CF- calcium flouride, A-aluminum oxide, N-nickel

Figure 5.12 D-T Neutron Spectra vs On-Target Flux for Selected Materials

A review of the results show that although the spectra differed, there was not an overall increase in the on-target flux by a factor greater than about one order of magnitude. The reference unmoderated D-T spectrum (the blue curve that did not extend lower than about 1E-4 MeV, labeled LLL) was plotted here as well to show that its spectra did not beneficially yield a significant increase in lower energy neutrons. Focusing on the energy region of interest, i.e., the (n, γ) resonances for Tc-99 and I-129

(between 1E-6 and 1E-2 MeV as shown in Figure 5.6), certain configurations appear to have about one order of magnitude advantage over other configurations.

The properties of the reflecting and moderating materials used in the MCPNX models are shown in Table 5.1.

Table 5.1: Properties of Moderating/ Reflecting Material

Material	Chemical formula	Density (g/cm)
Water	H_2O	1.0
Lead	Pb (nat)	11.35
Teflon	C_2F_4	2.2
Calcium Flouride	CaF_2	3.18
Aluminum Oxide	Al_2O_3	3.97
Nickel	Ni (nat)	8.9
Polyethylene	C_2H_4	0.93

The same set of analyses was performed on the D-D neutron generator in a moderated sphere (Figure 5.13).

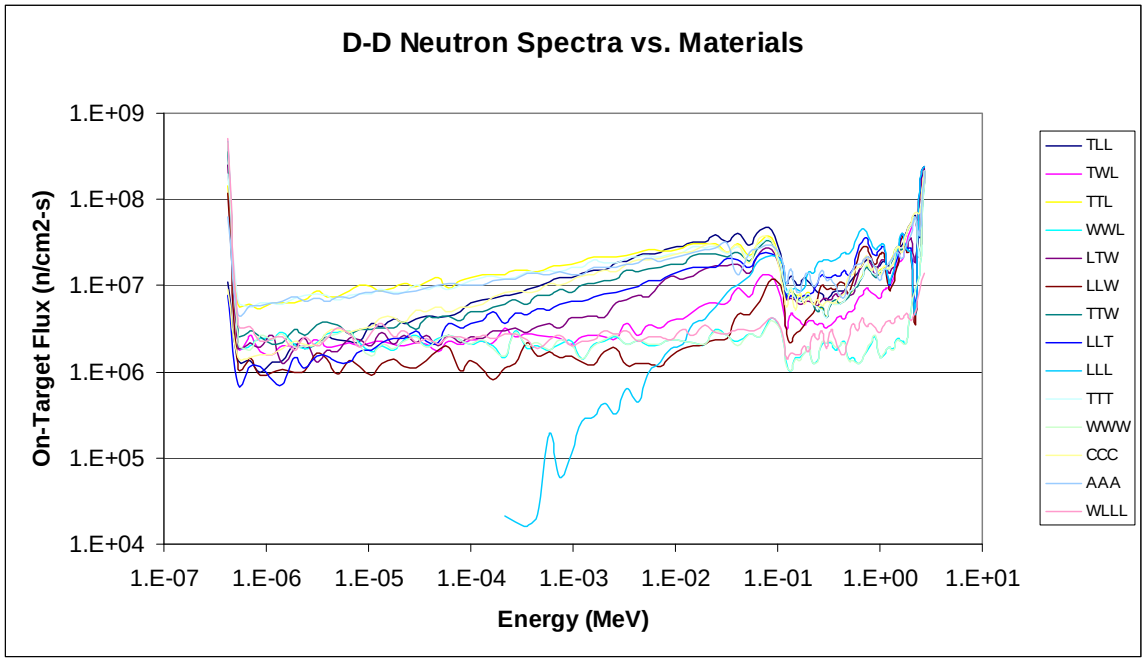

Legend: T-teflon, W-water, L-lead, CF- calcium flouride, A-aluminum oxide, N-nickel

Figure 5.13 D-D Neutron Spectra vs On-Target Flux for Selected Materials

As with the case of the D-T generator there was not a "magic" configuration that gave a huge advantage in total neutron flux. Note: the LLL labeled curve is the unmoderated D-D curve which showed no neutrons with energies below about $3x10^{-4}$ MeV; emphasizing the production of low energy neutrons in the moderated configurations. Ultimately, Teflon® was the chosen material for the moderating shell inside the sphere because it was the material that best met two important criteria: more lower energy neutrons and higher total flux.

5.8 Effect of Sphere Size on Moderated Spectrum

An investigation of the effect of overall sphere size on the flux using the moderating shell within the sphere was conducted. The D-T generator was modeled using the case of a 50 cm inner radius sphere and a smaller sphere of 20 cm inner radius. The minimum size of the sphere is limited by its ability to house the D-T or D-D neutron source. Figure 5.14 shows the results of the on-target neutron flux for both spheres for the D-T and the D-D generators. The D-T devices produced a higher neutron flux than the D-D device because the total source strength (n/s) of the device is about three orders of magnitude higher. The difference due to the size of the sphere is much less prominent. For most of the energy spectrum, the difference is less than a factor of two to five.

This evaluation was performed to determine if it is possible to reduce the size of the transmutation device such that increases of at least one to two orders of magnitude could be realized while maximizing the lower energy spectra. It was determined that the smaller sphere did not increase the on-target flux by a significant amount; however, there

are practical benefits of a smaller sphere such as weight and amount of material used for the sphere.

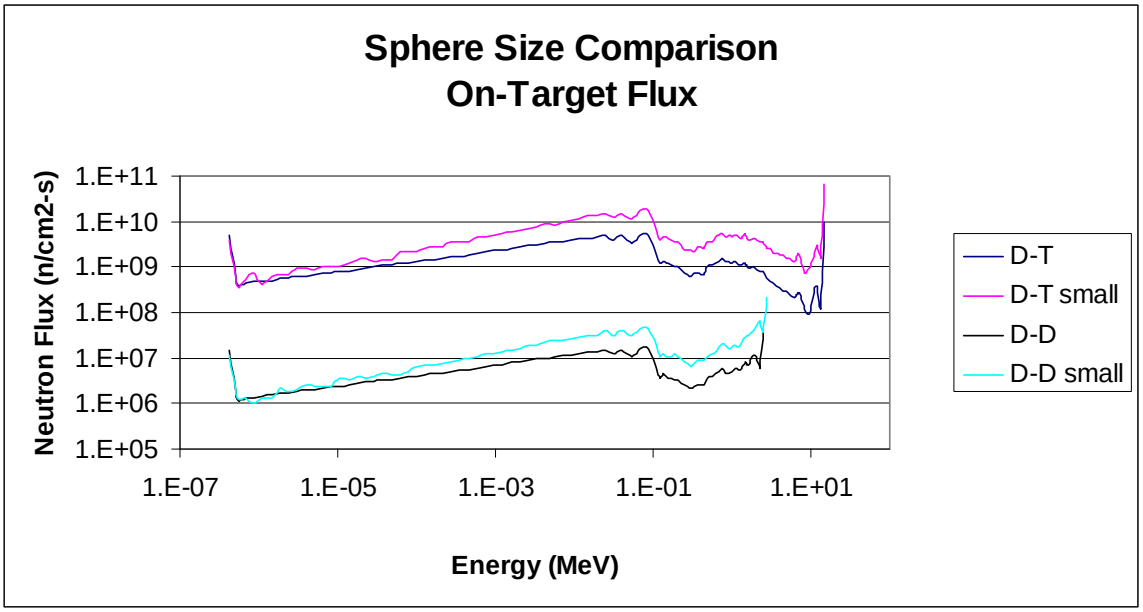

Figure 5.14: Sphere Size flux Comparison for Teflon Shell Moderated Spheres

5.9 Effect of Moderating the Target

The effect of moderating the target in addition to moderating the sphere was also evaluated. Again, the goal of this phase of the investigation was to increase the flux of lower energy neutrons in an effort to maximize the activation of the target nuclides. For the purpose of moderating the target, polyethylene material was placed both in front of and behind the target planchet. Comparing the moderated target configurations to the unmoderated target configurations, the moderated target configurations yielded a fairly constant flux across the low energy spectrum. By way of contrast, the flux decreased at the lower energies when using the unmoderated target configuration. Also the fluxes were slightly higher at the very low energy range with the moderated target. However,

the total neutron flux on-target did not differ much. Therefore, depending on the energy range of the desired reactions, it may or may not be beneficial to moderate the target in addition to moderating the sphere. Practical considerations include the fact that moderating a target would take up space inside the transmutation device

5.10 Maximizing Thermal Energy Spectrum in the Transmutation Device

To determine the maximum amount of thermal neutrons that could be generated on-target, the spherical transmutation device was modeled as filled with heavy water, D_2O. The MCNPX simulations included the thermal scattering cross sections associated with heavy water. Figure 5.15 shows the results of these simulations. The thermalized sphere with a D-T generator in moderated (with teflon shell) and unmoderated configurations have the same energy spectrum. This implies that the maximum moderation is achieved with the heavy water and that there is little effect of the Teflon shell. As expected, the energy spectrum using the thermalized sphere and the D-D generator was 2-3 orders of magnitude lower than for the similarly moderated the D-T case.

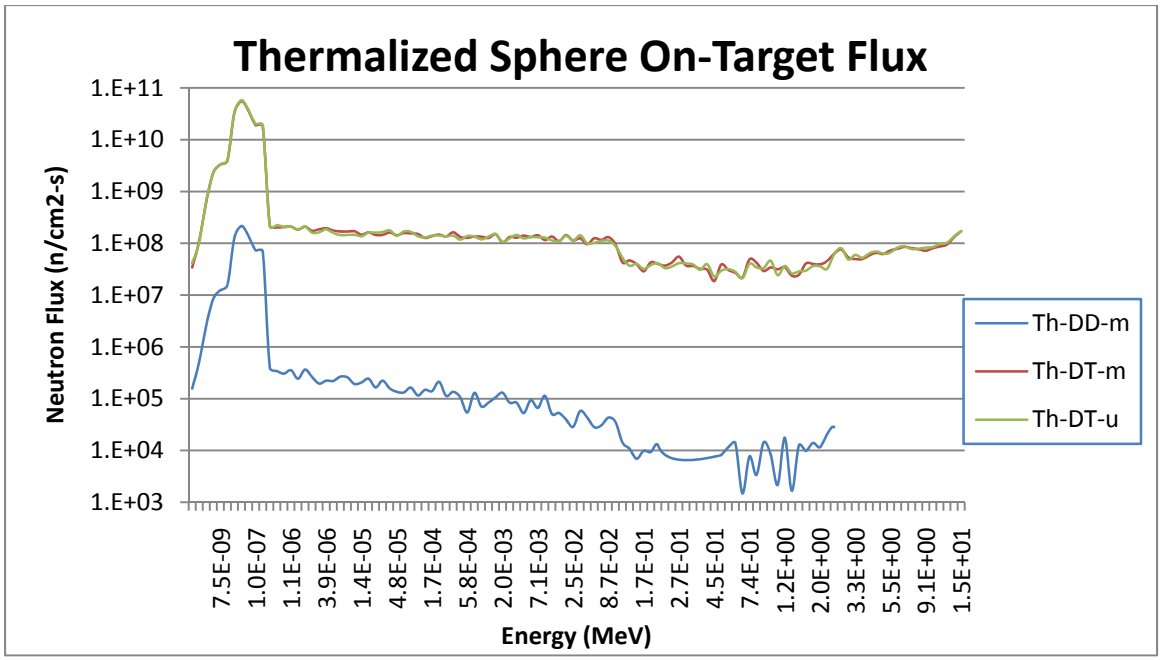

Figure 5.15 Neutron Flux with Sphere Filled with Heavy Water

Chapter 6

The Base Cases

The transmutation of radionuclides is a function of the following:

- the neutron energy spectrum,
- the radionuclide reaction crossections, and
- the total on-target neutron flux available.

As seen from Chapter 5, there are many conceptual design parameters that can affect the neutron spectrum. Therefore, it is important to define the base cases of the transmutation device which will be studied. Firstly, the spherical geometry will be used for the transmutation device. To maximize the number of neutrons inside the device, the volume to surface ratio must be minimized to reduce neutron leakage. Neutron leakage is a function of the surface area and assuming a given volume, the sphere provides the least surface area of most geometric objects.

Secondly, the inner diameter of the transmutation device will be one meter. This dimension was chosen to allow enough room for the neutron generator (26 cm diameter and 28 cm in length) and the target while allowing for future flexibility to increase the size of the generator for creation of higher fluxes.

Thirdly, the reflector shell of the transmutation device will be lead. Although results of analyses show that beryllium is a better reflector, the increase in the neutron multiplication factor of beryllium over lead is only a factor of less than two and not the

order of magnitude that was desired. In addition, lead is readily available, more economical, easy to machine, and is less toxic than beryllium. Therefore, based on these factors, lead was chosen.

Next, the thickness of the spherical reflector shell was set at 25 cm, the thickness above which there was little increase in the neutron multiplication. This thickness was chosen to minimize the amount of thickness and ultimately total lead volume used, as lead is a very heavy element. The moderator material used in the base cases was added to the inside of the existing spherical shell. Based on the results of the analyses shown in Section 5.7, Teflon® was chosen for the moderating material. Although the neutron energy spectra differed for the different configurations (including material type and the order of material placement), there was not an overall increase in the on-target flux of more than about one order of magnitude. Therefore, the choice was not just based on the total on-target neutron flux but also the total number of neutrons with energies in the lower energy range that favors the neutron capture cross sections using the adiabatic resonance crossing concept.

Figure 6.1 is a geometry plot generated in MCNPX of a simulation model of the transmutation device. The neutron source was modeled as a cylindrical shell source in MCNPX with an isotropic distribution of the source neutrons. The axis through the cylinder is lying in the horizontal plane such that the top and bottom lines represent the cylinder wall. The plot shows three concentric spherical shells which were used to iterate on reflector material. The target shown is the side view of a planchet on which the target material is assumed to be electroplated. This configuration was used to arrive at the four base cases for which the transmutation calculations were done.

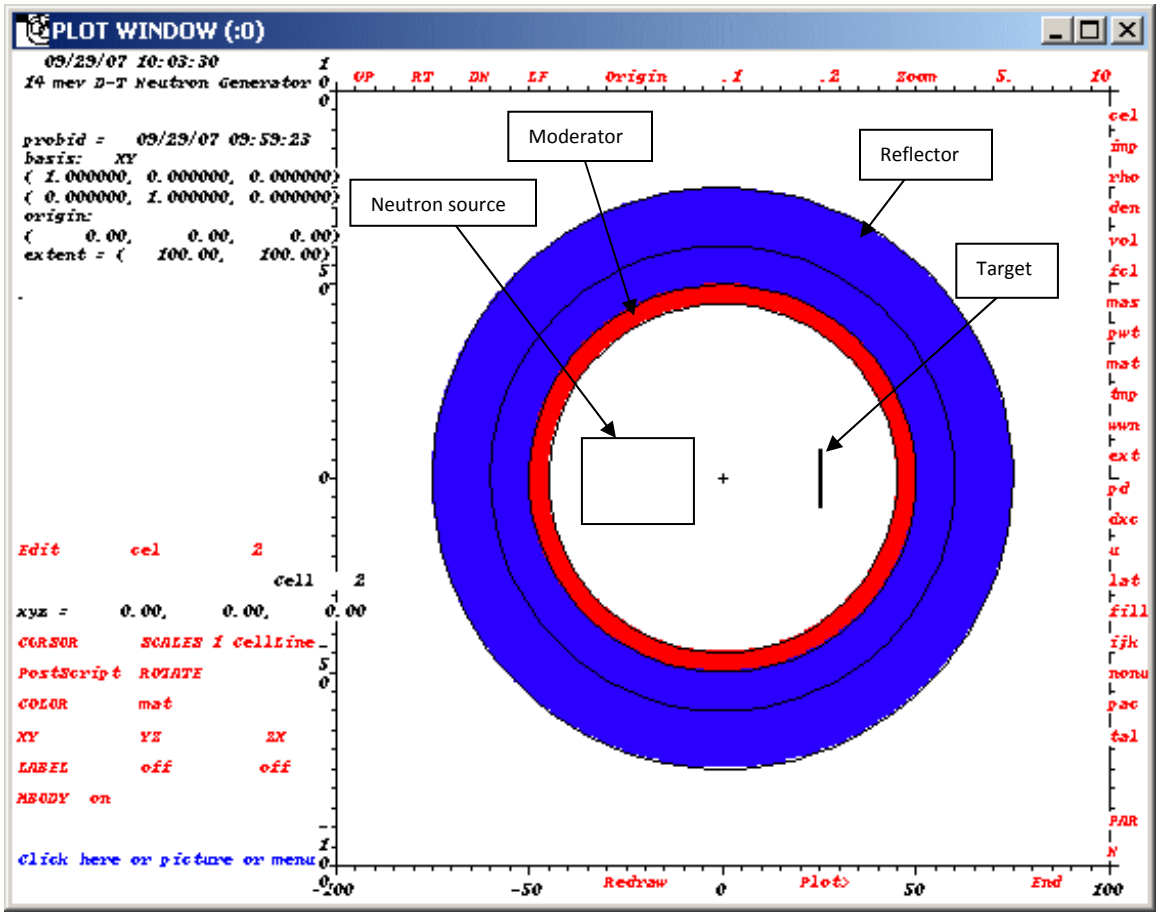

Figure 6.1 MCNPX Geometry Plot of Transmutation Device Model

The four base cases are:

- The D-T unmoderated configuration. This configuration takes advantage of the high flux produced by the D-T neutron generator (3.0 x 10^{14} n/s) producing 14 MeV mono-energetic neutrons. It has a 25 cm thick lead shell and a one meter inner diameter. The total on-target flux was 1.23 x 10^{11} n/s-cm^2.
- The D-T moderated configuration. This configuration takes advantage of the high flux produced by the D-T neutron generator (3.0 x 10^{14} n/s) producing 14 MeV mono-energetic neutrons. It has a 25 cm thick lead shell, a 5cm thick Teflon® lining, and a 0.9 meter inner diameter. The goal of this configuration was to

create a higher flux of lower energy neutrons. The total on-target flux was 1.55 x 10^{11} n/s-cm^2.

- The D-D moderated configuration. This configuration has a lower flux as produced by the D-D neutron generator (1.0 x 10^{12} n/s) of 2.5 MeV mono-energetic neutrons. It has a 25 cm thick lead shell, a 5 cm Teflon® lining, and a 0.9 meter inner diameter. The goal with this configuration was to produce a predominately lower energy neutrons in order to minimize, and in some cases prevent, unwanted reactions in the target (e.g., (n, 2n), (n, 3n), (n, α)), as well as other higher order reactions which could possibly create undesired activation products. The D-D unmoderated configuration is not a necessary base case because using the D-D generator would only be advantageous when seeking to maximize low energy neutrons. The total on-target flux was 5.14 x 10^8 n/s-cm^2.
- The thermalized configuration. This configuration is the D-T moderated configuration for which the inner chamber was filled with heavy water in an effort to maximize the thermal neutron flux on the target. The total on-target flux was 1.83 x 10^{11} n/s-cm^2 with about 85% of the neutrons in a distribution around the thermal energy range (~ 0.025 eV.)

Figure 6.2 shows the graphic representation of the neutron energy spectra of the four base cases. The following is evident:

- There are no neutrons above 2.5 MeV in the configuration using the D-D generator and the moderating shell (DD-m).
- The thermalized configuration (Th-DT-m). has a peak neutron flux around the thermal neutron energy of 2.5 x 10^{-8} MeV.

- The D-T unmoderated configuration (DT-u) has an insignificant number of neutrons in the lower energy range (less than about 1 x 10^{-4} MeV.)
- The DD-m and the DT-m spectra have roughly the same shape below energies of 2.5 MeV indicating that the moderator material has a similar effect on the lower energy distribution. The order of magnitude differences of these curves are attributed to the orders of magnitude difference in the source strength available in the generator.

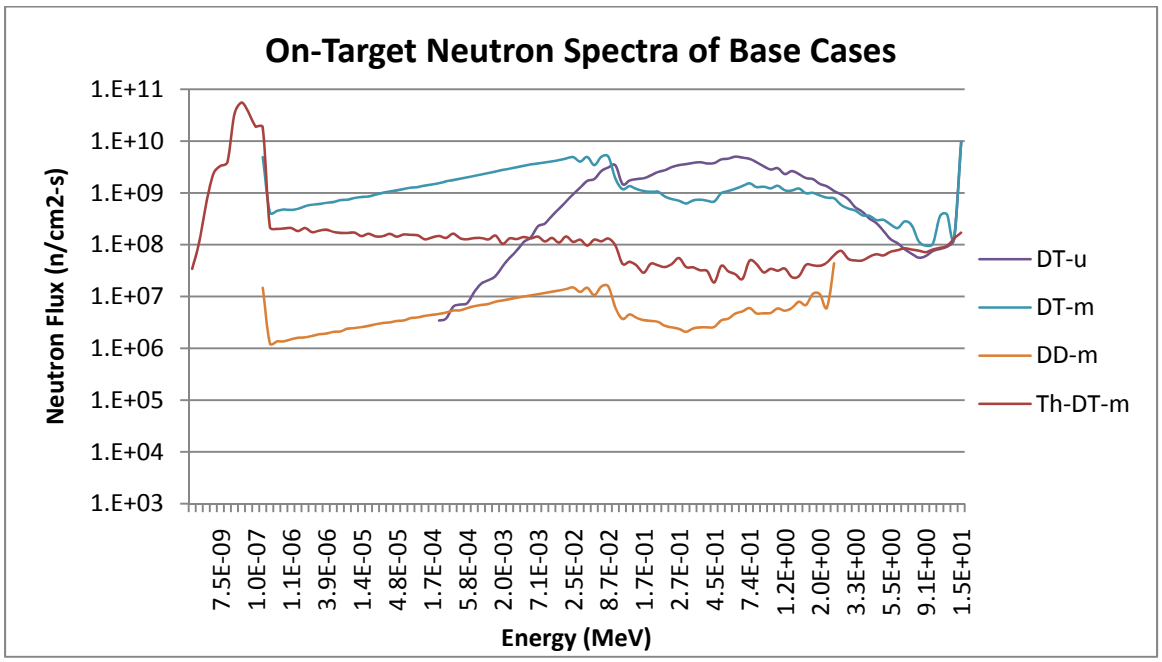

Figure 6.2 On-Target Neutron Energy Spectra of the Base cases

The neutron spectra represented by these four base cases are the neutron spectra incident upon the target planchet where the target radionuclide is assumed to be present. These energy spectra will be "folded in" with the energy dependent reaction cross-sections of the target radionuclide for the transmutation calculation. This methodology will be applied to the long-lived and short-lived fission product radionuclides as part of

this investigation. For the actinides, a slightly different methodology was used. Additional radionuclide neutron spectra were modeled. The reason for this is that the FISPACT software used to calculate activation/transmutation does not propagate neutrons created from fission which may be available for transmutation. Therefore, MCNPX was used to perform the KCODE calculation on a target cell filled with the actinide. The resulting F4 tally (average flux in a cell) included additional neutrons generated by the fissions that occur. These fission corrected spectra were then used for the transmutation calculations. This methodology was reviewed by the author of the transmutation code and found to be acceptable as long as the amount of actinides is small (subcritical amounts) [44].

Conclusions were made on which energy spectra is best for transmutation of each radionuclide. For each base case, the neutron source strength was iterated upon (increased and evaluated) by orders of magnitude until the radionuclide would be transmuted to a target level within a reasonable period of time. Consequently, these source strengths will be referred to as the "high flux" cases. As a result, one can determine how many orders of magnitude increase in the flux will be necessary to reach the point that transmutation may be feasible with the conceptual device.

Chapter 7

Results of Transmutation Calculations

The radionuclides chosen to be studied are shown in Table 7.1. Also shown are the radionuclides starting activity, specific activity, mass, density used in the calculations, radiological half-life, and the ending activity.

Table 7.1 Radionuclides and Their Characteristics [32, 43]

Nuclide	Starting Activity	Specific act.	Mass	Density	T ½	Ending Activity
	(Ci)	(Ci/gm)	(gm)	(g/cc)	(yr)	(uCi)
I-129	0.032	0.00016	200.000	4.93	1.57E+07	1
Tc-99	1.0	0.017	58.824	11.5	2.13E+05	100
Cs-137	1.0	88.000	0.011	1.87	3.02E+01	10
Sr-90	1.0	140.000	0.007	2.54	2.86E+01	0.1
Am-241	1.0	3.200	0.313	13.67	4.32E+02	0.001
Pu-239	1.0	0.062	16.129	19.84	2.41E+04	0.001
Pu-238	1.0	17.000	0.059	19.84	8.78E+01	0.001

The starting activity for each radionuclide was chosen as 1 Ci for ease in the scaling of results, with the exception of I-129. Because the specific activity of I-129 is so low, a more reasonable starting value was used which is the value that is equivalent to the amount of I-129 in a typical spent PWR fuel assembly with a burnup of 33 GWd/t and 10 year cooling [8]. The ending activity was chosen to be the activity above which the Nuclear Regulatory Commission requires radioactive material to be labeled [36].

For each radionuclide, the neutron reaction cross sections are presented as a function of energy, which can qualitatively show what energy range is more beneficial to

the transmutation process. It is then possible to eliminate the use of a particular base case; i.e., if the more beneficial energy is lower energy, then the D-T unmoderated base case would not need to be evaluated because the transmutation efficiency would be lower. Also presented are the neutron reaction thresholds as a function of energy, which can be used to qualitatively determine the activation products, as the activation products are a function of the reaction that occurs which in turn is a function of the neutron energy.

For each radionuclide, results of the transmutation calculations for each of the base cases used for that radionuclide up to and including the high flux cases are shown. These results include the amount of time and neutron fluence required to eliminate the target radionuclide from its starting activity to its ending activity, and the resulting irradiation effective half-life. The irradiation effective half-life is determined by starting with the typical decay equation:

$$A = A_o\, e^{-\lambda t} \tag{7.1}$$

Where: $\lambda = \ln 2 / T_{1/2}$

A_o: is the starting activity [Bq]

A: the ending activity [Bq]

t: irradiation time [s or consistent with $T_{1/2}$ unit]

Therefore, the irradiation effective half-life can be determined by:

$$T_{1/2} = (-\ln 2 * (t)) / (\ln(A/A_o)) \tag{7.2}$$

The neutron flux for each of the base cases used for that radionuclide was increased by an order of magnitude until the irradiation time was within a "reasonable" period of time; defined as < 100 years as discussed in Section 4.3. The flux at which the irradiation time is below 100 years was considered the high flux case for that base case.

Next, the activation products will be calculated and evaluated for each of the base cases used for a particular radionuclide and their associated high flux case. The activation products results shown include the total activation product activity in bequerels (Bq), the number of radionuclides and non-radioactive nuclides, and the major radionuclides present in the activation products.

Next, the radiation protection issues of the activation products from the cases studied were evaluated. These results include the gamma dose rate of the resulting activation products, the ingestion dose (committed effective dose equivalent, CEDE) that would result from the ingestion of the activation products, the inhalation dose (CEDE) that would result from the inhalation of the activation products, and the decay curve of the resulting activation products. The purpose of the decay curve of the activation products is to determine how long it would take for the activation products resulting from the transmutation to "cool" down to a gamma dose rate of 1 mR/hr. This information can reveal whether one creates a material that is even more hazardous than that of the material that was transmuted.

Finally, radionuclide specific observations and discussions were provided based on all the transmutation calculations for that radionuclide.

7.1 Iodine-129

For I-129 the more beneficial energy spectrum for transmutation would be lower energy neutrons. This can be seen in Figure 7.1.1 which depicts the neutron cross sections and the resonances that occur in the 50-4000 eV range. Therefore, the D-T unmoderated base case will not be used because the transmutation effectiveness would be lower than the other base cases. Only the other three base cases will be considered: D-T moderated, D-D moderated, and D-T thermalized.

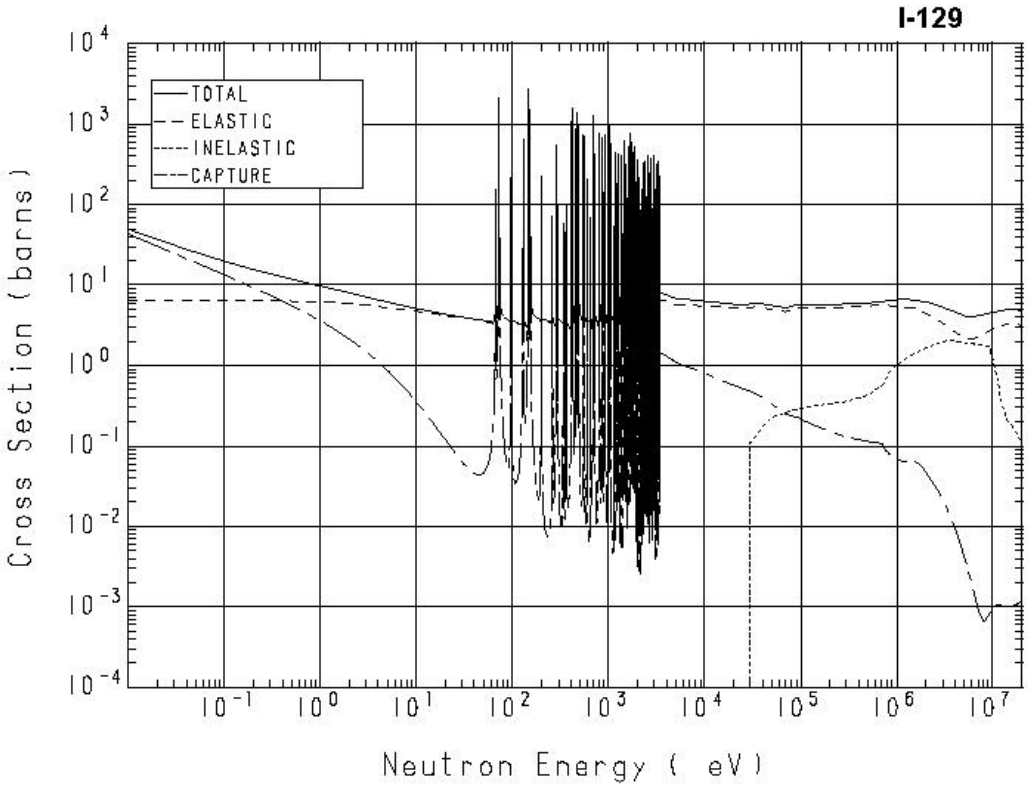

Figure 7.1.1 Neutron Reaction Cross Sections for I-129 [43]

Figure 7.1.2 shows the thresholds for different neutron reactions. As can be seen from Figure 7.1.2, inelastic processes predominate when using the D-D neutron generator for

transmutation since the maximum energy of the neutrons will be below 3 MeV. The figure also shows that when using the D-T neutron generator, some activation products may be generated by (n,2n), (n,p), and (n,α) reactions that would not be present in the activation products of the D-D neutron generator.

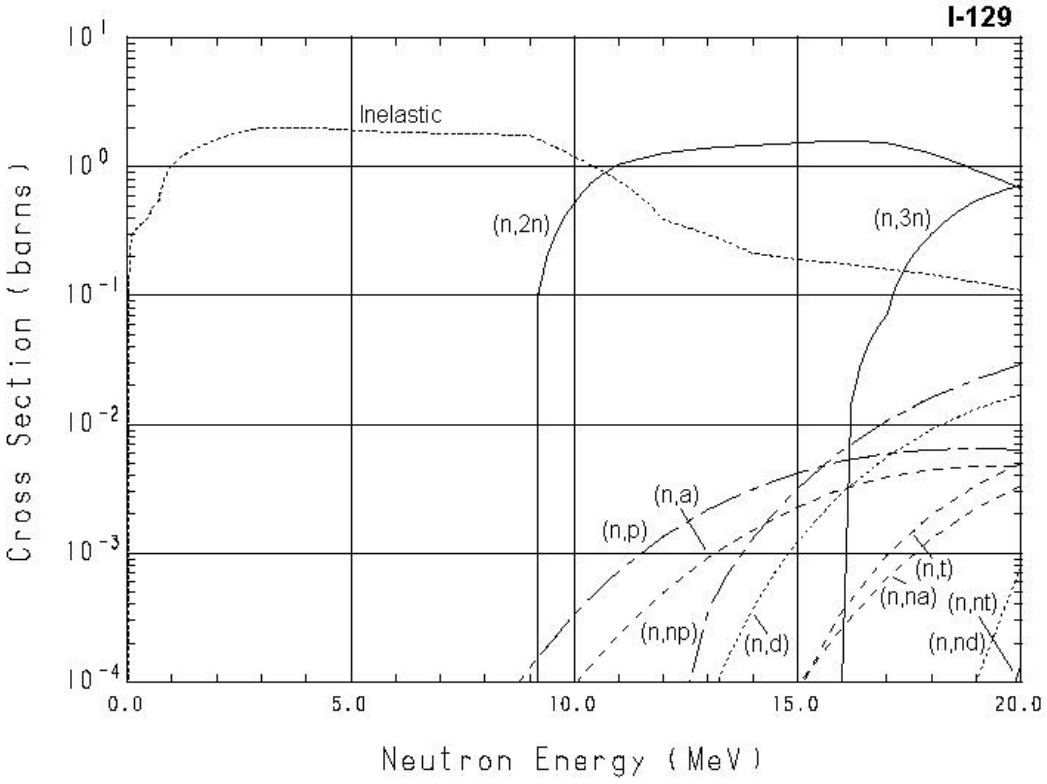

Figure 7.1.2 Neutron Reaction Thresholds for I-129 [43]

7.1.1 Results of Transmutation

Table 7.1.1hows the results of the transmutation calculations for I-129 with a radiological half-life of 1.57E+07 years. For I-129, the starting activity is 1.18e+09 Bq

(0.032 Ci) and the ending activity is 3.7e+04 Bq (0.001 mCi). Under the description of the neutron spectrum used for the transmutation calculation, the BC stands for base case and HFC stands for high flux case.

Table 7.1.1 Transmutation Results for I-129

Neutron Spectrum Used	On-target flux (n/s/cm2)	Irradiation Time (yrs)	Ending Activity (Bq)	Fluence Required (n/cm2)	Irradiation Effective Half-life (yrs)
D-T moderated BC	1.55E+11	2.00E+06	3.41E+04	9.77E+24	1.32E+05
	1.55E+12	2.00E+05	3.44E+04	9.77E+24	1.33E+04
	1.55E+13	2.00E+04	3.47E+04	9.77E+24	1.33E+03
	1.55E+14	2.00E+03	3.76E+04	9.77E+24	1.34E+02
	1.55E+15	2.00E+02	4.70E+04	9.77E+24	1.37E+01
D-T moderated HFC	1.55E+16	2.50E+01	3.71E+04	1.22E+25	1.67E+00
D-D moderated BC	5.14E+08	1.40E+08	3.06E+04	2.27E+24	9.17E+06
	5.14E+09	2.90E+07	3.41E+04	4.70E+24	1.92E+06
	5.14E+10	3.23E+06	3.71E+04	5.23E+24	2.16E+05
	5.14E+11	3.27E+05	3.71E+04	5.29E+24	2.18E+04
	5.14E+12	3.28E+04	3.64E+04	5.31E+24	2.18E+03
	5.14E+13	3.28E+03	3.64E+04	5.31E+24	2.19E+02
D-D moderated HFC	5.14E+14	3.28E+02	3.65E+04	5.31E+24	2.19E+01
D-T Thermalized BC	1.83E+11	6.00E+04	4.00E+04	3.46E+23	4.03E+03
	1.83E+12	6.10E+03	3.38E+04	3.52E+23	4.03E+02
	1.83E+13	6.10E+02	3.38E+04	3.52E+23	4.03E+01
D-T Thermalized HFC	1.83E+14	6.10E+01	3.38E+04	3.52E+23	4.03E+00

The results of the transmutation calculations show that any of the base cases produce effective half-lives lower than the radiological half-life of the I-129 (1.57E+07 years). The results also show that the neutron spectrum most effective for eliminating I-129 from the starting activity down to the ending activity is a thermalized neutron energy spectrum; with the least effective being the higher energy spectrum. This finding is

consistent with the information in the literature. The results also show that the fluence required for the transmutation is fairly consistent and doesn't change with the change in flux within a base case; subsequently, showing that the effective half-life is linearly and inversely proportional to the neutron flux. As seen in Figure 7.1.3, the increase in the flux required from present technology for transmutation of I-129 within a reasonable period of time is 5 orders of magnitude for the D-T moderated base case, 6 orders of magnitude for the D-D moderated base case, and only 3 orders of magnitude for the D-T thermalized base case.

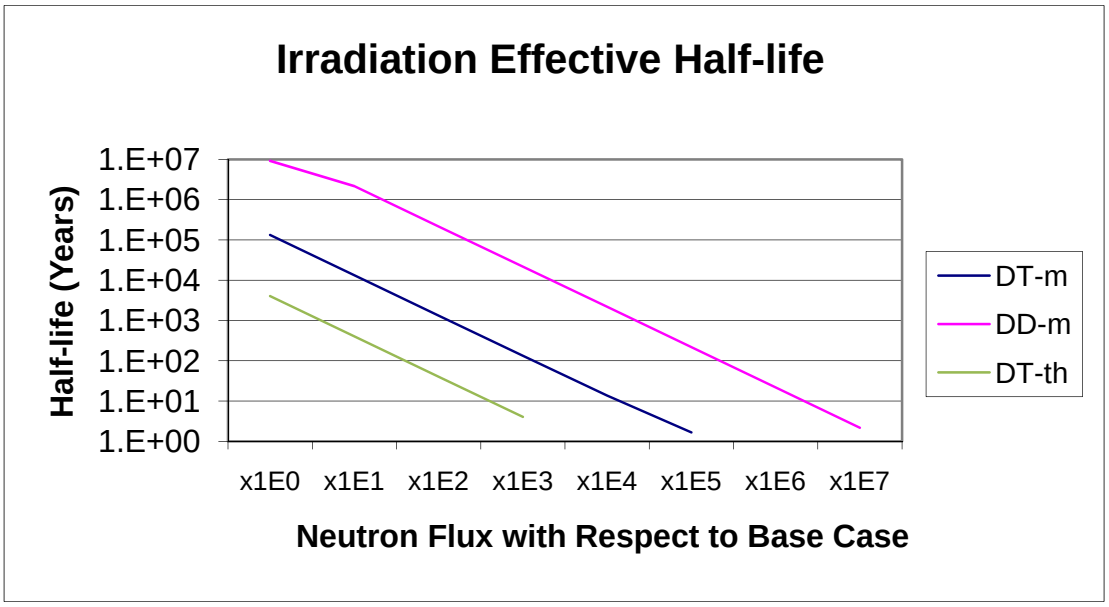

Figure 7.1.3: Irradiation Effective Half-life as a Function of Neutron Flux for I-129

7.1.2 Activation Products

Table 7.1.2 shows the summary of activation products generated by the transmutation of I-129 down to the ending activity level. The total activity of the results of the transmutation is given as well as the number of radioactive and non-radioactive

nuclides. Results show that using a higher energy spectrum for transmutation (D-T moderated case) generates many more radionuclides. The reason for this is the presence of higher order reactions which occur such as the (n,2n) or (n,p) reactions which do not occur using the D-D moderated base case or occur much less frequently using the D-T thermalized base case. Table 7.1.2 also shows that the total activity of activation products generated is directly proportional to the flux; subsequently, it is inversely proportional to the irradiation time.

Table 7.1.2 Activation Products Summary for I-129

Neutron Spectrum Used	On-target flux (n/s/cm2)	Total Activation (Bq)	Number of Radioactive Nuclides	Number of Non-radioactive Nuclides
D-T moderated BC	1.55E+11	3.02E+10	305	136
	1.55E+12	3.02E+11	332	136
	1.55E+13	3.02E+12	372	136
	1.55E+14	2.94E+13	427	136
	1.55E+15	2.80E+14	472	136
D-T moderated HFC	1.55E+16	2.29E+15	541	138
D-D moderated BC	5.14E+08	6.03E+07	50	69
	5.14E+09	7.55E+08	81	93
	5.14E+10	7.58E+09	101	96
	5.14E+11	7.57E+10	114	96
	5.14E+12	7.57E+11	130	97
	5.14E+13	7.57E+12	154	97
D-D moderated HFC	5.14E+14	7.49E+13	176	98
D-T Thermalized BC	1.83E+11	1.24E+11	64	56
	1.83E+12	1.24E+12	74	58
	1.83E+13	1.21E+13	92	60
D-T Thermalized HFC	1.83E+14	1.11E+14	103	66

In other words, the faster the I-129 is transmuted the more activation products are generated. Subsequent Tables show the most prominent radionuclides (with respect to activity) for each of the base cases at the base case flux level as well as at the high flux case level.

Table 7.1.3 show the most prominent activation products for transmutation of I-129 in a D-T moderated spectrum, both at base case and high flux case levels. The radionuclides shown are present at the end of the transmutation period. Results show that the activation products generated by transmutation are a function of the flux level used because the production of the different radionuclides is dependent upon each radionuclides production (or reaction) cross section and then their subsequent decay rate. The flux level, therefore, greatly affects the resulting products at the time of completion. For example, at the high flux level, the short lived Cs-136 comprises a much higher percentage of the activation products. Even though it is short-lived (~ 13 days half-life), it does have a significant contribution to gamma dose rate due to its decay with, among other radiations, an 818 keV gamma at a probability of 0.997 and a 1.05 MeV gamma at a probability of 0.795.

Table 7.1.4 shows the most prominent activation products for transmutation of I-129 in a D-D moderated spectrum, both at base case and high flux case levels. Likewise, Table 7.1.5 shows the most prominent activation products for the transmutation of I-129 in a D-T thermalized spectrum.

Table 7.1.3 Radionuclides and Percent Activity of the Activation Products of I-129 in a D-T Moderated Flux spectrum.

	Base Case Level				High Flux Case Level	
NUCLIDE	ACTIVITY	PERCENT		NUCLIDE	ACTIVITY	PERCENT
	(Bq)	ACTIVITY			(Bq)	ACTIVITY
Total	3.02E+10			Total	2.29E+15	
Cs134	8.41E+09	2.78E+01		Xe133	5.74E+14	2.50E+01
Xe133	7.60E+09	2.52E+01		Cs136	5.34E+14	2.33E+01
Xe131m	4.56E+09	1.51E+01		Ba135m	3.24E+14	1.41E+01
Ba135m	3.71E+09	1.23E+01		Xe131m	2.33E+14	1.02E+01
Ba137m	1.09E+09	3.62E+00		Ba137m	1.74E+14	7.58E+00
Ba136m	9.49E+08	3.14E+00		Ba136m	1.12E+14	4.89E+00
Xe133m	8.54E+08	2.83E+00		Xe133m	8.45E+13	3.69E+00
Ba133	8.05E+08	2.66E+00		Cs134m	6.50E+13	2.83E+00
Cs134m	7.83E+08	2.59E+00		Cs134	5.91E+13	2.58E+00
H 3	4.30E+08	1.42E+00		Ba139	2.39E+13	1.04E+00
Ba133m	4.03E+08	1.34E+00		Xe134m	2.04E+13	8.92E-01
Xe129m	2.01E+08	6.66E-01		La140	1.74E+13	7.61E-01
Ba139	1.26E+08	4.18E-01		Cs136m	1.68E+13	7.33E-01
La140	8.63E+07	2.86E-01		Xe135m	9.98E+12	4.36E-01
Cs132	7.41E+07	2.45E-01		Xe129m	7.32E+12	3.19E-01
Cs136	1.88E+07	6.21E-02		Cs137	5.70E+12	2.49E-01
Ce139	1.51E+07	4.99E-02		Cs138	4.94E+12	2.15E-01
I 128	1.40E+07	4.64E-02		Cs135m	4.30E+12	1.88E-01
I 132	1.17E+07	3.88E-02		Cs132	4.24E+12	1.85E-01
I 130	9.11E+06	3.01E-02		Ba133m	3.92E+12	1.71E-01
Rest	6.36E+07	2.11E-01		Rest	1.43E+13	6.24E-01

Table 7.1.4 Radionuclides and Percent Activity of the Activation Products of I-129 in a D-D Moderated Flux spectrum.

	Base Case Level				High Flux Case Level	
NUCLIDE	ACTIVITY	PERCENT		NUCLIDE	ACTIVITY	PERCENT
	(Bq)	ACTIVITY			(Bq)	ACTIVITY
Total	6.03E+07			Total	7.49E+13	
Xe133	2.35E+07	3.91E+01		Xe133	3.12E+13	4.17E+01
Cs134	2.27E+07	3.77E+01		Cs134	2.44E+13	3.25E+01
Xe131m	7.82E+06	1.30E+01		Cs136	6.68E+12	8.92E+00
Xe133m	2.65E+06	4.40E+00		Xe133m	3.53E+12	4.71E+00
Cs134m	2.12E+06	3.51E+00		Cs134m	2.97E+12	3.97E+00
Ba135m	1.27E+06	2.10E+00		Xe131m	2.78E+12	3.71E+00
Ba137m	4.52E+04	7.50E-02		Ba135m	2.24E+12	2.99E+00
I 129	3.06E+04	5.08E-02		Ba137m	8.10E+11	1.08E+00
Ba136m	2.94E+04	4.88E-02		Cs136m	1.10E+11	1.47E-01
I 130	2.00E+04	3.32E-02		Ba136m	7.86E+10	1.05E-01
I 130m	1.30E+04	2.16E-02		Ba139	4.31E+10	5.75E-02
Ba139	5.83E+02	9.68E-04		Cs135m	3.82E+10	5.10E-02
Xe129m	5.81E+02	9.63E-04		I 130	2.38E+10	3.18E-02
La140	9.14E+01	1.52E-04		Xe134m	2.00E+10	2.67E-02
Cs135	8.62E+00	1.43E-05		La140	1.57E+10	2.10E-02
I 131	3.96E+00	6.57E-06		I 130m	1.55E+10	2.07E-02
Xe135	3.56E+00	5.90E-06		Cs137	8.01E+09	1.07E-02
Xe134m	2.93E+00	4.86E-06		Xe135	6.50E+09	8.67E-03
Cs136	1.19E+00	1.97E-06		Ce141	3.01E+08	4.01E-04
Ce141	6.01E-01	9.97E-07		Xe135m	2.63E+08	3.50E-04
Rest	3.67E+00	6.08E-06		Rest	7.17E+08	9.57E-04

Table 7.1.5 Radionuclides and Percent Activity of the Activation Products of I-129 in a D-T Thermalized Flux spectrum.

	Base Case Level				High Flux Case Level	
NUCLIDE	ACTIVITY	PERCENT		NUCLIDE	ACTIVITY	PERCENT
	(Bq)	ACTIVITY			(Bq)	ACTIVITY
Total	1.24E+11			Total	1.11E+14	
Xe133	5.06E+10	4.09E+01		Xe133	4.99E+13	4.50E+01
Cs134	4.77E+10	3.85E+01		Cs136	2.16E+13	1.95E+01
Xe131m	1.42E+10	1.14E+01		Cs134	1.50E+13	1.35E+01
Xe133m	5.62E+09	4.55E+00		Xe131m	1.35E+13	1.21E+01
Cs134m	4.45E+09	3.59E+00		Xe133m	5.61E+12	5.06E+00
Ba135m	9.18E+08	7.42E-01		Cs134m	4.39E+12	3.96E+00
I 130	1.42E+08	1.14E-01		Cs136m	3.49E+11	3.14E-01
I 130m	9.22E+07	7.45E-02		Ba135m	2.88E+11	2.60E-01
Cs136	6.86E+07	5.54E-02		Cs135m	1.21E+11	1.09E-01
Ba136m	1.22E+07	9.83E-03		I 130	1.19E+11	1.08E-01
Ba137m	3.42E+06	2.77E-03		I 130m	7.78E+10	7.01E-02
Cs136m	1.11E+06	8.94E-04		Xe134m	4.22E+10	3.80E-02
Ba139	6.13E+05	4.96E-04		Ba137m	2.50E+10	2.26E-02
Cs135	4.33E+05	3.50E-04		Ba139	6.00E+09	5.41E-03
Cs135m	3.85E+05	3.11E-04		Ba136m	3.83E+09	3.45E-03
La140	1.70E+05	1.37E-04		Cs137	2.98E+09	2.69E-03
Xe135	4.95E+04	4.00E-05		La140	1.88E+09	1.70E-03
Xe134m	4.28E+04	3.46E-05		Xe135	1.86E+09	1.68E-03
I 129	4.00E+04	3.24E-05		Xe137	1.19E+09	1.07E-03
Ce141	3.51E+03	2.84E-06		Xe135m	5.22E+08	4.71E-04
Rest	7.93E+03	6.41E-06		Rest	3.24E+08	2.92E-04

7.1.3 Radiation Protection and Dose Rate Calculation

The activation products resulting from the transmutation of I-129 as shown in Section 7.1.2 will have hazards associated with them. These are referred to as the hazard indexes. As described in Section 4.4, the hazard indexes evaluated include gamma dose rate at the surface of the activation products, the ingestion dose (committed effective dose equivalent), and the inhalation dose (committed effective dose equivalent) from each of the base cases at both the base case flux level as well as the high flux case level. Table 7.1.6 shows the summary of the hazard indexes of the activation products generated by the transmutation of I-129 down to the ending activity level for each of the base cases considered.

Results show that the dose rate, ingestion hazard, and inhalation hazard are all directly proportional to the flux used for transmutation; i.e., the higher the flux, the higher the hazard indexes. Results also show that the hazards from the activation products from a D-D moderated neutron spectrum can have 3 orders of magnitude lower dose rates, ingestion hazard, and/or inhalation hazard than the D-T moderated and D-T thermalized base cases. The reason for this is the smaller activities of activation products generated. The hazard indexes for the D-T thermalized case are the highest

Table 7.1.6 Hazard Indexes Summary of the Activation Products for I-129

		Activation	Activation	Activation
Neutron Spectrum	On-target	Product	Ingestion	Inhalation
Used	flux	Dose rate	Dose	Dose
	(n/s/cm2)	(Sv/hr)	(Sv)	(Sv)
D-T moderated BC	1.55E+11	1.87E+01	1.82E+02	2.33E+02
	1.55E+12	1.87E+02	1.82E+03	2.33E+03
	1.55E+13	1.88E+03	1.80E+04	2.31E+04
	1.55E+14	1.91E+04	1.67E+05	2.15E+05
	1.55E+15	2.16E+05	1.09E+06	1.49E+06
D-T moderated HFC	1.55E+16	2.15E+06	4.23E+06	6.50E+06
D-D moderated BC	5.14E+08	4.03E-02	4.82E-01	5.82E-01
	5.14E+09	5.55E-01	6.42E+00	7.47E+00
	5.14E+10	5.61E+00	6.47E+01	7.49E+01
	5.14E+11	5.62E+01	6.47E+02	7.49E+02
	5.14E+12	5.63E+02	6.45E+03	7.48E+03
	5.14E+13	5.70E+03	6.33E+04	7.34E+04
D-D moderated HFC	5.14E+14	6.26E+04	5.34E+05	6.28E+05
D-T Thermalized BC	1.83E+11	8.47E+01	1.00E+03	1.21E+03
	1.83E+12	8.55E+02	9.94E+03	1.20E+04
	1.83E+13	8.63E+03	8.65E+04	1.06E+05
D-T Thermalized HFC	1.83E+14	8.71E+04	4.43E+05	6.08E+05

In evaluating the dose rate hazard index, the decay characteristics of the activation product is important as well, such as is common when evaluating the hazards of spent fuel. Figure 7.1.4 shows the comparison of the decay curves for the activation products between the base and high flux cases of the D-T moderated base case. Likewise, Figures 7.1.5 and 7.1.6 show the comparisons for the D-D moderated base case and the D-T thermalized base case, respectively. These figures designate a "recycling limit" and a "hands on" limit. The values for these limits are 1 R/h and 1mR/h, respectively [31].

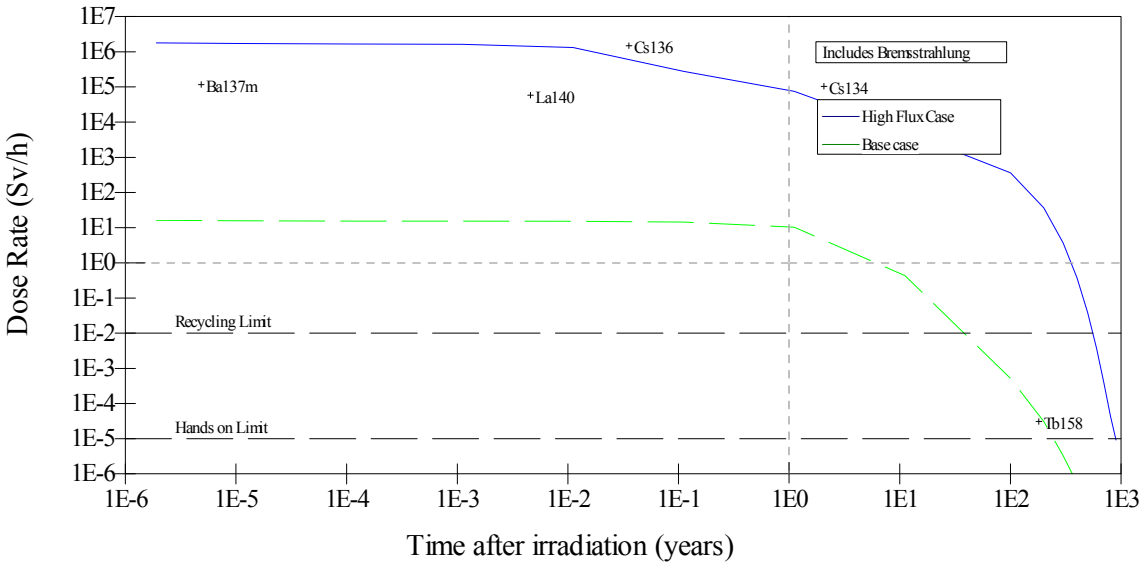

Figure 7.1.4 Decay Curve of I-129 Activation Products for the D-T moderated Base Case

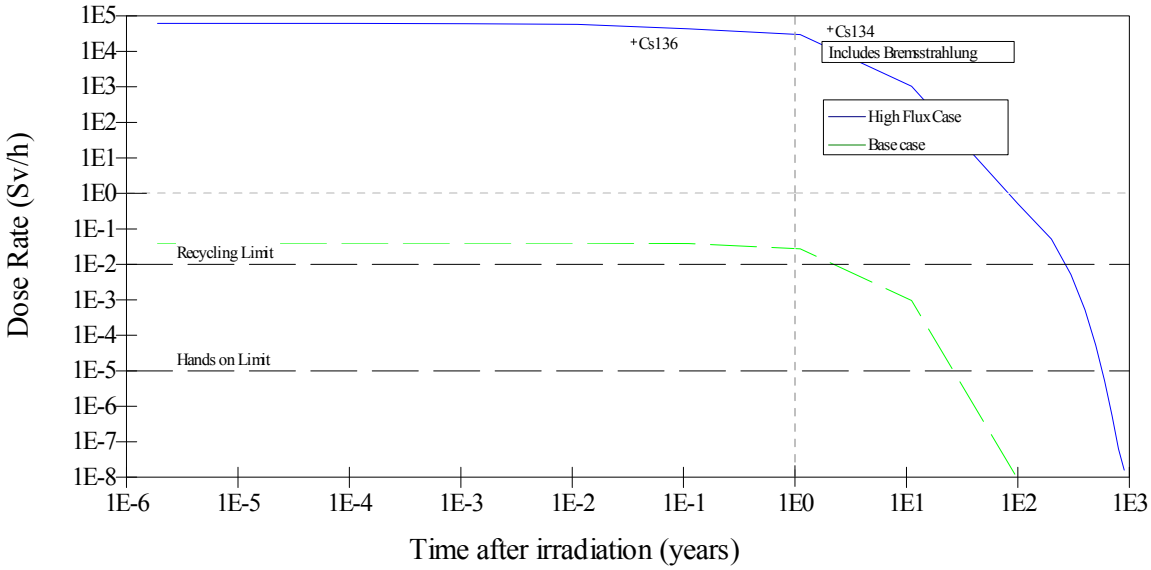

Figure 7.1.5 Decay Curve of I-129 Activation Products for the D-D moderated Base Case

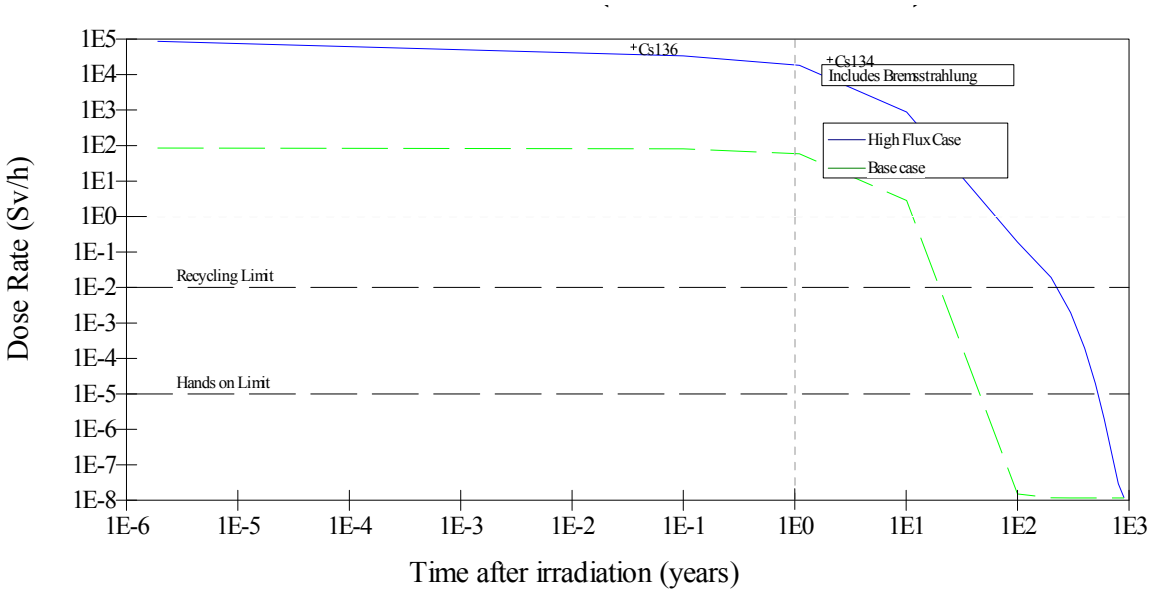

Figure 7.1.6 Decay Curve of I-129 Activation Products for the D-T Thermalized Base Case

Figures 7.1.4 through 7.1.6 show that for all three base cases, the high flux case yields activation products that take much longer to decay to the "hands on" value of 1 mR/h. The decay of the activation products may be an important parameter when evaluating for the optimum transmutation scheme. Table 7.1.7 summarizes the approximate cooling time for the activation products to reach 1 mR/h dose rate. In the case of I-129, the prominent activation products that drive the activity, hazards, and decay do not vary tremendously among the base cases; however, this is not necessarily true with all radionuclides when transmuted.

Table 7.1.7 Summary of Cooling Time for I-129 Activation Products

Neutron Spectrum Used	Approximate Cooling time To 1 mR/h (yrs)
D-T moderated BC	2.20E+02
D-T moderated HFC	9.00E+02
D-D moderated BC	2.30E+01
D-D moderated HFC	8.00E+02
D-T Thermalized BC	4.00E+01
D-T Thermalized HFC	5.00E+02

7.1.4 Discussion

The following observations were made regarding the transmutation of I-129:

- Any of the three base cases produce effective half-lives lower than the radiological half-life of the I-129.
- The lower energy spectrum is more advantageous to transmute I-129 with the thermalized spectrum as the best spectrum.
- Irradiation effective half-life is inversely proportional to the flux for all three base cases.
- Activation product generation is directly proportional to the flux for all three base cases.
- The hazard indexes correlate directly to amount of activation products that are generated for all three base cases.

- The decay of activation products are longer for activation products generated by the higher flux case than the base case flux for all three base cases.
- The minimum required improvement in technology for practical transmutation of I-129 is about 3 orders of magnitude increase in the neutron source strength (n/s) than the present source strength. This increase will produce an irradiation effective half-life of about 4 years for I-129.

7.2 Technetium-99

For Tc-99, similar to I-129, the more beneficial energy spectrum for transmutation would be lower energy neutrons. This can be seen in Figure 7.2.1 which depicts the neutron cross sections and the resonances that occur in the 5- 7000 eV range. Therefore, the D-T unmoderated base case will not be used because the transmutation effectiveness would be lower than the other base cases. Only the other three base cases will be considered: D-T moderated, D-D moderated, and D-T thermalized.

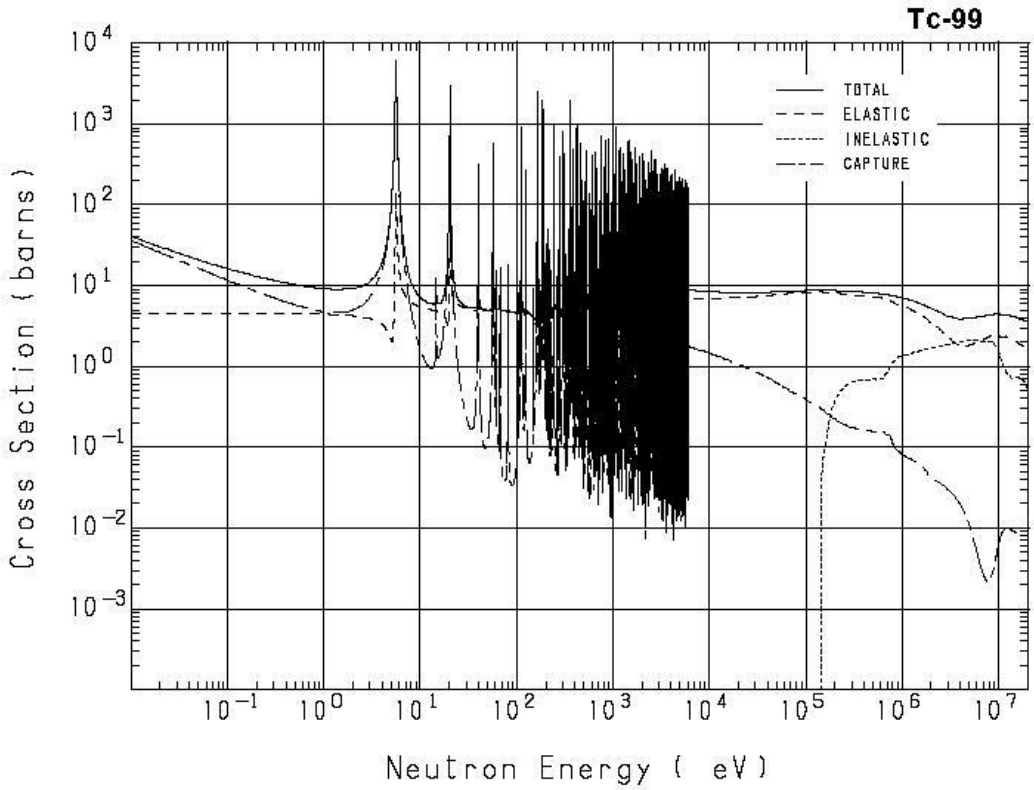

Figure 7.2.1 Neutron Reaction Cross Sections for T-99 [43]

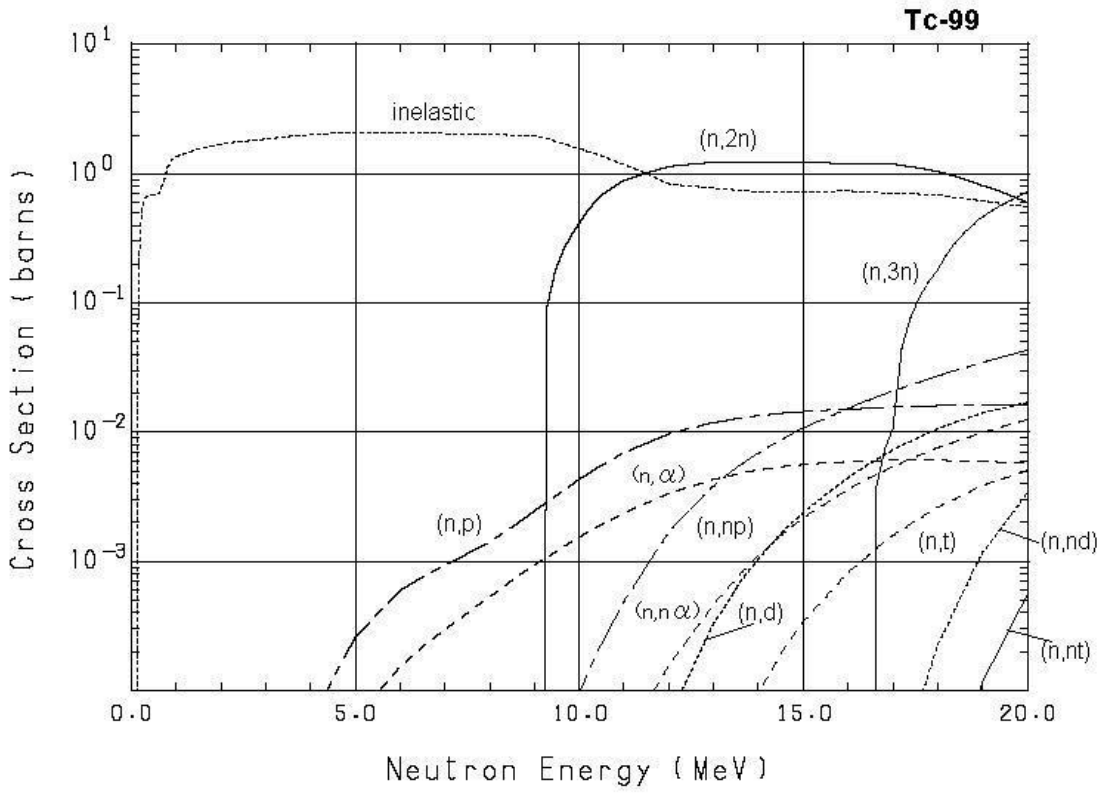

Figure 7.2.2 Neutron Reaction Thresholds for Tc-99 [43]

7.2.1 Results of Transmutation

Table 7.2.1 shows the results of the transmutation calculations for Tc-99 with a radiological half-life of 2.13E+05 years. For Tc-99, the starting activity is 3.7e+10 Bq (1.0 Ci) and the ending activity is 3.7e+06 Bq (0.1 mCi). Under the description of the neutron spectrum used for the transmutation calculation, the BC stands for base case and HFC stands for high flux case.

Table 7.2.1 Transmutation Results for Tc-99

Neutron Spectrum Used	On-target flux (n/s/cm2)	Irradiation Time (yrs)	Ending Activity (Bq)	Fluence Required (n/cm2)	Irradiation Effective Half-life (yrs)
D-T Moderated BC	1.55E+11	2.80E+05	3.54E+06	1.37E+24	2.10E+04
	1.55E+12	3.00E+04	3.54E+06	1.46E+24	2.25E+03
	1.55E+13	3.00E+03	3.60E+06	1.46E+24	2.25E+02
	1.55E+14	3.00E+02	3.60E+06	1.46E+24	2.25E+01
D-T Moderated HFC	1.55E+15	3.00E+01	3.60E+06	1.46E+24	2.25E+00
D-D Moderated BC	5.14E+08	2.80E+06	2.83E+06	4.53E+22	2.05E+05
	5.14E+09	2.20E+06	2.58E+06	3.56E+23	1.59E+05
	5.14E+10	6.60E+05	3.49E+06	1.07E+24	4.93E+04
	5.14E+11	8.40E+04	3.32E+06	1.36E+24	6.25E+03
	5.14E+12	8.60E+03	3.42E+06	1.39E+24	6.42E+02
	5.14E+13	8.60E+02	3.51E+06	1.39E+24	6.43E+01
D-D Moderated HFC	5.14E+14	8.60E+01	3.52E+06	1.39E+24	6.44E+00
D-T Thermalized BC	1.83E+11	9.00E+04	3.27E+06	5.19E+23	6.68E+03
	1.83E+12	9.00E+03	4.06E+06	5.19E+23	6.84E+02
	1.83E+13	9.10E+02	3.77E+06	5.25E+23	6.86E+01
D-T Thermalized HFC	1.83E+14	9.20E+01	3.41E+06	5.30E+23	6.86E+00

The results of the transmutation calculations show that the base cases utilizing the D-T neutron generator (moderated and themalized cases) produce effective half-lives lower than the radiological half-life of the Tc-99 (2.13E+05 years). However, the base case utilizing the D-D neutron generator results in an effective half-life similar to the radiological half-life of the Tc-99. The results also show that the neutron spectrum most effective for eliminating Tc-99 from the starting activity down to the ending activity is a thermalized neutron energy spectrum; with the least effective being the energy spectrum from the D-D generator because of the low flux. This finding is consistent with the

information in the literature. The results also show that the fluence required for the transmutation is fairly consistent and doesn't change with the change in flux within a base case; subsequently, showing that the effective half-life is linearly and inversely proportional to the neutron flux. As seen in Figure 7.2.3, the increase in the flux required from present technology for transmutation of I-129 within a reasonable period of time is 4 orders of magnitude for the D-T moderated base case, 6 orders of magnitude for the D-D moderated base case, and only 3 orders of magnitude for the D-T thermalized base case.

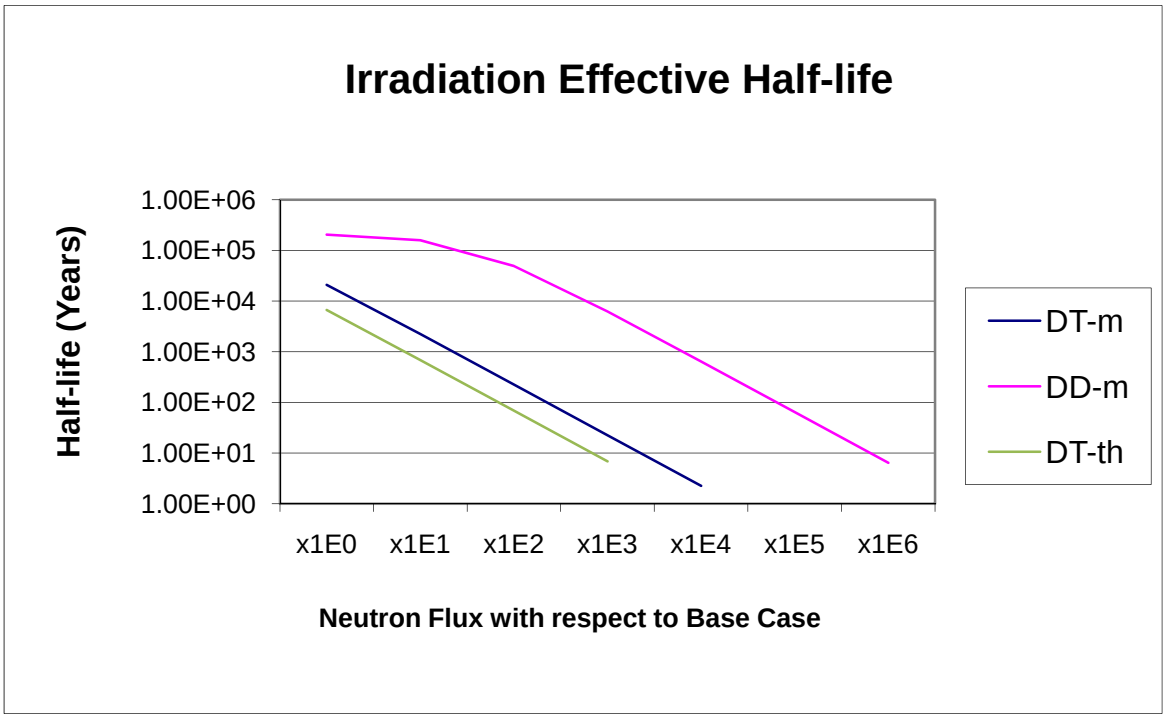

Figure 7.2.3 Irradiation Effective Half-life as a Function of Neutron Flux for Tc-99

7.2.2 Activation Products

Table 7.2.2 shows the summary of activation products generated by the transmutation of Tc-99 down to the ending activity level. The total activity of the results

of the transmutation is given as well as the number of radioactive and non-radioactive nuclides. Results show that using a higher energy spectrum for transmutation (D-T moderated case) generates many more radionuclides. The reason for this is the presence of higher order reactions which occur such as the (n,2n) or (n,p) reactions which do not occur using the D-D moderated base case or much less frequently using the D-T thermalized base case. Table 7.2.2 also shows that the total activity of activation products generated is directly proportional to the flux; subsequently, it is inversely proportional to the irradiation time. In other words, the faster the Tc-99 is transmuted the more activation products are generated.

Table 7.2.2 Activation Products Summary for Tc-99

Neutron Spectrum Used	On-target flux (n/s/cm2)	Total Activation (Bq)	Number of Radioactive Nuclides	Number of Non-radioactive Nuclides
D-T moderated BC	1.55E+11	1.59E+10	155	75
	1.55E+12	1.71E+11	169	76
	1.55E+13	1.70E+12	193	76
	1.55E+14	1.69E+13	207	76
D-T moderated HFC	1.55E+15	1.64E+14	227	77
D-D moderated BC	5.14E+08	2.94E+06	19	31
	5.14E+09	4.35E+07	44	43
	5.14E+10	3.39E+09	57	51
	5.14E+11	4.55E+10	66	54
	5.14E+12	4.67E+11	68	54
	5.14E+13	4.67E+12	77	54
D-D moderated HFC	5.14E+14	4.62E+13	84	54
D-T Thermalized BC	1.83E+11	9.55E+10	49	44
	1.83E+12	9.70E+11	54	44
	1.83E+14	9.78E+12	61	45
D-T Thermalized HFC	1.83E+13	9.72E+13	62	45

Table 7.2.3 show the most prominent activation products for transmutation of Tc-99 in a D-T moderated spectrum, both at base case and high flux case levels. The radionuclides shown are present at the end of the transmutation period. Results show that the activation products generated by transmutation are a function of the flux level used because the production of the different radionuclides is dependent upon each radionuclides production (or reaction) cross section and then their subsequent decay rate. For Tc-99, the flux level does not greatly affect the resulting products at the time of completion. The activation products at the high flux level are not much different than those at the base case level. Only the quantities are different because of the higher fluxes.

Table 7.2.4 shows the most prominent activation products for transmutation of Tc-99 in a D-D moderated spectrum, both at base case and high flux case levels. With a D-D moderated spectrum, the Tc-99 still dominates the resulting activity of all the activation products at the base case level. Likewise, Table 7.2.5 shows the most prominent activation products for the transmutation of Tc-99 in a D-T thermalized spectrum.

Table 7.2.3 Radionuclides and Percent Activity of the Activation Products of Tc-99 in a D-T Moderated Flux spectrum.

	Base Case Level				High Flux Case Level	
NUCLIDE	ACTIVITY	PERCENT		NUCLIDE	ACTIVITY	PERCENT
	(Bq)	ACTIVITY			(Bq)	ACTIVITY
Total	1.59E+10			Total	1.64E+14	
Rh103m	5.12E+09	3.22E+01		Rh103m	5.29E+13	3.22E+01
Ru103	4.88E+09	3.07E+01		Rh104	5.07E+13	3.09E+01
Rh104	4.87E+09	3.07E+01		Ru103	5.02E+13	3.05E+01
Rh104m	3.72E+08	2.34E+00		Rh104m	3.87E+12	2.36E+00
Pd103	2.53E+08	1.59E+00		Pd103	2.75E+12	1.68E+00
H 3	9.15E+07	5.76E-01		Tc100	8.30E+11	5.05E-01
Tc100	8.47E+07	5.33E-01		Ag109m	5.11E+11	3.11E-01
Ag109m	3.71E+07	2.34E-01		Pd109	5.08E+11	3.09E-01
Pd109	3.65E+07	2.30E-01		Ag110	4.36E+11	2.65E-01
Ag110	3.14E+07	1.97E-01		Ru105	3.69E+11	2.25E-01
Tc 99m	1.78E+07	1.12E-01		Rh105	3.25E+11	1.98E-01
Rh102	1.42E+07	8.94E-02		Tc 99m	1.67E+11	1.01E-01
Mo 99	1.28E+07	8.04E-02		Mo 99	1.37E+11	8.32E-02
Tc102	1.05E+07	6.63E-02		Tc102	1.12E+11	6.83E-02
Rh102m	9.70E+06	6.10E-02		Rh105m	1.05E+11	6.38E-02
Tc101	8.83E+06	5.55E-02		Tc101	8.67E+10	5.27E-02
Tc102m	7.49E+06	4.71E-02		Tc102m	7.98E+10	4.86E-02
Pd107m	6.08E+06	3.83E-02		Pd107m	7.87E+10	4.79E-02
Ru 97	5.79E+06	3.65E-02		Rh102m	5.47E+10	3.33E-02
Rh105	4.18E+06	2.63E-02		Rh106	4.90E+10	2.98E-02
Rest	1.30E+07	8.17E-02		Rest	1.18E+11	7.20E-02

Table 7.2.4 Radionuclides and Percent Activity of the Activation Products of Tc-99 in a D-D Moderated Flux spectrum.

	Base Case Level				High Flux Case Level	
NUCLIDE	ACTIVITY	PERCENT		NUCLIDE	ACTIVITY	PERCENT
	(Bq)	ACTIVITY			(Bq)	ACTIVITY
Total	2.94E+06			Total	4.62E+13	
Tc 99	2.83E+06	9.63E+01		Rh103m	1.52E+13	3.28E+01
Tc100	9.31E+04	3.16E+00		Ru103	1.51E+13	3.27E+01
Ru103	5.85E+03	1.99E-01		Rh104	1.44E+13	3.11E+01
Rh103m	5.78E+03	1.97E-01		Rh104m	1.09E+12	2.36E+00
Tc 99m	3.86E+03	1.31E-01		Tc100	1.16E+11	2.50E-01
Rh104	8.81E+02	2.99E-02		Ag109m	9.08E+10	1.97E-01
Rh104m	6.70E+01	2.28E-03		Pd109	9.04E+10	1.95E-01
Tc101	2.15E-01	7.32E-06		Ag110	7.55E+10	1.63E-01
Mo 99	5.63E-02	1.91E-06		Ru105	3.69E+10	7.98E-02
Ru105	1.22E-02	4.15E-07		Rh105	3.53E+10	7.62E-02
Rh105	1.22E-02	4.13E-07		Pd107m	1.72E+10	3.73E-02
Nb 96	7.56E-04	2.57E-08		Rh105m	1.03E+10	2.24E-02
Zr 93	1.82E-05	6.18E-10		Pd109m	1.98E+09	4.29E-03
Nb 93m	1.77E-05	6.03E-10		Ag111	1.97E+09	4.26E-03
Pd107	1.42E-05	4.82E-10		Ag110m	1.57E+09	3.39E-03
H 3	8.65E-06	2.94E-10		Rh106	1.50E+09	3.24E-03
Nb 95	3.22E-07	1.09E-11		Tc 99m	1.33E+09	2.87E-03
Nb 94	1.49E-07	5.06E-12		Ag111m	9.94E+08	2.15E-03
Ag108m	3.18E-09	1.08E-13		Cd111m	1.79E+08	3.87E-04
Ce141	6.01E-01	9.97E-07		Mo 99	1.60E+08	3.46E-04
Rest	3.67E+00	6.08E-06		Rest	3.73E+08	8.06E-04

Table 7.2.5 Radionuclides and Percent Activity of the Activation Products of Tc-99 in a D-T Thermalized Flux spectrum.

	Base Case Level				High Flux Case Level	
NUCLIDE	ACTIVITY	PERCENT		NUCLIDE	ACTIVITY	PERCENT
	(Bq)	ACTIVITY			(Bq)	ACTIVITY
Total	9.55E+10			Total	9.72E+13	
Ru103	3.12E+10	3.27E+01		Ru103	3.18E+13	3.27E+01
Rh103m	3.09E+10	3.24E+01		Rh104	3.14E+13	3.23E+01
Rh104	3.09E+10	3.23E+01		Rh103m	3.14E+13	3.23E+01
Rh104m	2.34E+09	2.45E+00		Rh104m	2.38E+12	2.45E+00
Tc100	1.00E+08	1.05E-01		Tc100	1.05E+11	1.08E-01
Ru105	7.83E+06	8.20E-03		Ru105	3.84E+10	3.95E-02
Rh105	7.81E+06	8.18E-03		Rh105	2.79E+10	2.88E-02
Tc 99	3.27E+06	3.42E-03		Rh105m	1.07E+10	1.11E-02
Pd109	2.46E+06	2.58E-03		Rh106	9.40E+09	9.68E-03
Ag109m	2.46E+06	2.58E-03		Pd109	2.94E+09	3.02E-03
Rh105m	2.19E+06	2.29E-03		Ag109m	2.93E+09	3.02E-03
Pd107m	2.13E+06	2.23E-03		Ag110	2.46E+09	2.53E-03
Ag110	2.05E+06	2.15E-03		Pd107m	2.41E+09	2.48E-03
Ag110m	9.90E+04	1.04E-04		Rh106m	9.99E+08	1.03E-03
Pd107	7.81E+04	8.19E-05		Pd109m	6.42E+07	6.61E-05
Ag108	5.90E+04	6.18E-05		Ag110m	6.25E+07	6.43E-05
Pd109m	5.38E+04	5.63E-05		Ag111	5.20E+07	5.36E-05
Cd111m	4.98E+03	5.22E-06		Ag111m	2.62E+07	2.70E-05
Cd109	4.05E+03	4.24E-06		Cd111m	5.96E+06	6.13E-06
Rh106	2.61E+03	2.74E-06		Tc 99	3.41E+06	3.51E-06
Rest	1.19E+04	1.25E-05		Rest	9.13E+06	9.40E-06

7.2.3 Radiation Protection and Dose Rate Calculation

The activation products resulting from the transmutation of Tc-99 as shown in Section 7.2.2 will have hazards associated with them. These are referred to as the hazard indexes. As described in Section 4.4, the hazard indexes evaluated include gamma dose rate at the surface of the activation products, the ingestion dose (committed effective dose equivalent), and the inhalation dose (committed effective dose equivalent) from each of the base cases at both the base case flux level as well as the high flux case level. Table 7.2.6 shows the summary of the hazard indexes of the activation products generated by the transmutation of Tc-99 down to the ending activity level for each of the base cases considered.

Results show that the dose rate, ingestion hazard, and inhalation hazard are all directly proportional to the flux used for transmutation; i.e., the higher the flux, the higher the hazard indexes. Results also show that the hazards from the activation products from a D-D moderated neutron spectrum can have 3 orders of magnitude lower dose rates, ingestion hazard, and/or inhalation hazard than the D-T moderated and D-T thermalized base cases. The reason for this is the smaller activities of activation products generated. The hazard indexes for the D-T thermalized case are the highest

Table 7.2.6 Hazard Indexes Summary of the Activation Products for Tc-99

Neutron Spectrum Used	On-target flux (n/s/cm2)	Activation Product Dose rate (Sv/hr)	Activation Ingestion Dose (Sv)	Activation Inhalation Dose (Sv)
D-T moderated BC	1.55E+11	8.48E+00	3.74E+00	1.52E+01
	1.55E+12	9.05E+01	3.99E+01	1.62E+02
	1.55E+13	9.04E+02	3.99E+02	1.62E+03
	1.55E+14	8.98E+03	3.96E+03	1.60E+04
D-T moderated HFC	1.55E+15	8.71E+04	3.82E+04	1.53E+05
D-D moderated BC	5.14E+08	3.67E-05	1.82E-03	3.69E-02
	5.14E+09	2.48E-02	1.25E-02	7.79E-02
	5.14E+10	1.89E+00	8.33E-01	3.43E+00
	5.14E+11	2.51E+01	1.11E+01	4.50E+01
	5.14E+12	2.57E+02	1.13E+02	4.61E+02
	5.14E+13	2.57E+03	1.13E+03	4.60E+03
D-D moderated HFC	5.14E+14	2.55E+04	1.12E+04	4.55E+04
D-T Thermalized BC	1.83E+11	5.23E+01	2.30E+01	9.39E+01
	1.83E+12	5.32E+02	2.34E+02	9.54E+02
	1.83E+13	5.36E+03	2.35E+03	9.61E+03
D-T Thermalized HFC	1.83E+14	5.33E+04	2.34E+04	9.54E+04

In evaluating the dose rate hazard index, the decay characteristics of the activation product is important as well, such as is common when evaluating the hazards of spent fuel. Figure 7.2.4 shows the comparison of the decay curves for the activation products between the base and high flux cases of the D-T moderated base case. Likewise, Figures 7.2.5 and 7.2.6 show the comparisons for the D-D moderated base case and the D-T thermalized base case, respectively. These figures designate a “recycling limit” and a “hands on” limit. The values for these limits are 1 R/h and 1mR/h, respectively [31].

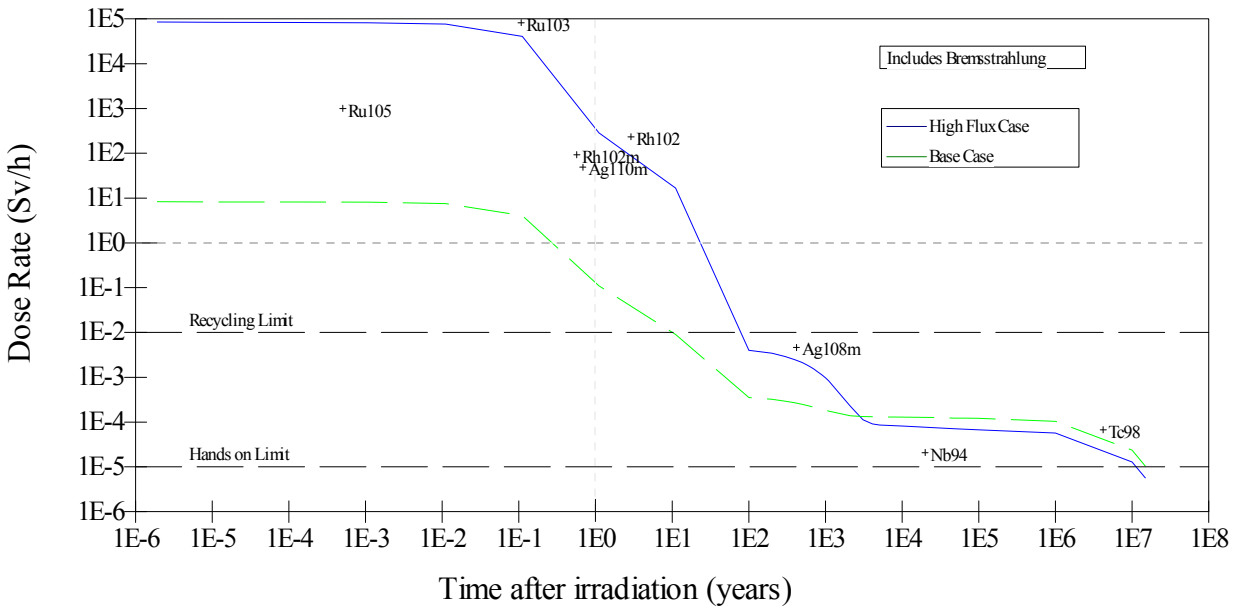

Figure 7.2.4 Decay Curve of Tc-99 Activation Products for the D-T moderated Base Case

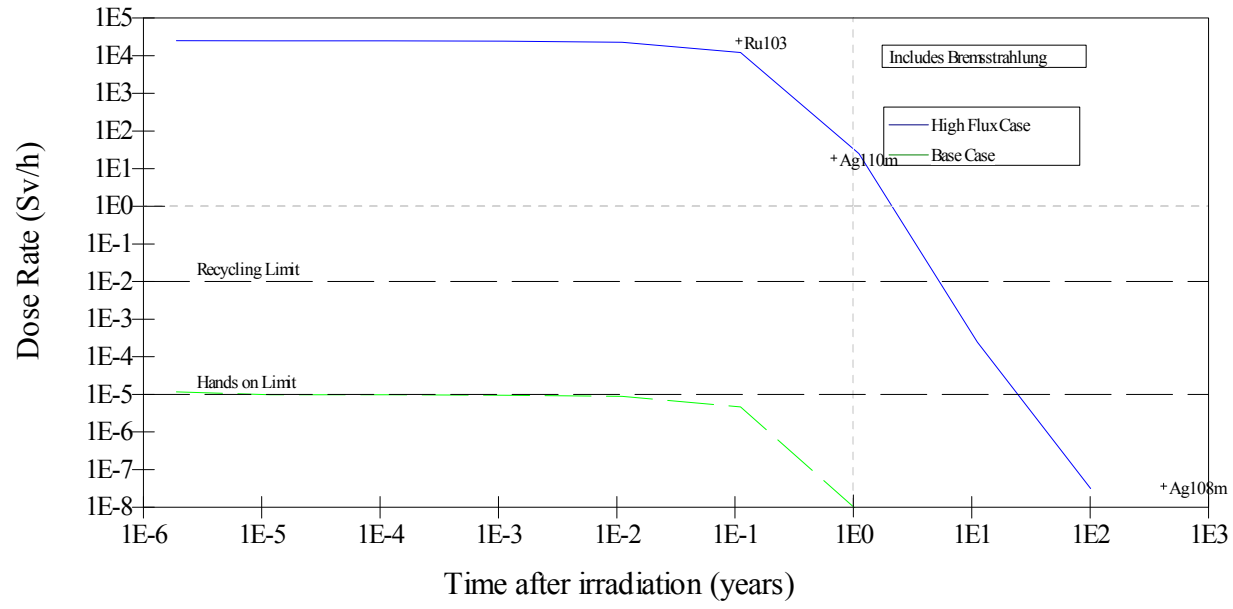

Figure 7.2.5 Decay Curve of Tc-99 Activation Products for the D-D moderated Base Case

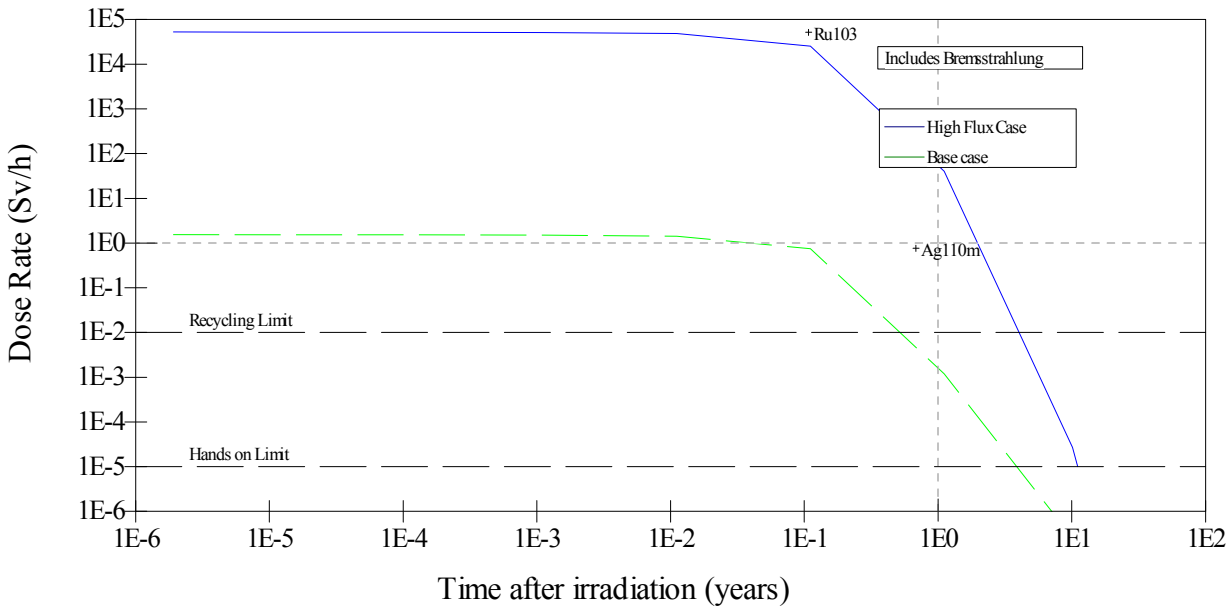

Figure 7.2.6 Decay Curve of Tc-99 Activation Products for the D-T Thermalized Base Case

Figure 7.2.4 shows that the D-T moderated case generates activation products that require an extremely long time to decay to the "hands on" value of 1 mR/h. This is not the case for the lower energy D-D moderated spectrum or the D-T thermalized spectrum. For the D-T moderated case, the radionuclide that dominates the long-lived characteristic of the activation product is Tc-98 which is produced from the (n, 2n) reaction with Tc-99. Tc-98 has a half-life is 4.2E+06 year and emits two gammas at 652 and 745 keV with 98% and 100% probability, respectively [43]. The threshold for this reaction, shown in Figure 7.2.2, is above 9 MeV; and therefore, is not generated in the D-D moderated case or the D-T thermalized case. In the D-D Moderated case, the dose rate from the total activation products at the end of irradiation is already as low as the "hands-on limit" while the D-T thermalized generates activation products that will decay down to 1 mR/h

in the matter of years. Table 7.2.7 summarizes the approximate cooling time for the activation products to reach 1 mR/h dose rate.

Table 7.2.7 Summary of Cooling Time for Tc-99 Activation Products

Neutron Spectrum Used	Approximate Cooling time To 1 mR/h (yrs)
D-T moderated BC	1.5E+07
D-T moderated HFC	1.1E+07
D-D moderated BC	2.00E-06 (~ 2 min.)
D-D moderated HFC	2.00E+01
D-T Thermalized BC	5.00E+00
D-T Thermalized HFC	1.10E+01

7.2.4 Discussion

The following observations were made regarding the transmutation of Tc-99:

- Only two of the three base cases produce effective half-lives lower than the radiological half-life of the Tc-99, with the D-D moderated case being the exception.
- The transmutation characteristics of Tc-99 is very similar to I-129 with the lower energy spectrum (thermalized) being most advantageous to transmute Tc-99
- Irradiation effective half-life is inversely proportional to the flux for all three base cases.
- Activation product generation is directly proportional to the flux for all three base cases.

- The hazard indexes correlate directly to amount of activation products that are generated for all three base cases.
- The decay of activation products are longer for activation products generated by the higher flux case than the base case flux for all three base cases. In the D-T moderated case the difference is not that substantial; however, the differences in the D-D moderated and D-T thermalized cases are more significant.
- The D-T moderated case produces radionuclides that are even longer-lived than the Tc-99. The use of lower energy transmutation (D-D moderated and D-T thermalized) produces significantly shorter-lived transmutation products than the D-T moderated case.
- The minimum required improvement in technology for practical transmutation of Tc-99 is about 3 orders of magnitude increase in the neutron source strength (n/s) of the present D-T neutron generator output. Also it must be used in the D-T thermalized configuration to prevent the higher order processes that would lead to long-lived radionuclides such as Tc-98.

7.3 Cesium-137

For Cs-137, it is difficult to determine the more advantageous energy spectrum to use for transmutation. Figure 7.3.1 shows the neutron cross sections for reactions for Cs-137. As can be seen from the figure, the total neutron cross section is dominated by the elastic scattering cross section and is very low (< ~ 20 barns with most of energy spectrum < 10 barns). The capture cross section, which was so important for the I-129 and Tc-99 transmutation is non-existent up to about 0.3 MeV and not very substantial thereafter. All four base cases, D-T unmoderated, D-T moderated, D-D moderated, and D-T thermalized, was used to determine which scheme would be most beneficial to use for transmutation. It would seem that whichever case is used, the probability of reactions will not be high so the transmutation efficiency will be low.

Figure 7.3.2 shows the thresholds for different reactions for Cs-137. For the D-D neutron generator case, the major reactions are inelastic collisions. For the D-T neutron generator cases, major reactions will also include (n, 2n) reactions. There will also be small amounts of (n, α) and (n, p) reactions.

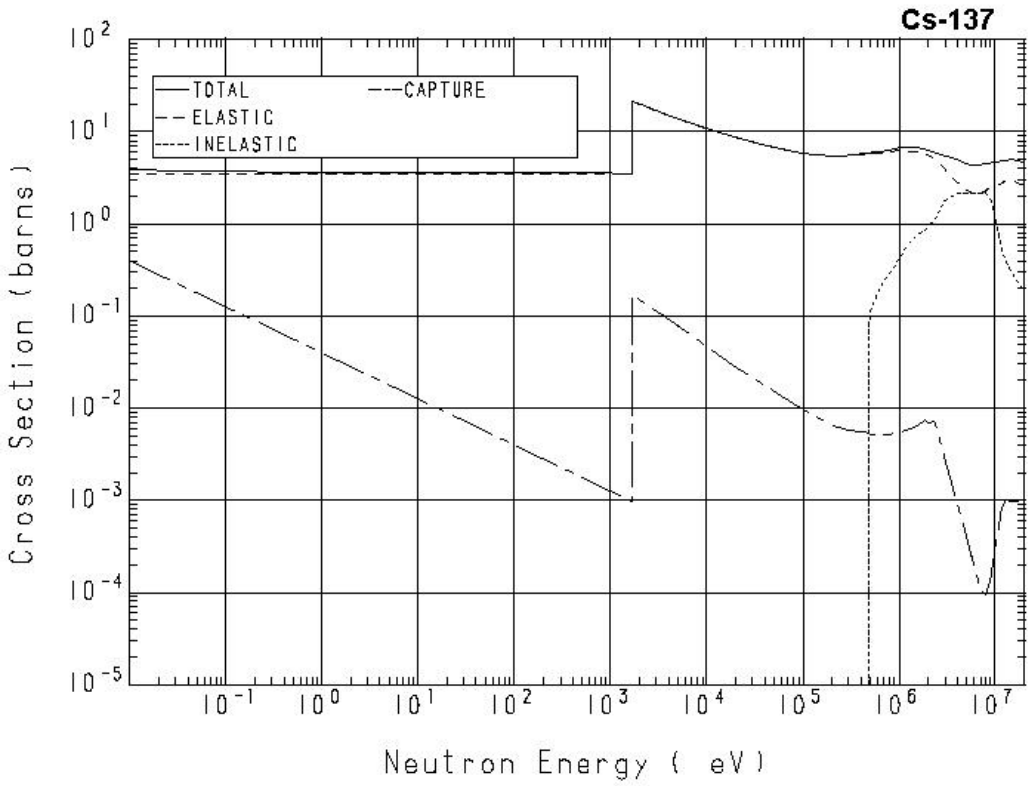

Figure 7.3.1 Neutron Reaction Cross Sections for Cs-137 [43]

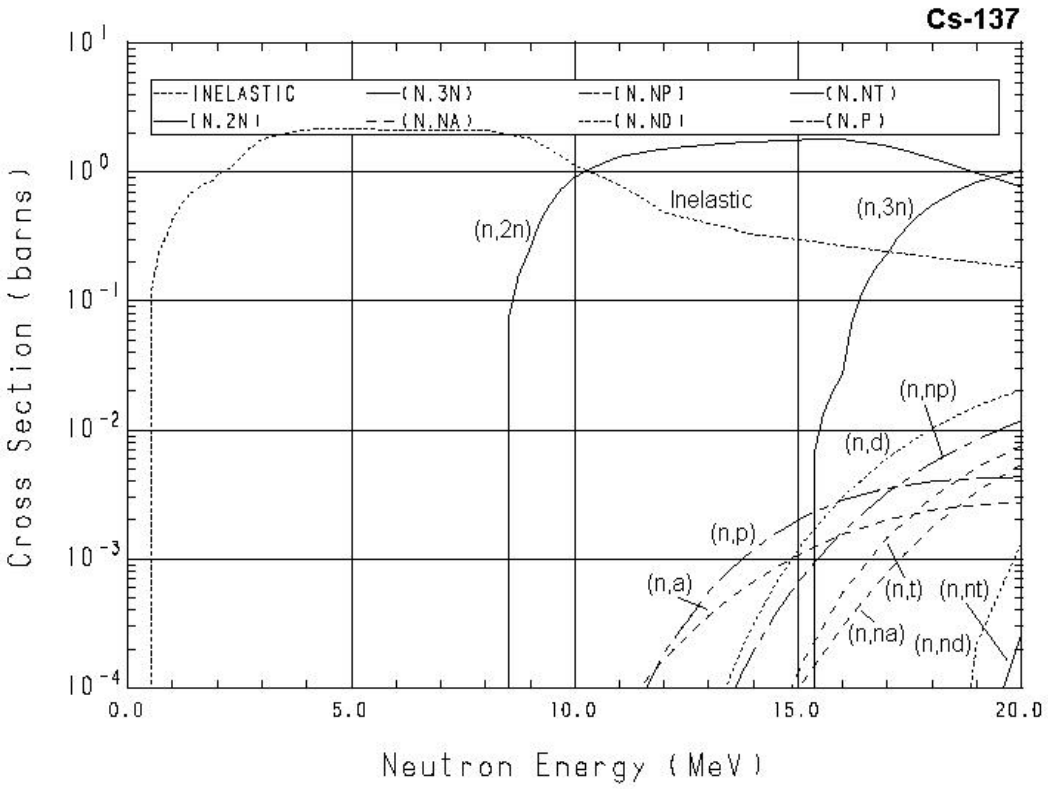

Figure 7.3.2 Neutron Reaction Thresholds for Cs-137 [43]

7.3.1 Results of Transmutation

Table 7.3.1 shows the results of the transmutation calculations for Cs-137 with a radiological half-life of 30.1 years. For Cs-137, the starting activity is 3.7e+10 Bq (1.0 Ci) and the ending activity is 3.7e+05 Bq (0.01 mCi). Under the description of the neutron spectrum used for the transmutation calculation, the BC stands for base case. Unlike the I-129 and Tc-99 cases, the neutron fluence requirements for transmutation do not stay consistent as the flux increases. The Table shows results of increasing the flux of the base case; however, the high flux case is not applicable in the case of Cs-137 because the increase in flux required to get the irradiation time down to < 100 years is

unreasonably high. The irradiation half-life is driven by the physical half-life of the Cs-137 (30.17 years) because of the predominant inelastic collision cross section and the low probability of reactions. The irradiation effective half-life will actually increase in the D-T neutron generator cases. The reason for this is that the higher order processes such as (n, 2n) and (n, p) results in the production of more Cs-137.

Table 7.3.1 Transmutation Results for Cs-137

					Irradiation
Neutron Energy spectrum	On-target flux (n/s/cm2)	Irradiation Time (yrs)	Ending Activity (Bq)	Fluence Required (n/cm2)	Effective Half-life (yrs)
D-T Unmoderated BC	1.23E+11	5.01E+02	3.68E+05	1.94E+21	3.02E+01
	1.23E+12	5.05E+02	3.68E+05	1.96E+22	3.05E+01
	1.23E+13	6.30E+02	3.69E+05	2.44E+23	3.80E+01
	1.23E+14	5.60E+03	3.70E+05	2.17E+25	3.38E+02
	1.23E+15	3.20E+03	3.66E+05	1.24E+26	1.93E+02
D-T Moderated BC	1.55E+11	5.01E+02	3.68E+05	2.45E+21	3.02E+01
	1.55E+12	5.05E+02	3.68E+05	2.47E+22	3.05E+01
	1.55E+13	5.93E+02	3.69E+05	2.90E+23	3.58E+01
	1.55E+14	1.60E+04	3.65E+05	7.81E+25	9.64E+02
	1.55E+15	7.00E+03	3.64E+05	3.42E+26	4.22E+02
D-D Moderated BC	5.14E+08	5.01E+02	3.65E+05	8.11E+18	3.02E+01
	5.14E+09	5.01E+02	3.65E+05	8.11E+19	3.02E+01
	5.14E+10	5.01E+02	3.65E+05	8.11E+20	3.02E+01
	5.14E+11	5.01E+02	3.65E+05	8.11E+21	3.02E+01
	5.14E+12	5.01E+02	3.64E+05	8.11E+22	3.02E+01
	5.14E+13	5.00E+02	3.63E+05	8.10E+23	3.01E+01
	5.14E+14	4.88E+02	3.69E+05	7.90E+24	2.94E+01
D-T Thermalized BC	1.83E+11	5.00E+02	3.73E+05	2.88E+21	3.02E+01
	1.83E+12	5.00E+02	3.72E+05	2.88E+22	3.02E+01
	1.83E+13	5.00E+02	3.60E+05	2.88E+23	3.01E+01
	1.83E+14	5.00E+02	2.60E+05	2.88E+24	2.93E+01
	1.83E+15	4.00E+02	2.05E+05	2.31E+25	2.30E+01

For example, Cs-136 can result from the (n, 2n) reaction on Cs-137. After which, neutron capture can occur thereby creating Cs-137 again. Also, Xe137 can result from (n, p) reactions on Cs-137; which then decays back to Cs-137 by beta decay. The irradiation effective half-life begins to fall again once the flux level is high enough to begin to overcome the production mechanisms of Cs-137.

These types of reactions do not occur in the lower energy spectra such as the D-D moderated case or the D-T thermalized case. So even though the irradiation half-life doesn't increase in the lower energy cases as it does for the D-T cases, higher fluxes do not decrease the irradiation effective half-life to a point where it is lower than the radiological half-life until there is at least six order of magnitude increase for the D-D case and four orders of magnitude for the D-T thermalized case.

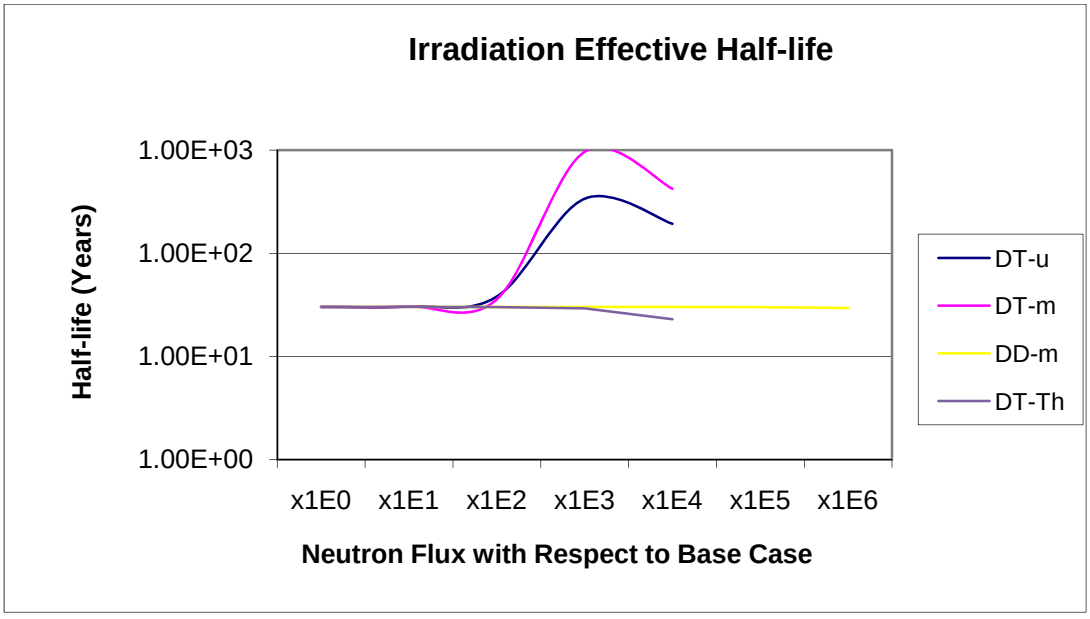

Figure 7.3.3 Irradiation Effective Half-life as a Function of Neutron Flux for Cs-137

Figure 7.3.3 shows the fact that in the lower energy cases, the radiological half-life dominates the irradiation effective half-life; therefore, there is no benefit in the timely destruction of the Cs-137 with increased flux; but rather, additional activation products will be created as discussed in the next section.

7.3.2 Activation Products

Table 7.3.2 shows the summary of activation products generated by the transmutation of Cs-137 down to the ending activity level. The total activity of the results of the transmutation is given as well as the number of radioactive and non-radioactive nuclides. Results show that using a higher energy spectrum for transmutation (D-T moderated case) generates many more radionuclides. The reason for this is the presence of higher order reactions which occur such as the (n,2n) or (n,p) reactions which do not occur using the D-D moderated base case or much less frequently using the D-T thermalized base case. In general, the number of activation products produced with Cs-137 is lower than in the cases of I-129 and Tc-99 transmutation. This can be explained by the low interaction cross sections and the predominance of the elastic scattering cross section. Table 7.3.2 also shows that the total activity of activation products generated is directly proportional to the flux. In other words, the higher the fluxes used, the more activation products are generated. Although there is not a high flux case as defined in Section 4.3 for Cs-137, the activation products for the iterative case of the highest flux evaluated for each of the base cases is presented to give a perspective on the difference in activation products generated.

Table 7.3.2 Activation Products Summary for Cs-137

Neutron Spectrum Used	On-target flux (n/s/cm2)	Total Activation (Bq)	Number of Radioactive Nuclides	Number of Non-radioactive Nuclides
D-T Unmoderated BC	1.23E+11	1.57E+06	28	19
	1.23E+12	9.26E+06	40	23
	1.23E+13	8.51E+07	57	32
	1.23E+14	8.48E+08	170	79
	1.23E+15	9.36E+09	386	152
D-T Moderated BC	1.55E+11	1.45E+06	32	21
	1.55E+12	8.01E+06	47	26
	1.55E+13	7.21E+07	75	38
	1.55E+14	1.99E+09	399	121
	1.55E+15	8.30E+09	426	119
D-D Moderated BC	5.14E+08	7.12E+05	5	8
	5.14E+09	7.30E+05	6	8
	5.14E+10	9.16E+05	8	12
	5.14E+11	2.77E+06	11	13
	5.14E+12	2.09E+07	22	19
	5.14E+13	1.73E+08	48	43
	5.14E+14	8.60E+08	161	89
D-T Thermalized BC	1.83E+11	7.60E+05	12	13
	1.83E+12	4.23E+06	25	19
	1.83E+13	3.26E+08	65	52
	1.83E+14	1.08E+10	158	85
	1.83E+15	2.46E+10	180	84

Table 7.3.3 shows the most prominent activation products for transmutation of Cs-137 in a D-T moderated spectrum, both at base case and the highest flux case evaluated. The radionuclides shown are present at the end of the transmutation period. Results show that the activation products generated by transmutation are a function of the flux level used because the production of the different radionuclides is dependent upon each radionuclides production (or reaction) cross section and then their subsequent decay

rate. For Cs-137, all the base cases show that the time required for transmutation down to the ending activity is about 500 years which is the amount of time the radiological half-life would reduce the Cs-137 down to the target level. In other words, transmutation is not practical for Cs-137. Trying to transmute Cs-137 would only serve to create additional activation products that would need to be handled appropriately. Also at the base cases, not many activation products are generated. For the D-D moderated case (Table 7.3.5), there is very few activation products. The reason for this is that the initial flux is so low (about three orders of magnitude lower than the D-T cases) and the cross sections as seen in Figure 7.3.1 are so low that there are not many neutron interactions occurring.

Table 7.3.4 shows the prominent activities for transmutation of Cs-137 in a D-T moderated spectrum. Table 7.3.5 shows the most prominent activation products for transmutation of Cs-137 in a D-D moderated spectrum, both at base case and high flux case levels. With a D-D moderated spectrum, the Cs-137 still dominates the resulting activity of all the activation products at the base case level. Likewise, Table 7.3.6 shows the most prominent activation products for the transmutation of Cs-137 in a D-T thermalized spectrum.

Table 7.3.3 Radionuclides and Percent Activity of the Activation Products of Cs-137 in a D-T Unmoderated Flux spectrum.

	Base Case Level				Highest Flux Case Level	
NUCLIDE	ACTIVITY	PERCENT		NUCLIDE	ACTIVITY	PERCENT
	(Bq)	ACTIVITY			(Bq)	ACTIVITY
Total	1.57E+06			Total	9.36E+09	
Ba137m	8.88E+05	5.65E+01		Xe131m	1.36E+09	1.45E+01
Cs137	3.68E+05	2.34E+01		Ba135m	9.57E+08	1.02E+01
Ba136m	3.15E+05	2.00E+01		Xe127	9.02E+08	9.64E+00
Cs136	4.03E+02	2.57E-02		Te125m	7.41E+08	7.91E+00
Xe134m	1.60E+02	1.02E-02		Xe129m	7.12E+08	7.60E+00
Ba135m	1.37E+02	8.71E-03		I 128	6.51E+08	6.96E+00
Cs136m	5.37E+01	3.42E-03		Ba133	6.37E+08	6.81E+00
H 3	3.91E+01	2.49E-03		Cs134	4.87E+08	5.21E+00
Xe133	5.37E+00	3.41E-04		I 126	4.25E+08	4.54E+00
Xe133m	2.55E+00	1.63E-04		Te123m	3.84E+08	4.10E+00
Xe135	1.41E+00	8.95E-05		Ba133m	3.61E+08	3.86E+00
Cs135m	1.33E+00	8.47E-05		Cs132	3.52E+08	3.76E+00
Xe135m	6.47E-01	4.12E-05		Te127	1.83E+08	1.95E+00
Ba139	4.71E-01	2.99E-05		Xe133	1.74E+08	1.86E+00
Cs138	2.50E-01	1.59E-05		Xe127m	1.60E+08	1.71E+00
Cs138m	3.97E-02	2.53E-06		Ba136m	9.44E+07	1.01E+00
Cs134	1.49E-02	9.47E-07		Xe125	9.32E+07	9.96E-01
Xe137	6.87E-03	4.37E-07		I 125	9.30E+07	9.94E-01
Cs135	5.72E-03	3.64E-07		Ba137m	8.08E+07	8.64E-01
I 134	3.94E-03	2.51E-07		Te121	7.75E+07	8.28E-01
Rest	7.95E-02	5.06E-06		Rest	4.35E+08	4.65E+00

Table 7.3.4 Radionuclides and Percent Activity of the Activation Products of Cs-137 in a D-T Moderated Flux spectrum.

	Base Case Level				Highest Flux Case Level	
NUCLIDE	ACTIVITY	PERCENT		NUCLIDE	ACTIVITY	PERCENT
	(Bq)	ACTIVITY			(Bq)	ACTIVITY
Total	1.45E+06			Total	8.30E+09	
Ba137m	7.58E+05	5.24E+01		Pb203	1.72E+09	2.07E+01
Cs137	3.68E+05	2.54E+01		Tl204	1.50E+09	1.81E+01
Ba136m	3.20E+05	2.21E+01		Pb203m	1.00E+09	1.21E+01
Cs136	4.03E+02	2.78E-02		Pb204m	8.32E+08	1.00E+01
Xe134m	1.62E+02	1.12E-02		Tl206	3.30E+08	3.98E+00
Ba135m	1.44E+02	9.97E-03		Hg203	2.04E+08	2.46E+00
Ba139	9.40E+01	6.50E-03		La140	1.57E+08	1.89E+00
H 3	5.61E+01	3.88E-03		Ba137m	1.42E+08	1.71E+00
Cs136m	5.36E+01	3.70E-03		Ce139	1.22E+08	1.48E+00
Xe133	5.33E+00	3.68E-04		Ce139m	1.19E+08	1.44E+00
Cs138	3.86E+00	2.67E-04		Tl202	1.05E+08	1.26E+00
Xe133m	2.54E+00	1.75E-04		Pb207m	1.03E+08	1.24E+00
Xe135	2.28E+00	1.58E-04		H 3	8.01E+07	9.65E-01
Cs135m	1.32E+00	9.15E-05		Pt197	6.95E+07	8.38E-01
Xe135m	9.71E-01	6.71E-05		Yb175	6.39E+07	7.69E-01
Cs138m	6.67E-01	4.61E-05		Pr142	6.36E+07	7.67E-01
Cs134	1.48E-01	1.02E-05		Os191	6.18E+07	7.44E-01
La140	6.58E-02	4.55E-06		Er169	6.12E+07	7.38E-01
Cs134m	1.60E-02	1.11E-06		Gd159	6.10E+07	7.35E-01
Xe137	8.01E-03	5.54E-07		Ce141	6.01E+07	7.24E-01
Rest	7.98E-02	5.51E-06		Rest	1.44E+09	1.73E+01

Table 7.3.5 Radionuclides and Percent Activity of the Activation Products of Cs-137 in a D-D Moderated Flux spectrum.

	Base Case Level				Highest Flux Case Level	
NUCLIDE	ACTIVITY	PERCENT		NUCLIDE	ACTIVITY	PERCENT
	(Bq)	ACTIVITY			(Bq)	ACTIVITY
Total	7.12E+05			Total	8.60E+08	
Cs137	3.65E+05	5.12E+01		Ba139	3.10E+08	3.60E+01
Ba137m	3.47E+05	4.88E+01		La140	2.76E+08	3.21E+01
Cs138	9.29E-03	1.31E-06		Ba137m	2.21E+08	2.56E+01
Ba139	8.65E-04	1.22E-07		Ce141	2.41E+07	2.81E+00
Cs135	3.71E-13	5.21E-17		Pr142	1.85E+07	2.16E+00
				Pr142m	6.45E+06	7.50E-01
				Nd147	7.63E+05	8.87E-02
				Sm153	4.88E+05	5.67E-02
				Eu156	4.21E+05	4.89E-02
				Cs137	3.69E+05	4.29E-02
				Pm148	2.93E+05	3.41E-02
				Gd159	2.73E+05	3.18E-02
				Dy165	2.26E+05	2.63E-02
				Ho166	2.09E+05	2.43E-02
				Tb160	2.09E+05	2.43E-02
				Pm147	2.02E+05	2.35E-02
				Pm149	1.53E+05	1.78E-02
				Dy165m	1.45E+05	1.69E-02
				Er167m	1.34E+05	1.56E-02
				Pm148m	1.16E+05	1.35E-02
				Rest	5.64E+05	6.56E-02

Table 7.3.6 Radionuclides and Percent Activity of the Activation Products of Cs-137 in a D-T Thermalized Flux spectrum

	Base Case Level				Highest Flux Case Level	
NUCLIDE	ACTIVITY	PERCENT		NUCLIDE	ACTIVITY	PERCENT
	(Bq)	ACTIVITY			(Bq)	ACTIVITY
Total	7.60E+05			Total	2.46E+10	
Cs137	3.73E+05	4.91E+01		Tl206	3.47E+09	1.41E+01
Ba137m	3.53E+05	4.64E+01		Hg203	2.77E+09	1.13E+01
Ba139	3.37E+04	4.44E+00		Pt197	2.18E+09	8.85E+00
La140	3.54E+02	4.66E-02		Au199	2.03E+09	8.24E+00
Cs138	1.15E+01	1.52E-03		Ir194	8.82E+08	3.59E+00
Cs138m	1.13E+00	1.49E-04		W 185	8.67E+08	3.52E+00
Ce141	1.62E-01	2.13E-05		Re186	8.59E+08	3.49E+00
Pr142	7.24E-04	9.52E-08		Os191m	7.55E+08	3.07E+00
Ba140	1.96E-04	2.59E-08		Ta183	7.06E+08	2.87E+00
Cs135	1.48E-09	1.94E-13		Os193	6.90E+08	2.81E+00
Nd144	2.62E-20	3.44E-24		Yb175	6.52E+08	2.65E+00
Ce142	5.23E-21	6.88E-25		Hf181	5.67E+08	2.30E+00
				Os191	4.98E+08	2.02E+00
				Lu176m	4.41E+08	1.79E+00
				Hf179m	4.30E+08	1.75E+00
				Tl204	3.98E+08	1.62E+00
				Er169	3.70E+08	1.50E+00
				Ir192m	3.59E+08	1.46E+00
				Dy165	3.32E+08	1.35E+00
				Gd159	3.31E+08	1.34E+00
				Rest	5.02E+09	2.04E+01

7.3.3 Radiation Protection and Dose Rate Calculation

The activation products resulting from the transmutation of Cs-137 as shown in Section 7.3.2 will have hazards associated with them. These are referred to as the hazard indexes. As described in Section 4.4, the hazard indexes evaluated include gamma dose rate at the surface of the activation products, the ingestion dose (committed effective dose equivalent), and the inhalation dose (committed effective dose equivalent) from each of the base cases at both the base case flux level as well as the highest flux case evaluated. Table 7.3.7 shows the summary of the hazard indexes of the activation products generated by the transmutation of Cs-137 down to the ending activity level for each of the base cases considered.

Results show that the dose rate of the activation products will increase with the increase in flux; however, the ingestion and inhalation hazards do not increase significantly with flux until a flux level is reached that would overcome the low cross section characteristics thereby generating more activation products. For all the base cases, the Cs-137 and it's daughter product Ba-137m dominates the ingestion and inhalation hazard index; which explains why these indexes do not change significantly with flux, initially. Results also show that the hazards from the activation products from a D-D moderated neutron spectrum have the lowest hazard indexes (dose rates, ingestion hazard, and/or inhalation hazard) than the D-T base cases. The reason for this is the smaller activities of activation products generated. The hazard indexes for the D-T unmoderated case are the highest for a given order of magnitude increase in flux applied to all base cases.

Table 7.3.7 Hazard Indexes Summary of the Activation Products for Cs-137

Neutron Spectrum Used	On-target flux (n/s/cm2)	Activation Product Dose rate (Sv/hr)	Activation Ingestion Dose (Sv)	Activation Inhalation Dose (Sv)
D-T Unmoderated BC	1.23E+11	2.48E+01	4.79E-03	1.44E-02
	1.23E+12	2.10E+02	4.82E-03	1.44E-02
	1.23E+13	2.01E+03	5.82E-03	1.52E-02
	1.23E+14	6.85E+03	1.86E+00	3.26E+00
	1.23E+15	3.59E+04	3.31E+01	7.36E+01
D-T Moderated BC	1.55E+11	2.35E+01	4.79E-03	1.44E-02
	1.55E+12	1.97E+02	4.81E-03	1.44E-02
	1.55E+13	1.78E+03	6.11E-03	1.54E-02
	1.55E+14	2.17E+04	1.45E+00	2.89E+00
	1.55E+15	7.78E+04	4.59E+00	4.80E+00
D-D Moderated BC	5.14E+08	4.09E+00	4.74E-03	1.42E-02
	5.14E+09	4.31E+00	4.74E-03	1.42E-02
	5.14E+10	6.49E+00	4.74E-03	1.42E-02
	5.14E+11	2.83E+01	4.75E-03	1.42E-02
	5.14E+12	2.42E+02	4.80E-03	1.42E-02
	5.14E+13	2.02E+03	9.00E-03	1.65E-02
	5.14E+14	1.90E+04	6.41E-01	4.49E-01
D-T Thermalized BC	1.83E+11	4.19E+00	4.86E-03	1.46E-02
	1.83E+12	2.36E+01	5.86E-03	1.50E-02
	1.83E+13	7.42E+03	2.88E-01	1.92E-01
	1.83E+14	1.18E+05	1.08E+01	1.67E+01
	1.83E+15	3.55E+04	1.69E+01	2.18E+01

In evaluating the dose rate hazard index, the decay characteristics of the activation product is important as well, such as is common when evaluating the hazards of spent fuel. Figure 7.3.4 shows the comparison of the decay curves for the activation products between the base and highest flux case evaluated for the D-T unmoderated base case. Likewise, Figures 7.3.5, 7.3.6 and 7.3.7 show the comparisons for the D-T moderated base case, the D-D moderated base case, and the D-T thermalized base case, respectively.

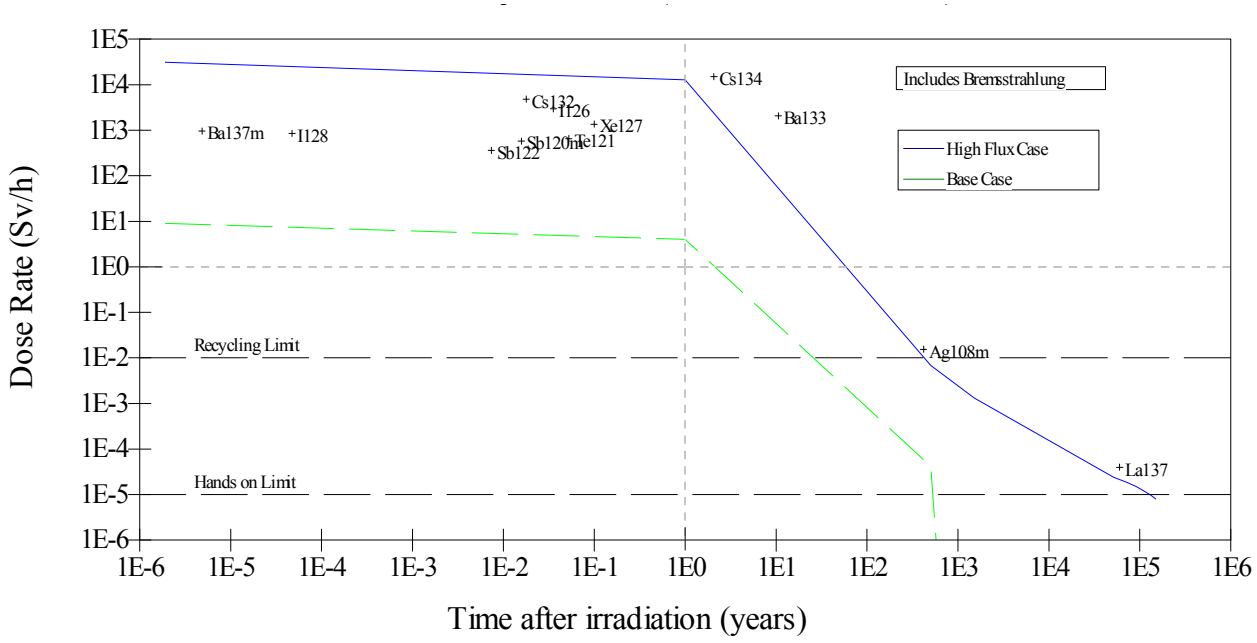

Figure 7.3.4 Decay Curve of Cs-137 Activation Products for the D-T Unmoderated Base Case

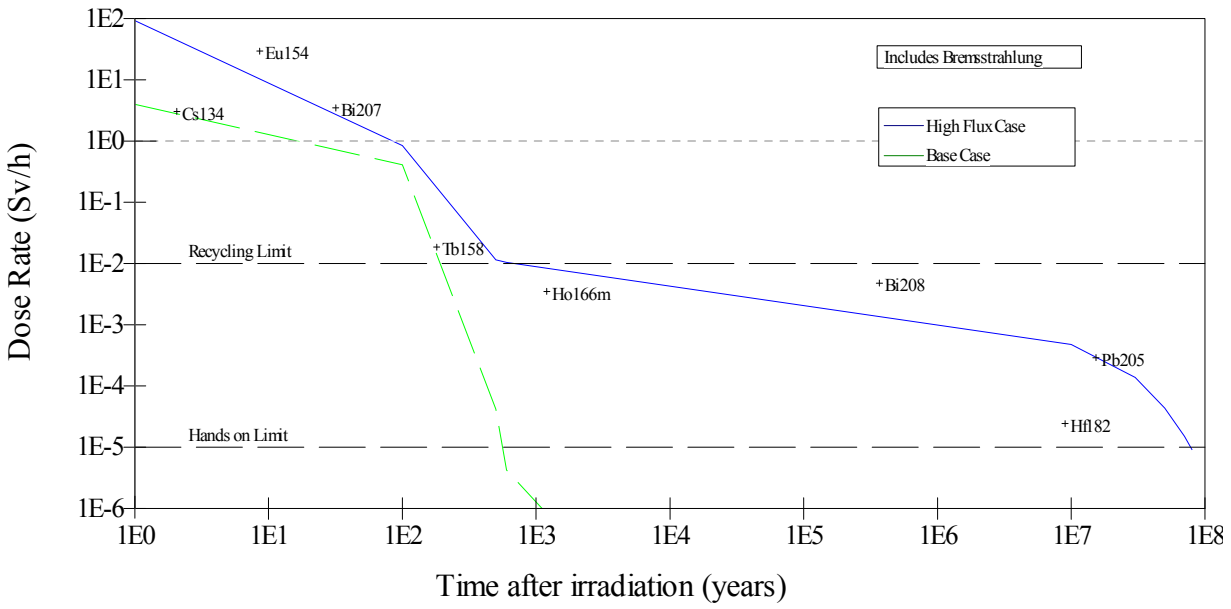

Figure 7.3.5 Decay Curve of Cs-137 Activation Products for the D-T Moderated Base Case

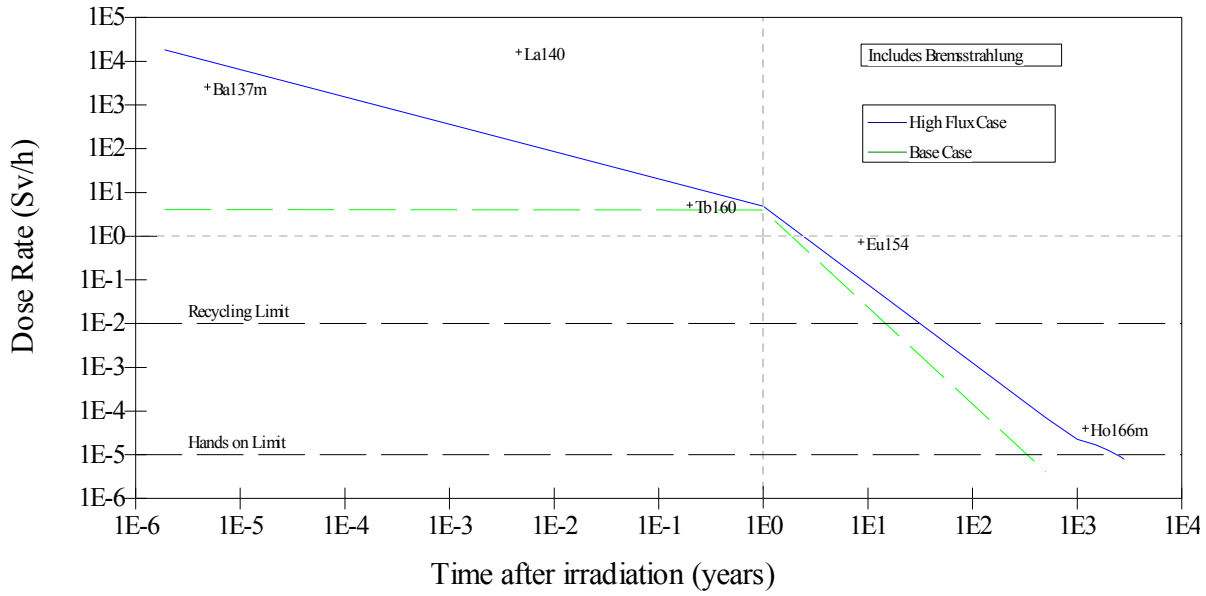

Figure 7.3.6 Decay Curve of Cs-137 Activation Products for the D-D Moderated Base Case

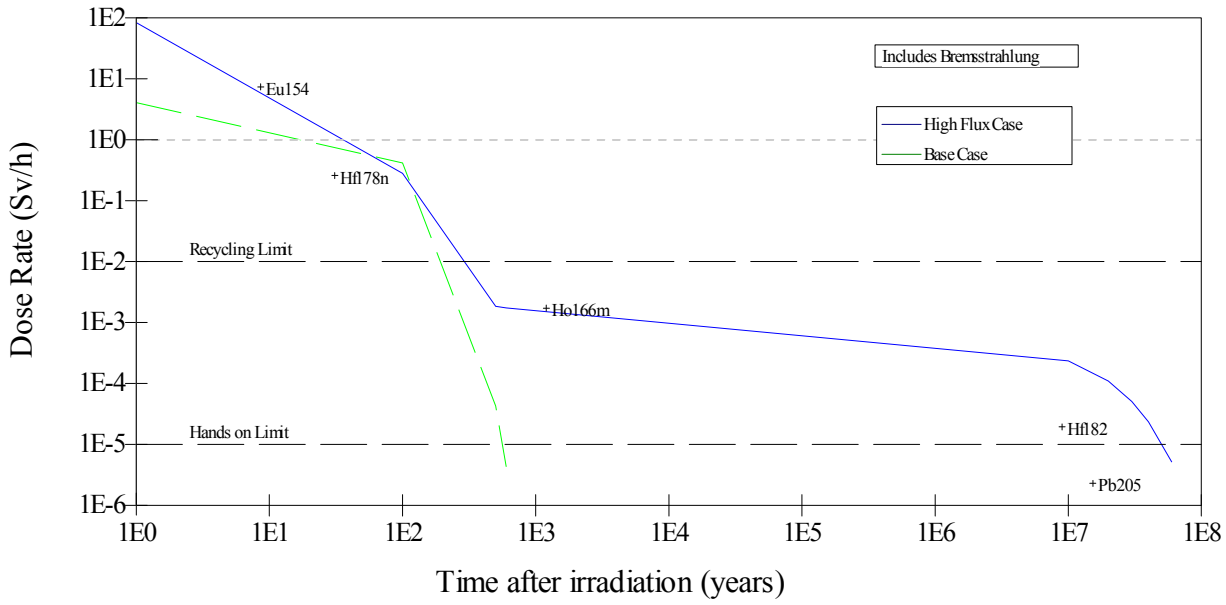

Figure 7.3.7 Decay Curve of Cs-137 Activation Products for the D-T Thermalized Base Case

Table 7.3.8 summarizes the approximate cooling time for the activation products to reach 1 mR/h dose rate. As noted above, for all the base cases, the cooling time is driven by the Cs-137 and its half-life. The long cooling times required for the activation products of the D-T Unmoderated highest flux case is due to La-137 (half-life of 6.0E+04 years) which beta decays to Ce-137 which contributes to the gamma dose rate. The long cooling times required by the D-T Moderated and Thermalized cases are due to the production of Pb-205 (half-life of 1.53E+07 years) which beta decays to Bi-205 which contributes to the gamma dose of the products.

Table 7.3.8 Summary of Cooling Time for Cs-137 Activation Products

Neutron Spectrum Used	Approximate Cooling time To 1 mR/h (yrs)
D-T Unmoderated BC	5.6E+02
D-T Unmoderated Highest Flux Case	1.2E+05
D-T Moderated BC	5.6E+02
D-T Moderated Highest Flux Case	7.5E+07
D-D Moderated BC	5.6E+02
D-D Moderated Highest Flux Case	2.4E+03
D-T Thermalized BC	5.6E+02
D-T Thermalized Highest Flux Case	7.0E+07

7.3.4 Discussion

The following observations were made regarding the transmutation of Cs-137:

- Transmutation is not recommended for Cs-137 with any of the base cases. Transmutation schemes at the base case levels will not transmute Cs-137 any faster than its radiological decay. Increasing the fluxes for all four base cases has either very little effect or serves to increase the effective half-life before decreasing it.
- Activation product generation is proportional to the flux for the base cases but increases very slowly for the first few orders of magnitude of flux increases; after which, the activation product activity will increase faster with flux but not as fast as in the case of I-129 or Tc-99 transmutation.

- The hazard indexes correlate directly to amount of activation products that are generated for all three base cases; but in general, these hazard indexes are not as high as with activation products of I-129 or Tc-99.
- The cooling time of the activation products are longer for activation products generated by the higher flux case than the base case flux for all four base cases. In the D-D moderated case the difference is not that substantial, about a factor of 25; however, in all the D-T cases the differences are more significant, from three to five orders of magnitude longer.

7.4 Strontium-90

For Sr-90, much like for Cs-137, it is difficult to determine the more advantageous energy spectrum to use for transmutation. Figure 7.4.1 shows the neutron cross sections for reactions for Sr-90. As can be seen from the figure, the total neutron cross section is dominated by the elastic scattering cross section and is very low (with most of the energy spectrum < 2 barns). The capture cross section, which was so important for the I-129 and Tc-99 transmutation is non-existent up to about 0.9 MeV and not very substantial thereafter. All four base cases, D-T unmoderated, D-T moderated, D-D moderated, and D-T thermalized, was used to determine which scheme would be most beneficial to use for transmutation. It would seem that whichever case is used, the probability of reactions will not be high so the transmutation efficiency will be low.

Figure 7.4.2 shows the thresholds for different reactions for Sr-90. For the D-D neutron generator case, the major reactions are inelastic collisions. For the D-T neutron generator cases, major reactions will also include (n, 2n) reactions. There will also be small amounts of (n, α) and (n, p) reactions.

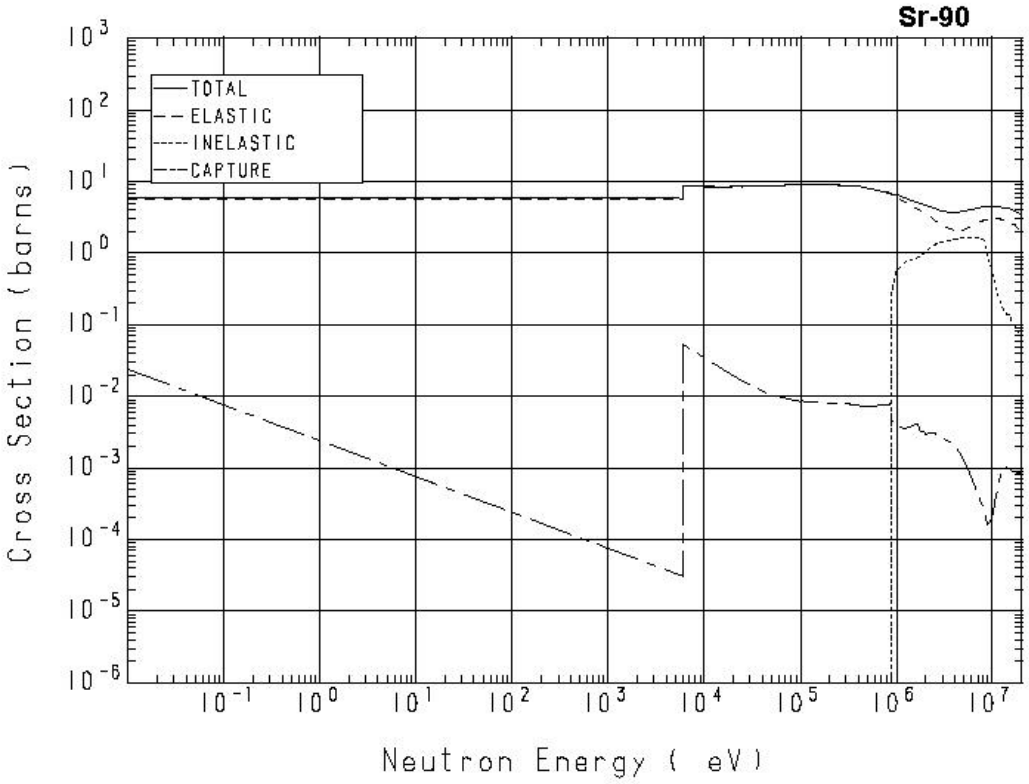

Figure 7.4.1 Neutron Reaction Cross Sections for Sr-90 [43]

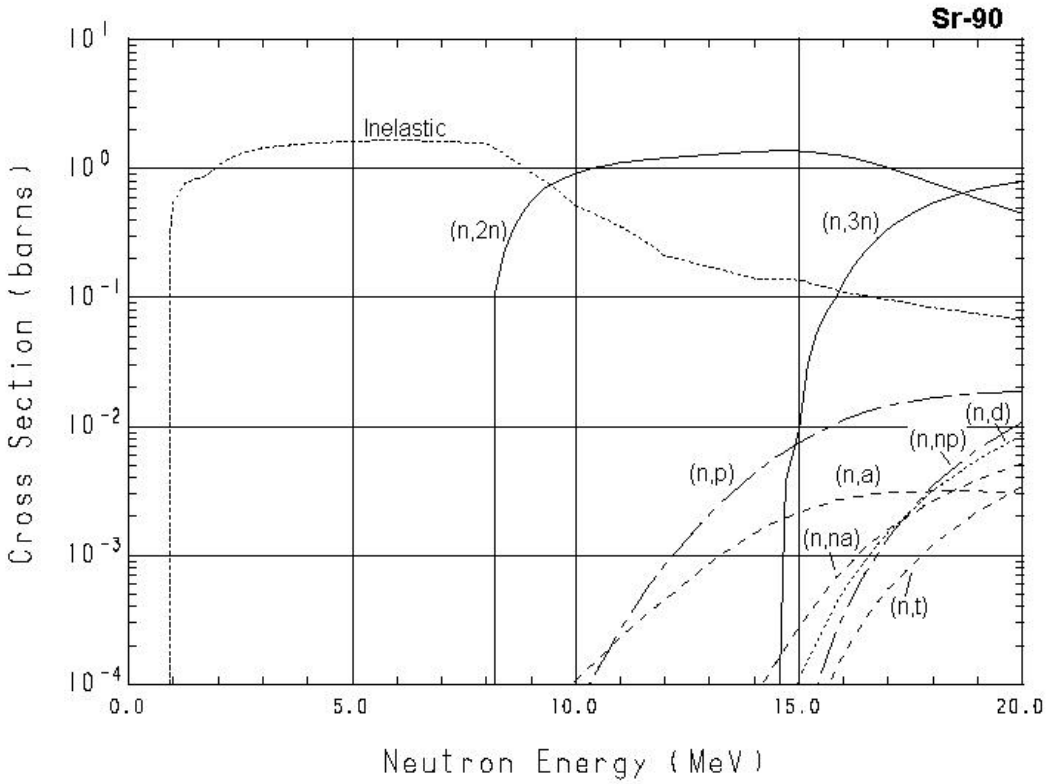

Figure 7.4.2 Neutron Reaction Thresholds for Sr-90 [43]

7.4.1 Results of Transmutation

Table 7.4.1 shows the results of the transmutation calculations for Sr-90 with a radiological half-life of 28.8 years. For Sr-90, the starting activity is 3.7e+10 Bq (1.0 Ci) and the ending activity is 3.7e+03 Bq (1.0E-4 mCi). Under the description of the neutron spectrum used for the transmutation calculation, the BC stands for base case. Like Cs-137, the neutron fluence requirements for transmutation of Sr-90 do not stay consistent as the flux increases. The Table shows results of increasing the flux of the base case; however, the high flux case is not applicable in the case of Sr-90 because the increase in flux required to get the irradiation time down to < 100 years is unreasonably high.

Table 7.4.1 Transmutation Results for Sr-90

Neutron Energy spectrum	On-target flux (n/s/cm2)	Irradiation Time (yrs)	Ending Activity (Bq)	Fluence Required (n/cm2)	Irradiation Effective Half-life (yrs)
D-T Unmoderated BC	1.23E+11	6.71E+02	3.66E+03	2.60E+21	2.89E+01
	1.23E+12	6.71E+02	3.65E+03	2.60E+22	2.89E+01
	1.23E+13	6.70E+02	3.64E+03	2.60E+23	2.88E+01
	1.23E+14	6.60E+02	3.58E+03	2.56E+24	2.84E+01
	1.23E+15	2.65E+03	3.56E+03	1.03E+26	1.14E+02
	1.23E+16	6.40E+02	3.60E+03	2.48E+26	2.75E+01
	1.23E+17	1.40E+02	3.67E+03	5.42E+26	6.02E+00
D-T Moderated BC	1.55E+11	6.71E+02	3.66E+03	3.28E+21	2.89E+01
	1.55E+12	6.71E+02	3.65E+03	3.28E+22	2.89E+01
	1.55E+13	6.70E+02	3.63E+03	3.27E+23	2.88E+01
	1.55E+14	6.71E+02	3.64E+03	3.28E+24	2.89E+01
	1.55E+15	1.00E+05	3.59E+03	4.88E+27	4.30E+03
	1.55E+16	1.38E+04	3.67E+03	6.74E+27	5.94E+02
	1.55E+17	1.12E+03	3.65E+03	5.44E+27	4.80E+01
	1.55E+18	6.16E+02	3.54E+03	3.01E+28	2.64E+01
D-D Moderated BC	5.14E+08	6.71E+02	3.66E+03	1.09E+19	2.89E+01
	5.14E+09	6.71E+02	3.66E+03	1.09E+20	2.89E+01
	5.14E+10	6.71E+02	3.66E+03	1.09E+21	2.89E+01
	5.14E+11	6.71E+02	3.66E+03	1.09E+22	2.89E+01
	5.14E+12	6.71E+02	3.66E+03	1.09E+23	2.89E+01
	5.14E+13	6.71E+02	3.63E+03	1.09E+24	2.88E+01
	5.14E+14	6.70E+02	3.44E+03	1.08E+25	2.87E+01
	5.14E+15	6.70E+02	2.53E+03	1.08E+26	2.82E+01
	5.14E+16	4.80E+02	3.67E+03	7.77E+26	2.07E+01
D-T Thermalized BC	1.83E+11	6.71E+02	3.66E+03	3.87E+21	2.89E+01
	1.83E+12	6.71E+02	3.66E+03	3.87E+22	2.89E+01
	1.83E+13	6.71E+02	3.65E+03	3.87E+23	2.89E+01
	1.83E+14	6.70E+02	3.63E+03	3.86E+24	2.88E+01
	1.83E+15	6.70E+02	2.69E+03	3.86E+25	2.83E+01
	1.83E+16	5.60E+02	3.26E+03	3.23E+26	2.39E+01

The irradiation half-life is driven by the radiological half-life of the Sr-90 (28.6 years) because of the predominant inelastic collision cross section and the low probability of reactions. The irradiation effective half-life will actually increase in the D-T neutron generator cases. The reason for this is that the higher order processes such as (n, 2n) and (n, p) results in the production of more Sr-90. For example, Sr-90 can result from the (n, 2n) reaction on Sr-91 which is generated from (n, γ) reaction on Sr-90. Also, the (n, 2n) reaction directly on Sr-90 could generate Sr-89 which can undergo (n, γ) and become Sr-90 again. Additionally, Sr-90 can result from (n, p) reactions on Y-90 which is a daughter product in secular equilibrium with Sr-90. The (n, p) reaction chain directly on Sr-90 could generate Rb-90 which then decays back to Sr-90. Therefore, there are many Sr-90 generation pathways. The irradiation effective half-life would begin to fall again once the flux level is high enough to begin to overcome the production mechanisms of Sr-90.

These types of reactions do not occur in the lower energy spectra such as the D-D moderated case or the D-T thermalized case. So even though the irradiation half-life doesn't increase in the lower energy cases as it does for the D-T cases, higher fluxes do not decrease the irradiation effective half-life to a point where it is lower than the radiological half-life until there is at least seven orders of magnitude increase for the D-D case and four orders of magnitude for the D-T thermalized case.

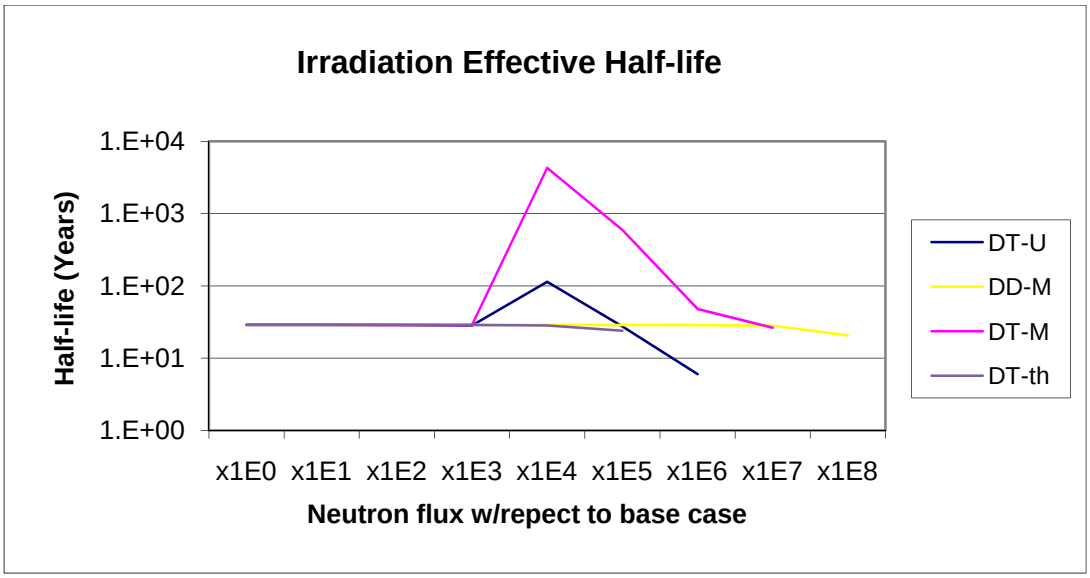

Figure 7.4.3 Irradiation Effective Half-life as a Function of Neutron Flux for Sr-90

Figure 7.4.3 shows the fact that in the lower energy cases, the radiological half-life dominates the irradiation effective half-life; therefore, there is no benefit in the timely destruction of the Sr-90 with increased flux; but rather, additional activation products will be created as discussed in the next section.

7.4.2 Activation Products

Table 7.4.2 shows the summary of activation products generated by the transmutation of Sr-90 down to the ending activity level. The total activity of the results of the transmutation is given as well as the number of radioactive and non-radioactive nuclides. Results show that using a higher energy spectrum for transmutation (D-T moderated case) generates many more radionuclides. The reason for this is the presence of higher order reactions which occur such as the (n,2n) or (n,p) reactions which do not occur using the D-D moderated base case or much less frequently using the D-T thermalized base case. In general, the number of activation products produced with Sr-90

is lower than in the cases of I-129 and Tc-99 transmutation. This can be explained by the low interaction cross sections and the predominance of the elastic scattering cross section. Table 7.4.2 also shows that the total activity of activation products generated is directly proportional to the flux. In other words, the higher the fluxes used, the more activation products are generated. Like Cs-137, there is not a high flux case as defined in Section 4.3; however, the activation products for the iterative case of the highest flux evaluated for each of the base cases is presented to give a perspective on the difference in activation products generated.

Table 7.4.2 Activation Products Summary for Sr-90

Neutron Spectrum Used	On-target flux (n/s/cm2)	Total Activation (Bq)	Number of Radioactive Nuclides	Number of Non-radioactive Nuclides
D-T Unmoderated BC	1.23E+11	1.01E+06	28	20
	1.23E+12	1.00E+07	37	23
	1.23E+13	9.99E+07	54	29
	1.23E+14	9.72E+08	90	44
	1.23E+15	5.02E+09	295	132
	1.23E+16	5.57E+10	438	175
	1.23E+17	4.40E+11	535	182
D-T Moderated BC	1.55E+11	1.05E+06	29	20
	1.55E+12	1.05E+07	39	26
	1.55E+13	1.05E+08	62	36
	1.55E+14	1.05E+09	130	70
	1.55E+15	3.81E+11	655	197
	1.55E+16	4.95E+10	688	192
	1.55E+17	3.65E+11	721	189
	1.55E+18	3.15E+12	750	185
D-D Moderated BC	5.14E+08	7.34E+03	7	8
	5.14E+09	7.47E+03	9	8
	5.14E+10	8.82E+03	11	11
	5.14E+11	2.23E+04	14	16
	5.14E+12	1.57E+05	19	22
	5.14E+13	1.48E+06	34	33
	5.14E+14	4.17E+07	104	74
	5.14E+15	3.25E+10	349	153
	5.14E+16	1.20E+10	353	152
D-T Thermalized BC	1.83E+11	7.32E+03	10	11
	1.83E+12	7.32E+03	14	17
	1.83E+13	7.50E+03	21	26
	1.83E+14	3.79E+06	66	51
	1.83E+15	5.20E+09	292	145
	1.83E+16	4.93E+10	315	146

Table 7.4.3 shows the most prominent activation products for transmutation of Sr-90 in a D-T moderated spectrum, both at base case and the highest flux case evaluated. The radionuclides shown are present at the end of the transmutation period. Results show

that the activation products generated by transmutation are a function of the flux level used because the production of the different radionuclides is dependent upon each radionuclides production (or reaction) cross section and then their subsequent decay rate. For Sr-90, all the base cases show that the time required for transmutation down to the ending activity is about 670 years which is the amount of time the radiological half-life would reduce the Sr-90 down to the target level. In other words, transmutation is not practical for Sr-90. Trying to transmute Sr-90 would only serve to create additional activation products that would need to be handled appropriately. Also at the base cases, not many activation products are generated. For the D-D moderated case (Table 7.4.5), there are very few activation products. The reason for this is that the initial flux is so low (about three orders of magnitude lower than the D-T cases) and the cross sections as seen in Figure 7.4.1 are so low that there are not many neutron interactions occurring.

Table 7.4.4 shows the prominent activities for transmutation of Sr-90 in a D-T moderated spectrum. Table 7.4.5 shows the most prominent activation products for transmutation of Sr-90 in a D-D moderated spectrum, both at base case and high flux case levels. With a D-D moderated spectrum, the Sr-90 still dominates the resulting activity of all the activation products at the base case level. Likewise, Table 7.4.6 shows the most prominent activation products for the transmutation of Sr-90 in a D-T thermalized spectrum.

Table 7.4.3 Radionuclides and Percent Activity of the Activation Products of Sr-90 in a D-T Unmoderated Flux spectrum.

	Base Case Level				Highest Flux Case Level	
NUCLIDE	ACTIVITY	PERCENT		NUCLIDE	ACTIVITY	PERCENT
	(Bq)	ACTIVITY			(Bq)	ACTIVITY
Total	1.01E+06			Total	4.40E+11	
Zr 90m	3.65E+05	3.62E+01		Se 77m	1.35E+11	3.08E+01
Y 89m	2.89E+05	2.87E+01		Se 79m	2.96E+10	6.74E+00
Zr 89	2.79E+05	2.77E+01		Kr 81m	2.83E+10	6.45E+00
Zr 89m	4.46E+04	4.42E+00		Ga 70	1.92E+10	4.37E+00
Y 90	1.97E+04	1.95E+00		Ge 71	1.90E+10	4.32E+00
Y 90m	5.65E+03	5.61E-01		Se 75	1.84E+10	4.20E+00
Sr 90	3.66E+03	3.63E-01		Kr 83m	1.55E+10	3.53E+00
Sr 87m	1.57E+03	1.56E-01		As 76	1.49E+10	3.38E+00
Y 88	7.74E+01	7.68E-03		Ge 73m	1.30E+10	2.97E+00
H 3	1.63E+01	1.62E-03		Kr 79	1.29E+10	2.93E+00
Sr 89	1.67E+00	1.66E-04		Br 80	1.20E+10	2.73E+00
Rb 86	4.21E-01	4.18E-05		As 74	9.18E+09	2.09E+00
Y 91	3.26E-01	3.23E-05		Ge 69	8.25E+09	1.88E+00
Y 91m	1.75E-01	1.73E-05		Cu 64	7.96E+09	1.81E+00
Rb 86m	1.30E-01	1.29E-05		Ga 68	6.92E+09	1.57E+00
Sr 85	2.51E-03	2.49E-07		Ga 72	6.78E+09	1.54E+00
Sr 91	1.27E-03	1.26E-07		Kr 79m	6.71E+09	1.53E+00
Rb 88	1.08E-03	1.07E-07		Br 79m	6.34E+09	1.44E+00
Zr 88	7.47E-04	7.41E-08		Zn 65	6.32E+09	1.44E+00
Sr 85m	5.93E-04	5.88E-08		Co 60m	3.51E+09	7.98E-01
Rest	4.85E-02	4.81E-06		Rest	5.95E+10	1.35E+01

Table 7.4.4 Radionuclides and Percent Activity of the Activation Products of Sr-90 in a D-T Moderated Flux spectrum.

	Base Case Level				Highest Flux Case Level	
NUCLIDE	ACTIVITY	PERCENT		NUCLIDE	ACTIVITY	PERCENT
	(Bq)	ACTIVITY			(Bq)	ACTIVITY
Total	1.05E+06			Total	3.15E+12	
Zr 90m	4.15E+05	3.95E+01		Tl206	7.98E+11	2.54E+01
Y 89m	2.85E+05	2.71E+01		Pb203	7.79E+11	2.48E+01
Zr 89	2.76E+05	2.62E+01		Pb204m	7.28E+11	2.31E+01
Zr 89m	4.40E+04	4.18E+00		Pb203m	6.27E+11	1.99E+01
Y 90	2.05E+04	1.95E+00		Pb207m	1.07E+11	3.40E+00
Y 90m	5.79E+03	5.51E-01		Pb203n	1.88E+10	5.98E-01
Sr 90	3.66E+03	3.48E-01		Hg203	1.59E+10	5.04E-01
Sr 87m	1.58E+03	1.51E-01		Tl202	1.30E+10	4.13E-01
Y 88	7.62E+01	7.25E-03		Hg205	1.26E+10	4.01E-01
H 3	2.61E+01	2.48E-03		Pb201	1.24E+10	3.93E-01
Sr 89	1.72E+00	1.64E-04		Tl201	1.03E+10	3.27E-01
Y 91	7.47E-01	7.10E-05		Pb202m	9.87E+09	3.14E-01
Rb 86	4.21E-01	4.00E-05		Pb201m	5.28E+09	1.68E-01
Y 91m	3.97E-01	3.78E-05		Tl204	3.67E+09	1.17E-01
Rb 86m	1.30E-01	1.23E-05		H 3	1.50E+09	4.78E-02
Rb 88	1.84E-02	1.75E-06		Hg199m	1.05E+09	3.33E-02
Sr 91	6.94E-03	6.60E-07		Tl206m	8.61E+08	2.73E-02
Sr 85	2.45E-03	2.33E-07		Au202	5.06E+08	1.61E-02
Zr 88	7.35E-04	6.99E-08		Bi208m	4.82E+08	1.53E-02
Sr 85m	5.79E-04	5.50E-08		Tl200	4.32E+08	1.37E-02
Rest	5.07E-02	4.83E-06		Rest	1.82E+09	5.79E-02

Table 7.4.5 Radionuclides and Percent Activity of the Activation Products of Sr-90 in a D-D Moderated Flux spectrum.

	Base Case Level				Highest Flux Case Level	
NUCLIDE	ACTIVITY	PERCENT		NUCLIDE	ACTIVITY	PERCENT
	(Bq)	ACTIVITY			(Bq)	ACTIVITY
Total	7.34E+03			Total	1.20E+10	
Y 90	3.66E+03	4.99E+01		Pb207m	7.50E+08	6.24E+00
Sr 90	3.66E+03	4.99E+01		Pb209	7.13E+08	5.93E+00
Zr 90m	1.46E+01	1.98E-01		Bi210	6.20E+08	5.15E+00
Y 90m	9.88E-05	1.35E-06		Po210	6.18E+08	5.14E+00
Y 91	2.13E-05	2.90E-07		Tl206	4.83E+08	4.02E+00
Sr 91	2.11E-05	2.87E-07		Hg203	3.58E+08	2.97E+00
Rb 87	3.24E-12	4.42E-14		Pt197	3.37E+08	2.80E+00
				Gd159	2.84E+08	2.37E+00
				Yb175	2.64E+08	2.19E+00
				Ho166	2.56E+08	2.13E+00
				Re188	2.55E+08	2.13E+00
				Au199	2.54E+08	2.11E+00
				Dy165	2.38E+08	1.98E+00
				Er169	2.33E+08	1.94E+00
				Ir194	2.30E+08	1.91E+00
				Os191m	2.26E+08	1.88E+00
				Ta183	2.23E+08	1.86E+00
				Tm172	2.16E+08	1.79E+00
				Hf183	2.14E+08	1.78E+00
				Os193	2.13E+08	1.77E+00
				Rest	5.04E+09	4.19E+01

Table 7.4.6 Radionuclides and Percent Activity of the Activation Products of Sr-90 in a D-T Thermalized Flux spectrum

	Base Case Level				Highest Flux Case Level	
NUCLIDE	ACTIVITY	PERCENT		NUCLIDE	ACTIVITY	PERCENT
	(Bq)	ACTIVITY			(Bq)	ACTIVITY
Total	7.32E+03			Total	4.93E+10	
Y 90	3.66E+03	5.00E+01		Tl206	1.34E+09	2.73E+00
Sr 90	3.66E+03	5.00E+01		Pt197	1.16E+09	2.36E+00
Y 91	9.00E-03	1.23E-04		Ba139	1.07E+09	2.16E+00
Sr 91	7.57E-03	1.03E-04		Gd159	1.06E+09	2.15E+00
Y 91m	4.13E-03	5.65E-05		La140	1.06E+09	2.15E+00
Sr 87m	8.74E-04	1.19E-05		Nd149	1.01E+09	2.04E+00
Zr 93	1.31E-05	1.79E-07		Au199	9.89E+08	2.01E+00
Nb 93m	1.16E-05	1.58E-07		Os193	9.79E+08	1.99E+00
Nb 94	6.00E-11	8.20E-13		Ho166	9.50E+08	1.93E+00
Rb 87	5.50E-13	7.51E-15		Yb175	9.21E+08	1.87E+00
				Tm172	9.07E+08	1.84E+00
				Ta183	9.04E+08	1.83E+00
				Pm150	8.95E+08	1.82E+00
				Eu157	8.40E+08	1.71E+00
				Hf183	8.22E+08	1.67E+00
				Hg203	8.20E+08	1.66E+00
				Sn121	8.00E+08	1.62E+00
				Os191m	7.86E+08	1.59E+00
				W 185	7.65E+08	1.55E+00
				Ir195	7.57E+08	1.54E+00
				Rest	3.05E+10	6.18E+01

7.4.3 Radiation Protection and Dose Rate Calculation

The activation products resulting from the transmutation of Sr-90 as shown in Section 7.4.2 will have hazards associated with them. These are referred to as the hazard indexes. As described in Section 4.4, the hazard indexes evaluated include gamma dose rate at the surface of the activation products, the ingestion dose (committed effective dose equivalent), and the inhalation dose (committed effective dose equivalent) from each of the base cases at both the base case flux level as well as the highest flux case evaluated. Table 7.4.7 shows the summary of the hazard indexes of the activation products generated by the transmutation of Sr-90 down to the ending activity level for each of the base cases considered.

Results show that the dose rate of the activation products will increase with the increase in flux; however, the ingestion and inhalation hazards do not increase significantly with flux until a flux level is reached that would overcome the low cross section characteristics thereby generating more activation products. For all the base cases, the Sr-90 and it's daughter product Y-90 dominates the ingestion and inhalation hazard index; which explains why these indexes do not change significantly with flux, initially. Results also show that the hazards from the activation products from a D-D moderated neutron spectrum have the lowest hazard indexes (dose rates, ingestion hazard, and/or inhalation hazard) than the D-T base cases, except for the D-T thermalized case. The reason for this is the smaller activities of activation products generated. The D-D Moderated case and the D-T thermalized case have very similar numbers of activation products and hazard indexes.

Table 7.4.7 Hazard Indexes Summary of the Activation Products for Sr-90

Neutron Spectrum Used	On-target flux (n/s/cm2)	Activation Product Dose rate (Sv/hr)	Activation Ingestion Dose (Sv)	Activation Inhalation Dose (Sv)
D-T Unmoderated BC	1.23E+11	5.31E+01	3.78E-04	7.70E-04
	1.23E+12	5.31E+02	2.77E-03	2.40E-03
	1.23E+13	5.32E+03	2.73E-02	2.11E-02
	1.23E+14	5.34E+04	3.14E-01	3.98E-01
	1.23E+15	5.83E+04	3.18E+00	1.56E+01
	1.23E+16	2.74E+05	1.77E+01	5.06E+01
	1.23E+17	3.38E+06	1.54E+02	1.58E+02
D-T Moderated BC	1.55E+11	5.84E+01	3.77E-04	7.69E-04
	1.55E+12	5.84E+02	2.79E-03	2.41E-03
	1.55E+13	5.84E+03	2.92E-02	2.21E-02
	1.55E+14	5.68E+04	4.55E-01	4.58E-01
	1.55E+15	1.18E+05	1.89E+01	9.96E+01
	1.55E+16	9.39E+05	1.32E+01	1.48E+01
	1.55E+17	8.48E+06	7.24E+01	1.05E+02
	1.55E+18	8.06E+07	4.88E+02	7.38E+02
D-D Moderated BC	5.14E+08	1.63E-03	1.12E-04	5.91E-04
	5.14E+09	1.60E-02	1.12E-04	5.91E-04
	5.14E+10	1.60E-01	1.13E-04	5.91E-04
	5.14E+11	1.60E+00	1.13E-04	5.92E-04
	5.14E+12	1.60E+01	1.23E-04	5.97E-04
	5.14E+13	1.57E+02	2.17E-04	6.51E-04
	5.14E+14	1.93E+03	1.91E-02	8.59E-02
	5.14E+15	4.07E+05	2.23E+01	3.91E+01
	5.14E+16	1.18E+05	7.49E+02	2.72E+03
D-T Thermalized BC	1.83E+11	3.42E-05	1.10E-04	5.77E-04
	1.83E+12	3.76E-05	1.12E-04	5.91E-04
	1.83E+13	4.60E-03	1.12E-04	5.90E-04
	1.83E+14	9.36E+01	2.95E-03	1.48E-02
	1.83E+15	5.96E+04	2.04E+00	6.20E+00
	1.83E+16	5.68E+05	2.27E+02	7.61E+02

In evaluating the dose rate hazard index, the decay characteristics of the activation product is important as well, such as is common when evaluating the hazards of spent fuel. Figure 7.4.4 shows the comparison of the decay curves for the activation products between the base and highest flux case evaluated for the D-T unmoderated base case. Likewise, Figures 7.4.5, 7.4.6 and 7.4.7 show the comparisons for the D-T moderated base case, the D-D moderated base case, and the D-T thermalized base case, respectively.

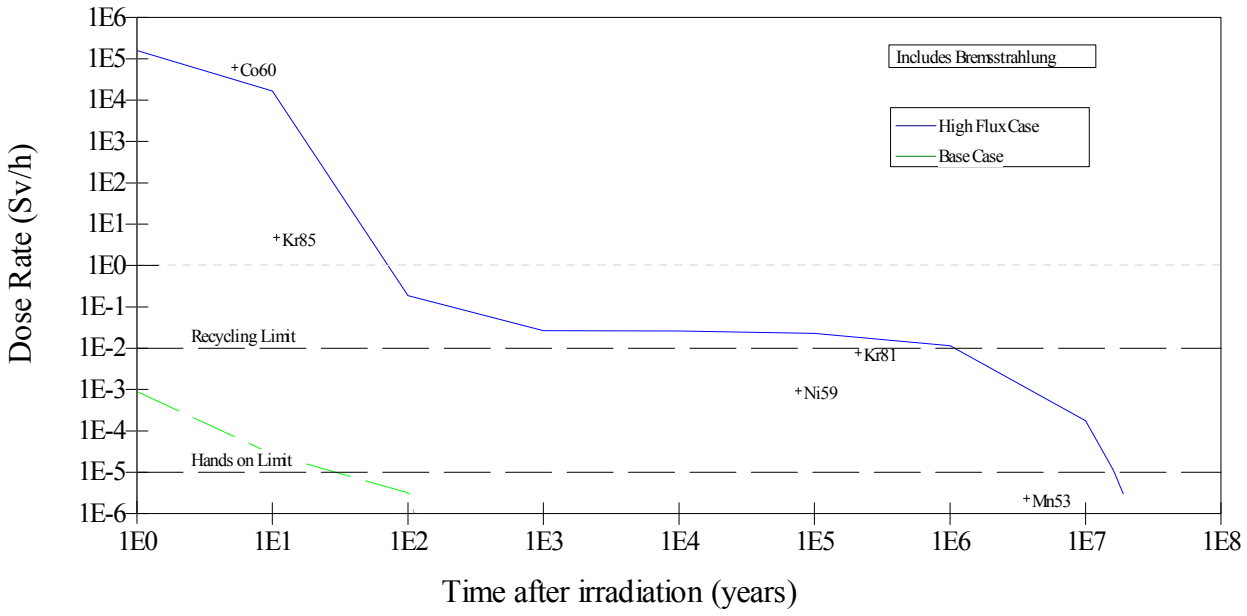

Figure 7.4.4 Decay Curve of Sr-90 Activation Products for the D-T Unmoderated Base Case

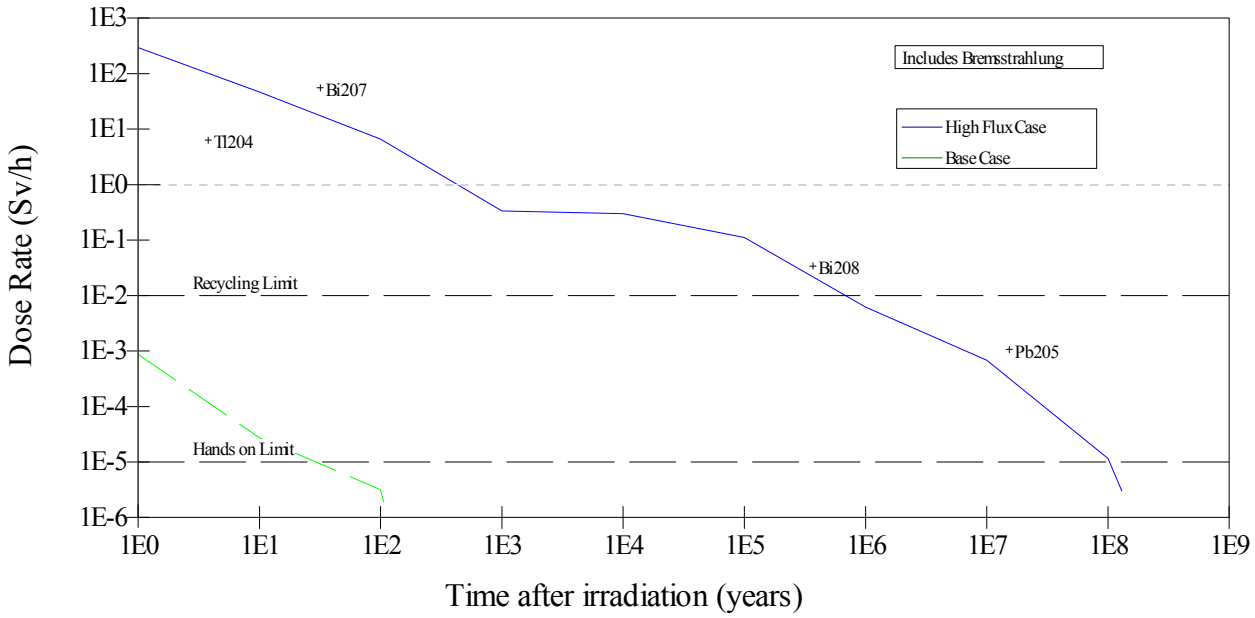

Figure 7.4.5 Decay Curve of Sr-90 Activation Products for the D-T Moderated Base Case

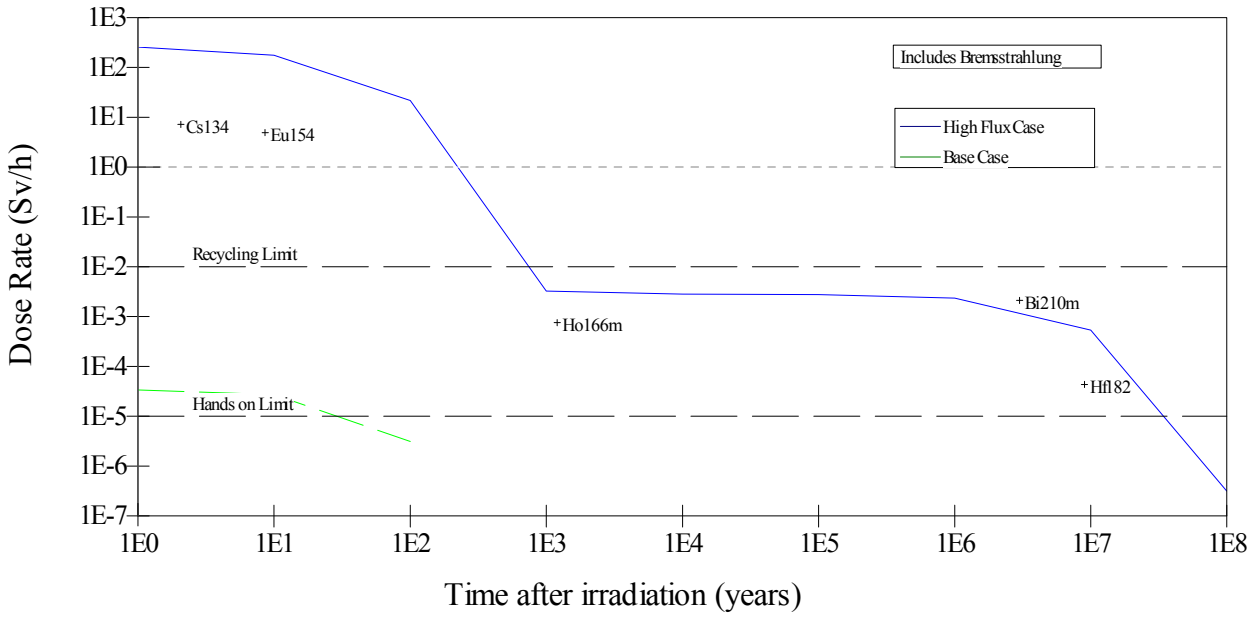

Figure 7.4.6 Decay Curve of Sr-90 Activation Products for the D-D Moderated Base Case

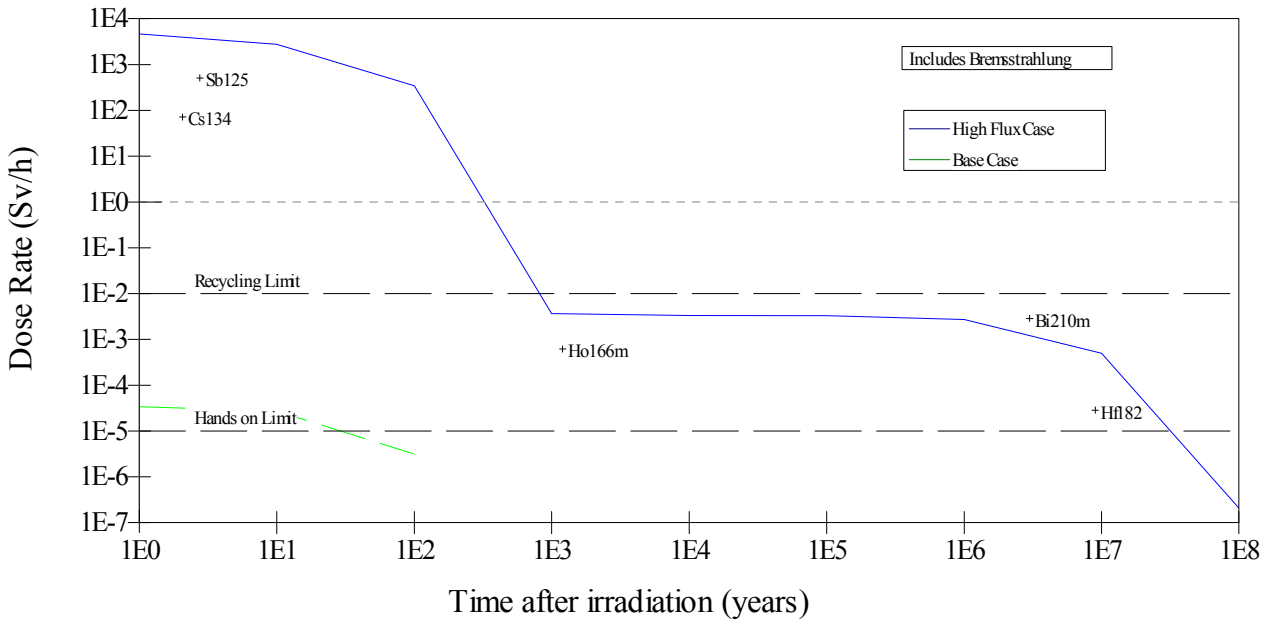

Figure 7.4.7 Decay Curve of Sr-90 Activation Products for the D-T Thermalized Base Case

Table 7.4.8 summarizes the approximate cooling time for the activation products to reach 1 mR/h dose rate. As noted above, for all the base cases, the cooling time is driven by the Sr-90 and its half-life. The long cooling times required for the activation products of the D-T Unmoderated highest flux case is due to Mn-53 (half-life of 3.74E+06 years); whereas, the dominant radionuclide which contributes to the gamma dose rate is Co-60. The long cooling times required by the D-T Moderated and Thermalized cases are due to the production of Pb-205 (half-life of 1.53E+07 years) which beta decays to Bi-205 which contributes to the gamma dose of the products.

Table 7.4.8 Summary of Cooling Time for Sr-90 Activation Products

Neutron Spectrum Used	Approximate Cooling time To 1 mR/h (yrs)
D-T Unmoderated BC	5.0E+01
D-T Unmoderated Highest Flux Case	1.6E+07
D-T Moderated BC	5.0E+01
D-T Moderated Highest Flux Case	1.0E+08
D-D Moderated BC	5.0E+01
D-D Moderated Highest Flux Case	5.0E+07
D-T Thermalized BC	5.0E+01
D-T Thermalized Highest Flux Case	3.0E+07

7.4.4 Discussion

The following observations were made regarding the transmutation of Sr-90:

- As in the case of Cs-137, transmutation is not recommended for Sr-90 with any of the base cases. In fact, it's even less practical for Sr-90 than Cs-137. Transmutation schemes at the base case levels will not transmute Sr-90 any faster than its radiological decay. Increasing the fluxes for all four base cases has either very little effect or serves to increase the effective half-life before decreasing it.
- Activation product generation is proportional to the flux for the base cases but increases very slowly for the first few orders of magnitude of flux increases; after which, the activation product activity will increase faster with flux but not as fast as in the case of I-129 or Tc-99 transmutation.

- The hazard indexes correlate directly to amount of activation products that are generated for all three base cases; but in general, these hazard indexes are not as high as with activation products of I-129 or Tc-99. In fact the hazard indexes for Sr-90 activation products are lower than those of the Cs-137 activation products as well.
- The cooling time of the Sr-90 activation products are much shorter for the base case activation products for Sr-90 than Cs-137. The cooling time of the Sr-90 activation products generated by the higher flux case than the base case flux for all four base cases. In all the base cases the differences between the cooling time for the case base and the highest flux case evaluated are very significant, from seven to eight orders of magnitude longer.

7.5 Americium-241

As explained in Chapter 6, the actinides required a slightly different methodology for analyzing the neutron spectrum for transmutation used in the base cases. For each actinide, the spectrum used for transmutation was calculated specifically for each base case and each radionuclide using MCNPX. There are called the fission-corrected spectra and include any fission generated neutrons. Figure 7.5.1 shows the fission corrected spectra for the Am-241 base cases.

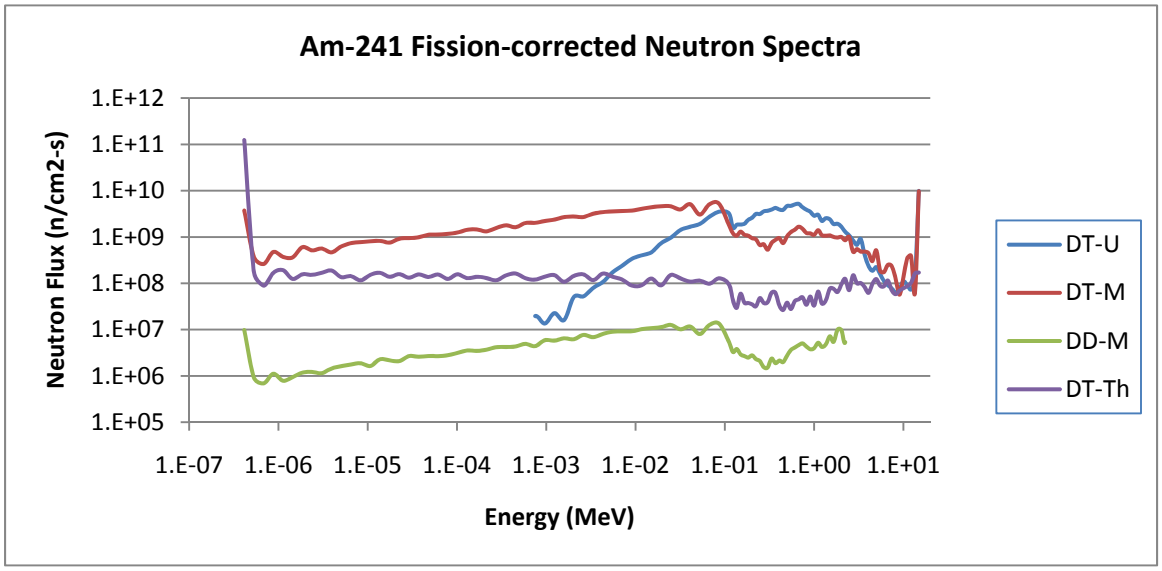

Figure 7.5.1 Am-241 Fission Corrected Neutron Spectra for the Base Cases

Figure 7.5.2 shows the neutron reaction cross sections for Am-241. As can be seen from the graph, the capture cross section is much larger than the fission cross section up to about 0.8 MeV. In fact, the capture cross sections dominate the total cross section up to that point. Capture reactions are less desirable than fission reactions because more actinides are created during capture whereas; during fissions, smaller atoms (fission products) result.

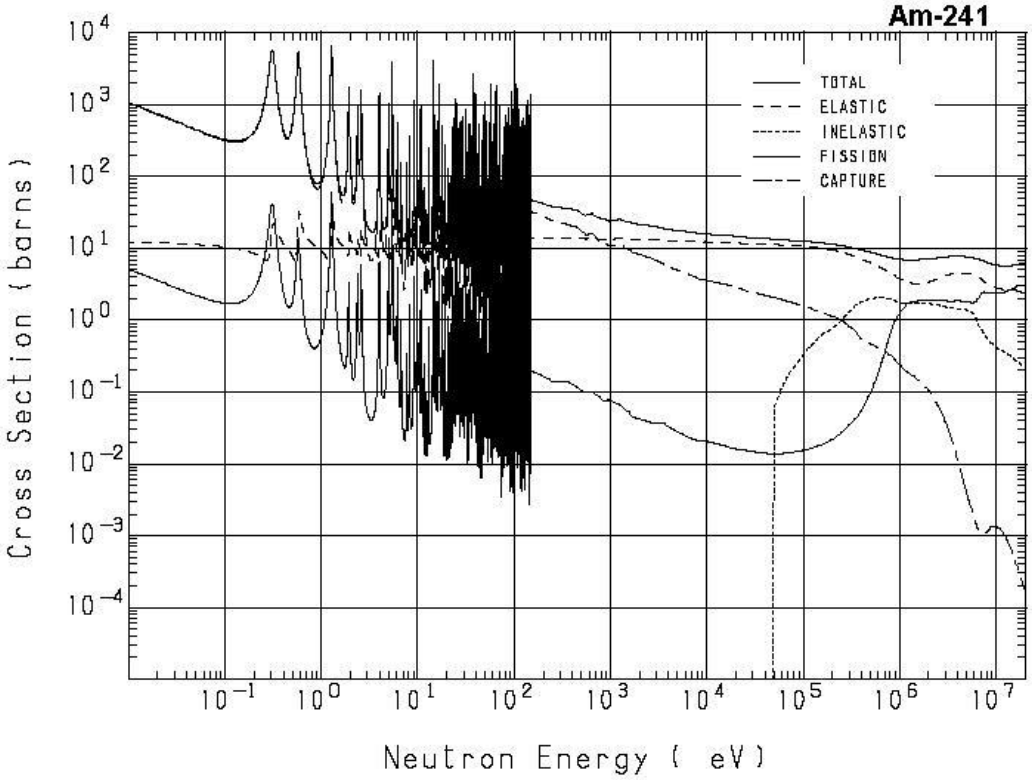

Figure 7.5.2 Neutron Reaction Cross Sections for Am-241 [43]

Figure 7.5.3 shows the reaction thresholds for higher processes. As seen with previous radionuclides, the (n, 2n) or higher processes will not occur with the D-D base case or is minimal with the D-T thermalized base case.

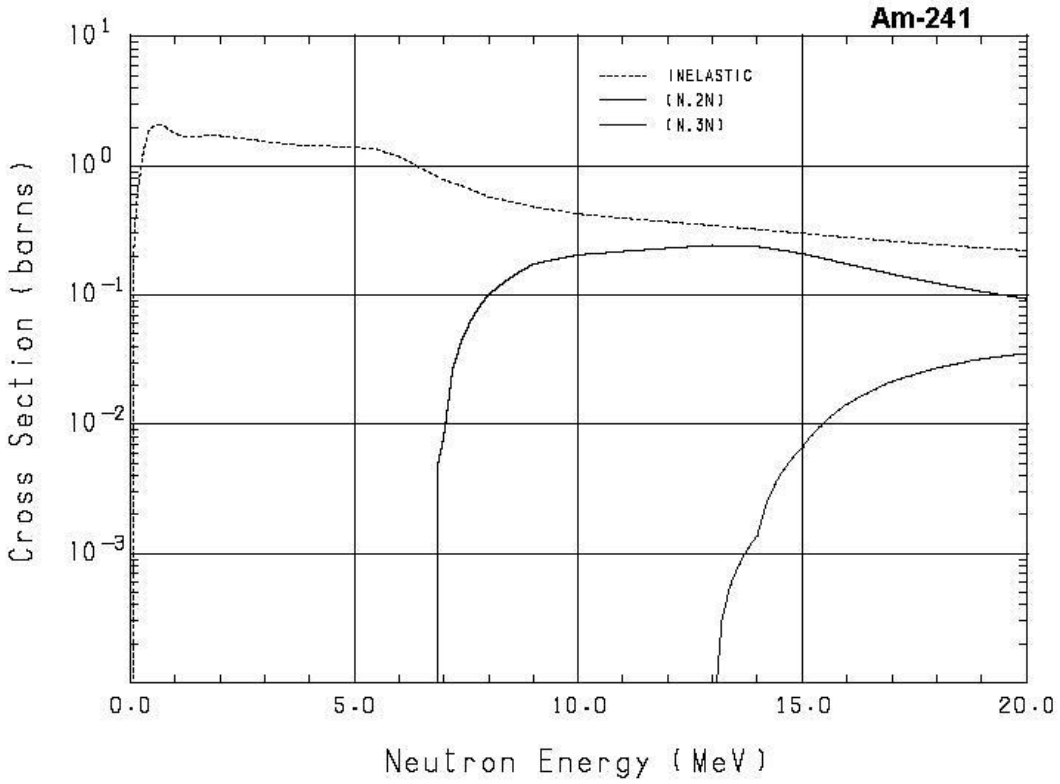

Figure 7.5.3 Neutron Reaction Thresholds for Am-241 [43]

7.5.1 Results of Transmutation

Table 7.5.1 shows the results of the transmutation calculations for Am-241 which has a radiological half-life of 4.32E+02 years. For Am-241, the starting activity is 3.7e+10 Bq (1.0 Ci) and the ending activity is 37 Bq (1.0E-6 mCi). Under the description of the neutron spectrum used for the transmutation calculation, the BC stands for base case and the HFC stands for the high flux case (that flux level at which the irradiation time required is less than 100 years.) Like the long-lived radionuclides, I-129 and Tc-99, the neutron fluence requirements for transmutation of Am-241 stay fairly consistent as the flux increases; however, only after a certain flux level. With the high

energy spectrum (D-T unmoderated case), initially, the irradiation effective half-life is driven by the radiological half-life because the flux is not sufficient to eliminate the Am-241.

Table 7.5.1 Transmutation Results for Am-241

Neutron Energy spectrum	On-target flux (n/s/cm2)	Irradiation Time (yrs)	Ending Activity (Bq)	Fluence Required (n/cm2)	Irradiation Effective Half-life (yrs)
D-T Unmoderated BC	1.26E+11	1.31E+04	3.06E+01	5.19E+22	4.34E+02
	1.26E+12	2.40E+05	3.65E+01	9.53E+24	8.02E+03
	1.26E+13	4.30E+04	3.67E+01	1.71E+25	1.44E+03
	1.26E+14	5.50E+03	3.64E+01	2.18E+25	1.84E+02
	1.26E+15	5.50E+02	3.36E+01	2.18E+25	1.83E+01
D-T Unmoderated HFC	1.26E+16	9.00E+01	1.60E+01	3.57E+25	2.89E+00
D-T Moderated BC	1.62E+11	4.10E+05	3.26E+01	2.09E+24	1.36E+04
	1.62E+12	5.90E+04	3.42E+01	3.01E+24	1.97E+03
	1.62E+13	7.50E+03	3.64E+01	3.82E+24	2.51E+02
	1.62E+14	5.70E+02	3.67E+01	2.90E+24	1.91E+01
D-T Moderated HFC	1.62E+15	2.90E+01	3.38E+01	1.48E+24	9.66E-01
D-D Moderated BC	4.37E+08	1.30E+04	3.56E+01	1.79E+20	4.34E+02
	4.37E+09	1.40E+04	3.77E+01	1.93E+21	4.69E+02
	4.37E+10	1.00E+06	3.42E+01	1.38E+24	3.33E+04
	4.37E+11	2.00E+05	3.91E+01	2.75E+24	6.71E+03
	4.37E+12	2.65E+04	3.48E+01	3.65E+24	8.84E+02
	4.37E+13	2.80E+03	3.59E+01	3.85E+24	9.35E+01
	4.37E+14	1.60E+02	3.08E+01	2.20E+24	5.30E+00
D-D Moderated HFC	4.37E+15	9.10E+00	3.65E+01	1.25E+24	3.04E-01
D-T Thermalized BC	1.34E+11	8.00E+05	3.19E+01	3.38E+24	2.66E+04
	1.34E+12	7.20E+04	3.35E+01	3.04E+24	2.40E+03
	1.34E+13	9.30E+03	3.62E+01	3.93E+24	3.11E+02
	1.34E+14	4.00E+02	3.25E+01	1.69E+24	1.33E+01
D-T Thermalized HFC	1.34E+15	1.25E+01	3.61E+01	5.28E+23	4.18E-01

The irradiation half-life then increases due to all the capture reactions that dominate. The increased flux level then reaches an equilibrium value where the fluence required to eliminate the Am-241 is consistent such that further increase in flux decrease the irradiation effective half-life. This pattern is also seen in the D-D moderated case. In the D-T moderated and D-T thermalized cases, the base cases result in irradiation effective half-lives much longer than the radiological half-life, then decrease with flux. Figure 7.5.4 shows these relationships with respect to the increase in flux for each of the base cases.

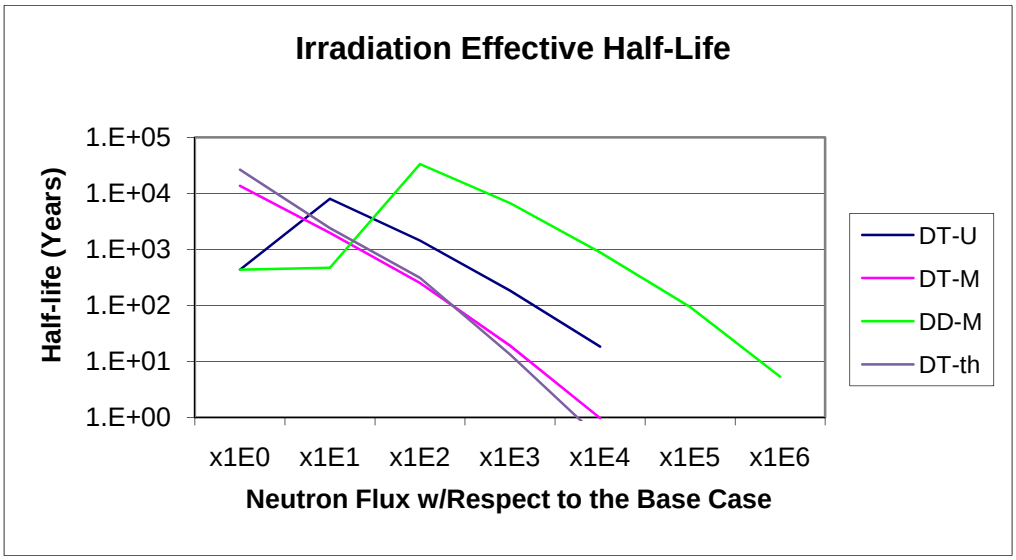

Figure 7.5.4 Irradiation Effective Half-life as a Function of Neutron Flux for Am-241

7.5.2 Activation Products

Table 7.5.2 shows the summary of activation products generated by the transmutation of Am-241 down to the ending activity level. The total activity of the results of the transmutation is given as well as the number of radioactive and non-radioactive nuclides. Results show that transmutation of Am-241 creates quite a lot more

activation products than the transmutation of the long-lived or short-lived fission products.

Table 7.5.2 Activation Products Summary for Am-241

Neutron Spectrum Used	On-target flux (n/s/cm2)	Total Activation (Bq)	Number of Radioactive Nuclides	Number of Non-radioactive Nuclides
D-T Unmoderated BC	1.26E+11	2.22E+07	580	191
	1.26E+12	2.93E+08	861	241
	1.26E+13	2.87E+09	905	247
	1.26E+14	3.39E+10	956	247
	1.26E+15	2.98E+11	1003	246
D-T Unmoderated HFC	1.26E+16	3.22E+12	1066	245
D-T Moderated BC	1.62E+11	1.30E+08	827	237
	1.62E+12	1.42E+09	863	238
	1.62E+13	1.69E+10	903	237
	1.62E+14	1.60E+11	949	236
D-T Moderated HFC	1.62E+15	1.88E+12	1012	234
D-D Moderated BC	4.37E+08	3.12E+07	523	178
	4.37E+09	1.49E+08	566	184
	4.37E+10	4.43E+07	631	216
	4.37E+11	4.14E+08	617	217
	4.37E+12	4.27E+09	621	218
	4.37E+13	4.86E+10	672	218
	4.37E+14	5.55E+11	734	218
D-D Moderated HFC	4.37E+15	4.76E+12	770	215
D-T Thermalized BC	1.34E+11	6.24E+08	554	220
	1.34E+12	5.00E+09	608	221
	1.34E+13	4.02E+10	662	221
	1.34E+14	3.24E+11	719	218
D-T Thermalized HFC	1.34E+15	2.85E+12	738	214

Table 7.5.3 shows the most prominent activation products for transmutation of Am-241 in a D-T moderated spectrum, both at base case and the high flux case levels. The radionuclides shown are present at the end of the transmutation period. Results show

that the activation products generated by transmutation are a function of the flux level used because the production of the different radionuclides is dependent upon each radionuclides production (or reaction) cross section and then their subsequent decay rate. Table 7.5.4 shows the prominent activities for transmutation of Am-241 in a D-T moderated spectrum, both at base case and high flux case levels. Table 7.5.5 shows the most prominent activation products for transmutation of Am-241 in a D-D moderated spectrum, both at base case and high flux case levels. Likewise, Table 7.5.6 shows the most prominent activation products for the transmutation of Am-241 in a D-T thermalized spectrum, both at base case and high flux case levels.

Table 7.5.3 Radionuclides and Percent Activity of the Activation Products of Am-241 in a D-T Unmoderated Flux spectrum.

	Base Case Level				High Flux Case Level	
NUCLIDE	ACTIVITY	PERCENT		NUCLIDE	ACTIVITY	PERCENT
	(Bq)	ACTIVITY			(Bq)	ACTIVITY
Total	2.22E+07			Total	3.22E+12	
Pa233	7.98E+06	3.59E+01		Rh103m	4.06E+11	1.26E+01
Np237	7.98E+06	3.59E+01		Ba135m	2.22E+11	6.90E+00
Pu238	5.48E+05	2.46E+00		Ag109m	1.82E+11	5.66E+00
Np238	5.48E+05	2.46E+00		Rh104	1.63E+11	5.06E+00
U 233	4.22E+05	1.90E+00		Xe131m	1.45E+11	4.52E+00
Ra225	1.76E+05	7.91E-01		Pd103	1.40E+11	4.36E+00
Th229	1.76E+05	7.91E-01		Ba133m	8.05E+10	2.50E+00
Ac225	1.76E+05	7.91E-01		Ru103	7.35E+10	2.28E+00
Fr221	1.76E+05	7.91E-01		Cs134	7.01E+10	2.18E+00
At217	1.76E+05	7.91E-01		Ce139	6.86E+10	2.13E+00
Bi213	1.76E+05	7.91E-01		Ag110	6.76E+10	2.10E+00
Pb209	1.76E+05	7.91E-01		Ba133	6.09E+10	1.89E+00
Po213	1.72E+05	7.74E-01		Cd109	5.67E+10	1.76E+00
Xe135	4.90E+04	2.21E-01		Nd141	5.06E+10	1.57E+00
Mo 99	4.64E+04	2.09E-01		Pr140	5.05E+10	1.57E+00
I 135	4.52E+04	2.04E-01		Xe129m	5.04E+10	1.57E+00
I 134	4.35E+04	1.96E-01		Zr 90m	4.75E+10	1.48E+00
Xe133	4.27E+04	1.92E-01		Ba137m	4.43E+10	1.38E+00
I 133	4.26E+04	1.92E-01		La136	4.40E+10	1.37E+00
Zr 99	4.23E+04	1.91E-01		Pd107m	4.39E+10	1.36E+00
Rest	3.04E+06	1.37E+01		Rest	1.15E+12	3.58E+01

Table 7.5.4 Radionuclides and Percent Activity of the Activation Products of Am-241 in a D-T Moderated Flux spectrum.

	Base Case Level				High Flux Case Level	
NUCLIDE	ACTIVITY	PERCENT		NUCLIDE	ACTIVITY	PERCENT
	(Bq)	ACTIVITY			(Bq)	ACTIVITY
Total	1.30E+08			Total	1.88E+12	
Rh103m	4.81E+06	3.71E+00		Ag109m	7.86E+10	4.19E+00
Rh104	4.78E+06	3.69E+00		Pd109	7.74E+10	4.13E+00
Mo 99	4.60E+06	3.55E+00		Ho166	7.50E+10	4.00E+00
Tc100	4.24E+06	3.27E+00		Ag110	7.50E+10	4.00E+00
Ho166	4.21E+06	3.25E+00		Dy165	7.40E+10	3.94E+00
Dy165	4.20E+06	3.24E+00		Gd159	6.74E+10	3.59E+00
Ru103	4.18E+06	3.22E+00		Rh104	6.33E+10	3.37E+00
Tc 99m	4.10E+06	3.17E+00		Rh103m	6.32E+10	3.37E+00
Tb160	4.08E+06	3.15E+00		Er167m	5.99E+10	3.19E+00
Tm170	4.07E+06	3.14E+00		Er169	5.79E+10	3.09E+00
Er169	4.06E+06	3.14E+00		Ru103	5.28E+10	2.82E+00
Gd159	3.98E+06	3.07E+00		Dy165m	4.77E+10	2.54E+00
H 3	3.93E+06	3.03E+00		Tc100	4.12E+10	2.20E+00
Er167m	3.42E+06	2.64E+00		Mo 99	4.11E+10	2.19E+00
Eu154	2.83E+06	2.18E+00		Tb160	4.10E+10	2.18E+00
Dy165m	2.68E+06	2.07E+00		Tm170	3.77E+10	2.01E+00
La140	2.68E+06	2.07E+00		Tc 99m	3.66E+10	1.95E+00
Cs134	2.28E+06	1.76E+00		Sm153	3.65E+10	1.95E+00
Nd147	2.21E+06	1.71E+00		Eu156	3.42E+10	1.82E+00
Pm147	2.21E+06	1.70E+00		In115m	3.28E+10	1.75E+00
Rest	5.60E+07	4.32E+01		Rest	7.83E+11	4.17E+01

Table 7.5.5 Radionuclides and Percent Activity of the Activation Products of Am-241 in a D-D Moderated Flux spectrum.

	Base Case Level				High Flux Case Level	
NUCLIDE	ACTIVITY	PERCENT		NUCLIDE	ACTIVITY	PERCENT
	(Bq)	ACTIVITY			(Bq)	ACTIVITY
Total	3.12E+07			Total	4.76E+12	
Np237	7.95E+06	2.55E+01		Ag109m	2.41E+11	5.05E+00
Pa233	7.95E+06	2.55E+01		Pd109	2.39E+11	5.02E+00
Pu238	6.12E+06	1.96E+01		Ag110	2.33E+11	4.90E+00
Np238	6.12E+06	1.96E+01		Dy165	2.24E+11	4.71E+00
U 233	4.17E+05	1.34E+00		Ho166	2.21E+11	4.64E+00
U 234	2.26E+05	7.24E-01		Gd159	2.14E+11	4.49E+00
Th229	1.73E+05	5.55E-01		Er167m	1.58E+11	3.31E+00
Ra225	1.73E+05	5.55E-01		Dy165m	1.46E+11	3.07E+00
Ac225	1.73E+05	5.55E-01		Tb161	1.34E+11	2.81E+00
Fr221	1.73E+05	5.55E-01		Rh103m	1.21E+11	2.54E+00
At217	1.73E+05	5.55E-01		Ru103	1.21E+11	2.54E+00
Bi213	1.73E+05	5.54E-01		Rh104	1.20E+11	2.53E+00
Pb209	1.73E+05	5.54E-01		Sm153	1.08E+11	2.27E+00
Po213	1.69E+05	5.43E-01		Er169	1.08E+11	2.26E+00
Xe135	1.36E+04	4.38E-02		Cs136	1.05E+11	2.20E+00
Th230	1.33E+04	4.27E-02		Eu156	9.47E+10	1.99E+00
I 135	1.26E+04	4.05E-02		Tc100	9.19E+10	1.93E+00
Mo 99	1.22E+04	3.92E-02		Mo 99	9.15E+10	1.92E+00
Tc101	1.17E+04	3.76E-02		La140	8.99E+10	1.89E+00
Mo101	1.17E+04	3.76E-02		Pr142	8.89E+10	1.87E+00
Rest	9.18E+05	2.95E+00		Rest	1.81E+12	3.81E+01

Table 7.5.6 Radionuclides and Percent Activity of the Activation Products of Am-241 in a D-T Thermalized Flux spectrum.

	Base Case Level				High Flux Case Level	
NUCLIDE	ACTIVITY	PERCENT		NUCLIDE	ACTIVITY	PERCENT
	(Bq)	ACTIVITY			(Bq)	ACTIVITY
Total	6.24E+08			Total	2.85E+12	
H 3	2.73E+08	4.37E+01		Sm153	1.37E+11	4.81E+00
Tm170	1.74E+07	2.79E+00		Ru103	1.09E+11	3.81E+00
Er169	1.74E+07	2.79E+00		Rh104	1.09E+11	3.81E+00
Tb160	1.62E+07	2.59E+00		Pd109	1.08E+11	3.77E+00
Dy165	1.61E+07	2.58E+00		Ag109m	1.08E+11	3.77E+00
Gd159	1.60E+07	2.56E+00		Rh103m	1.08E+11	3.77E+00
Ho166	1.56E+07	2.49E+00		Ag110	1.05E+11	3.68E+00
Yb175	1.23E+07	1.97E+00		Gd159	1.05E+11	3.67E+00
Er167m	1.19E+07	1.90E+00		Dy165	9.40E+10	3.29E+00
Hf181	1.13E+07	1.81E+00		Ho166	9.37E+10	3.28E+00
Ta182	1.08E+07	1.73E+00		Nd147	9.19E+10	3.22E+00
Eu154	1.04E+07	1.66E+00		Pm149	8.29E+10	2.91E+00
Dy165m	1.03E+07	1.65E+00		Tb161	8.24E+10	2.89E+00
Sm153	1.01E+07	1.62E+00		Eu157	7.98E+10	2.79E+00
Nd147	9.51E+06	1.52E+00		Eu156	7.47E+10	2.62E+00
Pm147	9.48E+06	1.52E+00		Er167m	6.91E+10	2.42E+00
Lu176m	8.08E+06	1.29E+00		Dy165m	6.32E+10	2.22E+00
Hf179m	7.35E+06	1.18E+00		Nd149	6.26E+10	2.19E+00
Pr142	7.15E+06	1.15E+00		Pr142	6.00E+10	2.10E+00
Ce141	7.15E+06	1.15E+00		Ce141	5.34E+10	1.87E+00
Rest	1.27E+08	2.04E+01		Rest	1.06E+12	3.71E+01

When evaluating the activation products for transmutation of an actinide such as Am-241, it is important to determine how much actinide activation products are generated. Actinides are defined here as radionuclides with atomic number from 89 (Actinium) and higher. Table 7.5.6.1 shows the total amount of actinides in the resulting activation products when the target actinide has been transmuted to the target level. Results are shown for the base case flux level and the high flux level for each of the four base cases.

Table 7.5.6.1 Actinides Generated By Transmutation of Am-241 Down to < 37 Bq

Neutron Spectrum Used	Total Activity of Actinides Generated (Bq)	Dominant Actinide
D-T Unmoderated BC	1.79E+07	Np-237
D-T Unmoderated Highest Flux Case	2.55E+05	Am-244
D-T Moderated BC	5.03E+04	Pu-238
D-T Moderated Highest Flux Case	5.83E+09	Cm-249
D-D Moderated BC	2.92E+07	Np-237
D-D Moderated Highest Flux Case	3.11E+10	Cm-249
D-T Thermalized BC	1.35E+03	Np-239
D-T Thermalized Highest Flux Case	1.53E+10	Cm-249

7.5.3 Radiation Protection and Dose Rate Calculation

The activation products resulting from the transmutation of Am-241 as shown in Section 7.5.2 will have hazards associated with them. These are referred to as the hazard indexes. As described in Section 4.4, the hazard indexes evaluated include gamma dose rate at the surface of the activation products, the ingestion dose (committed effective dose equivalent), and the inhalation dose (committed effective dose equivalent) from each of the base cases at both the base case flux level as well as the high flux case evaluated. Table 7.5.7 shows the summary of the hazard indexes of the activation products generated by the transmutation of Am-241 down to the ending activity level for each of the base cases considered.

Results show that the dose rate of the activation products will increase with the increase in flux; however, the radiotoxicity does not rise as fast with increased flux.

Table 7.5.7 Hazard Indexes Summary of the Activation Products for Am-241

Neutron Spectrum Used	On-target flux (n/s/cm2)	Activation Product Dose rate (Sv/hr)	Activation Ingestion Dose (Sv)	Activation Inhalation Dose (Sv)
D-T Unmoderated BC	1.26E+11	2.07E+00	1.22E+00	5.14E+02
	1.26E+12	6.93E+01	1.18E+00	6.20E+01
	1.26E+13	6.36E+02	4.29E+00	2.32E+01
	1.26E+14	6.33E+03	4.76E+01	1.44E+02
	1.26E+15	4.72E+04	3.96E+02	1.07E+03
D-T Unmoderated HFC	1.26E+16	4.59E+05	3.46E+03	8.57E+03
D-T Moderated BC	1.62E+11	2.29E+01	1.32E-01	2.19E+00
	1.62E+12	2.32E+02	1.31E+00	5.23E+00
	1.62E+13	2.87E+03	1.45E+01	4.52E+01
	1.62E+14	2.73E+04	1.33E+02	3.14E+02
D-T Moderated HFC	1.62E+15	3.18E+05	1.87E+03	1.38E+04
D-D Moderated BC	4.37E+08	3.07E+00	2.53E+00	1.13E+03
	4.37E+09	2.82E+01	1.53E+01	6.99E+03
	4.37E+10	9.50E+00	1.46E-01	2.40E+01
	4.37E+11	5.76E+01	3.37E-01	2.18E+00
	4.37E+12	5.87E+02	3.28E+00	1.29E+01
	4.37E+13	7.53E+03	3.61E+01	1.02E+02
	4.37E+14	8.80E+04	4.58E+02	1.44E+03
D-D Moderated HFC	4.37E+15	8.58E+05	4.20E+03	4.15E+04
D-T Thermalized BC	1.34E+11	5.17E+01	3.27E-01	1.48E+00
	1.34E+12	5.46E+02	3.44E+00	1.28E+01
	1.34E+13	5.24E+03	3.50E+01	9.80E+01
	1.34E+14	5.25E+04	3.28E+02	2.96E+03
D-T Thermalized HFC	1.34E+15	4.79E+05	2.83E+03	4.78E+04

In evaluating the dose rate hazard index, the decay characteristics of the activation product is important as well, such as is common when evaluating the hazards of spent fuel. Figure 7.5.5 shows the comparison of the decay curves for the activation products between the base and high flux case evaluated for the D-T unmoderated base case. Likewise, Figures 7.5.6, 7.5.7 and 7.5.8 show the comparisons for the D-T moderated base case, the D-D moderated base case, and the D-T thermalized base case, respectively.

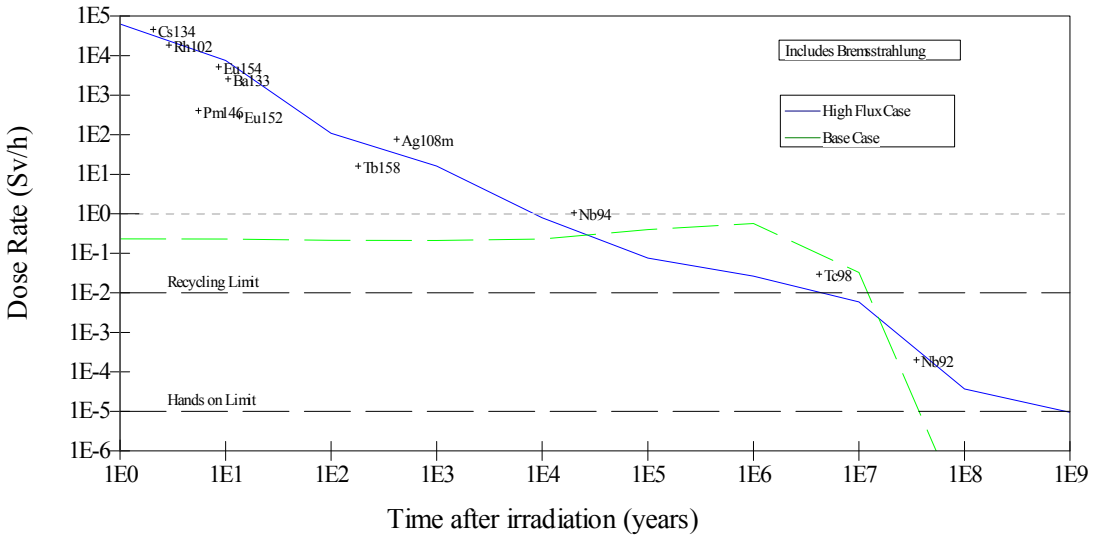

Figure 7.5.5 Decay Curve of Am-241 Activation Products for the D-T Unmoderated Base Case

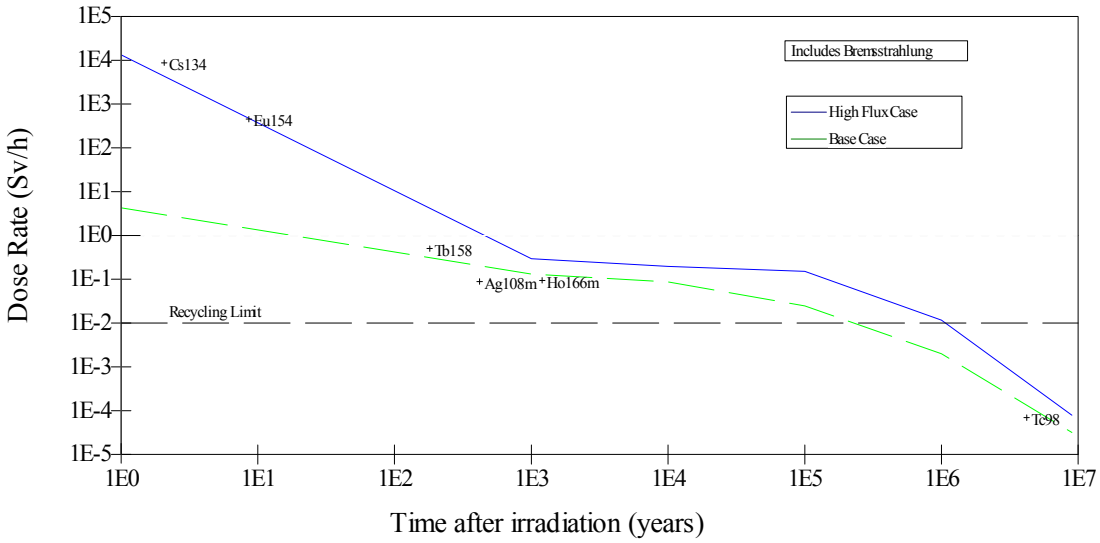

Figure 7.5.6 Decay Curve of Am-241 Activation Products for the D-T Moderated Base Case

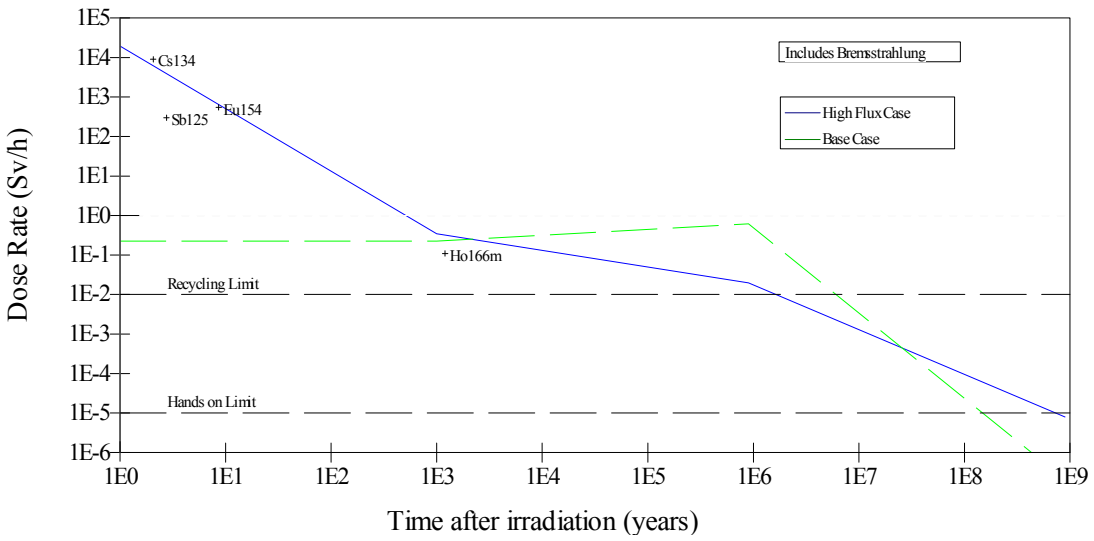

Figure 7.5.7 Decay Curve of Am-241 Activation Products for the D-D Moderated Base Case

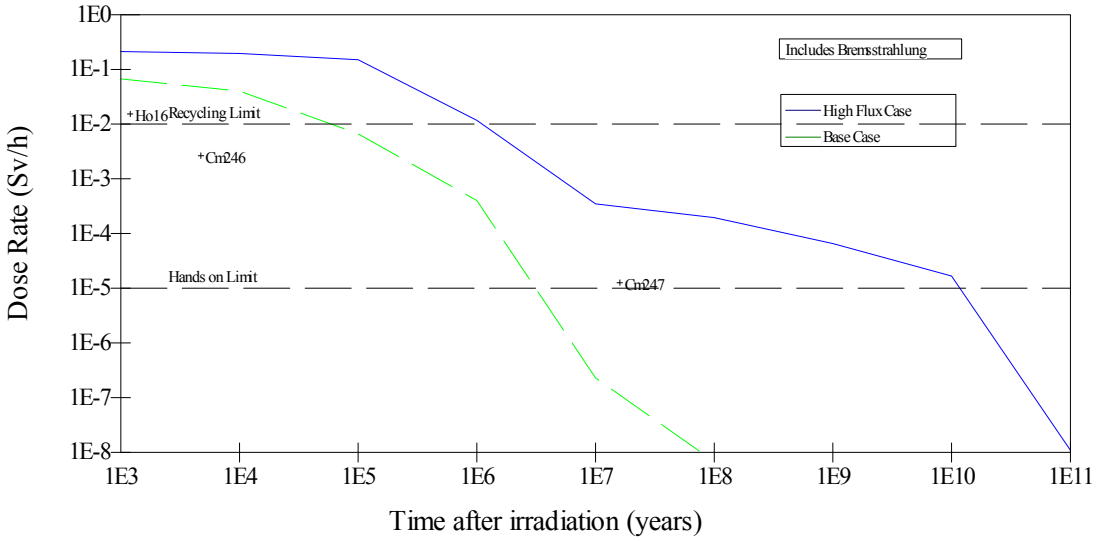

Figure 7.5.8 Decay Curve of Am-241 Activation Products for the D-T Thermalized Base Case

Table 7.5.8 summarizes the approximate cooling time for the activation products to reach 1 mR/h dose rate. In the D-T Unmoderated case, the long activation cooling time in the base case is driven by U-236 with a half-life of 2.3E+7 years and the activation cooling time of the high flux case is driven by La-138 with a half-life of 1.05E+11 years. In the D-T Moderated case, the long activation cooling time is driven by I-129 (with half-life of 1.57E+07 years) for both the base case and high flux cases. In the D-D Moderated case, the long activation cooling time is driven by U-235 (with half-life of 7.04E+08 years) and Rb-87 (with half-life 4.7E+10 years) for the base case and high flux case, respectively. In the D-T Thermalized case, the long activation cooling time is driven by Rb-87 (with half-life of 4.7E+10 years) for both the base case and high flux cases.

Table 7.5.8 Summary of Cooling Time for Am-241 Activation Products

Neutron Spectrum	Approximate Cooling time
Used	To 1 mR/h (yrs)
D-T Unmoderated BC	3.0E+07
D-T Unmoderated Highest Flux Case	1.0E+09
D-T Moderated BC	3.0E+07
D-T Moderated Highest Flux Case	2.0E+08
D-D Moderated BC	6.0E+07
D-D Moderated Highest Flux Case	5.0E+08
D-T Thermalized BC	3.0E+06
D-T Thermalized Highest Flux Case	1.0E+10

7.5.4 Discussion

The following observations were made regarding the transmutation of Am-241:

- The transmutation of Am-241 is much more complex than the long-lived fission products such as I-129 and short-lived fission products such as Cs-137. There are competing processes of capture and fission that determines the overall transmutation efficiency. Consequently, there are many more activation products created during the transmutation process of Am-241 than the long-lived or short-lived radionuclides.
- For Am-241, neutron capture is the dominant process as compared to fission for transmutation because the capture to fission ratio is about 200 for the thermal energies and about 100 across the resonance integrals. However, the capture to fission ration is extremely small, < 1.0E-06 at 14 MeV (D-T source neutron energies) [43].
- The lower energy spectra (D-T Moderated, D-D Moderated, and D-T Thermalized) transmute Am-241 more efficiently than the higher energy spectrum (D-T Unmoderated).
- The D-T Thermalized base case provides the most efficient process of the three lower energy spectra. At the base case flux level, the irradiation effective half-life far exceeds the radiological half-life (432 years); however, with a four order of magnitude increase in flux level, the irradiation effective half-life was down to about 5 months.
- At a given flux level, the higher energy spectrum (D-T Unmoderated) generates more actinides than the other base cases; however, when comparing the fluxes at

high flux case level to the base case level of each base case, the higher energy spectrum is the only case where the high flux case results in less actinides than the base case. For the other three base cases, the high flux level generates more actinides than their respective base case flux level. The reason for this is the higher number of neutron capture occurring in the radionuclides with the high atomic numbers.

- The total amount of actinides created even in the high flux cases is below 1 Ci (the starting activity of the Am-241).

7.6 Plutonium-238

Figure 7.6.1 shows the fission corrected spectra for the Pu-238 base cases calculated by MCNPX. These spectra were used in FISPACT to perform the transmutation calculations. Although the differences between the Pu-238 and the Am-241 spectra cannot be easily discerned in the figures, the spectra do differ slightly due to different energy dependent fission and capture cross sections.

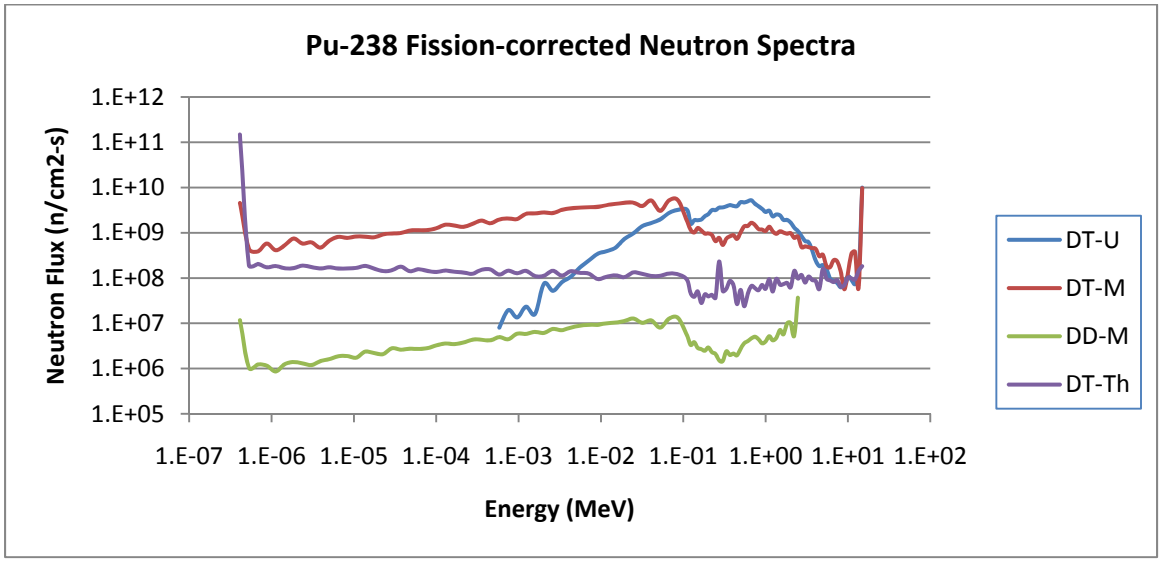

Figure 7.6.1 Pu-238 Fission Corrected Neutron Spectra for the Base Cases

Figure 7.6.2 shows the neutron reaction cross sections for Pu-238. As can be seen from the graph, the capture cross section is larger than the fission cross section up to about 0.08 MeV. In fact, the capture cross sections dominate the total cross section up to that point. Capture reactions are less desirable than fission reactions because more actinides are created during capture whereas; during fissions, smaller atoms (fission products) result.

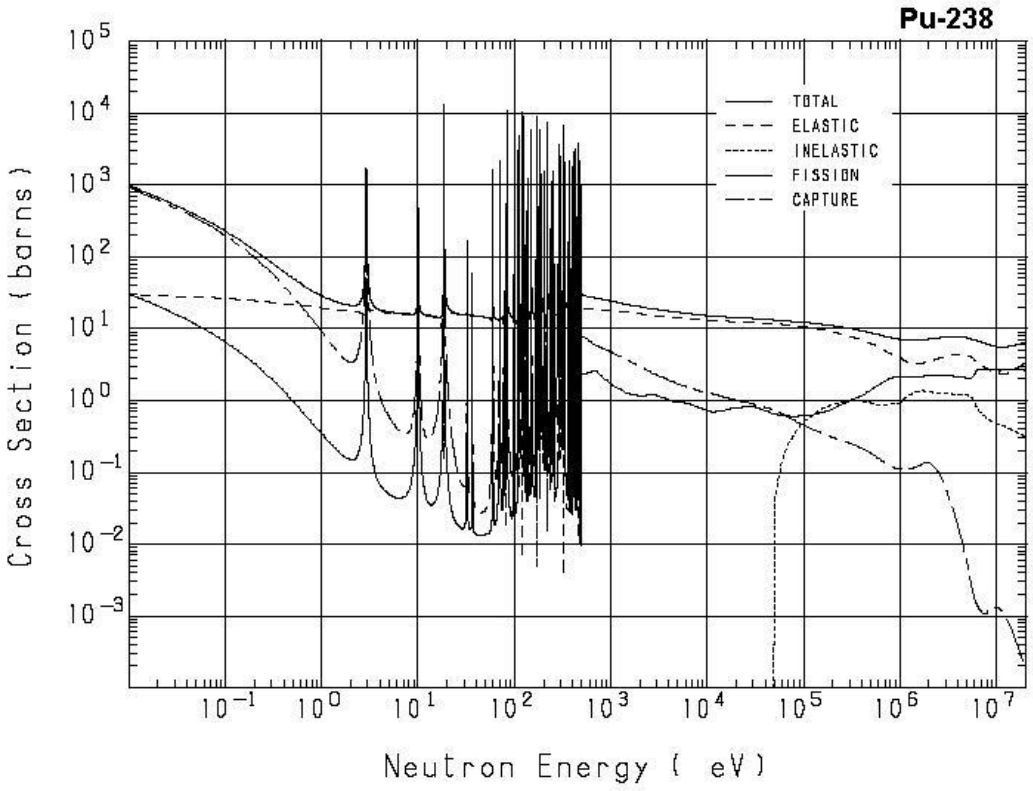

Figure 7.6.2 Neutron Reaction Cross Sections for Pu-238 [43]

Similar to Am-241, the capture cross-section is dominant over the fission cross-section at the lower energies; however, unlike Am-241, the fission cross-section for Pu-238 exceeds the capture cross-section at about 0.08 MeV rather than 0.8 MeV for Am-241. Figure 7.6.3 shows the reaction thresholds for higher processes. As seen with previous radionuclides, the (n, 2n) or higher processes will not occur with the D-D base case or is minimal with the D-T thermalized base case. As can be seen in the graphs, both the (n, 2n) and (n, 3n) cross-sections are lower for Pu-238 than for Am-241.

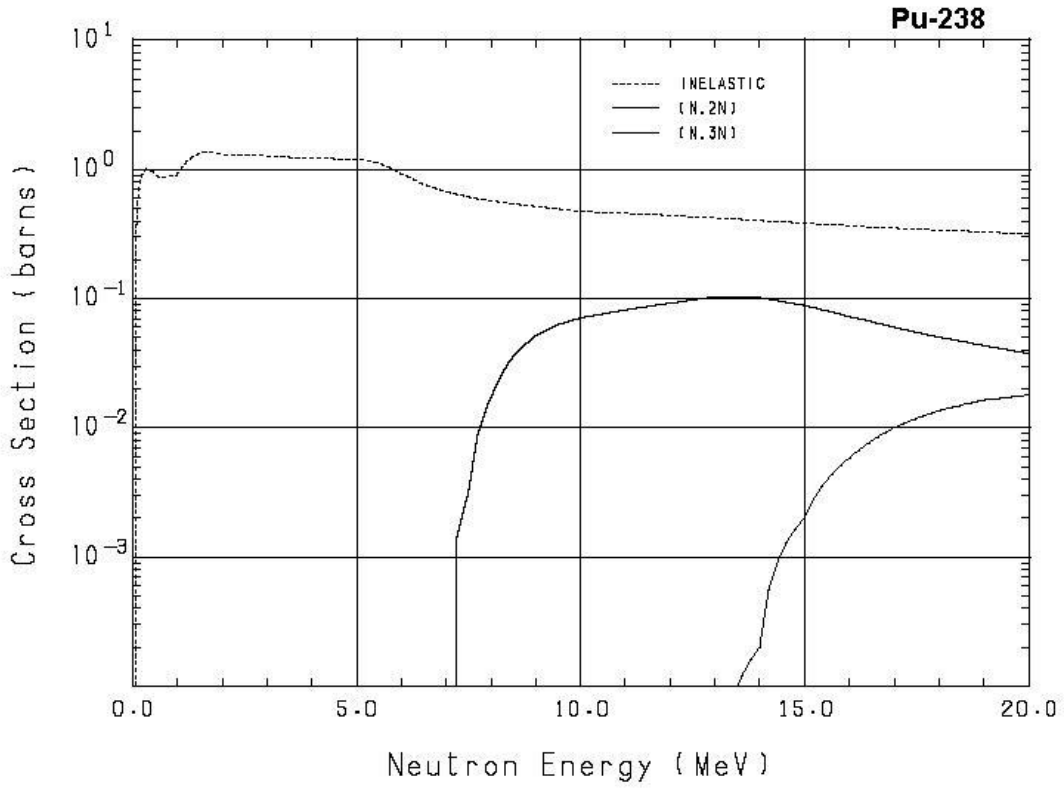

Figure 7.6.3 Neutron Reaction Thresholds for Pu-238 [43]

7.6.1 Results of Transmutation

Table 7.6.1 shows the results of the transmutation calculations for Pu-238 which has a radiological half-life of 87.75 years. For Pu-238, the starting activity is 3.7e+10 Bq (1.0 Ci) and the ending activity is 37 Bq (1.0E-6 mCi). Under the description of the neutron spectrum used for the transmutation calculation, the BC stands for base case and the HFC stands for the high flux case (that flux level at which the irradiation time required is less than 100 years.) Like the long-lived radionuclides, I-129 and Tc-99, the neutron fluence requirements for transmutation of Pu-238 stay fairly consistent as the flux increases; however, only after a certain flux level is achieved. With the high energy

spectrum (D-T unmoderated case), initially, the irradiation effective half-life is much higher than the radiological half-life because at these lower flux levels production processes increase the amount of Pu-238.

Table 7.6.1 Transmutation Results for Pu-238

Neutron Energy spectrum	On-target flux (n/s/cm2)	Irradiation Time (yrs)	Ending Activity (Bq)	Fluence Required (n/cm2)	Irradiation Effective Half-life (yrs)
D-T Unmoderated BC	1.26E+11	1.85E+04	6.83E+01	7.32E+22	6.37E+02
	1.26E+12	4.10E+03	7.34E+03	1.62E+23	1.84E+02
	1.26E+13	2.00E+03	6.03E+05	7.92E+23	1.26E+02
	1.26E+14	7.00E+03	3.69E+01	2.77E+25	2.34E+02
	1.26E+15	6.70E+02	3.36E+01	2.65E+25	2.23E+01
D-T Unmoderated HFC	1.26E+16	6.00E+01	2.11E+01	2.38E+25	1.95E+00
D-T Moderated BC	1.55E+11	1.80E+03	1.33E+05	8.77E+21	9.95E+01
	1.55E+12	1.00E+03	6.59E+07	4.87E+22	1.09E+02
	1.55E+13	7.20E+03	3.80E+01	3.51E+24	2.41E+02
	1.55E+14	5.70E+02	3.41E+01	2.78E+24	1.90E+01
D-T Moderated HFC	1.55E+15	4.10E+01	3.18E+01	2.00E+24	1.36E+00
D-D Moderated BC	4.22E+08	2.60E+03	4.43E+01	3.46E+19	8.77E+01
	4.22E+09	2.60E+03	4.42E+01	3.46E+20	8.77E+01
	4.22E+10	2.50E+03	1.21E+03	3.32E+21	1.00E+02
	4.22E+11	2.40E+03	4.26E+06	3.19E+22	1.83E+02
	4.22E+12	2.90E+04	3.55E+01	3.86E+24	9.68E+02
	4.22E+13	2.70E+03	4.10E+01	3.59E+24	9.07E+01
	4.22E+14	1.95E+02	3.84E+01	2.59E+24	6.53E+00
D-D Moderated HFC	4.22E+15	1.50E+01	4.87E+01	1.99E+24	5.08E-01
D-T Thermalized BC	1.59E+11	6.30E+05	3.92E+01	3.16E+24	2.11E+04
	1.59E+12	6.00E+04	3.18E+01	3.01E+24	1.99E+03
	1.59E+13	6.00E+03	3.71E+01	3.01E+24	2.01E+02
	1.59E+14	3.80E+02	3.14E+01	1.90E+24	1.26E+01
D-T Thermalized HFC	1.59E+15	2.30E+01	3.57E+01	1.15E+24	7.68E-01

This trend continues until the flux level is high enough to eliminate the Pu-238 faster than production. This pattern is also seen in the D-T moderated case and the D-D moderated cases. In the D-T thermalized case, the base case flux level results in an irradiation effective half-life much longer than the radiological half-life, but then decreases with increasing flux. Figure 7.6.4 shows these relationships with respect to the increase in flux for each of the base cases.

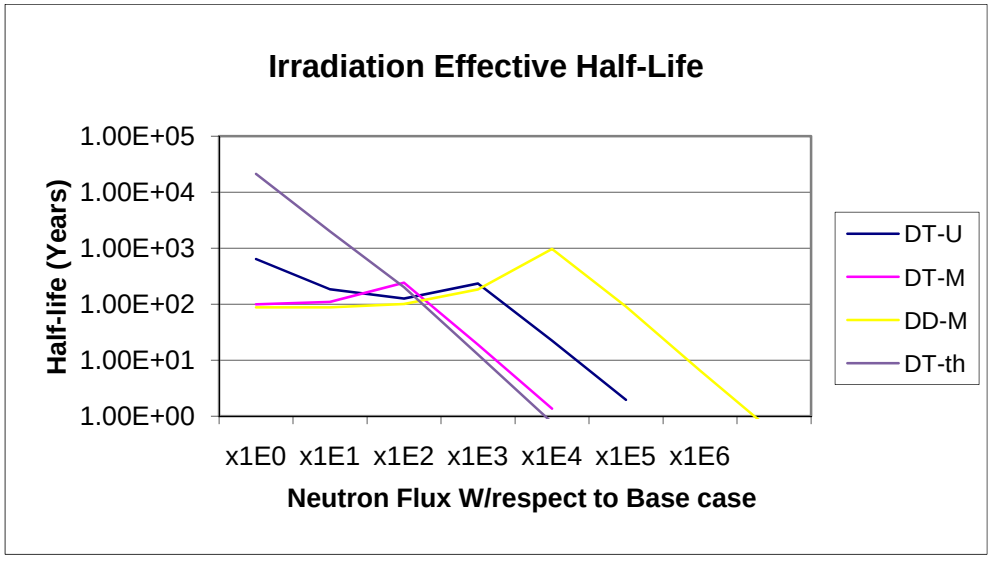

Figure 7.6.4 Irradiation Effective Half-life as a Function of Neutron Flux for Pu-238

7.6.2 Activation Products

Table 7.6.2 shows the summary of activation products generated by the transmutation of Pu-238 down to the ending activity level. The total activity of the results of the transmutation is given as well as the number of radioactive and non-radioactive nuclides. Results show that transmutation of Pu-238 creates quite a lot more activation products than the transmutation of the long-lived or short-lived fission products. However, in the lower energy spectra (D-D moderated and D-T thermalized),

the activation products are lower than for Am-241 transmutation. In the higher energy spectra (D-T unmoderated and moderated) there is initially more activation products but after a few orders of magnitude increase in flux level, then there is less activation products than for Am-241.

Table 7.6.2 Activation Products Summary for Pu-238

Neutron Spectrum Used	On-target flux (n/s/cm2)	Total Activation (Bq)	Number of Radioactive Nuclides	Number of Non-radioactive Nuclides
D-T Unmoderated BC	1.26E+11	9.48E+07	693	210
	1.26E+12	6.63E+08	747	212
	1.26E+13	4.62E+09	822	221
	1.26E+14	6.12E+09	909	249
	1.26E+15	6.77E+10	945	245
D-T Unmoderated HFC	1.26E+16	6.55E+11	1013	241
D-T Moderated BC	1.55E+11	5.48E+08	702	202
	1.55E+12	8.53E+09	784	211
	1.55E+13	3.33E+09	875	237
	1.55E+14	2.77E+10	925	236
D-T Moderated HFC	1.55E+15	3.56E+11	983	233
D-D Moderated BC	4.22E+08	1.51E+07	464	172
	4.22E+09	2.09E+07	515	181
	4.22E+10	1.03E+08	566	183
	4.22E+11	2.06E+09	632	190
	4.22E+12	7.46E+08	563	217
	4.22E+13	8.04E+09	645	217
	4.22E+14	8.86E+10	705	217
D-D Moderated HFC	4.22E+15	8.91E+11	728	214
D-T Thermalized BC	1.59E+11	1.33E+08	527	218
	1.59E+12	9.62E+08	565	218
	1.59E+13	8.62E+09	648	219
	1.59E+14	8.03E+10	693	217
D-T Thermalized HFC	1.59E+15	3.99E+11	717	214

Table 7.6.3 shows the most prominent activation products for transmutation of Pu-238 in a D-T moderated spectrum, both at base case and the high flux case levels. The radionuclides shown are present at the end of the transmutation period. Results show that the activation products generated by transmutation are a function of the flux level used because the production of the different radionuclides is dependent upon each radionuclide's production (or reaction) cross section and then their subsequent decay rate. Table 7.6.4 shows the prominent activities for transmutation of Pu-238 in a D-T moderated spectrum, both at base case and high flux case levels. Table 7.6.5 shows the most prominent activation products for transmutation of Pu-238 in a D-D moderated spectrum, both at base case and high flux case levels. Likewise, Table 7.6.6 shows the most prominent activation products for the transmutation of Pu-238 in a D-T thermalized spectrum, both at base case and high flux case levels.

Table 7.6.3 Radionuclides and Percent Activity of the Activation Products of Pu-238 in a D-T Unmoderated Flux spectrum.

	Base Case Level				High Flux Case Level	
NUCLIDE	ACTIVITY	PERCENT		NUCLIDE	ACTIVITY	PERCENT
	(Bq)	ACTIVITY			(Bq)	ACTIVITY
Total	9.48E+07			Total	6.55E+11	
U 234	1.17E+07	1.23E+01		Rh103m	8.08E+10	1.23E+01
U 235m	2.82E+06	2.97E+00		Ba135m	5.14E+10	7.85E+00
Th230	1.91E+06	2.02E+00		Xe131m	3.52E+10	5.38E+00
Ra226	1.70E+06	1.79E+00		Rh104	3.24E+10	4.95E+00
Po218	1.70E+06	1.79E+00		Pd103	2.75E+10	4.20E+00
Rn222	1.70E+06	1.79E+00		Ag109m	2.13E+10	3.25E+00
Bi214	1.70E+06	1.79E+00		Ba133m	1.92E+10	2.94E+00
Pb214	1.70E+06	1.79E+00		Zr 90m	1.52E+10	2.32E+00
Po214	1.70E+06	1.79E+00		Ba133	1.52E+10	2.31E+00
Bi210	1.69E+06	1.79E+00		Ru103	1.50E+10	2.29E+00
Po210	1.69E+06	1.79E+00		Y 89m	1.44E+10	2.20E+00
Pb210	1.69E+06	1.79E+00		Cs134	1.41E+10	2.16E+00
I 134	9.69E+05	1.02E+00		Ce139	1.40E+10	2.15E+00
Xe135	9.51E+05	1.00E+00		Xe129m	1.31E+10	2.00E+00
Xe133	9.31E+05	9.82E-01		Xe127	1.07E+10	1.64E+00
I 133	9.18E+05	9.68E-01		La136	1.04E+10	1.59E+00
Mo 99	9.11E+05	9.61E-01		Nd141	1.04E+10	1.58E+00
Nb 97	8.60E+05	9.08E-01		Pr140	1.02E+10	1.56E+00
Zr 97	8.57E+05	9.04E-01		Cs132	9.92E+09	1.52E+00
I 135	8.24E+05	8.70E-01		Tc 99m	8.00E+09	1.22E+00
Rest	5.59E+07	5.90E+01		Rest	2.26E+11	3.46E+01

Table 7.6.4 Radionuclides and Percent Activity of the Activation Products of Pu-238 in a D-T Moderated Flux spectrum.

	Base Case Level				High Flux Case Level	
NUCLIDE	ACTIVITY	PERCENT		NUCLIDE	ACTIVITY	PERCENT
	(Bq)	ACTIVITY			(Bq)	ACTIVITY
Total	5.48E+08			Total	3.56E+11	
U 235m	1.68E+08	3.06E+01		Ag109m	1.53E+10	4.31E+00
U 234	1.14E+07	2.07E+00		Pd109	1.52E+10	4.26E+00
I 134	5.77E+06	1.05E+00		Rh104	1.46E+10	4.10E+00
Xe135	5.53E+06	1.01E+00		Rh103m	1.46E+10	4.09E+00
Xe133	5.46E+06	9.96E-01		Ag110	1.45E+10	4.08E+00
I 133	5.44E+06	9.93E-01		Ru103	1.22E+10	3.44E+00
Mo 99	5.35E+06	9.78E-01		Er169	1.20E+10	3.38E+00
Nb 97	5.11E+06	9.33E-01		Tc100	1.03E+10	2.90E+00
Zr 97	5.09E+06	9.29E-01		Mo 99	1.03E+10	2.88E+00
I 135	4.86E+06	8.88E-01		Ho166	1.01E+10	2.83E+00
Zr 99	4.84E+06	8.84E-01		Dy165	9.92E+09	2.79E+00
Nb 97m	4.82E+06	8.80E-01		Tc 99m	9.15E+09	2.57E+00
La140	4.72E+06	8.62E-01		Gd159	9.12E+09	2.56E+00
Y 92	4.72E+06	8.62E-01		Er167m	8.57E+09	2.41E+00
Tc 99m	4.72E+06	8.62E-01		Tm170	8.25E+09	2.32E+00
Ba139	4.71E+06	8.60E-01		In115m	6.40E+09	1.80E+00
Cs137	4.71E+06	8.59E-01		Cd115	6.39E+09	1.80E+00
Ba140	4.70E+06	8.58E-01		Dy165m	6.39E+09	1.80E+00
Sr 92	4.70E+06	8.58E-01		Sm153	6.02E+09	1.69E+00
Y 93	4.66E+06	8.50E-01		Tb160	5.61E+09	1.58E+00
Rest	2.79E+08	5.09E+01		Rest	1.51E+11	4.24E+01

Table 7.6.5 Radionuclides and Percent Activity of the Activation Products of Pu-238 in a D-D Moderated Flux spectrum.

	Base Case Level				High Flux Case Level	
NUCLIDE	ACTIVITY	PERCENT		NUCLIDE	ACTIVITY	PERCENT
	(Bq)	ACTIVITY			(Bq)	ACTIVITY
Total	1.51E+07			Total	8.91E+11	
U 234	1.32E+07	8.72E+01		Ag109m	4.34E+10	4.87E+00
U 235m	4.74E+05	3.13E+00		Pd109	4.31E+10	4.84E+00
Th230	2.98E+05	1.97E+00		Ag110	4.11E+10	4.61E+00
Ra226	1.16E+05	7.64E-01		Er169	3.43E+10	3.85E+00
Po218	1.16E+05	7.64E-01		Ho166	3.11E+10	3.49E+00
Rn222	1.16E+05	7.64E-01		Dy165	3.10E+10	3.48E+00
Bi214	1.16E+05	7.64E-01		Rh103m	2.96E+10	3.32E+00
Pb214	1.16E+05	7.64E-01		Ru103	2.95E+10	3.31E+00
Po214	1.16E+05	7.64E-01		Rh104	2.94E+10	3.30E+00
Pb210	1.13E+05	7.47E-01		Gd159	2.87E+10	3.22E+00
Bi210	1.13E+05	7.47E-01		Er167m	2.61E+10	2.93E+00
Po210	1.13E+05	7.47E-01		Mo 99	2.53E+10	2.84E+00
Th231	3.89E+03	2.57E-02		Tc100	2.50E+10	2.81E+00
Pu239	3.62E+03	2.39E-02		Tc 99m	2.25E+10	2.53E+00
I 134	2.06E+03	1.36E-02		Dy165m	2.02E+10	2.27E+00
Xe135	2.00E+03	1.32E-02		In115m	1.83E+10	2.06E+00
Xe133	1.96E+03	1.30E-02		Cd115	1.83E+10	2.05E+00
I 133	1.96E+03	1.29E-02		Tb161	1.80E+10	2.02E+00
Mo 99	1.94E+03	1.28E-02		Sm153	1.77E+10	1.98E+00
Nb 97	1.85E+03	1.22E-02		Tm170	1.57E+10	1.76E+00
Rest	1.16E+05	7.68E-01		Rest	3.43E+11	3.85E+01

Table 7.6.6 Radionuclides and Percent Activity of the Activation Products of Pu-238 in a D-T Thermalized Flux spectrum.

	Base Case Level				High Flux Case Level	
NUCLIDE	ACTIVITY	PERCENT		NUCLIDE	ACTIVITY	PERCENT
	(Bq)	ACTIVITY			(Bq)	ACTIVITY
Total	1.33E+08			Total	3.99E+11	
H 3	5.79E+07	4.35E+01		Sm153	1.97E+10	4.93E+00
Tm170	3.97E+06	2.98E+00		Gd159	1.93E+10	4.84E+00
Er169	3.97E+06	2.98E+00		Ho166	1.79E+10	4.48E+00
Tb160	3.80E+06	2.86E+00		Dy165	1.77E+10	4.43E+00
Dy165	3.77E+06	2.83E+00		Tb161	1.57E+10	3.95E+00
Gd159	3.77E+06	2.83E+00		Er169	1.42E+10	3.56E+00
Ho166	3.65E+06	2.74E+00		Er167m	1.34E+10	3.36E+00
Er167m	2.78E+06	2.09E+00		Rh104	1.34E+10	3.35E+00
Yb175	2.48E+06	1.86E+00		Ru103	1.33E+10	3.34E+00
Eu154	2.46E+06	1.85E+00		Rh103m	1.31E+10	3.30E+00
Sm153	2.46E+06	1.85E+00		Eu157	1.24E+10	3.12E+00
Dy165m	2.41E+06	1.81E+00		Dy165m	1.20E+10	3.01E+00
Nd147	2.25E+06	1.69E+00		Pm149	1.15E+10	2.89E+00
Pm147	2.24E+06	1.69E+00		Nd147	1.15E+10	2.88E+00
Hf181	2.20E+06	1.65E+00		Nd149	1.03E+10	2.57E+00
Ta182	2.08E+06	1.56E+00		Eu156	9.84E+09	2.47E+00
Lu176m	1.61E+06	1.21E+00		Tm172	9.38E+09	2.35E+00
Pr142	1.60E+06	1.20E+00		Pd109	7.29E+09	1.83E+00
Ce141	1.60E+06	1.20E+00		Ag109m	7.28E+09	1.83E+00
Ba139	1.60E+06	1.20E+00		Ag110	6.98E+09	1.75E+00
Rest	2.45E+07	1.84E+01		Rest	1.43E+11	3.58E+01

When evaluating the activation products for transmutation of an actinide such as Pu-238, it is important to determine how much actinide activation products are generated. Actinides are defined here as radionuclides with atomic number from 89 (Actinium) and higher. Table 7.6.6.1 shows the total amount of actinides in the resulting activation products when the target actinide has been transmuted to the target level. Results are shown for the base case flux level and the high flux level for each of the four base cases.

Table 7.6.6.1 Actinides Generated By Transmutation of Pu-238 Down to < 37 Bq

Neutron Spectrum Used	Total Activity of Actinides Generated (Bq)	Dominant Actinide
D-T Unmoderated BC	1.71E+07	U-234
D-T Unmoderated Highest Flux Case	7.25E+03	U-237
D-T Moderated BC	1.85E+08	U-235
D-T Moderated Highest Flux Case	8.58E+07	Cm-249
D-D Moderated BC	1.40E+07	U-234
D-D Moderated Highest Flux Case	2.82E+08	Cm-249
D-T Thermalized BC	1.91E+02	Np-238
D-T Thermalized Highest Flux Case	8.17E+08	Cm-249

7.6.3 Radiation Protection and Dose Rate Calculation

The activation products resulting from the transmutation of Pu-238 as shown in Section 7.6.2 will have hazards associated with them. These are referred to as the hazard indexes. As described in Section 4.4, the hazard indexes evaluated include gamma dose rate at the surface of the activation products, the ingestion dose (committed effective dose equivalent), and the inhalation dose (committed effective dose equivalent) from each of the base cases at both the base case flux level as well as the high flux case evaluated. Table 7.6.7 shows the summary of the hazard indexes of the activation products generated by the transmutation of Pu-238 down to the ending activity level for each of the base cases considered.

Results show that the dose rate of the activation products will increase with the increase in flux; however, the radiotoxicity does not rise as fast with increased flux.

Table 7.6.7 Hazard Indexes Summary of the Activation Products for Pu-238

		Activation	Activation	Activation
Neutron Spectrum	On-target	Product	Ingestion	Inhalation
Used	flux	Dose rate	Dose	Dose
	(n/s/cm2)	(Sv/hr)	(Sv)	(Sv)
D-T Unmoderated BC	1.26E+11	1.94E+02	7.47E+00	3.94E+02
	1.26E+12	1.83E+03	3.10E+00	3.29E+02
	1.26E+13	1.25E+04	1.03E+01	9.53E+02
	1.26E+14	7.40E+03	9.23E+00	2.56E+01
	1.26E+15	6.84E+04	9.63E+01	2.47E+02
D-T Unmoderated HFC	1.26E+16	5.93E+05	7.46E+02	1.82E+03
D-T Moderated BC	1.55E+11	1.09E+03	1.88E+00	4.04E+02
	1.55E+12	2.15E+04	3.65E+01	1.28E+04
	1.55E+13	2.94E+03	2.95E+00	9.49E+00
	1.55E+14	2.46E+04	2.41E+01	5.61E+01
D-T Moderated HFC	1.55E+15	3.01E+05	3.39E+02	9.67E+02
D-D Moderated BC	4.22E+08	1.08E+00	1.13E+00	1.58E+02
	4.22E+09	5.51E+00	1.14E+00	1.61E+02
	4.22E+10	1.33E+02	1.22E+00	2.02E+02
	4.22E+11	5.13E+03	5.91E+00	1.50E+03
	4.22E+12	5.28E+02	5.76E-01	2.32E+00
	4.22E+13	6.29E+03	6.12E+00	1.75E+01
	4.22E+14	7.15E+04	7.08E+01	1.68E+02
D-D Moderated HFC	4.22E+15	7.33E+05	7.37E+02	1.97E+03
D-T Thermalized BC	1.59E+11	5.94E+01	7.14E-02	3.31E-01
	1.59E+12	6.19E+02	7.51E-01	2.72E+00
	1.59E+13	6.50E+03	8.25E+00	2.35E+01
	1.59E+14	6.53E+04	8.03E+01	2.79E+02
D-T Thermalized HFC	1.59E+15	3.00E+05	3.60E+02	1.19E+03

In evaluating the dose rate hazard index, the decay characteristics of the activation product is important as well, such as is common when evaluating the hazards of spent fuel. Figure 7.6.5 shows the comparison of the decay curves for the activation products

between the base and high flux case evaluated for the D-T unmoderated base case. Likewise, Figures 7.6.6, 7.6.7 and 7.6.8 show the comparisons for the D-T moderated base case, the D-D moderated base case, and the D-T thermalized base case, respectively.

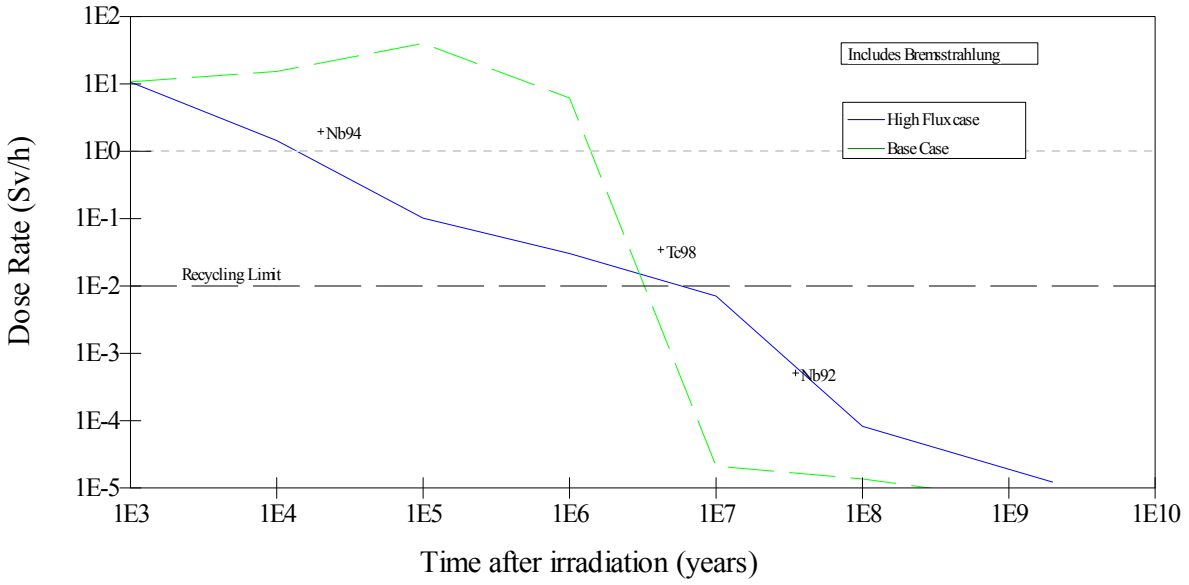

Figure 7.6.5 Decay Curve of Pu-238 Activation Products for the D-T Unmoderated Base Case

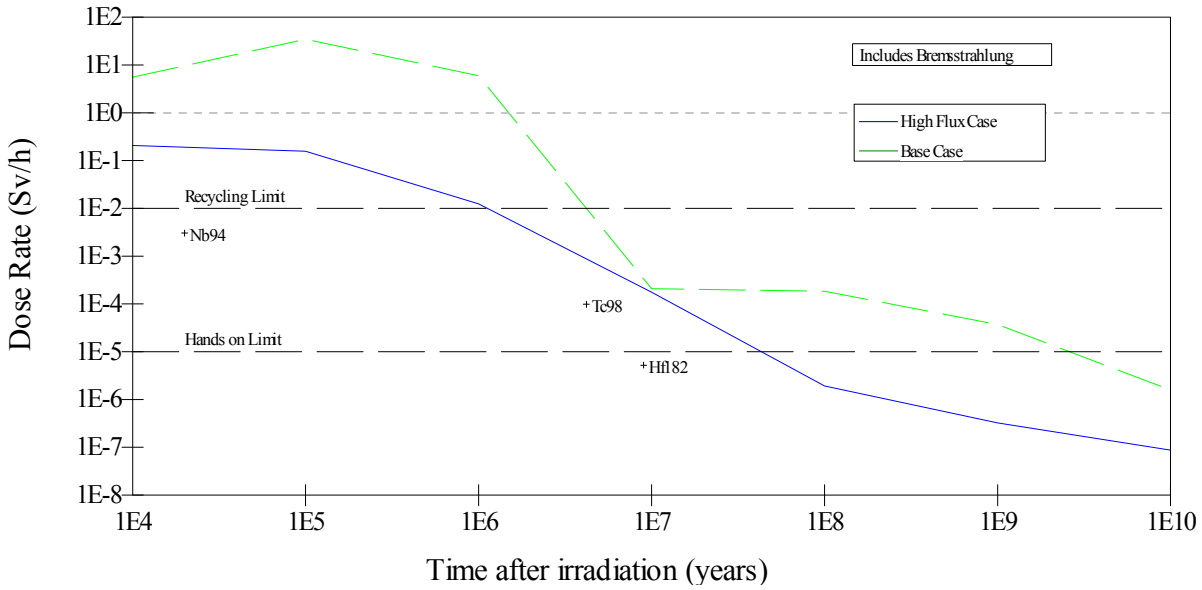

Figure 7.6.6 Decay Curve of Pu-238 Activation Products for the D-T Moderated Base Case

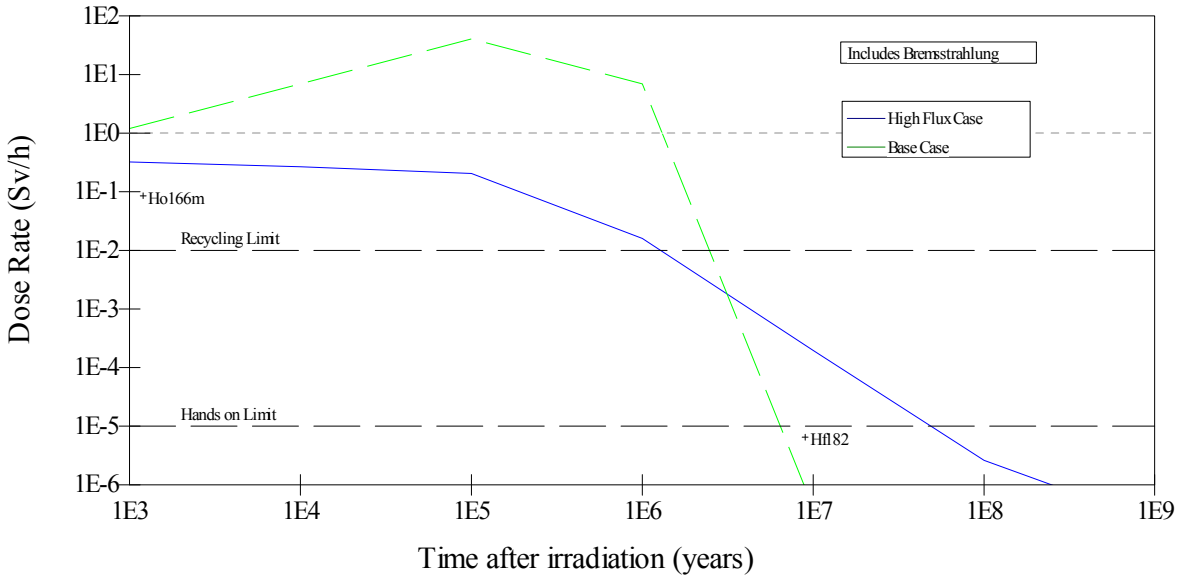

Figure 7.6.7 Decay Curve of Pu-238 Activation Products for the D-D Moderated Base Case

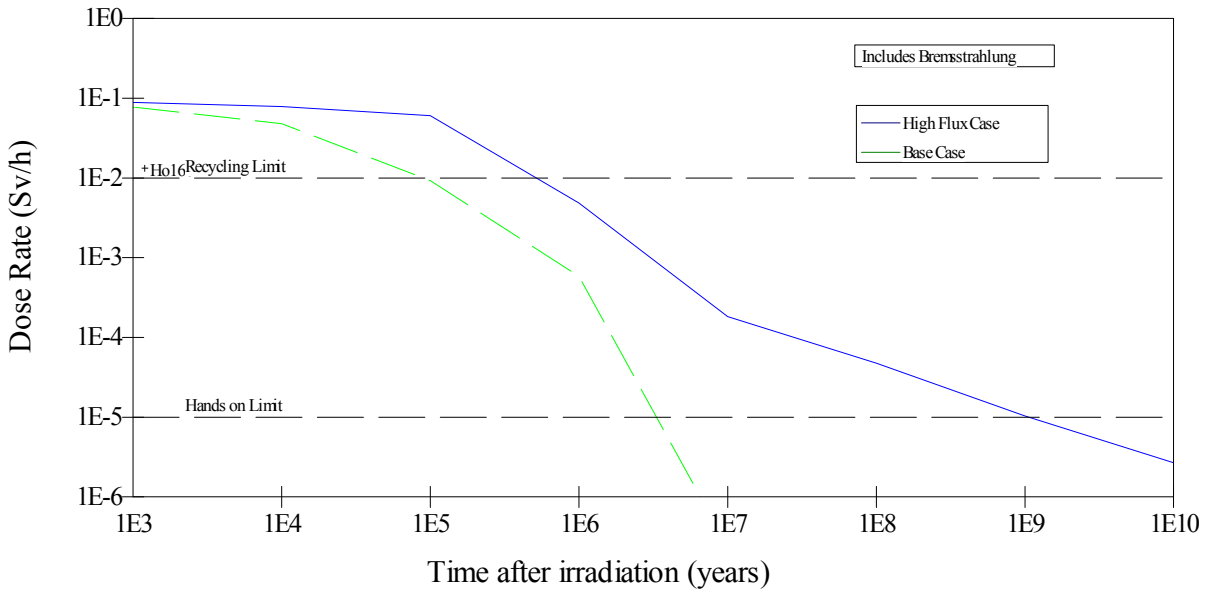

Figure 7.6.8 Decay Curve of Pu-238 Activation Products for the D-T Thermalized Base Case

Table 7.6.8 summarizes the approximate cooling time for the activation products to reach 1 mR/h dose rate. In the D-T Unmoderated case, the long activation cooling time in the base case is driven by U-235 with a half-life of 7.0E+8 years and the activation cooling time of the high flux case is driven by La-138 with a half-life of 1.05E+11 years. In the D-T Moderated case, the long activation cooling time is also driven by U-235 (with half-life of 7.0E+08 years) and La-138 (with half-life of 1.05E+11 years) for both the base case and high flux cases, respectively. In the D-D Moderated case, the long activation cooling time is driven by U-235 (with half-life of 7.04E+08 years) and Hf-182 (with half-life 9.2E+6 years) for the base case and high flux case, respectively. In the D-T Thermalized case, the long activation cooling time for the base case is driven by I-129 (with half-life of 1.57E+7 years) and for the high flux case s driven by Lu-176 (with half-life of 3.6E+10 years).

Table 7.6.8 Summary of Cooling Time for Pu-238 Activation Products

Neutron Spectrum Used	Approximate Cooling time To 1 mR/h (yrs)
D-T Unmoderated BC	2.0E+08
D-T Unmoderated Highest Flux Case	2.0E+09
D-T Moderated BC	3.0E+09
D-T Moderated Highest Flux Case	6.0E+07
D-D Moderated BC	8.0E+06
D-D Moderated Highest Flux Case	7.0E+07
D-T Thermalized BC	3.0E+06
D-T Thermalized Highest Flux Case	1.0E+09

7.6.4 Discussion

The following observations were made regarding the transmutation of Pu-238:

- In all three base cases other than the D-T thermalized, increases in flux creates more Pu-238 (thus, increasing the irradiation effective half-life) up to a few orders of magnitude before further increases begin to decrease the irradiation effective half-life. For the D-T thermalized case, the base case causes more Pu-238 to be generated so the irradiation effective half-life is longer than the radiological half-life; but subsequent increase in flux decreases the irradiation effective half-life proportionately.
- For Pu-238, neutron capture is the dominant process as compared to fission for transmutation because the capture to fission ratio is about 30 for the thermal energies and about 4.7 across the resonance integrals. However, the capture to

fission ration is extremely small, < 1.0E-08 at 14 MeV (D-T source neutron energies) [43].

- The lower energy spectra (D-T Moderated, D-D Moderated , and D-T Thermalized) transmutes Pu-238 more efficiently than the higher energy spectrum (D-T Unmoderated).
- The D-T Thermalized base case provides the more efficient process of the three lower energy spectra. At the base case flux level, the irradiation effective half-life far exceeds the radiological half-life (87.75 years); however, with a four order of magnitude increase in flux level, the irradiation effective half-life was down to about 10 months.
- For the D-T unmoderated and moderated cases, more actinides are generated in the base case than the high flux case; whereas, for the D-D moderated and D-T thermalized cases, more actinides are generated in the high flux cases than the base cases.

7.7 Plutonium-239

Figure 7.7.1 shows the fission corrected spectra for the Pu-239 base cases calculated by MCNPX. These spectra were used in FISPACT to perform the transmutation calculations. The largest differences between the Pu-238 and the Pu-239 spectra can be seen in the DD-moderated spectrum and the D-T thermalized spectrum. In the D-D moderated spectrum, there are neutrons above the source neutron energy of 2.5 MeV. In the D-T thermalized spectrum, there are much more neutrons in the energy range up to the maximum source energy of 14 MeV. The reason for the higher energy

neutrons for both of these spectra is from fission for which there are many more based on the higher fission cross-section for Pu-239 than Pu-238.

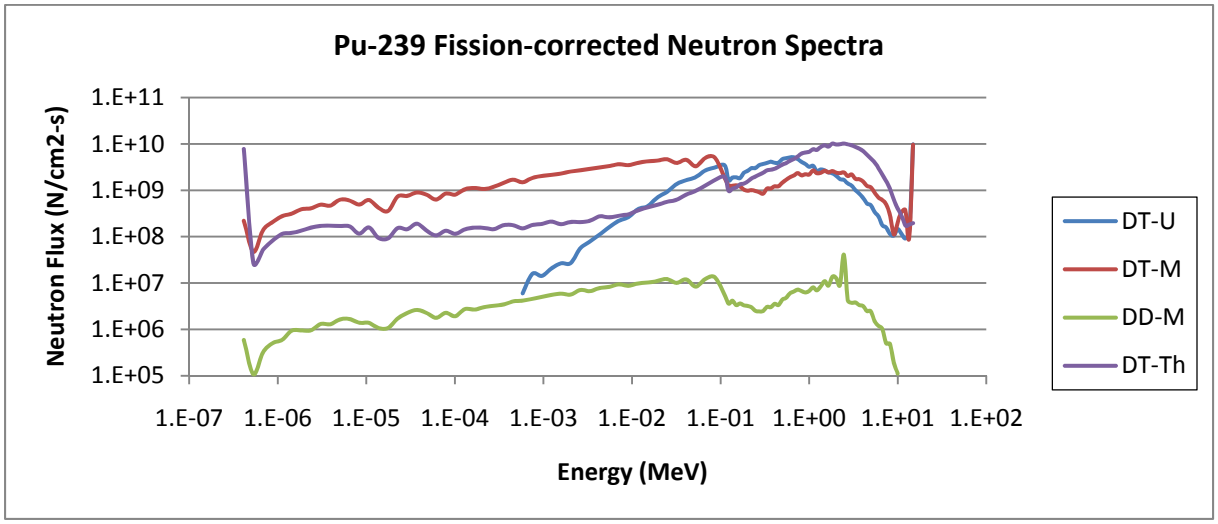

Figure 7.7.1 Pu-239 Fission Corrected Neutron Spectra for the Base Cases

Figure 7.7.2 shows the neutron reaction cross sections for Pu-239. As can be seen from the graph, the capture cross section is larger than the fission cross section up to about 0.08 MeV. In fact, the capture cross sections dominate the total cross section up to that point. Capture reactions are less desirable than fission reactions because more actinides are created during capture whereas; during fissions, smaller atoms (fission products) result.

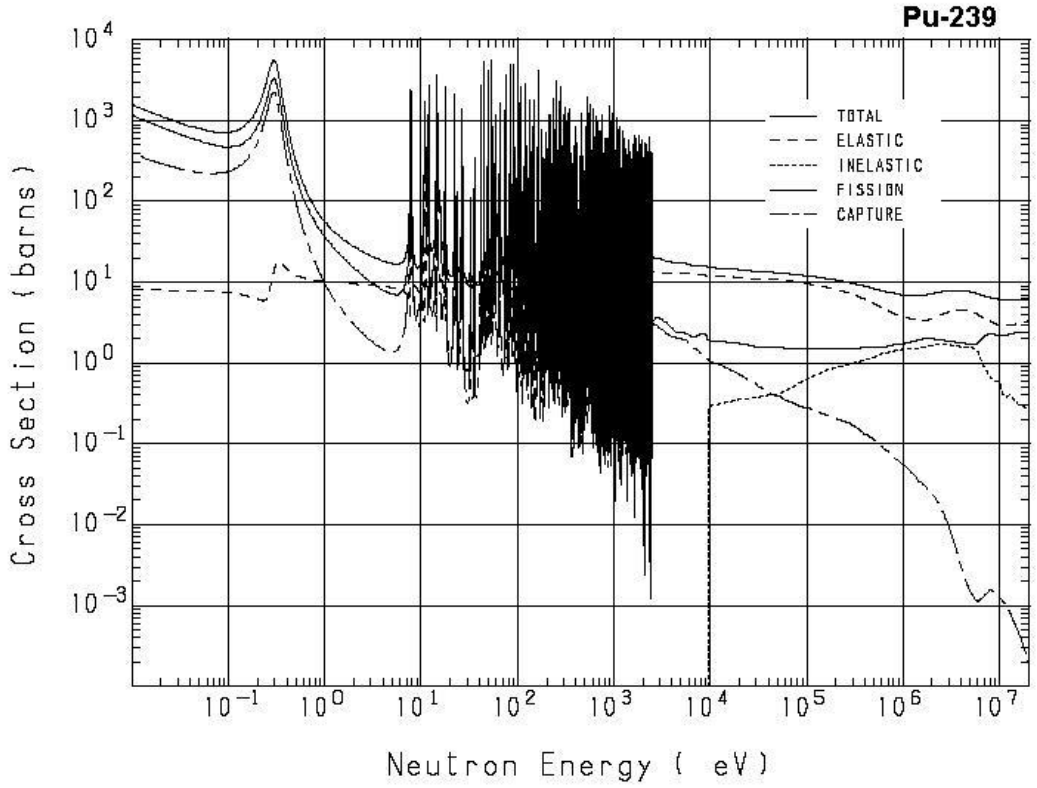

Figure 7.7.2 Neutron Reaction Cross Sections for Pu-239 [43]

Unlike Am-241 and Pu-238, the fission cross-section is dominant over the capture cross-section throughout most of the energy spectrum. In addition, the resonance region (where the cross-sections peak) covers a much wider energy range. Figure 7.7.3 shows the reaction thresholds for higher processes. Unlike with previous radionuclides, the (n, 2n) or higher processes may still occur with the D-D base case or the D-T thermalized base case due to the fact that there are neutrons above the D-D source energies and more neutrons in the D-T case up to the D-T source energies. As can be seen in the graphs, both the (n, 2n) and (n, 3n) cross-sections are higher for Pu-239 than for either Am-241 or Pu-238.

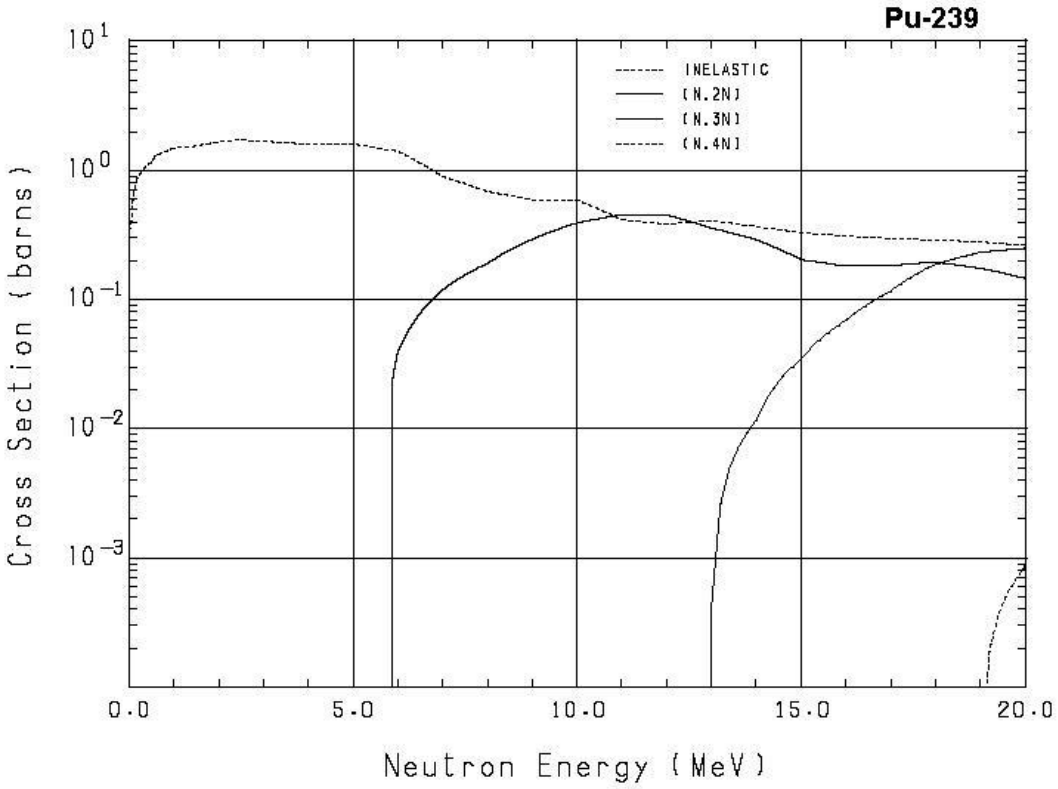

Figure 7.7.3 Neutron Reaction Thresholds for Pu-239 [43]

7.7.1 Results of Transmutation

Table 7.7.1 shows the results of the transmutation calculations for Pu-239 which has a radiological half-life of 2.41E+04 years. For Pu-239, the starting activity is 3.7e+10 Bq (1.0 Ci) and the ending activity is 37 Bq (1.0E-6 mCi). Under the description of the neutron spectrum used for the transmutation calculation, the BC stands for base case and the HFC stands for the high flux case (that flux level at which the irradiation time required is less than 100 years.)

Like the long-lived radionuclides, I-129 and Tc-99, the neutron fluence requirements for transmutation of Pu-239 stay fairly consistent as the flux increases for three of the four base cases: the base cases using the D-T neutron generator. For the base case using the D-D neutron generator, the irradiation effective half-life actually increases slightly over a three order of magnitude increase in flux before it starts to decrease with subsequent increases in the order of magnitude of flux. With the high energy spectrum (D-T unmoderated case), initially, the irradiation effective half-life is higher than the radiological half-life because at these lower flux levels production processes increase the amount of Pu-238. With the D-D case, the irradiation effective half-life is initially driven by the radiological half-life. For the D-T moderated and thermalized cases, the irradiation effective half-life is immediately lower than the radiological half-life at the base case flux level.

Table 7.7.1 Transmutation Results for Pu-239

Neutron Energy spectrum	On-target flux (n/s/cm2)	Irradiation Time (yrs)	Ending Activity (Bq)	Fluence Required (n/cm2)	Irradiation Effective Half-life (yrs)
D-T Unmoderated BC	1.34E+11	2.50E+06	3.76E+01	1.05E+25	8.37E+04
	1.34E+12	4.20E+05	3.24E+01	1.77E+25	1.40E+04
	1.34E+13	5.00E+04	3.35E+01	2.11E+25	1.66E+03
	1.34E+14	5.00E+03	4.31E+01	2.11E+25	1.68E+02
	1.34E+15	4.60E+02	3.88E+01	1.94E+25	1.54E+01
D-T Unmoderated HFC	1.34E+16	4.20E+01	3.02E+01	1.77E+25	1.39E+00
D-T Moderated BC	1.71E+11	5.00E+05	3.04E+01	2.70E+24	1.66E+04
	1.71E+12	5.70E+04	3.47E+01	3.07E+24	1.90E+03
	1.71E+13	6.20E+03	3.51E+01	3.34E+24	2.07E+02
	1.71E+14	4.40E+02	4.06E+01	2.37E+24	1.48E+01
D-T Moderated HFC	1.71E+15	2.60E+01	3.64E+01	1.40E+24	8.69E-01
D-D Moderated BC	4.75E+08	7.50E+05	2.72E+01	1.12E+22	2.47E+04
	4.75E+09	5.00E+05	3.27E+04	7.48E+22	2.49E+04
	4.75E+10	1.70E+06	3.14E+01	2.54E+24	5.64E+04
	4.75E+11	2.10E+05	4.22E+01	3.14E+24	7.07E+03
	4.75E+12	2.40E+04	2.82E+01	3.59E+24	7.92E+02
	4.75E+13	2.20E+03	3.84E+01	3.29E+24	7.37E+01
	4.75E+14	1.30E+02	2.81E+01	1.95E+24	4.29E+00
D-D Moderated HFC	4.75E+15	9.00E+00	2.62E+01	1.35E+24	2.96E-01
D-T Thermalized BC	2.40E+11	4.40E+05	3.16E+01	3.33E+24	1.46E+04
	2.40E+12	3.60E+04	3.48E+01	2.72E+24	1.20E+03
	2.40E+13	3.30E+03	3.42E+01	2.49E+24	1.10E+02
	2.40E+14	1.60E+02	3.22E+01	1.21E+24	5.31E+00
D-T Thermalized HFC	2.40E+15	8.00E+00	3.75E+01	6.05E+23	2.68E-01

Figure 7.6.4 shows these relationships with respect to the orders of magnitude increase in flux for each of the base cases.

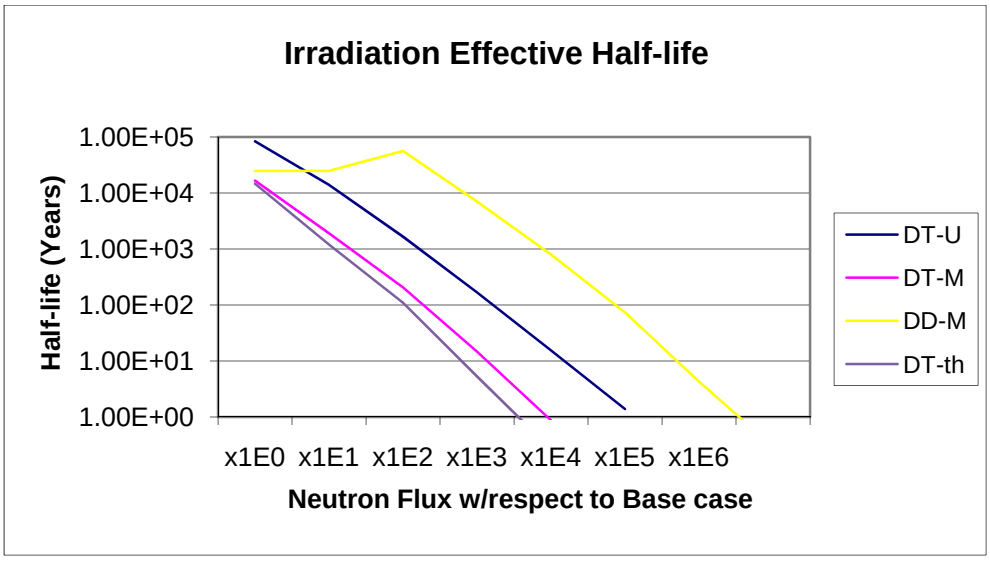

Figure 7.7.4 Irradiation Effective Half-life as a Function of Neutron Flux for Pu-239

7.7.2 Activation Products

Table 7.7.2 shows the summary of activation products generated by the transmutation of Pu-239 down to the ending activity level. The total activity of the results of the transmutation is given as well as the number of radioactive and non-radioactive nuclides. Results show that transmutation of Pu-239 creates quite a lot more activation products than the transmutation of the long-lived or short-lived fission products. The amount of activation products generated in Pu-239 transmutation is also higher than for Am-241 and Pu-238 as well. This can be explained with the higher reaction cross-sections for Pu-239; especially the fission cross-section which will result in radioactive fission products.

Table 7.7.2 Activation Products Summary for Pu-239

Neutron Spectrum Used	On-target flux (n/s/cm2)	Total Activation (Bq)	Number of Radioactive Nuclides	Number of Non-radioactive Nuclides
D-T Unmoderated BC	1.34E+11	2.09E+09	857	249
	1.34E+12	2.17E+10	909	254
	1.34E+13	2.20E+11	951	253
	1.34E+14	2.18E+12	1004	252
	1.34E+15	2.12E+13	1046	247
D-T Unmoderated HFC	1.34E+16	2.03E+14	1101	246
D-T Moderated BC	1.71E+11	1.05E+10	887	241
	1.71E+12	1.06E+11	911	241
	1.71E+13	1.12E+12	969	240
	1.71E+14	1.19E+13	1008	237
D-T Moderated HFC	1.71E+15	1.34E+14	1041	236
D-D Moderated BC	4.75E+08	1.65E+09	594	192
	4.75E+09	4.03E+09	642	200
	4.75E+10	2.34E+09	641	218
	4.75E+11	2.50E+10	647	218
	4.75E+12	2.56E+11	674	218
	4.75E+13	2.59E+12	722	218
	4.75E+14	2.64E+13	764	218
D-D Moderated HFC	4.75E+15	2.99E+14	771	215
D-T Thermalized BC	2.40E+11	6.86E+10	626	222
	2.40E+12	3.94E+11	677	221
	2.40E+13	3.34E+12	727	220
	2.40E+14	3.17E+13	747	218
D-T Thermalized HFC	2.40E+15	1.18E+15	744	215

Table 7.7.3 shows the most prominent activation products for transmutation of Pu-239 in a D-T moderated spectrum, both at base case and the high flux case levels. The radionuclides shown are present at the end of the transmutation period. Results show that the activation products generated by transmutation are a function of the flux level used because the production of the different radionuclides is dependent upon each radionuclide's production (or reaction) cross section and then their subsequent decay rate.

Table 7.7.4 shows the prominent activities for transmutation of Pu-239 in a D-T moderated spectrum, both at base case and high flux case levels. Table 7.7.5 shows the most prominent activation products for transmutation of Pu-239 in a D-D moderated spectrum, both at base case and high flux case levels. Likewise, Table 7.7.6 shows the most prominent activation products for the transmutation of Pu-239 in a D-T thermalized spectrum, both at base case and high flux case levels.

Table 7.7.3 Radionuclides and Percent Activity of the Activation Products of Pu-239 in a D-T Unmoderated Flux spectrum.

	Base Case Level				High Flux Case Level	
NUCLIDE	ACTIVITY	PERCENT		NUCLIDE	ACTIVITY	PERCENT
	(Bq)	ACTIVITY			(Bq)	ACTIVITY
Total	2.09E+09			Total	2.03E+14	
Rh103m	1.49E+08	7.12E+00		Rh103m	2.65E+13	1.30E+01
Ba135m	1.01E+08	4.82E+00		Ba135m	1.36E+13	6.68E+00
Xe131m	8.89E+07	4.25E+00		Rh104	1.06E+13	5.22E+00
Cs134	8.21E+07	3.92E+00		Xe131m	1.01E+13	4.97E+00
Ba133	6.72E+07	3.21E+00		Pd103	8.97E+12	4.41E+00
Ce139	5.88E+07	2.81E+00		Ag109m	8.30E+12	4.08E+00
Rh104	5.83E+07	2.78E+00		Ba133m	5.18E+12	2.55E+00
Ba137m	5.64E+07	2.70E+00		Cs134	4.99E+12	2.45E+00
Zr 90m	5.64E+07	2.69E+00		Ru103	4.93E+12	2.42E+00
Y 89m	5.06E+07	2.42E+00		Ce139	4.67E+12	2.29E+00
Pr140	4.49E+07	2.14E+00		Ba133	3.71E+12	1.82E+00
Cs132	4.34E+07	2.07E+00		Zr 90m	3.49E+12	1.71E+00
Pd103	4.23E+07	2.02E+00		Pr140	3.46E+12	1.70E+00
Ru103	4.07E+07	1.94E+00		Xe129m	3.42E+12	1.68E+00
Nb 93m	3.95E+07	1.88E+00		Nd141	3.35E+12	1.65E+00
La137	3.86E+07	1.84E+00		Tc 99m	3.13E+12	1.54E+00
Nd141	3.75E+07	1.79E+00		Y 89m	3.05E+12	1.50E+00
Xe133	3.46E+07	1.65E+00		Ag110	3.04E+12	1.50E+00
Ba133m	3.37E+07	1.61E+00		Cs132	2.97E+12	1.46E+00
Ba136m	3.07E+07	1.47E+00		Ba137m	2.87E+12	1.41E+00
Rest	9.39E+08	4.49E+01		Rest	7.31E+13	3.59E+01

Table 7.7.4 Radionuclides and Percent Activity of the Activation Products of Pu-239 in a D-T Moderated Flux spectrum.

	Base Case Level				High Flux Case Level	
NUCLIDE	ACTIVITY	PERCENT		NUCLIDE	ACTIVITY	PERCENT
	(Bq)	ACTIVITY			(Bq)	ACTIVITY
Total	1.05E+10			Total	1.34E+14	
Rh103m	4.17E+08	3.99E+00		Ho166	5.41E+12	4.05E+00
Rh104	4.16E+08	3.98E+00		Ag109m	5.39E+12	4.04E+00
Ru103	3.56E+08	3.40E+00		Dy165	5.32E+12	3.99E+00
Ag109m	3.42E+08	3.27E+00		Pd109	5.32E+12	3.98E+00
H 3	3.35E+08	3.20E+00		Ag110	5.13E+12	3.84E+00
Ag110	3.24E+08	3.09E+00		Gd159	4.84E+12	3.62E+00
Tm170	3.22E+08	3.08E+00		Rh104	4.79E+12	3.59E+00
Pd109	3.22E+08	3.08E+00		Rh103m	4.79E+12	3.58E+00
Mo 99	3.20E+08	3.06E+00		Er167m	4.38E+12	3.28E+00
Er169	3.17E+08	3.03E+00		Er169	4.38E+12	3.28E+00
Tc100	2.99E+08	2.86E+00		Ru103	4.01E+12	3.00E+00
Tc 99m	2.85E+08	2.72E+00		Dy165m	3.43E+12	2.57E+00
Ho166	2.45E+08	2.34E+00		Tc100	3.35E+12	2.51E+00
Dy165	2.44E+08	2.33E+00		Mo 99	3.35E+12	2.51E+00
Tb160	2.38E+08	2.27E+00		Tc 99m	2.98E+12	2.23E+00
Gd159	2.33E+08	2.22E+00		Tb160	2.87E+12	2.15E+00
Yb175	2.05E+08	1.96E+00		Tm170	2.81E+12	2.10E+00
Er167m	2.05E+08	1.96E+00		Sm153	2.65E+12	1.98E+00
Eu154	1.82E+08	1.74E+00		Eu156	2.46E+12	1.84E+00
La140	1.67E+08	1.60E+00		Tb161	2.17E+12	1.63E+00
		4.48E+01				
Rest	4.69E+09	5.09E+01		Rest	5.37E+13	4.02E+01

Table 7.7.5 Radionuclides and Percent Activity of the Activation Products of Pu-239 in a D-D Moderated Flux spectrum.

	Base Case Level				High Flux Case Level	
NUCLIDE	ACTIVITY	PERCENT		NUCLIDE	ACTIVITY	PERCENT
	(Bq)	ACTIVITY			(Bq)	ACTIVITY
Total	1.65E+09			Total	2.99E+14	
I 134	2.38E+07	1.44E+00		Ag109m	1.37E+13	4.58E+00
Cs138	2.07E+07	1.26E+00		Pd109	1.36E+13	4.55E+00
Xe133	2.06E+07	1.25E+00		Dy165	1.36E+13	4.54E+00
I 133	2.06E+07	1.25E+00		Ho166	1.36E+13	4.54E+00
Ba139	2.04E+07	1.24E+00		Ag110	1.30E+13	4.36E+00
Y 94	2.03E+07	1.23E+00		Gd159	1.25E+13	4.20E+00
Zr 95	2.02E+07	1.23E+00		Er167m	1.08E+13	3.60E+00
Nb 95	2.02E+07	1.23E+00		Er169	9.79E+12	3.28E+00
Xe135	2.02E+07	1.23E+00		Rh103m	9.12E+12	3.06E+00
Cs139	2.02E+07	1.23E+00		Ru103	9.10E+12	3.05E+00
Y 95	2.01E+07	1.22E+00		Rh104	9.05E+12	3.03E+00
Cs137	1.96E+07	1.19E+00		Dy165m	8.85E+12	2.96E+00
Te134	1.95E+07	1.19E+00		Tb161	8.12E+12	2.72E+00
Xe138	1.95E+07	1.18E+00		Mo 99	7.81E+12	2.62E+00
Sr 94	1.94E+07	1.18E+00		Tc100	7.70E+12	2.58E+00
Xe137	1.93E+07	1.17E+00		Tc 99m	6.96E+12	2.33E+00
I 135	1.92E+07	1.17E+00		Sm153	6.65E+12	2.23E+00
La140	1.91E+07	1.16E+00		Eu156	5.63E+12	1.89E+00
Tc 99	1.91E+07	1.16E+00		Cs136	5.53E+12	1.85E+00
Mo 99	1.91E+07	1.16E+00		Ru105	5.10E+12	1.71E+00
Rest	1.25E+09	7.57E+01		Rest	1.09E+14	3.64E+01

Table 7.7.6 Radionuclides and Percent Activity of the Activation Products of Pu-239 in a D-T Thermalized Flux spectrum.

	Base Case Level				High Flux Case Level	
NUCLIDE	ACTIVITY	PERCENT		NUCLIDE	ACTIVITY	PERCENT
	(Bq)	ACTIVITY			(Bq)	ACTIVITY
Total	6.86E+10			Total	1.18E+15	
H 3	3.48E+10	5.08E+01		Sm153	5.81E+13	4.93E+00
Tm170	1.57E+09	2.29E+00		Gd159	5.32E+13	4.51E+00
Er169	1.57E+09	2.29E+00		Rh104	4.90E+13	4.16E+00
Tb160	1.45E+09	2.12E+00		Ru103	4.90E+13	4.16E+00
Dy165	1.44E+09	2.11E+00		Rh103m	4.84E+13	4.11E+00
Gd159	1.44E+09	2.10E+00		Ho166	4.82E+13	4.09E+00
Ho166	1.40E+09	2.04E+00		Dy165	4.66E+13	3.95E+00
Yb175	1.14E+09	1.66E+00		Eu157	4.51E+13	3.83E+00
Er167m	1.07E+09	1.55E+00		Tb161	4.36E+13	3.70E+00
Hf181	1.05E+09	1.53E+00		Nd149	3.66E+13	3.10E+00
Ta182	9.85E+08	1.44E+00		Er167m	3.60E+13	3.05E+00
Sm153	9.50E+08	1.39E+00		Nd147	3.28E+13	2.79E+00
Dy165m	9.23E+08	1.35E+00		Dy165m	3.26E+13	2.76E+00
Eu154	9.01E+08	1.32E+00		Pm149	3.25E+13	2.76E+00
Nd147	8.78E+08	1.28E+00		Pd109	3.20E+13	2.71E+00
Pm147	8.74E+08	1.27E+00		Ag109m	3.19E+13	2.71E+00
Lu176m	7.47E+08	1.09E+00		Ag110	3.09E+13	2.62E+00
Ba139	7.08E+08	1.03E+00		Pm150	2.87E+13	2.44E+00
La140	7.06E+08	1.03E+00		Er169	2.85E+13	2.42E+00
Ce141	6.87E+08	1.00E+00		Eu156	2.39E+13	2.03E+00
Rest	1.33E+10	1.94E+01		Rest	3.91E+14	3.32E+01

When evaluating the activation products for transmutation of an actinide such as Pu-239, it is important to determine how much actinide activation products are generated. Actinides are defined here as radionuclides with atomic number from 89 (Actinium) and higher. Table 7.7.6.1 shows the total amount of actinides in the resulting activation products when the target actinide has been transmuted to the target level. Results are shown for the base case flux level and the high flux level for each of the four base cases.

Table 7.7.6.1 Actinides Generated By Transmutation of Pu-239 Down to < 37 Bq

Neutron Spectrum Used	Total Activity of Actinides Generated (Bq)	Dominant Actinide
D-T Unmoderated BC	3.23E+06	U-237
D-T Unmoderated Highest Flux Case	9.73E+06	Am-244
D-T Moderated BC	8.11E+04	Pu-238
D-T Moderated Highest Flux Case	1.37E+11	Cm-249
D-D Moderated BC	2.91E+07	U-235
D-D Moderated Highest Flux Case	4.70E+11	Cm-249
D-T Thermalized BC	3.62E+04	Np-239
D-T Thermalized Highest Flux Case	4.31E+11	Cm-249

7.7.3 Radiation Protection and Dose Rate Calculation

The activation products resulting from the transmutation of Pu-239 as shown in Section 7.7.2 will have hazards associated with them. These are referred to as the hazard indexes. As described in Section 4.4, the hazard indexes evaluated include gamma dose rate at the surface of the activation products, the ingestion dose (committed effective dose equivalent), and the inhalation dose (committed effective dose equivalent) from each of the base cases at both the base case flux level as well as the high flux case evaluated. Table 7.7.7 shows the summary of the hazard indexes of the activation products generated by the transmutation of Pu-239 down to the ending activity level for each of the base cases considered.

Results show that the dose rate of the activation products will increase with the increase in flux; however, the radiotoxicity does not rise as fast with increased flux.

Table 7.7.7 Hazard Indexes Summary of the Activation Products for Pu-238

Neutron Spectrum Used	On-target flux (n/s/cm2)	Activation Product Dose rate (Sv/hr)	Activation Ingestion Dose (Sv)	Activation Inhalation Dose (Sv)
D-T Unmoderated BC	1.34E+11	9.49E+00	4.82E+00	1.89E+02
	1.34E+12	8.48E+01	3.11E+01	1.50E+02
	1.34E+13	7.57E+02	3.12E+02	1.00E+03
	1.34E+14	7.18E+03	3.08E+03	9.03E+03
	1.34E+15	6.73E+04	2.91E+04	7.57E+04
D-T Unmoderated HFC	1.34E+16	6.14E+05	2.31E+05	5.53E+05
D-T Moderated BC	1.71E+11	3.25E+01	9.88E+00	4.30E+01
	1.71E+12	3.31E+02	9.61E+01	3.45E+02
	1.71E+13	3.63E+03	9.49E+02	2.80E+03
	1.71E+14	3.78E+04	9.95E+03	2.39E+04
D-T Moderated HFC	1.71E+15	4.20E+05	1.32E+05	5.37E+05
D-D Moderated BC	4.75E+08	1.69E+01	5.62E+00	1.00E+03
	4.75E+09	3.22E+01	1.63E+02	2.21E+04
	4.75E+10	6.45E+00	1.96E+00	1.48E+01
	4.75E+11	6.75E+01	2.02E+01	8.88E+01
	4.75E+12	7.21E+02	1.94E+02	7.04E+02
	4.75E+13	7.68E+03	1.90E+03	5.22E+03
	4.75E+14	7.79E+04	2.27E+04	7.05E+04
D-D Moderated HFC	4.75E+15	9.37E+05	2.53E+05	1.03E+06
D-T Thermalized BC	2.40E+11	9.85E+01	3.22E+01	1.35E+02
	2.40E+12	9.90E+02	3.25E+02	1.09E+03
	2.40E+13	9.65E+03	3.30E+03	1.12E+04
	2.40E+14	9.74E+04	3.33E+04	1.52E+05
D-T Thermalized HFC	2.40E+15	3.17E+06	9.98E+05	2.41E+06

In evaluating the dose rate hazard index, the decay characteristics of the activation product is important as well, such as is common when evaluating the hazards of spent fuel. Figure 7.7.5 shows the comparison of the decay curves for the activation products between the base and high flux case evaluated for the D-T unmoderated base case.

Likewise, Figures 7.7.6, 7.7.7 and 7.7.8 show the comparisons for the D-T moderated base case, the D-D moderated base case, and the D-T thermalized base case, respectively.

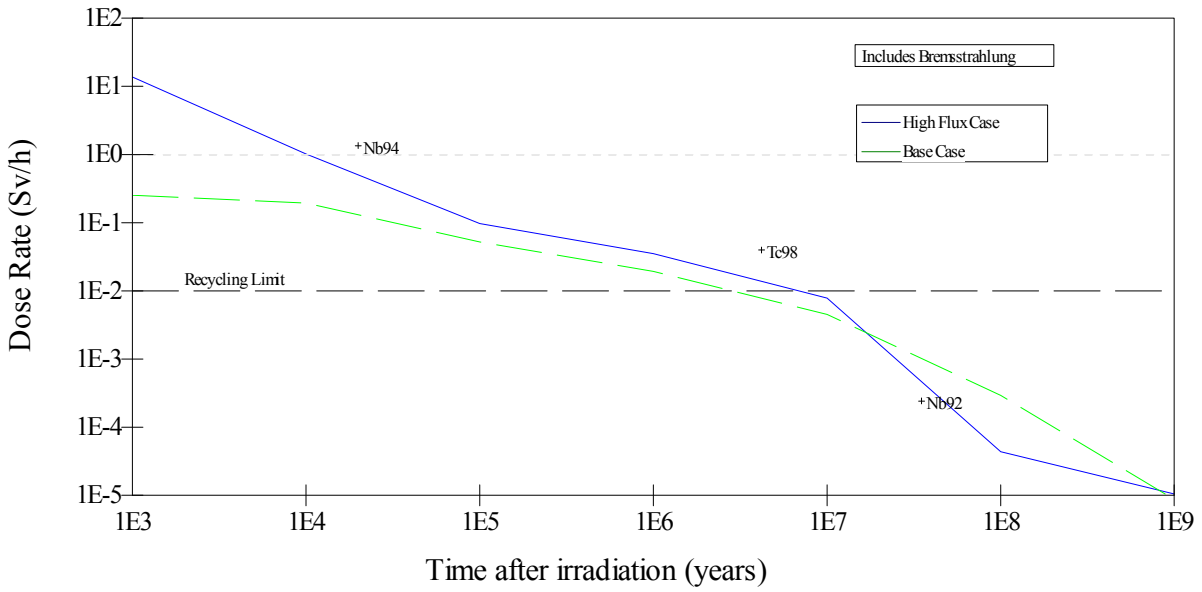

Figure 7.7.5 Decay Curve of Pu-239 Activation Products for the D-T Unmoderated Base Case

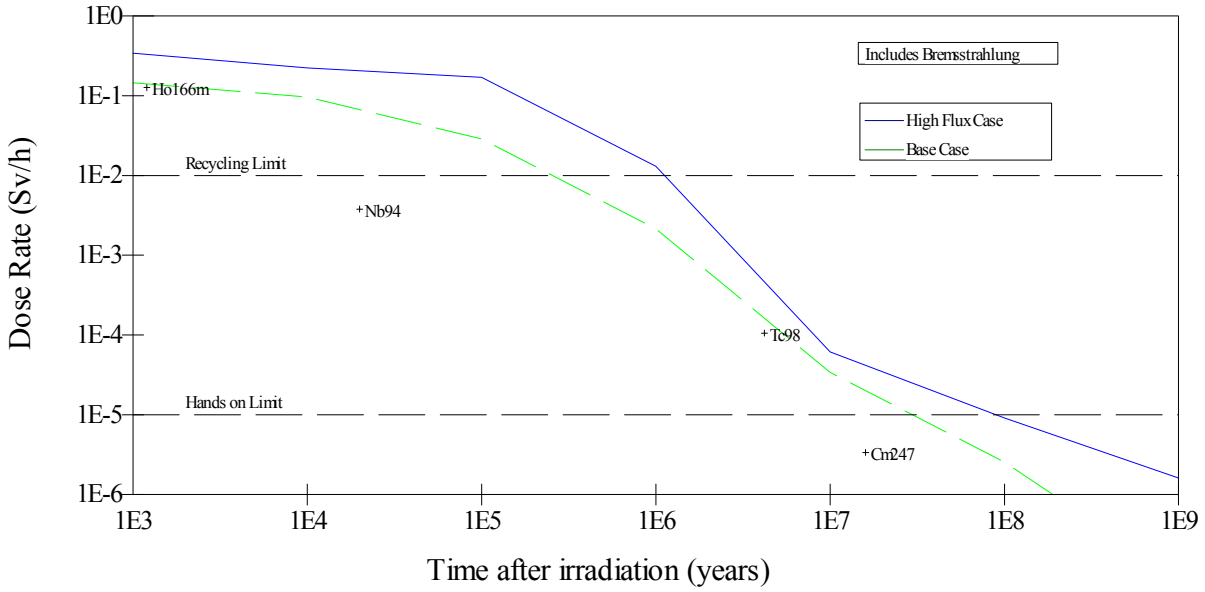

Figure 7.7.6 Decay Curve of Pu-239 Activation Products for the D-T Moderated Base Case

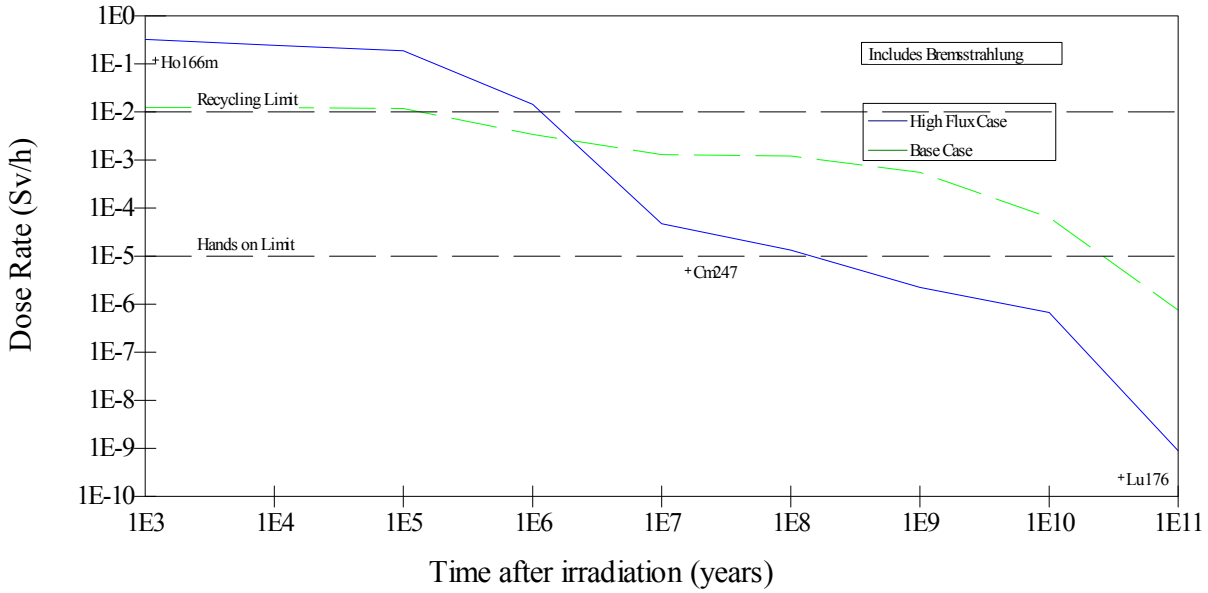

Figure 7.7.7 Decay Curve of Pu-239 Activation Products for the D-D Moderated Base Case

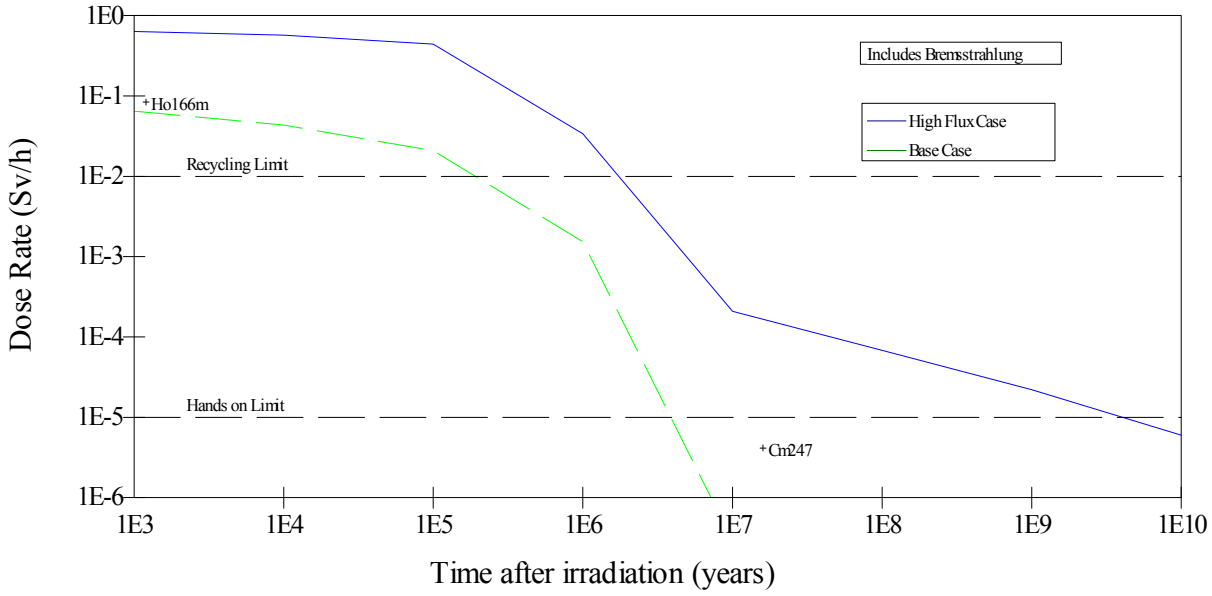

Figure 7.7.8 Decay Curve of Pu-239 Activation Products for the D-T Thermalized Base Case

Table 7.7.8 summarizes the approximate cooling time for the activation products to reach 1 mR/h dose rate. In the D-T Unmoderated case, the long activation cooling time in both the base case and the high flux case is driven by Nb-92 with a half-life of 3.6E+7 years. In the D-T Moderated case, the long activation cooling time in the base case is also driven by Nb-92; but the long activation cooling time in the high flux case is driven by Cm-247 (with half-life of 1.5E+07 years). In the D-D Moderated case, the long activation cooling time is driven by U-235 (with half-life of 7.04E+08 years) and Hf-182 (with half-life 9.2E+6 years) for the base case and high flux case, respectively. In the D-T Thermalized case, the long activation cooling time is driven by Hf-182 for the base case and Cm-247 in the high flux case.

Table 7.7.8 Summary of Cooling Time for Pu-239 Activation Products

Neutron Spectrum Used	Approximate Cooling time To 1 mR/h (yrs)
D-T Unmoderated BC	9.0E+08
D-T Unmoderated Highest Flux Case	1.0E+09
D-T Moderated BC	3.0E+07
D-T Moderated Highest Flux Case	9.0E+07
D-D Moderated BC	3.0E+10
D-D Moderated Highest Flux Case	1.0E+08
D-T Thermalized BC	3.0E+06
D-T Thermalized Highest Flux Case	3.0E+09

7.7.4 Discussion

The following observations were made regarding the transmutation of Pu-239:

- In all the cases utilizing the D-T generator, an increase in flux from the base case decreases the irradiation effective half-life. With the D-D generator case, initial increases in flux creates more Pu-239 (thus, increasing the irradiation effective half-life) up to a few orders of magnitude before further increases begin to decrease the irradiation effective half-life.
- For Pu-239, unlike Am-241 and Pu-238, fission is the dominant process over capture; i.e., the capture to fission ratio < 1. The capture to fission ratio is about 0.36 for the thermal energies and about 0.6 across the resonance integrals. The capture to fission ration is the smallest, 0.03 at 14 MeV (D-T source neutron energies) [43]; however, the fission cross-section is much smaller at this energy than at thermal or resonance energies.
- The lower energy spectra for the D-T generators (D-T Moderated, and D-T Thermalized) transmute Pu-239 more efficiently than the higher energy spectrum (D-T Unmoderated).
- The D-T Thermalized base case provides the most efficient process than the other base cases. At the base case flux level, the irradiation effective half-life was already slightly lower than the radiological half-life (2.4E+04 years); and, with a four order of magnitude increase in flux level, the irradiation effective half-life was down to about 3 - 4 months.

- With all base cases, more actinides are generated at the high flux case level than the base case level. For the D-T unmoderated case, the increase is small but for the lower energy spectra, the increase was orders of magnitude.

7.8 Summary of Results

The following is a summary of the results from this Chapter. Details of the results are found in the respective Sections, Figures, and Tables:

Tc-99 and I-129: The transmutation characteristics of these long-lived fission products are very similar due to the fact that they have very similar neutron reaction cross sections. The thermalized neutron energy spectrum is the most beneficial for transmuting these radionuclides and a three order magnitude increase in the base case flux level can produce irradiation effective half lives of only a few year for these radionuclides. The irradiation effective half life is inversely proportional to the increase in neutron flux. The hazard indices are directly proportional to the increase in flux. At the high flux levels for all three base cases, activation products generated takes longer to decay down to a surface dose rate of 1 mRem/h than activation products generated at the base case flux levels. For Tc-99 specifically, higher energy neutrons (above about 10 MeV) will create activation products with half lives even longer than the Tc-99 half life; therefore, there should be no high energy component in the transmutation strategy.

Cs-137 and Sr-90: The transmutation characteristics of these short-lived fission products are very similar due to the fact that they have similar neutron reaction cross sections. The reaction cross sections are very small so transmutation is very inefficient. Transmutation is not recommended for these radionuclides with any of the transmuter

base cases in this dissertation. Over several orders of magnitude increases in the base case fluxes, the irradiation effective half life actually increases over the radiological half life due to production processes of these radionuclides. The irradiation effective half life will become smaller than the radiological half life only after a four to five order of magnitude increase in the base case fluxes; while generating unwanted activation products. The activation products generation is proportional to the flux but at a lower rate of increase than for the long-lived fission products. At the high flux levels for all four base cases, activation products generated takes longer to decay down to a surface dose rate of 1 mRem/h than activation products generated at the base case flux levels.

Am-241, Pu-238 and Pu-239: The transmutation efficiency, activation product generation, and hazard indices of the activation products are highly dependent on the neutron reaction cross sections of these radionuclides. Transmutation of these radionuclides does generate other actinides. The fission-to-capture cross section ratios play a major role in the amounts of actinides generated and their subsequent hazard indices. The irradiation effective half life is not directly proportional to the increase in neutron flux due to the complex reaction cross section and the competing processes of production and depletion; however, the irradiation effective half life does become proportional to the increase in flux after a few orders of magnitude increase. The thermalized neutron spectra is the more beneficial energy spectrum and a four order magnitude increase in the base case flux level can produce irradiation effective half lives of less than a year for these radionuclides. The very long time scale for activation products to reach 1 mrem/h surface dose rate is similar at both the base case and high flux case levels.

Chapter 8

Shielding Requirements for Conceptual Transmutation Device

Shielding calculations were conducted for the conceptually designed transmutation device to determine the amount of shielding material required for operating the device based on a 30-cm and one-meter dose rate. The 30-cm dose rate is important to determine posting requirements such as "Radiation", and "High Radiation" areas defined as > 5.0 mrem in any one hour or > 100 mrem in any one hour respectively. The one meter reading is important to determine facility shielding requirements (such as requiring a shielded vault for the device) or to determine a posting requirement for "Very High Radiation" area defined as 500 rads in any one hour at one meter from the surface of the source. These definitions are found in the Nuclear Regulatory Commission radiation protection regulations [36.]

Because the transmutation device emits neutrons isotropically and is inside a spherical shell, one would expect the dose rate outside the device to be symmetrical around the device. However, as seen in Figure 6.1, the neutron generator source is not located directly in the center of the sphere but is off-centered on the x-axis to make room for a target. One would expect to see that the dose rates outside the device would still be symmetrical in the y and z directions, slightly higher in the (–x) direction and slightly lower in the (+x) direction (at a given distance from the sphere). Calculations were made using the highest dose rate scenario; the D-T generator in an unmoderated sphere

configuration. This is considered the "worst case" and would determine the maximum amount of shielding required.

MCNPX was used to calculate the dose rates. Specifically, a point detector tally (F5) outside the sphere was used to calculate both a neutron and a photon dose rate. Although this is a neutron source, one would expect a photon dose resulting from neutron interactions with the materials in the sphere surrounding the source. The tally includes the neutron and photon flux along with their energy distribution at the dose point. As explained in Section 4.5, the dose rate was calculated using these energy dependent fluxes and the energy dependent neutron and photon flux-to-dose conversion factors from references [41] and [40], respectively.

Table 8.1 shows the results of dose rate calculations using the D-T unmoderated base case (neutron source strength of 3.0E+14 n/s) from a bare transmutation device (no shielding) at one meter from the surface of the sphere on axes in the +x, -x, +y, -y, +z, and –z directions.

Table 8.1 Dose Rates Around Bare Transmutation Device Using D-T Neutron Source

Dose Rate Location	Neutron Dose Rate (mrem/h)	Photon Dose Rate (mrem/h)	Total Dose Rate (mrem/h)
1 meter in x direction	1.04E+08	3.22E+04	1.04E+08
1 meter in -x direction	2.01E+08	9.01E+04	2.01E+08
1 meter in y direction	1.23E+08	4.27E+04	1.23E+08
1 meter in -y direction	1.21E+08	4.32E+04	1.21E+08
1 meter in z direction	1.23E+08	4.34E+04	1.23E+08
1 meter in -z direction	1.23E+08	4.37E+04	1.23E+08

The results confirm that the dose rate is symmetrical in the y and z directions while the (–x) direction is slightly higher and the (+x) direction is slightly lower. Consequently, the worst case is in the (–x) direction. All subsequent shielding calculations tallied the dose only in one location due to the computation requirements in the radiation transport modeling. Layers of shielding material were added in one foot increments until the dose rate dropped to < 5 mrem in any one hour. Due to the intense computation times required to perform shielding calculations, the MCNPX model employed variance reduction techniques (as explained in Section 4.5) in order to get reliable results in shorter periods of time, especially as shielding thickness increased. The number of histories used in each calculation ensured that the relative error (defined as the ratio of the standard deviation of the tally mean to the mean [63])of the dose tally was < 0.05.

Table 8.2 shows the results of the dose rate calculations with varying thicknesses of shielding material from no shielding through seven feet of concrete. The composition

and density of normal concrete taken from ANSI/ANS 6.6.1standard was used [65]. As the concrete thickness increased the photon dose rate increased due to increased (n,γ) reactions in concrete. Therefore, when the neutron dose rate was sufficiently low (a few mrem/h), a layer of lead was added on the outside of the concrete to shield the capture gammas produced inside the concrete. This exercise was not performed to optimize shielding but only to get an idea of how much shielding would be required for the device to be considered a self-shielded device. Results show that seven feet of concrete with five cm lead would be necessary in order for the device to be operated as a self-shielded device requiring a posting of "Radiation Area". Figure 8.1 shows a graphical representation of the dose rate data found in Table 8.2.

Table 8.2 Dose Rate at 30-cm with from the Surface of the Transmuter with Varying Shielding Thicknesses

	Neutron	Photon	Total
Dose Rate 1 foot from Transmuter	Dose rate	Dose rate	Dose rate
Surface With Shielding Thickness	mrem/hr	mrem/hr	mrem/hr
0'	6.84E+08	3.23E+05	6.84E+08
1'	4.67E+07	1.62E+06	4.83E+07
2'	3.83E+06	6.22E+05	4.46E+06
3'	3.46E+05	1.63E+05	5.10E+05
4'	2.86E+04	1.41E+04	4.27E+04
5'	2.46E+03	2.05E+03	4.51E+03
6'	4.36E+01	1.82E+02	2.25E+02
7' + Lead	2.53E+00	2.67E+00	5.20E+00

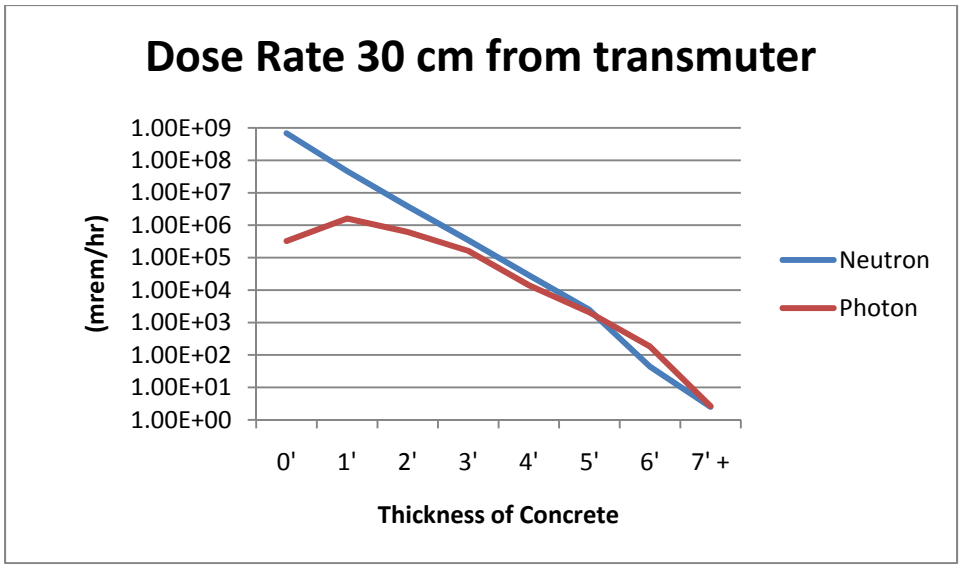

Figure 8.1 Dose Rate at 30-cm from the Surface of the Transmuter with Varying Shielding Thicknesses

Figure 8.2 shows a geometry plot of the transmutation device with the total amount of shielding required. The plot shows the composite structure of the shield in the model to incorporate the variance reduction techniques for the simulation.

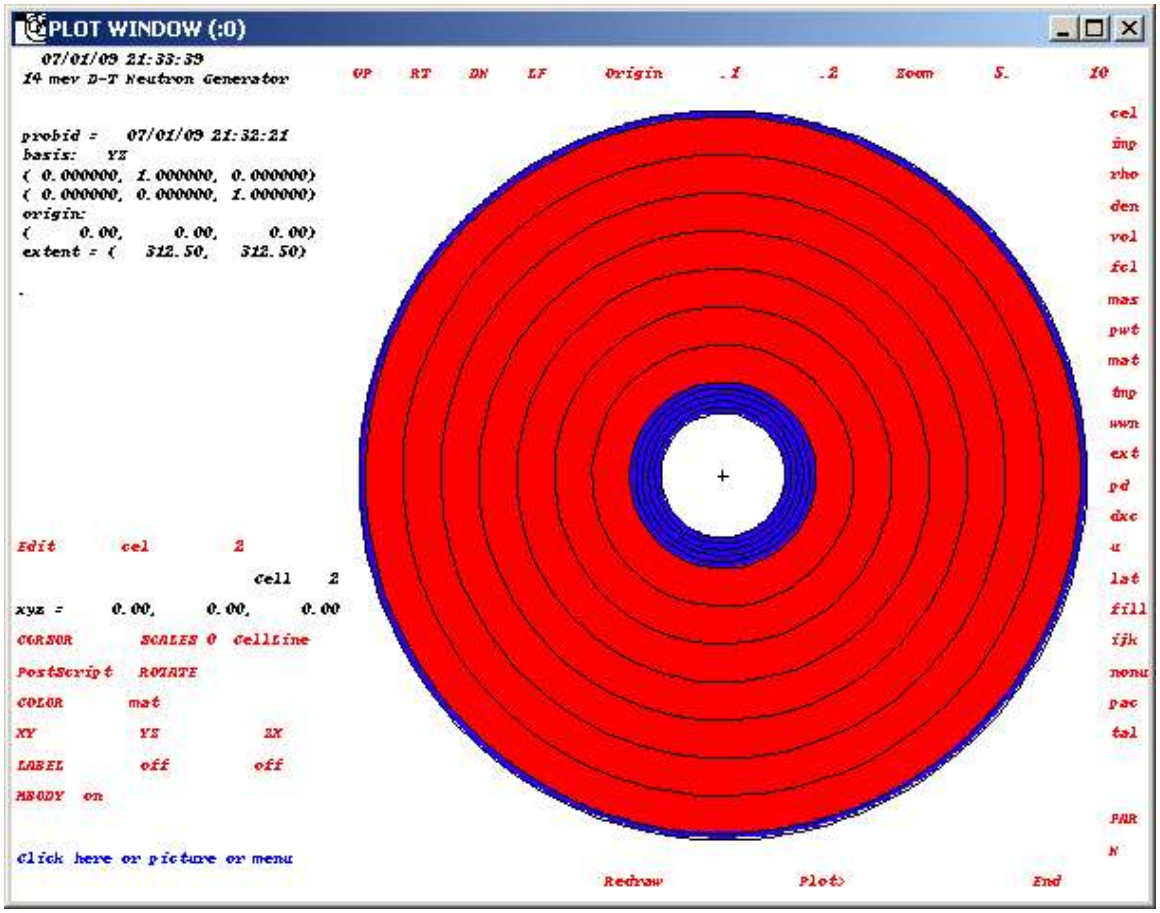

Figure 8.2 Geometry Plot of Transmutation Device Surrounded by Layers of Concrete Shielding Material

The calculations show that there will be a considerable dose rate outside the transmutation device during operations, and radiation shielding will be required. About seven feet of concrete plus a layer of lead would be required to operate the device as a self-shielded device. This amount of shielding is reasonable for localized shielding when one considers the amount of facility shielding required for a nuclear reactor. The containment building requires up to six feet of concrete [66]. A medical accelerator might require up to four feet of concrete thickness for a much lower neutron flux level [67].

Chapter 9

Heat Load Calculations for Conceptual Transmutation Device

The purpose for this Chapter is to describe the computational methodology used to determine the heat load in the lead spherical shell during operations of the device. A qualitative conclusion was made on whether the device would need active cooling, based on a quantitative evaluation of the heat generated in the shell of the device. No attempt was made to determine heat removal requirements as this would be more appropriate at an engineering design phase.

For the heat load calculations, the D-T unmoderated base case was utilized. This is the same base case that was used for the shielding calculations in Chapter 8. The lead shell of the transmutation device is the location of interest for the heat load calculations to determine if any cooling may be necessary. The D-T unmoderated case was assumed to be the worst case because preliminary analyses of radiation transport calculations showed more collision heating and more activation products generated in this case than the D-T and the D-D moderated cases. As explained in Section 4.6, two sources of heat load were evaluated: collision heating from the radiation interactions and the decay of the radioactive activation products in the lead spherical shell. In MCNPX, the +F6 tally was used for collision heating (accounting for energy deposition from all particles and photons in the problem) which resulted in units of MeV/sec which were then converted to kW. In FISPACT, the activation products in the lead spherical shell were calculated

using the neutron flux and energy distribution impinging upon the lead shell calculated by MCNPX. The heat load from those activation products summed up to 0.305 kW.

The FISPACT results showed the highest amount of activation product (saturation level) produced in the lead spherical shell was 1.82E+14 Bq resulting in a heat load of 0.0453 kW. The total heat load on the lead spherical shell was therefore, 0.305 + 0.0453 = 0.351 kW.

The specific heat capacity of lead is 0.13 J/gm-°C [68]. The total amount of lead in a 25 cm thick spherical shell with a density of 11.35g/cc [68] was determined to be 1.407E+07 grams. The total heat load or power in the lead shell of 0.351 kW can be converted to Joules by using:

$$1\ J = 2.8E\text{-}07\ kW\text{-}hr \quad [32] \tag{9.1}$$

Therefore:

$$(0.351\ kW)x\frac{1\ J}{2.8E-07\ kW-hr/J)} = 1.25E+06\ J/hr \tag{9.2}$$

Then using the specific heat capacity of lead, the temperature rise in the lead sphere is:

$$\left(0.13\frac{J}{gm-°C}\right)x\frac{1.407E+07\ gm}{1.25E+06\ J/hr} = 1.46\ hr/°C \tag{9.3}$$

Or

0.69 °C/hr

This result shows that the transmutation device will require cooling when operating continuously for many hours. The melting point of lead is about 327 °C. Without heat

removal, the transmutation device could be operated for no more than about 474 hours, depending on the ambient temperature, before the lead exceeds its melting point.

Chapter 10

Conclusions and Future Work

This dissertation presents the design and feasibility of a small-scale, fusion-based transmutation device incorporating a commercially available neutron generator. It also presents the design features necessary to optimize the device and render it practical for the transmutation of selected long-lived fission products and actinides.

Four conceptual designs of a transmutation device were used to study the transformation of seven radionuclides: long-lived fission products (Tc-99 and I-129), short-lived fission products (Cs-137 and Sr-90), and selective actinides (Am-241, Pu-238, and Pu-239). These radionuclides were chosen because they are major components of spent nuclear fuel and also because they exist as legacy sources that are being stored pending a decision regarding their ultimate disposition.

The four designs include the use of two different devices; a Deuterium-Deuterium (D-D) neutron generator (for one design) and a Deuterium-Tritium (D-T) neutron generator (for three designs) in configurations which provide different neutron energy spectra at the target location containing the radionuclide for transmutation. Key parameters analyzed include total fluence and flux requirements; transmutation effectiveness measured as irradiation effective half-life; and activation products generated along with their characteristics: activity, dose rate, decay, and ingestion and inhalation radiotoxicity.

From this investigation, conclusions were drawn about the feasibility of the device, the design and technology enhancements that would be required to make transmutation practical, the most beneficial design for each radionuclide, the consequence of the transmutation, and radiation protection issues that are important for the conceptual design of the transmutation device.

10.1 Main Results and Conclusions from this Investigation

The following conclusions were drawn during the course of this research:

- A rigorous calculation methodology for transmutation analyses was developed by coupling the MCNPX radiation transport code with the FISPACT activation code. The methodology includes calculation of "a fission corrected neutron spectrum" as input into the FISPACT code for activation calculations when evaluating actinides because the FISPACT code does not propagate fission neutrons. The methodology used in this research allowed for evaluations of issues that are not typically investigated during transmutation studies; the consequence of the transmutation, including the activation products generated during transmutation and their hazardous characteristics (radioactivity and radiotoxicity).
- The neutron source strength of the D-T and D-D neutron generators used in this investigation was not sufficient to perform transmutation in a reasonable period of time as defined herein; however, the transmutation of long-lived fission products and select actinides can be practical through a combination of technological enhancements to the neutron source and system design optimization.

- A three order of magnitude increase in the source strength, if possible, could result in irradiation effective half-lives of a few years for long-lived fission products. The ideal neutron energy spectrum for transmutation of long-lived fission products is the thermalized energy spectrum.
- A four order magnitude increase in the source strength could result in irradiation effective half-lives of < 1 year for select actinides. The ideal neutron energy spectrum for transmuting actinides is highly dependent on the particular radionuclide and its fission-to-capture ratio as these parameters determine the generation rate of other actinides.
- There is no overall benefit in using the D-D generator as the neutron source for a transmutation device. The D-D neutron generator has one advantage over the D-T generator in producing a lower neutron energy spectrum. This lower energy spectrum increases transmutation efficiencies for radionuclides with resonances in the lower energy ranges and eliminates higher order processes such as (n, 2n), (n, 3n) or (n, a) reactions which could lead to longer-lived activation products. However, this advantage is easily compensated for by moderating or thermalizing the neutron energy spectrum inside the D-T neutron generator device, as seen with the D-T moderated and D-T thermalized base cases.
- The long-lived fission products, Tc-99 and I-129, behave similarly with regards to transmutation characteristics due to the fact that they have very similar neutron reaction cross sections. The irradiation effective half-life is inversely proportional to the flux in an almost linear fashion. Unfortunately, the activity, dose rate, ingestion radiotoxicity and inhalation radiotoxicity of activation products all

increase with increasing flux. Consequently, one must balance how quickly the transmutation is accomplished with how much activation products will be managed. Because of the neutron resonances in the low energy range and the overall higher cross-sections, the lower neutron energy spectrum is the most beneficial for transmutation of these radionuclides. For the D-T thermalized configuration, only a three order of magnitude increase in flux is required to transmute the Tc-99 and I-129 within a reasonable period of time. This constitutes reducing the radiological half-life of I-129 (1.57E+07 years) down to an irradiation effective half-life of about four years and reducing the radiological half-life of Tc-99 (2.13E+05 years) down to an irradiation effective half-life of about seven years. The three order magnitude in flux can be accomplished by a combination of increasing the source strength of the D-T generator and optimizing the design of the transmutation device. In Chapter 5, it was shown that decreasing the size of the sphere or incorporating alternate materials such as beryllium as a reflector/multiplying material could increase the flux.

- This investigation confirmed industry opinion that there is no benefit in trying to transmute short-lived fission products due to low neutron reaction cross sections and the generation of a multiplicity of counterproductive activation products. The short-lived fission products Cs-137 and Sr-90 behave similarly with regards to transmutation characteristics due to the fact that they have very similar neutron reaction cross sections. Results from all four base cases studied for both radionuclides show that radionuclide depletion is dominated by its radiological half-life, not only at the design neutron generator flux (considered the base cases)

but also for several orders of magnitude increase in the flux (the high flux cases). The irradiation effective half-life falls below the radiological half-life (30.17 years for Cs-137 and 28.8 years for Sr-90) only after a five or more order in magnitude increase in the flux. Similar to the long-lived fission products, the activity, dose rate, ingestion dose and inhalation dose of the activation products of these short-lived fission products all increase with an increase in the flux. As discussed in Chapter 7, the cross-sections for any beneficial reactions are extremely low resulting in the low transmutation efficiency. Using higher fluxes for the transmutation generates longer-lived activation products which can ultimately become more radiotoxic than the fission products themselves.

- In the case of actinide transmutation additional actinides were created in all four base cases; whereas no actinides were created with the transmutation of the long or short-lived fission products. The actinides' transmutation characteristics are radionuclide specific. For example, Am-241 has the highest capture-to-fission ratio over the energy spectrum as compared to Pu-238 and Pu-239; while Pu-239 has the lowest. The magnitude of the cross-section and the resonance integrals are also important the transmutation results. For each of the three lower energy base cases, the increase in flux increased the amount of actinides generated; however, for the higher energy base case, the higher fluxes produced less or about the same amount of actinides generated. The reason for this is that, even for Am-241, the fission cross section is higher than the capture cross-section at high energies (above about 1 MeV). The fluxes are small in this higher energy range but are greater for the D-T unmoderated case than for the other base cases.

- For Am-241, the lowest energy spectrum (D-T thermalized) is the most beneficial for transmutation. The radiological half-life of 432 years can be reduced to an irradiation effective half-life of 0.42 years with a four order of magnitude increase in the on-target flux. However, for all base cases, the resulting activation products are much longer lived than the Am-241 itself. The flux level at all four base cases was not sufficient to eliminate the Am-241. In some base cases, an increase in flux tended to increase the irradiation effective half-life until a certain flux level was reached. At that point elimination factors exceeded production factors so that the irradiation effective half life could begin to decrease. For the lowest energy spectrum, irradiation half-life decreases proportionately with increase in flux. The fluence required for transmutation was highest for the higher energy spectrum (D-T unmoderated).
- For Pu-238 and Pu-239, there is not a significantly more beneficial transmutation base case. Large amounts of activation products are created in each case which are sensitive to the different energy spectra. This is due to the complex neutron reaction cross-sections. The more efficient transmutation scheme is again, the D-T thermalized case. A four order of magnitude increase in the base case flux level can reduce the radiological half-life of Pu-238 from 87.7 years to an irradiation effective half-life of 0.77 years and the radiological half-life of Pu-239 from 2.4E+04 years to an irradiation effective half-life of 0.27 years.
- Because the thermal-to-slow energy spectrum is obviously more beneficial for Tc-99 and I-129 transmutation, targets should be thin to reduce self-shielding effects and maximize transmutation processes. For actinides, the research results

demonstrated that thicker targets increase the number of fission reactions, thereby generating more fission products instead of to capture reactions that would generate other actinides. This would decrease the "consequence" of the transmutation.

- The conceptual transmutation device using a D-T neutron generator would require significant shielding for personnel and general public safety. This research shows that for the transmuter to be a self-shielded device and posted with only a "Radiation Area" sign, the amount of shielding required would be about seven feet of concrete plus some lead to eliminate photon dose resulting from capture gammas originating in the concrete. As stated in Chapter 8, the shielding evaluation was not optimized. Obviously, the amount of shielding required could be reduced if different shielding materials (e.g., borated concrete, polyethylene lined concrete or different aggregates of concrete) were studied.
- The conceptual transmutation device using a D-T neutron generator would require cooling for the device to be operated for significant periods of time. As mentioned in Chapter 9. A comprehensive engineering design was not performed; only an empirical calculation of the temperature increase in the transmutation device based on power deposition from radiation and activation products was conducted.

10.1 Future Work

As a result of this investigation, the following is a listing of recommended additional research using the conceptual design presented in this dissertation:

- The D-T and D-D neutron generator were not modeled in detail in this research. Future work could determine the effect of the generator within the transmutation device on the neutron flux and the energy spectrum. Neither effect is expected to be significant.
- The conceptual transmutation device could be optimized for each radionuclide under investigation. This research included broad parameters and general application to different radionuclides. Reflecting on the results of different reflector/moderator materials, sphere size, target size, etc., on the neutron energy spectrum and flux, one can choose the best combinations of parameters can be chosen based on what is most beneficial for a specific radionuclide.
- The methodology developed in this dissertation provides a mechanism that can be used for studying the feasibility of transmuting other radionuclides of interest such as other long-lived fission products. For example, Pd-107 which has a fairly wide resonance integral similar to Tc-99 or I-129; and for Cs-135, Zr-93, or Se-79 which have much smaller resonance integrals could be investigated.
- The application of the methodology developed in this dissertation can be extended to studying the production of radionuclides of interest; medical use radionuclides, for example.

Bibliography

1. Seltborg, P. Source Efficiency and High-Energy Neutronics in Accelerator Driven Systems. Diss. Department of Nuclear and Reactor Physics. Royal Institute of Technology, Stockholm, 2005.
2. Lou, T. P. Compact D-D/D-T Neutron Generators and Their Applications. Diss. Department of Nuclear Engineering. University of California, Berkeley, 2003.
3. Verbeke, J. M., Development of High-Intensity D-D and D-T Neutron Sources and Neutron Filters for Medical and Industrial Applications, Diss. Department of Nuclear Engineering, University of California, Berkeley, May 2000
4. Hoffman, E. A. Neutron Transmutation of Nuclear Waste. Department of Nuclear and Radiological Engineering. Georgia Institute of Technology, 2002.
5. Liu, Y. A Study on the Feasibility of Electron-based Accelerator Driven Systems for Nuclear Waste Transmutation. Diss. Department of Nuclear Engineering. North Carolina State University, 2006.
6. Kang, C. H. Transmutation Effects on Transuranic Waste Inventory and Its Repository Risk. MS Thesis. Department of Nuclear Engineering. Massachusetts Institute of Technology, 1993.
7. Ganda, F. Optimization of a Sub-Critical Multiplier and a Beam-Shaping Assembly for a D-D Compact Neutron Source Driven BNCT Facility. MS Thesis. Department of Nuclear Engineering. University of California, Berkeley, 2002.

8. Physics and Safety of Transmutation Systems – A Status Report. Nuclear Energy Agency, NEA No.6090. OECD, 2006.
9. Overview of Physics Aspects of Different Transmutation Concepts. Nuclear Energy Agency, NEA/Nsc/Doc(94)11. OECD, 1994.
10. Partitioning and Transmutation Current Developments – 2004. Swedish Nuclear Fuel and Waste Management Company. May 2004.
11. Status of Nuclear Fuel Processing, Partitioning and Transmutation. Nuclear Waste Management Organization. NWMO Background Papers. November 2003.
12. Implications of Partitioning and Transmutation in Radioactive Waste Management. Waste Technology Section, International Atomic Energy Agency. Technical Report Series no. 435. December 2004.
13. Fusion Transmutation of waste and the Role of the In-Zinerator in the Nuclear Fuel Cycle. Sandia Report, SAND2006-3522. June, 2006.
14. Compact Neutron Generators. E.O. Lawrence Berkeley National Laboratory. November, 2007. <http://www.lbl.gov/tt/techs/lbnl1764.html>.
15. Portable Neutron Generators. Del Mar Ventures. November, 2007. <http://www.sciner.com/Neutron/>.
16. Offsite Source Recovery Project. Los Alamos National Laboratory. September, 2008. <http://osrp.lanl.gov/index.shtml>
17. Cerullo, N et al. "An Irradiation Facility for Boron Neutron Capture Therapy Application Based on a Radio Frequency driven D-T Neutron Source and a New Beam Shaping Assembly". Review of Scientific Instruments, Volume 73, Number 10. October 2002: 3614-3618.

18. M. Angelone et al., "Conceptual Study of a Compact Accelerator-Driven Neutron Source for Radioisotope Production, Boron Neutron Capture Therapy, and Fast Neutron Therapy," Nuclear Instruments and Methods in Physics Research A, 487**,** 2002: 585-594.
19. Magill, J., Schoerer, H., et al. "Laser Transmutation of Iodine-129". Applied Physics B – Lasers and Optics. 5 September 2003.
20. Dagani, R. "Tabletop Nuclear Fusion Device". Chemical & Engineering News. Volume 83, Number 18. 2 May 2005: 10.
21. Ridikas, D. et al. "Conceptual Study of Neutron Irradiator driven by Electron Accelerator". 7th Information Exchange Meeting on Actinide and Fission Product P&T (NEA/OCDE), Jeju, Korea, 14-16 Oct. 2002.
22. Cipiti, B.B. "The Advantage of Fusion Sources for Nuclear Waste Transmutation". Proceedings of the 2005 ANS Annual Meeting, Washington, D.C. 13-17 November 2005: 278-279.
23. Brolly, A. and Vertes, P. "Transmutation: towards solving problem of spent nuclear fuel". Proceedings of the Wigner Centennial Conference, Pecs, Hungary, 8-12 July, 2002: 19-1 – 19-8.
24. Venneri, F. et al. "Disposition of Nuclear Wastes Using Subcritical Accelerator-Driven Systems". The Uranium Institute, Twenty Fourth Annual International Symposium, 1999.
25. Forsberg, C.W. "Disposal of Partioning-Transmutation Wastes in a Yucca-Mountain-Type Repository with Separate Management of High-Heat

Radionuclides (Sr-90 and Cs-137)". 4th Topical Meeting on Nuclear Applications of Accelerator Technology, Washington, D.C. 12-16 November 2000.

26. Billebaud, A., et al. "The Muse-4 Experiment: Prompt Reactivity and Neutron Spectrum Measurements". PHYSOR 2002, Seoul, Korea, October 7-10, 2002.
27. Stacey, W. et al. "Subcritical Transmutation Reactors with Tokamak Fusion Neutron Sources". 16th ANS Topical Meeting on the Technology of Fusion Energy, Madison, Wisconsin, September 14-16, 2004.
28. Leung, K.N. et al. "Compact neutron generator development and application." Proceedings of 16th world conference on nondestructive testing. Montreal, Canada, August 30–September 3, 2004.
29. Lahey, R. et al. "Sonofusion – Fact or Fiction?" Proceedings of the 11th International Topical Meeting on Nuclear Reactor Thermal-Hydraulics (NURETH-11). Avignon, France, October 2-6, 2005.
30. Pelowitz, D.B. MCNPX™ User's Manual Version 2.5.0. LA-CP-05-0369. Los Alamos National Laboratory. April 2005.
31. Forrest, R. EASY-2003 Documentation Series. UKAEA FUS 484 through 488. Culham Science Center. December 2002.
32. Shleien, Bernard. The Health Physics and Radiological Health Handbook, Third Edition, 1998.
33. Science Daily. "Double Crystal Fusion Could Pave Way for Portable Devices". Rensselaer Polytechnic Institute. February 14, 2006. <www.sciencedaily.com/releases/2006/02/060213101716.htm>

34. DOE Fundamentals Handbook: Nuclear Physics and Reactor Theory, Volume 1 and 2. DOE-HDBK-1019/1-93. January 1993. U.S. Department of Energy, Washington D.C. 20585.

35. R.A. Forrest, "EASY- a tool for activation calculations," Fusion Engineering and Design, **37**, 1997: 167-174.

36. "Standards for Protection Against Radiation". Code of Federal Regulations, Title 10, Part 20, Appendix C.

37. Forrest, R. et al. EAF-2003 Cross Section Library. UKAEA FUS 486. UKAEA Fusion Association, Culham Science Center. December 2002.

38. Forrest, R. EAF-2003 Decay Data Library. UKAEA FUS 487. UKAEA Fusion Association, Culham Science Center. December 2002.

39. Forrest, R. EAF-2003 Biological, Clearance, and Transport Libraries. UKAEA FUS 488. UKAEA Fusion Association, Culham Science Center. December 2002.

40. ICRP Publication 51: Data for Use in Protection Against External Radiation: Annals of the ICRP Volume 17/2-3: Annals of the ICRP v. 17/2-3. 1987.

41. "Protection against Neutron Radiation," NCRP Report 38, National Council on Radiation Protection and Measurements, Washington D.C., 1971.

42. National Nuclear Data Center. Brookhaven National Laboratory. September, 2008. < http://www.nndc.bnl.gov/>.

43. WWW Chart of the Nuclides, Japan Energy Atomic Research Institute. September, 2008. <http://wwwndc.jaea.go.jp/CN04/index.html>.

44. Forrest, R. "Question about FISPACT." E-mail to Roger Sit. March 17, 2008.

45. The ITER Project. The ITER Organization. October, 2008. <http://www.iter.org/index.htm>.

46. Spheromaks. California Institute of Technology. October, 2008. <http://ve4xm.caltech.edu/Bellan_plasma_page/spheroma.htm>.

47. Radiation Source Use and Replacement, Abbreviated Version. National Research Council of the National Academies. National Academy of Sciences, 2008.

48. "Bubble Fusion Scientist Disciplined", Issues and Events Section, pages 28 – 30. Physics Today, November 2008.

49. Ledingham, K. W., et al. "Laser-driven Photo-Transmutation of Long-Lived Nuclear Waste: Application to Iodine-129". Central Laser Facility Annual Report 2002/2003. Council for the Central Laboratory of the Research Councils 2003. ISSN 1358-6254

50. Transmutation of Nuclear Waste. Textbook by Janne Wallenius. Royal Institute of Technology. Stockholm, Sweden. November 2008. <http://www.neutron.kth.se/courses/transmutation/TextBook.shtml>.

51. Edwards, R. "Giant laser Transmutes Nuclear Waste." New Scientist, 14 August 2003: 16:19.

52. Considerations for Extended Interim Storage of Low-Level Radioactive Waste by Fuel Cycle and Material Licensees. Nuclear Regulatory Issue Summary 2008-12. Nuclear Regulatory Commission, May 9, 2008.

53. Naranjo, B. et al. "Observation of Nuclear Fusion Driven by a Pyroelectric Crystal". Nature. Volume 434, 28 April 2005: 1115.

54. Geuther, J. et al. “Nuclear Reactions Induced by a Pyroelectric Accelerator.” Physical Review Letters. Volume 96, Number 5, 10 February 2006: 054803-1.

55. MCNP- A General Monte Carlo N-Particle Transport Code. Los Alamos National Laboratory. November, 2008. < http://mcnp-green.lanl.gov/index.html>.

56. LAHET. Los Alamos National Laboratory. November, 2008. < http://www-xdiv.lanl.gov/XCI/PROJECTS/LCS/index.html >.

57. FLUKA. Fluka Team. November, 2008. < http://www.fluka.org/fluka.php>.

58. Joint Evaluated File. Los Alamos National Laboratory. November, 2008. <http://t2.lanl.gov/data/jef22.html>.

59. National Nuclear Data Center, Brookhaven National Laboratory. November, 2008. < http://www.nndc.bnl.gov//>.

60. “Dose coefficients for Intakes of Radionuclides by Workers”, International Commission on Radiological Protection, ICRP Publication 68, 1995.

61. “Age-dependent Doses to Members of the Public from Intake of Radionuclides: Part 5 Compilation of Ingestion and Inhalation Dose Coefficients”, International Commission on Radiological Protection, ICRP Publication 72, 1996.

62. Phipps, A. W., Kendall G. M., Stather J. W., and Fell,T. P., “Committed Equivalent Organ Doses and Committed Equivalent Doses from Intakes of Radionuclides”, NRPB-R245, 1991.

63. Shultis, J.K. and Faw, R.E., “An MCNP Primer”, Department of Mechanical and Nuclear Engineering, Kansas State University, 28 July, 2006.

64. Kimura, I. et al., "Neutron Spectrum in Small Iron Pile Surrounded by Lead Reflector", Journal of Nuclear Science and Technology. Vol.15, No.3(1978), pp. 183-191.

65. "Calculation and Measurement of Direct and Scattered Gamma Radiation from LWR Nuclear Power Plants." ANSI/ANS 6.6.1. American Nuclear Society, 1987 (revised 1998).

66. Heinloth, K. et al., Landolt-Bornstein Group VIII Advance Materials and Technologies, Volume 3B, Nuclear Energy, 2005.

67. "Radiation Protection for Particle Accelerator Facilities" NCRP Report 144, National Council on Radiation Protection and Measurements, Washington D.C., 2003.

68. CRC Handbook of Chemistry and Physics, 89th Edition, 2008-2009. "Section 4: Properties of the Elements and Inorganic Compounds", p. 4-127.

69. LIFE: Clean Energy from Nuclear Waste, Lawrence Livermore Natioanl Laboratory. July, 2009. <https://lasers.llnl.gov/missions/energy_for_the_future/life/index.php>.

70. Hermanne, A. "Transmutation of Long Lived Fission Products: The Possibilities of Proton Induced Reactions". Journal of Nuclear Science and Technoloy. Supplement 2, p.1202-1205. August 2002.

71. Kase, T. at al. "Transmutation Fission ProductsWith the Use of an Accelerator". Progress in Nuclear Energy. Vol. 29 (Supplement 2), pp. 335-341. 1995.

72. "Transmutation is Technically Feasible", Radioactive Waste Management Research. CLEFS CEA- No. 46, pp34-39. Spring 2002.